UNIVERSITY OF TASMANIA

MIXTURE PREPARATION IN PETROL ENGINES

by

HOANG DINH LONG

Submitted in partial fulfilment of the requirements for the degree of

MASTER OF TECHNOLOGY

in the faculty of Engineering, University of Tasmania

February 1996

I hereby declare that this thesis contains no material which has been accepted for the award of any other degree or diploma in any university, and that, to the best of my knowledge and belief, the thesis contains no copy or paraphrase of material previously published or written by another person, except where due reference is made in the text of this thesis.

D. L. Hoang

Table of content

Acknowledgments

The author extends his gratitude and appreciation to his supervisor, Dr. A.C. Pittas for his advice, assistance and encouragement, to Dr. P.E. Doe for his guidance in the course, and also to Mr. R. Kennedy and all the staffs in the Engineering Workshop for their technical assistance.

The author also expresses his thanks to all the other people who have helped him during his study at the University of Tasmania.

Abstract

The aim of this work is to study the aspects of mixture preparation in petrol engines which are of interest to the mechanical engineers and researchers. The work reviewed the characteristics and behaviour of fuel and air flow in the intake manifolds of petrol engines and emphasised on investigation of fuel distribution between cylinders in a carburation engine and a multi-point injection engine.

Characteristics of the flows of liquid fuel film, fuel droplets, fuel evaporation and process of mixing of fuel and air were analysed. The presence and behaviour of a large amount of liquid fuel film and fuel droplets in the intake manifolds was confirmed to be a main cause of inhomogeneity of mixture supplied to the cylinders. Atomising fuel spray and heating inlet manifolds are good methods for improving fuel evaporation and mixing of fuel and air in the intake manifolds to achieve homogeneous mixture for good operations of the engines.

Fuel distribution between cylinders of a carburation engine and a multi-point injection engine was investigated, using the method of exhaust gas analysis. The results showed that in the multi-point injection engine fuel distribution between the cylinders is much better than in the carburation engine although the injection engine is equipped with a pneumatically controlled fuel injection pump (delta A/F ratio of 0.35 to 0.93 in the injection engine in contrast of delta A/F ratio of 0.76 to 1.7 in the carburation engine at normal running conditions). Injection engines equipped with an electronically controlled fuel injection system would have much better improvement in fuel distribution than the injection engine used for the present study.

Heating the intake manifold in the carburation engine (by increasing coolant temperature) indicated a good improvement in fuel distribution between the cylinders while heating inlet air was not an effective way. In the injection engine, fuel distribution between the cylinders was seen to be not significantly affected by heating.

1. Introduction.

It is well known that mixture preparation in petrol engines has a significant effect on the ability of the engines to operate smoothly, powerfully, and efficiently, as well as on the exhaust emissions. Poor quality air-fuel mixture prohibits an engine to give high power output and high efficiency and causes high concentration of toxic components in the exhaust gas.

Therefore, in the field of petrol engine, engineers and researchers always want to find effective methods to create correct air-fuel mixtures. At the early stage of petrol engine development, preparation of mixture in the engines was done by carburation systems, but soon after, fuel injection engines were developed and indicated more advantages over carburation engines in terms of power output, efficiency and cleanness of exhaust gas, and now more and more carburation engines are replaced by injection engines. To confirm how fuel injection engines give such more advantages over carburation engines and find the methods to improve the performance of the engines, this report reviews characteristics of mixture preparation in both of the types of petrol engines and investigates fuel distribution between cylinders of these engines.

The report contains 3 main sections. A general overview of petrol engines is presented in section 2 to give a basic understanding about these types of engines. Characteristics of mixture preparation in the intake manifolds of petrol engines are presented in section 3. Section 4 presents results of the present investigation of fuel distribution in a carburation engine and an injection engine. In addition to these three sections, section 5 gives conclusions of the study, and recommendations and suggestions for further research based on the present facility in the Thermodynamics Laboratory.

2. General introduction to petrol engines.

A petrol engine is one type of internal combustion engines, which uses petrol as fuel. Unlike diesel engines in the group, in which diesel fuel is sprayed directly into the combustion chamber of the engine and ignited due to high air temperature resulting from compression, in conventional petrol engines the mixture of air and petrol is prepared outside the engine cylinders in a special device before being supplied to the cylinders, and then the mixture is ignited by a spark discharged from the electrodes of a plug. Petrol engines are therefore called *spark ignition engines* or *pre-mixed charged ignition engines.*

2.1 Petrol fuel.

Petrol is one type of products resulting from refinement of petroleum. It is a complex mixture of several hydrocarbon compounds whose chemical composition varies widely, depending on the base crude oil and the methods used in the refinement. Petrol burns violently in the open air, releasing a large amount of thermal energy. A typical petrol has an energy content of 44 MJ/kg. The two most important characteristics of petrol to engine performance are its volatility and octane number. Volatility of fuel affects the mixture preparation while the octane number affects the anti-knock in combustion. Both of them therefore determine design characteristics of the engines.

2.1.1 Volatility.

Volatility is closely defined as the tendency of a liquid to evaporate. In spark ignition engines, this property of fuel is very important because it affects the evaporation rate of fuel in the intake manifold, and therefore affects the uniformity of the air- fuel mixture in the cylinders at the time of ignition.

Measurement of volatility of petrol is usually based on its distillation characteristics. For example, motor petrol consists essentially of a mixture of hydrocarbons boiling at temperatures in the range of 20° to 200° C, and the volatility of each type of petrol is expressed by the volume percentage that is

distilled (or evaporate) at or below a fixed temperature. The distillation curves for two types of petrol are shown in Figure 2.1-1 as an example

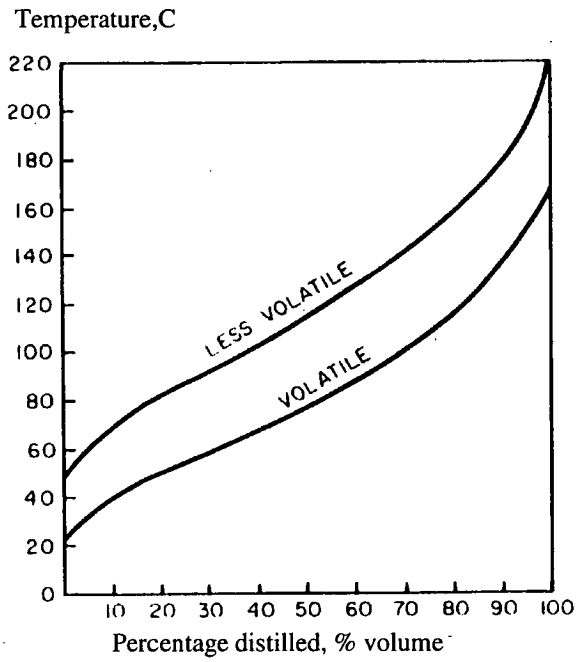

Figure 2.1-1. Distillation curves for two types of petrol (A.G. Bell, 1977)

As shown in the Figure, at the same temperature, the volatile petrol has a larger percentage distilled than the less volatile petrol does. The petrol that has the lower curve has the greater volatility.

Effect of fuel volatility on the engine operation.

Since the volatility influences the proportion of the fuel evaporated in the intake manifolds and in the cylinders of engines, it affects the quality of in-cylinder mixture before combustion starts. Therefore, it strongly affects the engine performance.

Theory and experiments indicate that in the normal type of spark ignition engine, operation will be satisfactory only if the various cylinders receive approximately the same air-fuel ratio and if nearly all of the fuel in the cylinders is evaporated by the time of ignition. Thus, if the fuel used is not sufficiently volatile, the proportion of fuel supplied to the engine, which evaporates in the induction system, will be small. This leads to a large amount of fuel depositing in the intake manifolds and flowing into cylinders, causing maldistribution of fuel between cylinders and net liquid fuel present in the

cylinders. This liquid fuel will not be able to fully vaporise before ignition starts, so it cannot burn completely or may not be able to burn at all, leading to a decrease in engine efficiency and engine power output, and an increase in emissions of unburnt hydrocarbons (HC) and carbon monoxide, which are causing widespread concern today.

Low volatility of fuel makes the engine difficult to start, especially at low ambient temperatures. For example, examining engine startability at the ambient temperature of -20°C Nakajima et al (1978) showed that engine cranking duration to the first fire with n-hexane fuel, which has a boiling point of 69°C (low volatility), is 5 times longer than that with n-pentane fuel, which has a boiling point of 36°C (high volatility), (15 seconds compared with 3 seconds). The explanation for this is that engine startability depends on the supply of a combustible mixture to the cylinder at the moment of ignition. During start, mixture preparation is carried out under unfavourable conditions, ie both temperature and turbulence, which are the main factors contributing to accelerating fuel evaporation, are very low. This makes a satisfactory air-vapour ratio difficult to achieve.

Taylor (1985) indicated that the amount of fuel vapour present in cylinders increases with the amount of fuel supplied by the fuel system. In other words, the fuel vapour-air ratio in cylinders increases with the ratio of fuel to air supplied by the induction system. Therefore, to obtain a required air-fuel vapour mixture for starting engines at low ambient air temperature, it is necessary to supply more fuel than that at high ambient air temperature. This solution is also applied to the case of using a less volatile petrol fuel. To start and warm up engines with less volatile petrol, more fuel should be supplied to the intake manifold than with volatile petrol. Similarly for the case of warming up the engine, Bell (1977) indicated that the use of fuel with high volatility reduces considerably the time required for this period, which in turn improves fuel economy.

In brief, the less volatile the petrol, the greater the amount that should be supplied to the engine to compensate the amount of non vaporised fuel. Thus, with a given engine in a given set of running conditions, there is a certain minimum volatility of fuel to be used, below which operation will be unsatisfactory, ie. the volatility of the available fuel influences engine design, particularly regarding the size, shape and arrangement of the inlet manifolds,

and the minimum temperature of the manifold walls, as well as the minimum temperature of inlet air required for satisfactory engine operation.

However, if a petrol is too volatile , it can cause some problems for engine operations at high ambient air temperatures. That is, the petrol is liable to vaporise in the fuel lines, leading to vapour locks, which can cause a stoppage of fuel flow in the fuel supply system or in the carburettor. This problem can be seen in engines that are being restarted, since in that case the engine compartment is usually hottest.

2.1.2 Octane number.

Octane number of a fuel is the percentage of isooctane in the mixture of isooctane and normal heptane that will give borderline detonation under the same conditions as the fuel under test. In terms of resistance to detonation, isooctane has great resistance to detonation (its octane number is considered to be equal to 100) while normal heptane detonates readily (its octane number is considered to be equal to 0). To determine the octane number of some petrol that has greater resistance to detonation than isooctane, a mixture of isooctane and a lead based compound is used in the test. In this case, one percent of lead based compound in isooctane is equal to one octane unit. For fuel test a specified engine is used under a specified set of operating conditions. The octane number is accepted for evaluating the resistance to detonation (anti-knock performance) of any fuel.

A method of measuring the influence of design characteristics and operating conditions of an engine on the detonation tendency is to determine the percentage of isooctane in normal heptane that will give incipient detonation under the prevailing conditions.

Fuel with high octane number has a high anti-knock performance. The octane requirement of an engine varies with compression ratio, geometrical and mechanical considerations, and with its operating conditions. Typically, for example, an engine that has compression ratio of 7.5 requires 85 octane fuel, while an engine that has compression ratio of 10 would require 100 octane fuel (Richard Stone, 1992).

In other words, fuel with high octane number enables the engines to be designed with high compression ratios, which give increased efficiency and power output, as well as improved fuel economy.

In effect, an increase in engine efficiency with compression ratio in petrol engines can be seen from the equation determining the thermal efficiency of a theoretical Otto cycle under ideal conditions.

$$\eta_t = 1 - \frac{1}{r_v^{\gamma-1}} \qquad (2.1\text{-}1)$$

Where η_t is thermal efficiency of an ideal Otto cycle,

r_v is compression ratio of an engine,

γ is the ratio of gas specific heat capacities, c_p / c_v. (C_p and C_v are specific heat at constant pressure and specific heat at constant volume, respectively, of the working gas).

However, for a given compression ratio, the octane number requirement varies widely, depending on the design characteristics of an engine.

An effective mean of increasing the octane number of a petrol is to use fuel additives, for example, lead-based compounds. Lead-based compounds indicate a significant improvement for the octane rating of petrol and they have been widely used for this purpose for a few years. However, using lead compounds as fuel additives is found to cause severe air pollution. Therefore, most countries now have restrictions on the use of lead in automotive fuels.

2.2 Combustion in petrol engines.

Combustion in engines is a process of burning air-fuel mixture to release heat for power output. In spark ignition engines fuel-air mixture is ignited by the ignition spark discharged from the electrodes of a plug. Except in the case where charge stratification is used to control detonation, conventional spark ignition engines are supplied with a mixture of fuel and air that is quite homogeneous in approximately gaseous form by the time of ignition. The ignition is started at the point where the spark discharges, and then a flame is formed and propagates throughout the whole combustion chamber. If all the petrol (HC) burned with the oxygen (O_2) trapped in the cylinder, only water (H_2O) and carbon dioxide (CO_2) would be formed. However, complete combustion is never obtained in the engines because of inhomogeneity of the mixture, the variations of conditions of the combustion process and other

factors. Under these conditions, some of the carbon of fuel does not get enough oxygen, and therefore, instead of CO_2 , carbon monoxide (CO) is formed. Some of the hydrogen does not unite with oxygen, so some hydrocarbon (HC) remains unburnt.

In addition, during combustion there are also some other reactions occurring. At the high temperature of combustion, some of the nitrogen can unite with oxygen to form nitrogen oxides (NO_x). As a result, the exhaust gas emitted from the exhaust manifold contains not only the products of perfect combustion (water and carbon dioxide) but also pollutants (carbon monoxide, unburnt hydrocarbon, and oxides of nitrogen). Components of these emissions and the factors influencing their formation will be discussed later.

Clearly, engine performance is influenced by the characteristics and efficiency of the combustion of fuel-air mixture in the cylinders. The completion of combustion depends on the quality of the mixture at the time of ignition. Therefore, it depends on the mixture preparation in the intake manifold. Thus, mixture preparation and combustion are the two interrelated factors affecting engine performance. Study of combustion in engines in detail is beyond the scope of this project, but understanding the main points of a combustion process is necessary in the analysis of mixture preparation in petrol engines.

Depending on the characteristics of the combustible mixture in the cylinder and the engine running conditions, combustion can occur normally or abnormally.

2.2.1 Normal combustion.

In the normal combustion process, ignition starts from the position of electric sparks discharged, following which the flame front propagates steadily through out the whole mixture volume. The flame front divides the volume of the mixture in the cylinder into two zones, burned mixture and unburnt mixture; the burned mixture volume increases and the unburnt mixture volume decreases with combustion time. The mechanism of combustion is very complicated and difficult to determine because combustion of fuel-air mixture occurs with a great rapidity at very high temperature and pressure. There have been many studies on this subject and a theory now generally accepted is that combustion of fuel-air mixtures depends on chain reactions, in which a few highly active constituents cause reactions which in turn generate additional active

constituents in addition to end products, thus multiplying the number of reactions until the combustion is complete. First active constituents are created due to high temperature at the points where electric sparks are discharged. Heat released from the combustion of mixture causes the temperature and pressure of gas to rise. The rate of pressure rise depends on the combustion speed that is influenced by the quality of mixture preparation and engine operating conditions. Figure 2.2-1 shows a hypothetical pressure time diagram of a spark ignition engine.

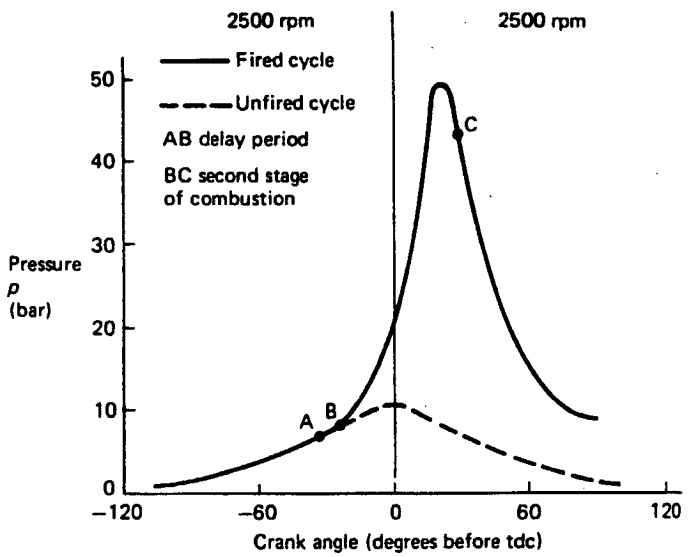

Figure 2.2-1. Hypothetical pressure diagram for a spark ignition engine.

Most authors assume that the combustion process consists of two stages. In the first stage (indicated by AB on the diagram), there is no pressure rise resulting from combustion because the amount of reactants is still very small (less than 10% of the total mixture). The duration of this stage, called the delay period, depends on many factors, such as energy and configuration of the spark, vapour-air ratio at the position where the spark is discharged, and air motion. These factors are sometimes random so the delay duration is even not the same for different cycles within individual cylinders. This leads to a *cyclic dispersion* within a cylinder. Richard Stone (1992) stated that the delay period is typically about 0.5 ms duration, which corresponds to about 7.5° of crank angle at 2500 rpm.

Following the delay period is the main stage of combustion that takes a finite time and ends shortly after the peak pressure of the cycle (point C). Benson and

Whitehouse (1979) stated that in reciprocating engines , high cycle efficiency is obtained if the maximum cylinder pressure occurs 5-20° after top dead centre. To obtain this, the mixture is usually ignited some time before top dead centre (near the end of the compression stroke). This means that there is a pressure rise associated with combustion before the end of the combustion stroke, and an increase in the compression work (negative work). If the ignition starts at the top dead centre, there will be an increase in time loss due to combustion during expansion and a decrease in cycle efficiency. The rate of pressure rise during combustion depends on flame speed that is influenced by such factors as the air-fuel ratio and uniformity of the mixture, engine speed, and load. Experimental investigation from Kneen et al (1983) showed that flame speed is strongly influenced by the turbulence of in-cylinder charge; increasing the turbulence by means of an intake centre body port may increase the flame speed by 30% to 50%. Similarly, Ma (1975) stated that the lean burn limit can be extended with improved combustion resulting from increased cylinder charge motion. With a fuel-air ratio of 1.05 to 1.2 times stoichiometric (lightly rich mixture), the flame speed is highest (Taylor, 1985).

One of the most prominent characteristics of a spark ignition combustion process is a wide variation (from cycle to cycle) of the pressure-crank angle diagram (**cyclic dispersion**). That is a difference of pressure-time diagrams of successive cycles within a cylinder. This can be easily seen in the difference of the peak pressures and of the crank angle of peak pressure of the successive cycles within a cylinder.

Experiments showed that cyclic dispersion in spark ignition engines is inevitable because the turbulence of charge within the cylinder varies from cycle to cycle, the fuel-air mixture is not homogeneous and the exhaust gas residuals is not fully mixed with the unburnt charge. In particular, the formation of the first highly active constituents and the early flame development have a profound effect on the subsequent combustion. The formation of the flame kernel depends on the local fuel-air ratio, the mixture motion, and the exhaust gas residuals in spark plug gap at the time of ignition, which are not stable, but randomly fluctuated. This causes variations in duration of delay period of combustion and affects the early stage of flame propagation. De Soete (1983) stated that combustion starts as self-ignition, occurring in the volume of very hot gases, and after that ignited flames pass though a non-steady propagation period before reaching a steady speed. This transient period is relatively

important compared with the total time available for combustion in an engine cycle. In the early stage of flame growth, the flame is small and very sensitive to mixture conditions. If the flame nucleus is moved into the thermal-boundary layer surrounding the combustion chamber, then it will burn slowly. In addition, at a given flame radius, the greater contact with the wall will reduce the flame front area. Conversely, if the flame is moved away from the combustion chamber surfaces, it will burn more quickly. Therefore, it can be concluded that cyclic dispersion is increased by anything that tends to slow-up the combustion process, for example, lean mixture operation, inhomogeneous mixture, exhaust gas residuals, and low load operation.

If all cycles were alike and equal to the average cycle, maximum cylinder pressure would be lower, efficiency would be greater and, particularly, the detonation limit would be higher, thus allowing appreciable increases in efficiency and mean effective pressure with a given fuel. Soltau (1960) indicated that if cyclic dispersion could be eliminated, there would be about 10 per cent increase in the power output for the same fuel consumption with weak mixture. Similarly, Lyon (1986) stated that 6 per cent improvement in fuel economy could be achieved if all cycles burned at the optimum rate.

2.2.2 Abnormal combustion.

Other forms of combustion different from the normal form described above are called **abnormal combustion**. Abnormal combustion can take several forms; the main ones are **pre-ignition** and **self-ignition**.

Pre-ignition is an ignition that occurs due to the contact of the mixture with a hot surface, such as an exhaust valve or incandescent carbon combustion deposits. Pre-ignition is often characterised by the engine continuing to fire after the ignition has been switched off. If the engine is operating with the correct mixture strength, ignition timing and adequate cooling, yet there is pre-ignition, the usual explanation is a build-up of combustion deposits, or coke. Early ignition causes an increase in the compression work and this causes a reduction in power. In a multi-cylinder engine with pre-ignition in just one cylinder, the consequence can be particularly serious as the other cylinders continue to operate normally. Pre-ignition leads to higher peak pressure, which increases the charge temperature and this in turn can cause self-ignition.

Self-ignition is an ignition that occurs when the pressure and temperature of the unburnt gas are such as to cause spontaneous ignition. The flame front propagates away from the sparking plug, and the unburnt gas is heated by radiation from the flame front and compressed as a result of the combustion process. If spontaneous ignition of the unburnt gas occurs, there is a rapid pressure rise characterised by a knocking. As a result, the thermal boundary layer at the combustion chamber walls can be destroyed, leading to an increased heat transfer. Therefore, the chamber walls can become too hot, which can cause pre-ignition. Severe self-ignition sustained over long periods of time often damages aluminium pistons and cylinder heads. Exhaust valves and piston rings also suffer. Damage due to self-ignition may eventually lead to a complete failure of the affected parts. A more likely explanation of the damage mechanism is that the pressure waves increase the rate of heat transfer to, and the temperature of the susceptible parts, thereby causing either local melting of the material or softening to such a point that the high local pressure causes erosion.

Because of noise, or the possibility of serious damage, self-ignition is a significant factor limiting the power output and efficiency of spark ignition engines. Without self-ignition, higher compression ratios could be used, giving higher efficiency and power output, or else higher inlet pressures could be used in supercharged engines, giving increased output. Using the fuel with high octane number, cooling engine adequately and retarding ignition timing usually reduces the possibility of self-ignition. An increase in either inlet temperature or inlet pressure increases end gas temperature and therefore increases a tendency to self-ignition. In addition, all design factors that increase heat transfer to end gas and combustion time increase the tendency to self-ignition.

In brief, a combustion process in which fuel burns completely and pressure rises smoothly is considered to be good combustion. The good combustion enable the engine to have high efficiency, high power output, and low specific fuel consumption. In petrol engines, the quality of combustion strongly depends on the quality of the air-fuel mixture present in the cylinder at the time of ignition. This depends on characteristics of the mixture preparation systems in the engines.

2.3 Exhaust emissions.

Exhaust gas from petrol engines usually consists of carbon dioxide CO_2, oxygen O_2, water vapour H_2O, nitrogen N_2, oxides of nitrogen NO_x, carbon monoxide CO, and unburnt hydrocarbon HC. Of these components, carbon dioxide, oxygen, water vapour, and nitrogen are the normal products of fuel combustion while carbon monoxide, oxides of nitrogen, and unburnt hydrocarbon are the products of incomplete combustion, association or dissociation of different components during combustion process and are harmful.

The fraction of HC, NO_x, and CO substances found in engine exhaust gases varies from engine to engine and depends on almost every aspect of engine operating conditions, such as ignition timing, load, speed, and in particular, fuel-air ratio. Typical variations of emissions with fuel-air ratio is shown in Figure 2.3-1.

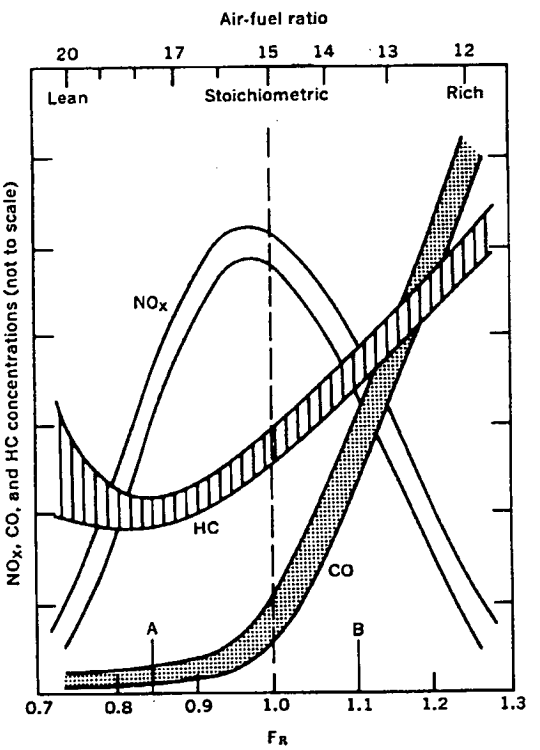

Figure 2.3-1 Effect of fuel-air ratio on exhaust emissions in petrol engines, (Taylor, 1985)

2.3.1 Carbon monoxide.

Carbon monoxide (CO) is always present in the exhaust gases due to the dissociation processes and incomplete combustion of fuel in the engine

cylinders. The CO formed due to the latter factor is most concentrated with fuel-rich mixtures (with a fuel-air ratio above stoichiometric). In this case there is a lack of oxygen to unite with the carbon of fuel, so some of the carbon cannot be completely oxidated.

With lean mixtures some CO is formed because complete chemical equilibrium is not always reached before exhaust valve opening, due to a shortage of time. Therefore, some of the hydrocarbons fails to burn to carbon dioxide (CO_2). Detailed studies of the relevant chemical reactions in the burnt gas have shown that the formation and decomposition of CO are controlled by the reaction:

$$CO + OH \leftrightarrow CO_2 + H$$

Theoretical studies have indicated that the reaction shown by the above equation is rapid enough to maintain equilibrium over the range of temperature and pressure encountered during a normal engine cycle. However, the discrepancy between the equilibrium calculations and the observed concentrations of CO usually exists. This is a result of other simultaneous reactions. The hydroxyl radical (OH) and hydrogen (H) are controlled by trimolecular reactions which are not rapid enough for equilibration of these species in the burned gas (Watfa et al, 1975).

2.3.2 Unburnt hydrocarbons.

Hydrocarbon (HC) emissions in spark ignition engines come from many sources and are normal components in exhaust gases. Possible sources of unburnt hydrocarbon emissions are intake fuel transients, plug thread crevice, fuel short circuiting, exhaust valve leakage, gasket crevice, oil absorption, wall quench layer, post flame kinetics, and ring pack crevice. The illustration of these sources can be seen in Figure 2.3-2.

It was first believed that these unburnt hydrocarbons were formed, in the main, because of quenching at the relatively cool cylinder walls. Many previous theoretical studies (eg., Kurkov and Mirsky, 1969; Adamczyk and Lavoie, 1978; Lavoie and Blumberg, 1980) and the experimental work by Watfa et al, 1979 were motivated by this belief. By sampling and analysing burned gas in the combustion chamber and exhaust manifold of a conventional spark ignition engine Watfa et al (1979) showed that the concentration of unburnt hydrocarbons in exhaust gas is relatively high immediately after exhaust valve

opens and then decreases sharply to the minimum value when the piston reaches BDC; during exhaust stroke the concentration of unburnt hydrocarbons increases and reaches the peak at TDC of the piston. The authors supported the belief that HC was formed in the quench layers on the walls of the chamber and stated that the high concentrations of HC at the beginning of the exhaust process were probably due to the quench layer near the exhaust valve; the high concentration at the end of exhaust stroke represented the quench layer on the cylinder walls, scraped and collected by the piston in its motion, and then discharged near the end of the exhaust stroke.

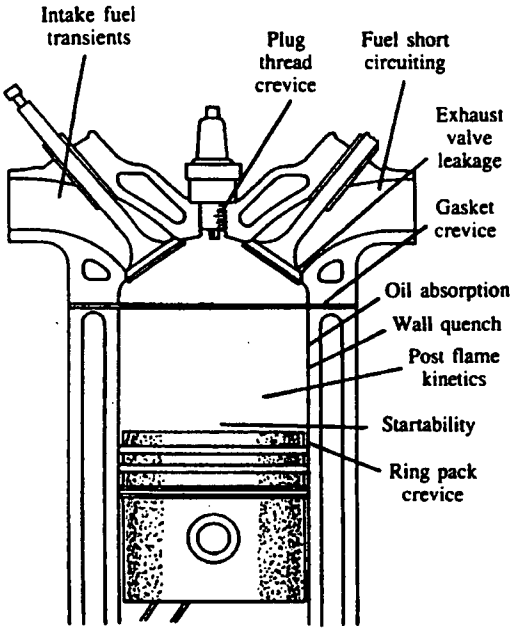

Figure 2.3-2. Potential sources of unburnt HC emissions.

However, the later experimental studies of wall quench layer (Lorusso et al, 1980; Lorusso et al, 1981; Lorusso et al, 1983) using a wall mounted sampling valve and theoretical studies (Shyy et al, 1983; Fendell et al, 1983) of wall layer hydrocarbons in spark ignition engines indicated that hydrocarbons remaining in a wall quench layer are not a major source of exhaust hydrocarbon emissions. Measurements of hydrocarbon concentrations during the combustion cycle (Lorusso et al, 1981 and Lorusso, 1983) show a rapid and extensive burn up (oxidation) of quench layer hydrocarbons after the time of flame arrival at the wall. This could be the result of both the diffusion of hydrocarbon material from the quench layer into the hot burned gases, or the diffusion of radicals into the quench layer from the burned gases. The fraction of HC which reacts in this manner is dependent on mixing rate (turbulence), gas temperatures,

concentrations of HC and O_2, and wall conditions (eg. wall temperature, deposits, etc). Further oxidation of HC from quench layers also occurs in the exhaust gas in the exhaust manifold. Lorusso et al showed that hydrocarbons arising from quench layers could account for no more than 12 percent of the hydrocarbons measured in the exhaust. The measurements also show a sharp increase in hydrocarbon concentration during the expansion stroke and up to the time of exhaust valve opening. The authors stated that this could be due to convection of unburnt material into the sampling zone from sources other than wall quenching, ie., ring crevices, oil films, etc, but quantities of these sources were not determined.

Boam et al (1994) experimentally investigated sources of unburnt hydrocarbon emissions and indicated that unburnt hydrocarbon emissions due to sources other than wall quench layer are significant. Of them mass flow of HC emissions due to crevices (piston ring crevices) represents about 0.6 percent of the total mass flow of fuel entering the engine, and represents 20 percent of the total amount of HC in the exhaust gas. The value can be more in the case of engine warm-up. The cause is the failure of the flame to penetrate the narrow gap between the cylinder and the piston while the mixture can be squeezed through the ring gap and into the region between the top and the second rings to re-emerge later when the cylinder pressure falls below the ring pack pressure. Similarly, HC emissions due to oil-film effects represent about 0.5 % of fuel entering the engine; HC concentrations from other sources depend on engine operating conditions.

2.3.3 Oxides of nitrogen.

The formation of oxides of nitrogen (NO_x) is very complex since it is dependent on a series of reactions which were suggested by many authors. These reactions were summarised by Sano (1982). Some major reactions had been suggested before by Newhall and Starkman (1967), called the Zeldovich mechanism as follows:

$$O_2 \leftrightarrow 2O$$

$$O + N_2 \leftrightarrow NO + N$$

$$N + O_2 \leftrightarrow NO + O$$

Equilibrium calculations at high temperature predict that the principal oxide of nitrogen present in the combustion products is nitric oxide (NO). The other oxides, such as nitrogen dioxide (NO_2), are present in much lower concentrations. Sano (1982) showed that NO_2 is mainly formed in early flames but after that much of NO_2 is destroyed mainly by the reaction with species H

$$NO_2 + H \rightarrow NO + OH$$

In fuel-lean flames, NO_2 is also destroyed by the reaction with oxygen:

$$NO_2 + O \rightarrow NO + O_2$$

Thus, NO is formed mainly in post-flame. Experiments by Newhall and Shahed (1971) using spectroscopic techniques to record the time rate of formation of NO in a reaction of hydrogen and air in a closed vessel also showed that NO formation occurred predominantly in the post-flame combustion products. This result agreed with the experimental result of Lavoie (1970) who showed that after the passage of the flame the NO concentration increases up to a maximum and then remains steady.

Experimental studies indicate that the formation of NO_x (in the main, NO) is at the highest temperature reached during combustion. It increases very strongly with increasing flame temperature. Ahtisham et al (1982) showed that relatively small changes in the flame temperature can significantly affect the amount of NO_x formed at any given equivalence ratio. Therefore, this would imply that the highest concentration of NO_x should be for slightly rich mixtures, those that have the highest flame temperature. However, NO_x formation will also be influenced by the flame speed because the flame speed affects the time for NO_x to form. Lower flame speed with lean mixtures causes a longer time and more available oxygen for formation of NO_x, therefore, it can also increase concentration of NO_x.

2.3.4 Factors affecting exhaust emissions.

a) Effects of air-fuel ratio on exhaust emissions.

At a very early stage of I.C. engine development, the influence of the air-fuel ratio on the engine operation has been recognised. Experimental data from Taylor (1985) shown in Figure 2.3-1 illustrate briefly this effect. Other investigators such as Watfa and Daneshyar (1975), Nakajima et al (1979),

Gruden and Hahn (1979) also indicated similar results at different conditions. In general, concentrations of CO and HC in the exhaust gas increase with a richer mixture while concentration of NO_x has a peak at the value of air-fuel ratio of mixture close to stoichiometric, with this mixture the flame temperature is highest.

Taylor (1985) and Gruden and Hahn (1979) also indicated that concentration of CO decreases with lean mixture, but the variation is very small with the fuel-air equivalence ratio less than unit. Concentration of HC, however, has a minimum value at about the point of maximum temperature which reaches with the fuel-air equivalence ratio between 1 and 1.05 (Lavoie and Blumberg, 1980) and then remaining almost constant. If the mixture is too lean the concentration will slightly increase due to misfiring. During the expansion and exhaust process some unburnt HC continues to be oxidated.

b) Effect of mixture inhomogeneity on exhaust emissions.

The presence of liquid fuel in the mixture in cylinders has different effects on each exhaust gas components. The formation of oxides of nitrogen can be affected by fuel droplets size. According to Ahtisham et al (1982), who studied the formation of NO_x in monodisperse spray combustion of hydrocarbon fuels, the concentration of NO_x has a minimum value at the optimum droplet size of about 40-50 μm depending on fuel types. Beyond this point, NO_x increases with either increasing or decreasing droplet size. This is explained as that NO_x formation depends on the flame temperature of burning fuel droplets; the flame temperature is dependent on the ratio of heat of combustion to latent heat of vaporisation of fuel droplets.

CO and HC are affected by quantity of liquid fuel present in the cylinders. Hasson and Flint (1989) studied this problem by removing wall fuel film flow from entering cylinders to get a homogenous mixture in the cylinders and showed that the removal of wall fuel film significantly reduces CO and HC emissions compared with a conventional engine because the wall fuel film usually consists of heavy fractions of the original petrol and enters the engine cylinders in the form of relatively large drops that will not evaporate readily during the conduction and compression strokes of the cycle and they can evaporate after the passage of the flame front. This leads to the existence of unburnt hydrocarbon.

c) Effect of mixture maldistribution on exhaust emissions.

Carbon monoxide emission.

As noted earlier, carbon monoxide formation is mainly due to incomplete combustion of fuel in the cylinders. The concentration of carbon monoxide in the exhaust gas of an engine is dependent on several factors including the factor concerned with fuel distribution. Eltinge (1968) stated that combustion occurs within an infinite number of volume elements in a chamber, each of which has a given air-fuel ratio and burns completely to the degree of available oxygen without mixing with gases from other elements. At the ideal conditions of combustion (assuming reactions reaching an equilibrium and no product remained due to dissociation), rich elements produce no oxygen, but produce some carbon monoxide (as mentioned earlier, the richer the mixture the more the CO is produced); lean elements produce no carbon monoxide or hydrogen but produce carbon dioxide, water and oxygen. Maldistribution of fuel means air-fuel ratios of the mixtures in volume elements are different. Therefore, this always leads to the formation of carbon monoxide in the cylinders although some oxygen is still available. That is why all experiments of Taylor (1985), Gruden and Hahn (1979), Watfa et al (1975), Nakajima et al (1979), and etc, who study effects of air-fuel ratio on the exhaust emissions, showed the presence of CO in the exhaust even though at very lean mixture. Of course, some carbon monoxide can be produced from dissociation reaction of carbon dioxide but in every case fuel maldistribution is an important factor. Thus, with the same overall air-fuel ratio, the poorer the fuel distribution, the more the CO is produced. In addition, for poorer fuel distribution, the overall fuel-air ratio should be higher than that would be in the case of uniform distribution to compensate the leanest volume element or cylinder, therefore this causes higher carbon monoxide emissions.

Hydrocarbon emissions.

Effect of fuel distribution on hydrocarbon emissions is not analysed theoretically but it can be understood that good fuel distribution allows an engine to operate at leaner mixture and therefore lowers hydrocarbon emissions, because a rich mixture always gives high concentration of hydrocarbon emissions.

Nitrogen oxide emissions.

As mentioned earlier, the formation of nitrogen oxides in the combustion chamber is dependent on the temperature, the oxygen present after combustion, and the time the mixture is held at these conditions. The formation of nitrogen oxides appears to reach a maximum value at the operating conditions that give good economy and power. This point is quite close to stoichiometric conditions for single-cylinder engine. With multi-cylinder engines, it has been noted that non uniform distribution of the fuel to the different cylinders results in lower nitrogen oxide emissions because in this case some of the fuel is burning under lean or rich conditions, both of which give lower concentrations of nitrogen oxides.

2.3.5 Method of reducing exhaust emissions.

Based on the above analysis, it can be deduced that emissions of CO can be reduced by operating engines with lean and uniform mixture. However, uniform mixture is never obtained, so with lean mixture it is difficult to ensure satisfactory mixtures in all cylinders; in addition, lean mixtures can reduce engine output.

NO_x emissions can be reduced by either reducing the flame temperature or burning duration. Retarding the ignition, using lean mixture or increasing the concentration of residuals in the cylinders by exhaust gas recirculation (EGR) always reduce the flame temperature, therefore NO_x decrease. Experimental and theoretical data from Lavoie and Blumberg (1980) show that the highest exhaust temperature is reached at a slightly rich mixture (equivalence ratio $F_R \approx$ 1.05), decreasing by about 50-70° C if equivalence ratio decreases to F_R=0.8. A significant decrease in exhaust temperature is also observed when using EGR (Gat and Kauffman, 1980 and Lavoie and Blumberg, 1980). Lavoie and Blumberg (1980). Studying the effect of EGR on exhaust emissions, Nakajima and Takagi (1979) and Lavoie and Blumberg (1980) showed that increasing EGR significantly decreases NO_x emission, but leads to an increase in HC emissions and specific fuel consumption. Nakajima and Takagi (1979) indicated that with the conventional engine, a marked reduction of NO_x is achievable only by the combination of rich mixture and EGR. Fuel economy penalty is then indispensable. They also showed that if some method is used to increase burning rate in engine (in fast burn engine), a great reduction of NO_x can be achieved by stoichiometric mixture with heavy EGR.

2.4 Mixture preparation systems.

Mixture preparation systems in a petrol engine are used to supply a satisfactory mixture of fuel and air to the engine to enable the engine to operate powerfully and effectively under different operating conditions.

Preparation and supply of fuel-air mixture into the cylinders of an engine can be done by either a carburettor or a fuel injection system. Although operating in different principles, both the carburetted fuel system and the fuel injection system supply fuel in the form of fuel sprays into the air stream in the induction systems of the engines (except for the case of stratified charge), and then mixture formation occurs and continues until the time of ignition.

The process of mixture formation consists of the discharge of fuel into the intake manifold, evaporation of fuel, mixing of fuel and air, and transportation of the mixture to the cylinders. All of these occur simultaneously in the intake manifold of the engine. However, characteristics of the process are different in a carburetted fuel system and in a fuel injection system.

2.4.1 Carburetted fuel systems.

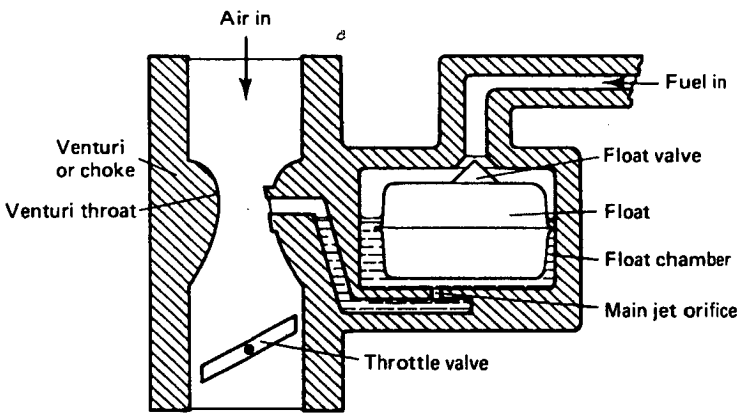

Figure 2.4-1. Simple fixed jet carburettor.

A carburetted fuel system consists of two main parts, the first is a carburettor that is used for creating and metering air-fuel mixture, and the second is an intake manifold system used for conducting and distributing air-fuel mixture to the cylinders. Both the carburettor and the intake manifold play an important role in creating and supplying homogeneous air-fuel mixture into cylinders.

Fuel is metered and mixed with air in the carburettor venturi in the proper proportion, and then flows along the intake manifold to the cylinders. The mixing of fuel and air occurs from the venturi and continues in the intake manifold. Figure 2.4-1 shows the principle in a diagram of a simple fixed jet carburettor.

The main operating principle of a carburettor is pulling fuel to an air stream and mixing them in the venturi. As the air flows at a high velocity through the venturi, a partial vacuum is produced, which is proportional to the air flow rate. This causes the fuel nozzle to deliver a fine spray of petrol into the passing air stream. The rate of fuel sprayed is proportional to the degree of vacuum in the venturi, and therefore, proportional to the air flow rate. This can be seen by analysing a flow of fluid through a venturi.

Air is compressible, and for flow through the venturi air flow rate can be determined by the following formula (R. Stone, 1992):

$$\dot{m}_a = A_t C_v \sqrt{(2\rho_a \Delta p)} \left\{ r^{1/\gamma} \sqrt{\left[\frac{\gamma}{\gamma-1} \frac{1-r^{(\gamma-1)/\gamma}}{1-r}\right]} \right\} \qquad (2.4\text{-}1)$$

Where $\dot{m}_a$ = mass flow rate of air,

A_t = area of venturi throat,

C_v = discharge coefficient for the venturi,

ρ_a = density of air at entry to the venturi,

Δp = pressure drop between entry and the venturi throat,

γ = ratio of gas specific heat capacity or adiabatic index.

$r = 1 - p/p_a$

p = pressure of air at the venturi,

p_a = pressure of air at entry to the venturi.

Fuel can be treated as incompressible, and for flow through an orifice fuel flow rate is determined by the following equation (R. Stone, 1992):

$$\dot{m}_f = A_o C_o \sqrt{(2\rho_f \Delta p)} \qquad (2.4\text{-}2)$$

Where $\dot{m}_f$ = mass flow rate of fuel,

A_o = orifice area,

C_o = coefficient of discharge for the orifice,

ρ_f = density of fuel,

Δp = pressure difference across the orifice.

The pressure of air at entry to the venturi and pressure in the float chamber of the carburettor are approximately unchanged (equal to atmospheric pressure) during operation. Therefore, as can be seen from the above diagram and equations, the pressure difference across the orifice is dependent on the pressure of air at the venturi throat or the pressure drop between entry and the venturi throat. This means that fuel flow rate is dependent on air flow rate.

When the throttle plate is stepwise opened, the flow rate and therefore the velocity of air passing through the venturi will increase. The increased air velocity in the venturi throat then causes the vacuum to increase, which in turn increases the pressure difference across the orifice and therefore increases fuel sprayed into the venturi. However, since r is always less than unity the pointed bracket term in equation (2.4-1) will always be less than unity (for a compressible flow). Thus, for a given mass flow rate the pressure drop will be greater than that predicted by a simple approach, assuming incompressible flow. This leads to the fact that the fuel flow will also be greater than expected and the air-fuel ratio will be richer as well at larger flow rate of air (when throttle opening is larger). Because of that, a practical main fuel metering system of a carburettor is constructed in such a way that it can make allowance for the mixture becoming richer at larger flow rates. Thus, when increasing the quantity of mixture by further opening the throttle plate the fuel-air ratio does not vary very much in a certain range of load as required by the engine.

In practice, a modern carburettor is equipped with different fuel supply systems, such as an idle system, main metering system, power system, accelerator pump system, and starting system. The starting system helps the carburettor supply a very rich-fuel mixture for starting a cold engine easily and rapidly, but as the engine speed increases, the mixture leans out. The idle system of the carburettor supplies a rich-fuel mixture to make the engine operate steadily at a given speed at idling conditions, and it continues to work together with the main metering system in the range of part load to create mixtures appropriate for the engines operating economically. When the engine

runs at full load, beside the main metering system, the power system supplies extra fuel to enrich the mixture as required to give the highest power. With a sudden throttle opening to increase torque, the accelerator pump system sprays some extra fuel into the venturi to create a rich mixture, meeting the transient mixture requirement of the engine.

2.4.2 Fuel injection systems.

In fuel-injected engines, fuel is introduced into the intake manifold in a different way from that used in carburetted engines. The injected engines use pressure to spray fuel into the intake manifold (or intake ports), so they do not have pressure loss due to venturi effect. There are two types of fuel injection systems, **single-point injection** and **multi-point injection**.

In a single-point injection engines, the injectors (usually one injector) spray fuel into the throttle body and then the fuel is transported in the intake manifold as in carburetted engines. So, as in carburetted fuel systems, in single point injection engines the throttle plate and intake manifold also have significant effects on mixture preparation.

The multi-point injection system employs injectors usually mounted close to the inlet ports of each cylinder. Each injector is responsible for supplying fuel to one individual cylinder, so precise metering of fuel can be obtained. As a result, a good distribution of fuel is also obtained.

In both the single point-injection system and the multi-point injection system, fuel can be injected in a pulse (time injection) or continuously. The metering of fuel is then carried out by controlling the duration of injection in the case of pulse injection and by controlling the flow rate of injection in the case of continuous injection. Controlling the injection in the modern fuel injection systems is now carried out by microprocessor systems in respect to manifold pressure, engine speed, air temperature, coolant temperature, composition of exhaust gas, and characteristics of acceleration. As a result, the fuel injection systems can adjust more precisely the amount of fuel sprayed to get the correct fuel-air ratio as required by the engine at different operating conditions. A block diagram of an electronic fuel injection system is illustrated in Fig. 2.4-2.

A comparison of the carburetted fuel systems with single-point injection systems and multi-point injection systems reveals that the multi-point injection systems have many advantages over the two others. The multi-point injection

systems eliminate many carburation and fuel distribution problems due to fuel transportation in the intake manifold because fuel is supplied individually to the intake port of each cylinder. In addition, the injectors can be adjusted to spray the same amounts of fuel for each cylinder. As a result, the uniform fuel-air ratio in the cylinders is easily obtained. With the uniform fuel distribution the engine can operate on a leaner overall fuel-air mixture. This reduces HC and CO in the exhaust gas and improves the fuel economy. Moreover, because of using separate injectors for each cylinder, the intake manifold does not need to heat, it can be designed in a simpler shape than in a carburetted engine and single point injected engine. This helps to have the highest overall volumetric efficiency and uniform air distribution.

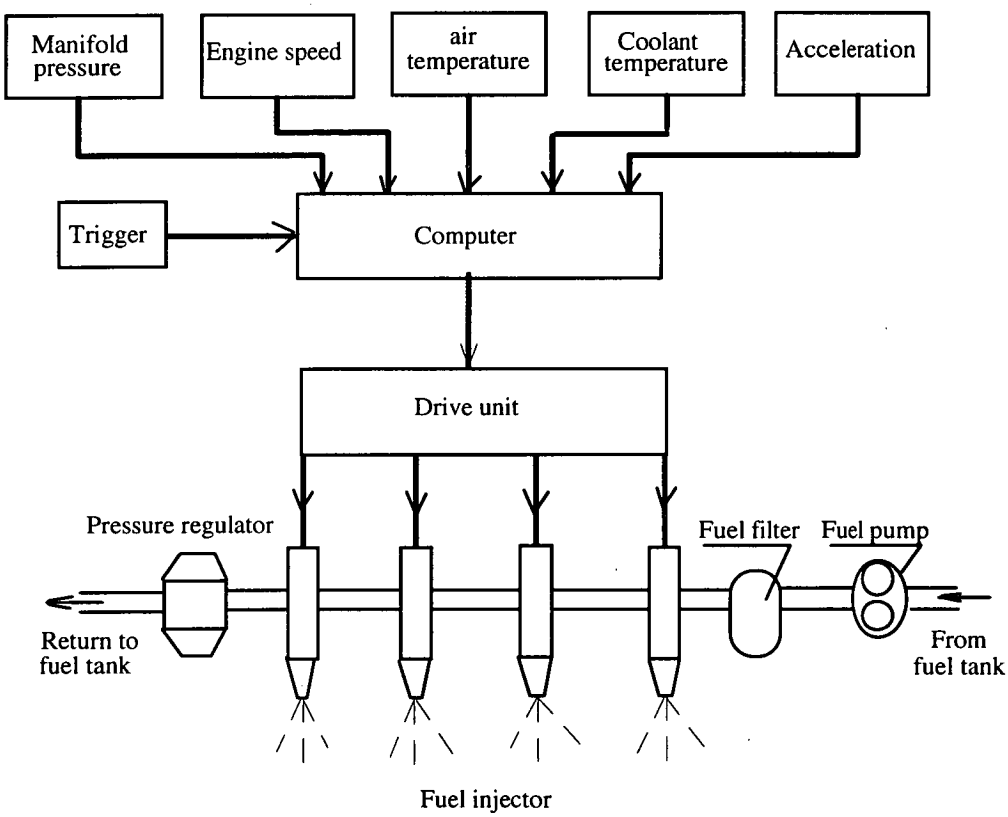

Figure 2.4-2. Electronic fuel injection system

However, under transient operating conditions the multi-point injection systems show some problems. When the throttle is rapidly opened , the inlet manifold pressure will rise more quickly than the fuel supply pressure, leading to an instantaneous fall in differential pressure across the injector which is different from the mean pressure differential being controlled by the pressure regulator. This reduces fuel sprayed, causing an instantaneously lean mixture in the

engine. A similar problem can occur as a result of pressure pulsations in the fuel supply rail and in the inlet manifold. These pressure pulsations are an inevitable consequence of the unsteady flow.

At very light loads, control of injection in the case of pulse injection becomes more difficult because the injectors then will open for a very short period of time, and under these conditions the differences in the response time become significant while exhaust gas sensors for controlling the overall fuel-air ratio cannot compensate for inter-cylinder variations. Therefore at light loads the mixture distribution will be worst in the multi-point injection systems. In contrast, under these loads, conditions the mixture mal-distribution will be least in carburetted or single-point injection systems because the manifold pressure is low, leading to a higher proportion of fuel evaporating and entering the cylinders as vapour.

The following section will discuss the mixture requirement for engine operating at different conditions, and how the fuel supply system can meet the mixture requirement.

2.5 Mixture requirements in petrol engines.

Mixture requirements in petrol engines are usually discussed in terms of air/fuel ratio or fuel/air ratio. In some cases, the relative proportions of fuel and air can be stated more generally in terms of fuel/air equivalence ratio (the definition is given in appendix B). In this section, fuel-air equivalence ratio is usually used for analysis and the term fuel air ratio refers to fuel-air equivalence ratio.

Unlike diesel engines, petrol engines can only normally operate in a certain range of air/fuel ratio. Moreover, at a certain set of engine operating conditions the engine can only operate efficiently and powerfully with a mixture at a certain value of air/fuel ratio called optimum air/fuel ratio. In principle, the optimum air/fuel ratio is that at any given engine speed, which will develop the required torque, or brake mean effective pressure with the lowest fuel consumption consistent with smooth and reliable operation. The optimum fuel-air ratio is not constant but varies according to engine running conditions, ie. under different running conditions, an engine needs different fuel-air ratios to give the best performances.

This section deals with a concept and determination of optimum fuel-air ratios of the mixture under different engine operating conditions by analysing the effect of fuel-air ratio on engine performance at each operating condition, using the experimental data from previous studies. Two typical operating conditions are considered. Those are **steady running condition** and **transient condition**. The analysis is mainly based on carburetted engines, however, the result is also applied to fuel injected engines.

2.5.1 Mixture requirements at steady conditions.

The effect of fuel-air ratio of a mixture on engine performance is determined in the following way. Under different running conditions the rate of fuel flow supplied to the engine is changed and the engine response is measured. The data are then expressed in diagrams, from which the optimum fuel-air ratio is determined.

a) Effect of fuel-air ratio on engine performance at full throttle opening.

Figure 2.5-1, established from experimental studies, shows typical curves of indicated mean effective pressure (imep) and indicated specific fuel

consumption (isfc) with varying mixture ratios at a full throttle opening (Definitions of engine operating parameters are given in appendix A).

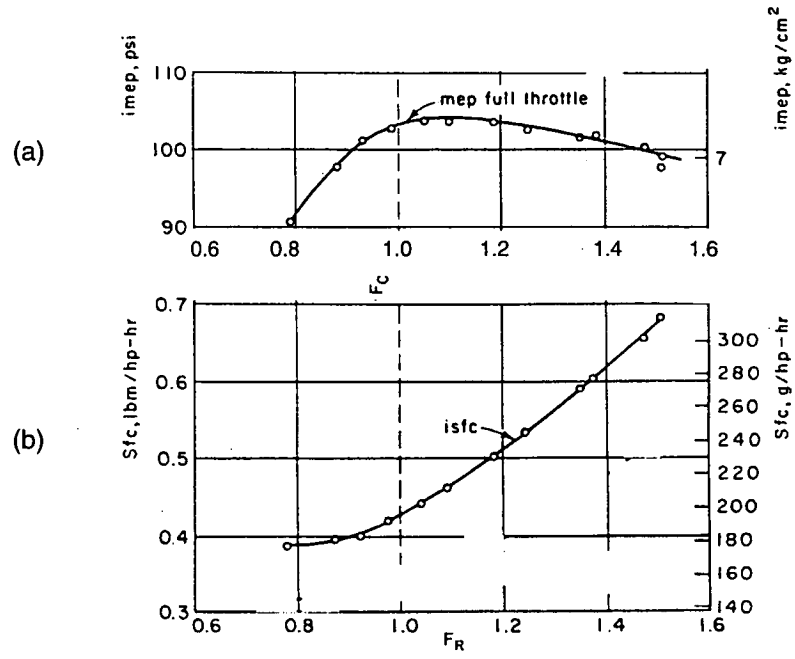

Figure 2.5-1. Effect of fuel-air ratio on indicated mep (a) and fuel economy (b),with V-8 engine, 3.6 litres, compression ratio r=6.3, at 3000 rpm, (Taylor, 1985b)

F_R is equivalent fuel-air ratio, and is defined as follows:

$$F_R = \frac{actual\ fuel-air\ ratio}{stoichiometric\ fuel-air\ ratio},$$

$F_R<1$: poor fuel mixture; $F_R>1$: rich fuel mixture.

(these parameters are defined in detail in appendix B).

As seen from figure 2.5-1, the imep reaches a peak between $F_R=1$ and $F_R=1.1$. This means that lightly rich mixture gives a maximum power output. This is because the density of constituents attending chemical reactions is highest and there is an equilibrium between the various chemical compounds evolved during the chemical reaction, which increases combustion speed and rate of heat released.

The specific fuel consumption increases with fuel-air ratio in the range of experimental mixture ratios ($F_R=0.8$ to 1.6) because with $F_R>1$ (rich mixture),

there is not enough air to burn fuel, so some fuel does not burn completely and some remains unburnt, leading to an increase in losses. Other experimental data with a larger range of fuel-air ratio indicated that leaning out the mixture beyond the fuel-air ratio of 0.8 also leads to an increase in specific fuel consumption due to misfire.

b) Effect of fuel-air ratio on engine performance at part throttle openings.

A similar effect of varying the fuel-air ratio of the mixture on mep and sfc is seen when running the engine at different throttle openings. Figure 2.5-2 and 2.5-3 express the dependence of indicated mean effective pressure (imep), brake mean effective pressure (bmep), indicated specific fuel consumption (isfc), and brake specific fuel consumption (bsfc) on fuel-air ratio at four positions of throttle opening (Test with 3.6 litreV-8 engine, compression ratio r=6.3, at 3000 rpm)

As seen in Figure 2.5-2, the shape of the imep and bmep versus fuel-air ratio curves is little affected by throttle positions. The highest imep and bmep occur at the same fuel-air ratio in each curve (between $F_R=1$ and $F_R=1.1$) provided that the mixture is homogeneous. The explanation for the shape of the imep curves is similar to that for the case of full throttle opening mentioned above. The shape of bmep curves is similar to that of imep curves because the difference between values of imep and bmep is friction mep (definition is given in appendix A) which is approximately independent of fuel-air ratio (Taylor,1985a).

The isfc and bsfc curves in Figure 2.5-1 show that there is a minimum point at each curve and the minimum point tends to occur at higher fuel-air ratios as the throttle is closed. This may be due to a reduction in effective flame speed caused by relatively increased fraction of residuals in the cylinders. However, at every throttle setting, the minimum isfc and bsfc occur at fuel-air ratios less than stoichiometric ($F_R=0.9$-1).

c) Effect of fuel-air ratio on engine performance at different engine speeds.

At different engine speeds, the shape of mep and sfc versus F_R curves are also similar to that indicated in Figures 2.5-2 and 2.5-3 but the values are different. The values of fuel-air ratios giving the highest power or best economy are also similar to those shown in these Figures.

(a)

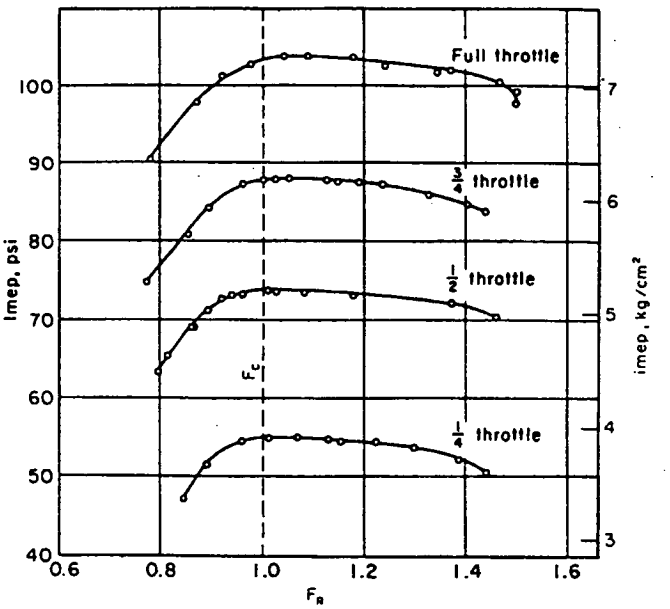

(b)

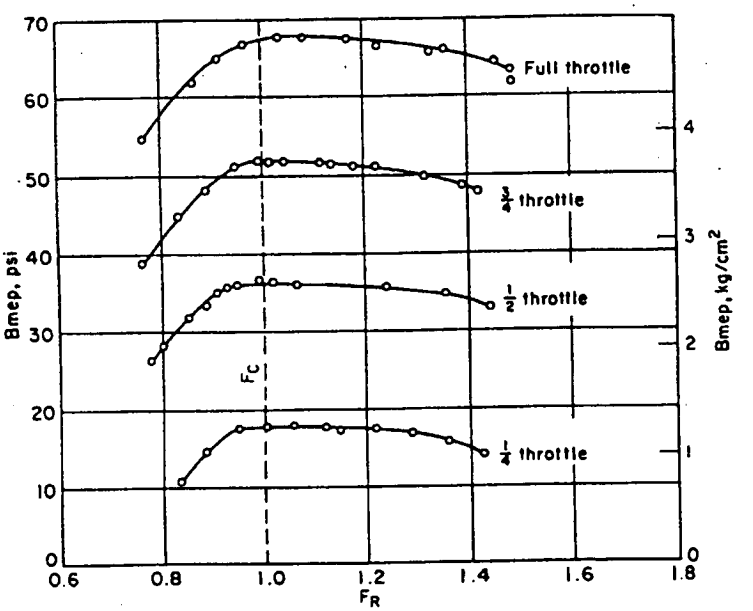

Figure 2.5-2. Effect of fuel-air ratio on imep (a) and bmep (b) at various throttle settings (Taylor, 1985)

(a)

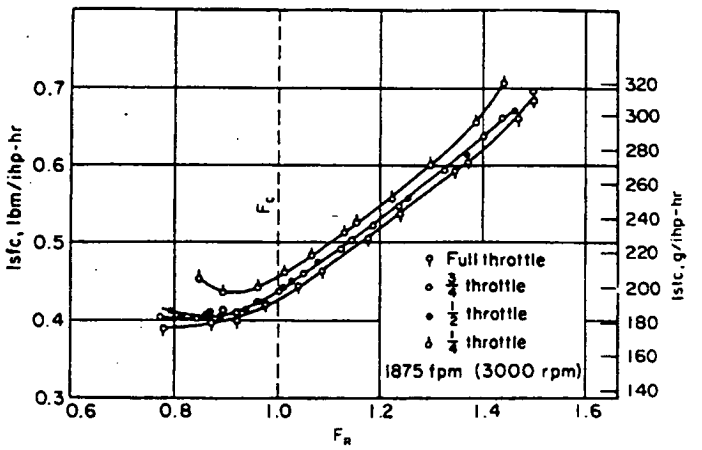

(b)

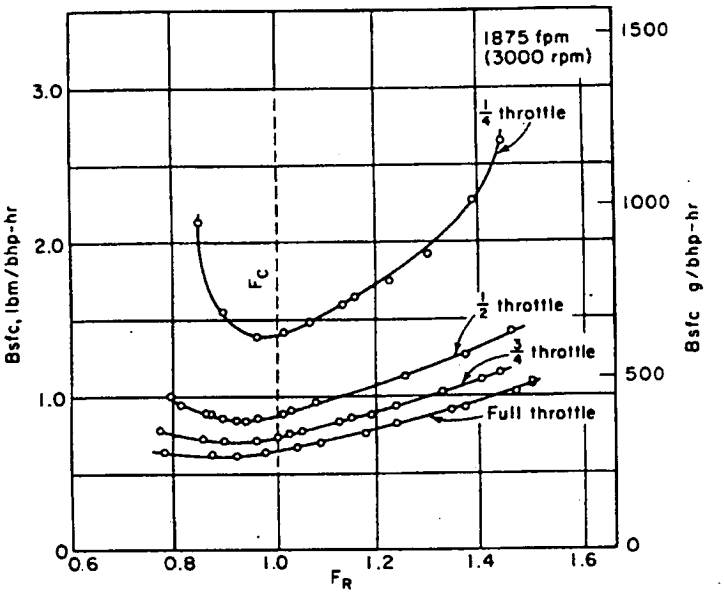

Figure 2.5-3. Effect of fuel-air ratio on isfc (a) and bsfc (b) at various throttle settings (Taylor, 1985)

d) Optimum fuel-air ratio.

In practice, engines can be required to give the highest power or to operate with the best fuel economy, depending on the use. Therefore, the optimum fuel-air ratio of mixture can be that with which the engine gives the highest power or the best fuel economy.

To analyse optimum fuel-air ratio conveniently, the optimum fuel-air ratio should be expressed in terms of a parameter which characterises the engine operation. Practically, the duty which an engine has to perform at a given instant can always be defined in terms of a required brake mean effective pressure at a given speed. Therefore, it can perform the optimum fuel-air ratios at different engine speeds versus brake mean effective pressure on a diagram. For this purpose, the data from Figures 2.5-2 and 2.5-3 are replotted to show the highest power and best economy curves. The mixture with the fuel-air ratio giving the highest bmep is called the **best power mixture**. It is clear from the above data that the best power mixtures at any throttle positions are approximately the same in fuel-air ratio and a little richer than stoichiometric ($F_R \approx 1.05$). Thus, the F_R versus bmep curve for the best power is approximately a horizontal line. In order to express the relationship between F_R and bmep for the case of best fuel economy, from Figures 2.5-2 and 2.5-3 with the addition of data for other speeds, the minimum bsfc at each throttle position and F_R corresponding to it are determined. Plotting the values of F_R versus bmep gives F_R versus bmep curve for the case of best fuel economy at different speeds. The shape of the curve is shown in Figure 2.5-4.

The Figure shows that the mixture required to give the best fuel economy is slightly lean ($F_R = 0.9\text{-}1$) while the mixture required to give the highest power is slightly rich ($F_R > 1.05$). It can be seen from the Figure that the fuel-air ratio depends on engine speed, but the fuel-air ratio versus bmep curves at different speeds corresponding to the throttle position from small opening to full opening are similar in shape. Therefore, plotting fuel-air ratio versus the fraction of maximum bmep at full throttle opening (this fraction is called load) at a given speed shows that the curves corresponding to different speeds approximately coincide to a curve, so it is more convenient to use this curve than the others in analysing mixture requirement. A typical curve expressing fuel-air ratio in terms of load is shown in Figure 2.5-5. The fuel-air ratio required for the best power is expressed by a horizontal line ($F_R \approx 1.05$) on the fuel-air ratio versus load diagram; the fuel-air ratio required for the best economy is expressed by

the dash curve. Thus, any curve between the best power and the best economy curves will meet both power and economy requirements. In practice, engines are not required to give the highest power output at part loads, but rather it is preferred that they consume least fuel, so at part loads the mixture should be somewhere between the best power and the best economy mixture, close to the best economy; only at full load or nearly full load the best power mixture is required to give the highest power.

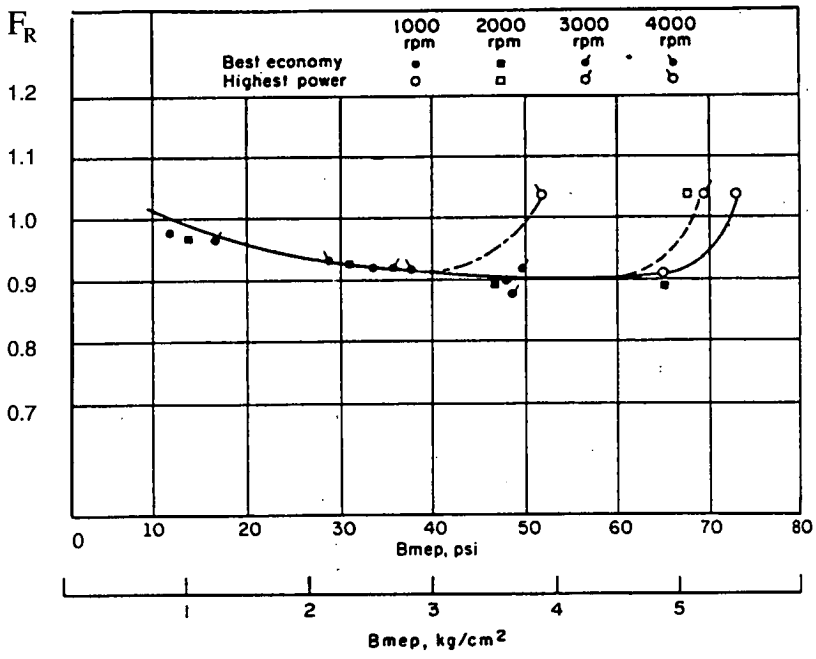

Figure 2.5-4. Fuel-air ratio versus bmep, (Taylor, 1985).

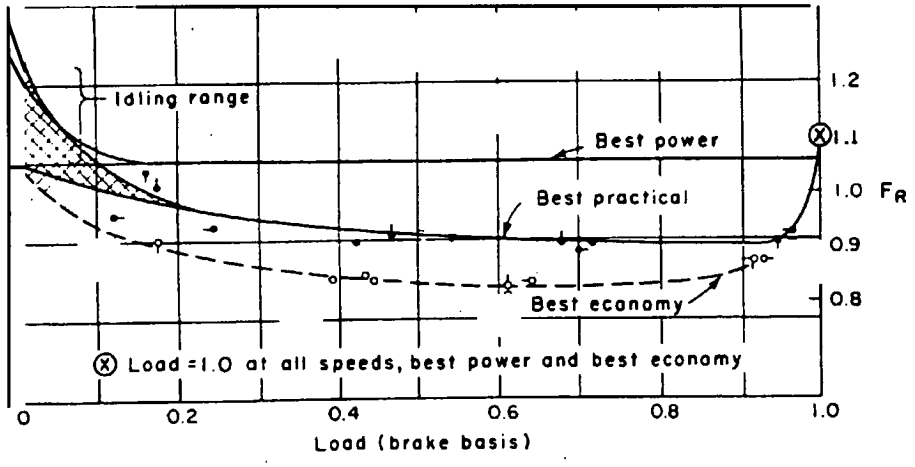

Figure 2.5-5. Fuel-air ratio versus load, (Taylor, 1985)

At idling, there is no useful work done, so optimum fuel-air ratio is that which uses the least fuel at the chosen idling speed, and that which makes the engine work steadily. Experimental results showed that the normal idling mixtures usually range between 1.2 and 1.5 times stoichiometric because at idling running conditions the engine temperature and air motion in engine are lower than those at load running conditions, leading to a decrease in fuel evaporation.

In brief, under steady running conditions, the optimum mixture is not the same in the full range of load, but is varied to ensure the engine operates well, meeting both economy and power requirements. It is rich at idling (F_R =1.2 to 1.5) to keep the engine running steadily, lightly poor (F_R =0.85 to 0.95) at part loads to give the best economy, and lightly rich ($F_R \approx 1.05$) at full load to give the highest power. A typical optimum fuel-air ratio versus load curve for steady running conditions is shown in Figure 2.5-5 (the best practical curve). In practical operations, there is a number of factors influencing the optimum fuel-air ratio, so for different types of engine running at different conditions, the optimum fuel-air ratio can be different. In general, however, fuel-air ratio versus load curves have a similar shape to the typical curve above.

2.5.2 Mixture requirements at transient conditions.

Under steady running conditions, an equilibrium is established at the inlet system, and the average fuel-air ratio received by the cylinders is equal to the fuel-air ratio supplied by the carburettor. Engine temperatures then are high enough for approximately all the fuel in the mixture to evaporate before ignition occurs. In the transient operation, however, an equilibrium is not obtained. The engine operates at abnormal speeds, loads, temperatures or pressures, or in rapidly changing conditions. The principal transient conditions of operation are starting, warming up, acceleration (increase of load), and deceleration (decrease of load). Under these conditions, experiments show that the air-fuel vapour ratio of the mixture received by cylinders is very different from the air-fuel ratio supplied by the fuel supply system. Also, the air- fuel vapour ratio received by a cylinder is not the same as that which it receives under steady conditions, even though the mixture ratio supplied at the inlet system may be exactly the same in both cases.

An acceleration and deceleration in gasoline engines mean an increase and decrease, respectively, in engine torque resulting from opening and closing the

throttle; whether or not a change in engine speed follows depends on the nature of the load. In carburetted engines and throttle body injected engines, mixture becomes momentarily leaner immediately after sudden throttle openings and momentarily richer after sudden throttle closing (Tanaka and Durbin, 1977, Hires and Overington, 1981, Aquino, 1981 and Taylor, 1985), ie. a lean excursion accompanies sudden throttle openings, and a rich excursion accompanies sudden throttle closings.

During start and warm up, the engine temperature is usually low, therefore most of the fuel discharged from the fuel nozzles does not evaporate but deposits in the intake manifold, leading to the mixture entering to the cylinders being leaner than that supplied at the carburettor.

Therefore under transient conditions, to ensure that the fuel vapour-air ratio received by the cylinders is satisfactory, the fuel-air ratio required from the carburettor or injector may be quite different from that required under steady operations, even at the same engine speed and load.

Thus, for starting and accelerating the engine, a very rich mixture must be supplied to the carburation system to compensate the amount of fuel that deposits in the intake manifold. This can be done by injecting an extra amount of fuel into the intake manifold during this period. The amount of fuel injected varies with engine speed, load, throttle position and characteristics of fuel. The fuel-air ratio will be progressively reduced from this point during the warm-up period until the engine will run satisfactorily with the normal steady running fuel-air ratio.

In the case of port-injected engines where fuel is injected separately into the intake port of each cylinder, air-fuel ratio excursions during transient operating conditions are smaller than in carburetted engines and throttle body injected engines because the fuel delay effect in these engines is relatively small. As a result, mixture requirement at transient operating conditions for these engines is not as rich as that for carburetted and throttle body injected engines.

In brief, under transient conditions, mixture required is generally richer, and sometimes much richer than that under steady running conditions. The value of fuel-air ratio depends on transient conditions and varies until the engine reaches a steady operation.

3. Mixture preparation in petrol engines.

3.1 Introduction.

Mixture preparation in petrol engines involves metering of fuel in a proper proportion with air, mixing of fuel and air to form a homogeneous mixture, and distribution of the mixture to the engine cylinders. In principle, the mixture should be homogeneous and uniformly distributed between different engine cylinders as required to enable the engines to operate optimally at different conditions. However, in practice, it is hard to achieve completely homogeneous mixture in the cylinders.

Either prepared by carbureted fuel systems or by fuel injection systems, fuel-air mixture results from the combined action of many processes occurring simultaneously in the intake manifold. Those are the processes of metering, spray and atomisation of fuel, evaporation and condensation of fuel from and to fuel droplets and fuel film, including complicated heat transfer processes between the intake manifold walls and fuel film, and between air flow and fuel droplets, and the transfer of mass and momentum between the highly turbulent and pulsating air flow and liquid fuel.

The details of the air and fuel flow in intake manifolds are therefore extremely complex. The combination of pulsating flow into each cylinder, different geometry flow paths from the plenum beneath the throttle through each runner and branch of the manifold to each inlet port, liquid fuel vaporisation and transport phenomena, and the mixing of air and fuel are truly difficult areas to untangle. During engine transients, when the throttle position is changed, the fact that the processes which govern the air and the fuel flow to the cylinder are substantially different introduces additional problems.

In fuel metering systems of conventional petrol engines, the supplied fuel usually enters the air stream as liquid jets, and then the liquid jets atomise into droplets. These mix with air and also deposit on the walls of the intake manifolds as liquid fuel film. Vaporisation of the fuel droplets and of the liquid

fuel film on the walls occur. The flow of liquid fuel along the walls can be significant. The transport and behaviour of fuel vapour, fuel droplets, and liquid fuel streams or fuel films in the intake manifolds affect fuel evaporation and are all important for mixture formation and distribution in the engines.

The transport phenomena of fuel and air in induction systems are different in multi-point fuel injection systems and in carburettor and throttle-body injection systems. In carburettor and throttle-body injection systems, fuel must travel past the throttle plate and along the intake manifolds, while in the multi-point fuel-injection systems, the liquid fuel is injected into the inlet ports, toward the back of the intake valve.

In general, in both cases the mixture entering the engines is not as homogeneous as required. The fuel is not fully vaporised as it enters the cylinders. The mixture going to each cylinder is not usually uniform in fuel/air ratio throughout its volume, and the distribution of fuel between different engine cylinders is not exactly uniform. This is a result of several processes.

In carburetted and throttle-body injection systems, deposition of liquid fuel in the intake manifolds makes the mixture formation complicated. In these systems, fuel must pass the throttle plate, so when the throttle opening is less than fully opened, most of the fuel metered into the air stream impacts on the throttle plate and throttle-body walls. only a small fraction of the fuel vaporises upstream of the throttle. The liquid is re-entrained as the air flows at high velocity past the throttle plate. The air undergoes a 90° bend in the plenum beneath the throttle; much of the fuel which has not evaporated is impacted on the manifold floors. Vaporised fuel and liquid droplets which remain suspended in the air stream will be transported with the air stream. However, droplet deposition on the manifold walls may occur due to gravity and to inertial effects as the flow goes round bends in the manifold.

The transport phenomena in port fuel-injection systems are different and significantly dependent on the timing and duration of the injection pulse. Fuel is injected onto the back of the inlet valve and surrounding port walls. Vaporisation of liquid fuel off the valve and walls occurs, enhanced by the back flow of hot residual gases from the cylinder, but some fuel is carried as liquid drops into the cylinders.

In brief, the flow in the intake manifold usually consists of several components such as air, fuel vapour, fine fuel droplets, and liquid fuel. A large proportion of the liquid fuel is often attached to the manifold wall as a fuel film; the remainder exists in the form of large droplets suspended in the stream. In general, there is a continuous interchange between these modes of fuel during transportation and mixing as the flow proceeds (Pao, 1982). Figure 3.1-1 shows a general model of an intake pipe of a carburetted petrol engine with different forms of fuel present.

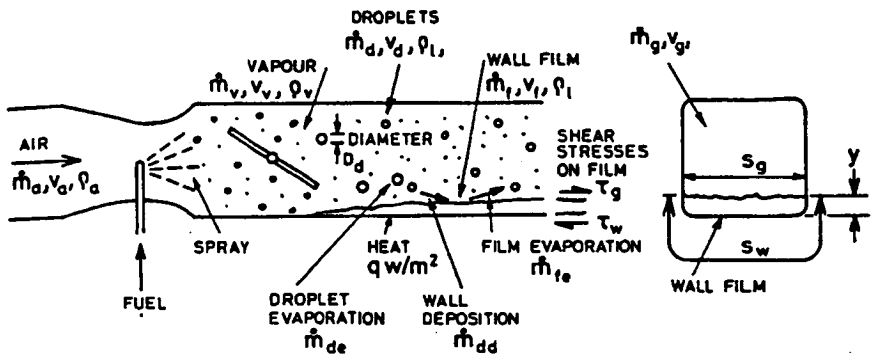

Figure 3.1-1 Different fuel forms in the intake pipe.

3.2 Flow past throttle plate.

Controlling power output in petrol engines is usually carried out by throttling the intake pipe, using throttle plate. Except at or close to wide-open throttle, the throttle provides the minimum flow areas in the entire intake system and has significant effect on the flow. At part-throttle operating conditions the throttle plate angle is in the 20 to 50° range and jets issue from open areas on either side of the throttle plate. These jets are not identical after passing the throttle plate. According to Liimata et al (1971), in carburetted fuel systems, the flow accelerates through the carburettor venturi and then divides on either side of the throttle plate. There is a stagnation point on the upstream side of the throttle plate. The wake of the throttle plate contains two vortices which rotate in opposite directions. The jets on either side of the wake (at part throttle) are at or near sonic velocity. There is little or no mixing between the two jets. Thus, if maldistribution of the fuel-air mixture occurs above the throttle plate, it is not corrected immediately below the throttle plate.

The mass flow rate through the throttle valve can be calculated from standard orifice equations for compressible flow based on the theory of fluid mechanic. In the case of pressure ratios across the throttle less than the critical value (below sonic flow), the mass flow rate is given by equation (3.2-1) (Taylor, 1985).

$$m_{th} = \frac{C_D A_{th} p_o}{\sqrt{RT_o}} \left(\frac{p_T}{p_o}\right)^{1/\gamma} \left\{\frac{2\gamma}{\gamma - 1}\left[1 - \left(\frac{p_T}{p_o}\right)^{(\gamma - 1)/\gamma}\right]\right\}^{1/2} \qquad (3.2\text{-}1)$$

where A_{th} is the throttle plate open area, p_o and T_o are the upstream pressure and temperature, p_T is the pressure downstream of the throttle plate (pressure at the minimum area), C_D is the discharge coefficient. For pressure ratios greater than the critical ratio (supersonic flow), the mass flow rate is given by equation (3.2-2) (Taylor, 1985).

$$m_{th} = \frac{C_D A_{th} p_o}{\sqrt{RT_o}} \gamma^{1/2} \left(\frac{2\gamma}{\gamma + 1}\right)^{(\gamma-1)/2(\gamma-1)} \qquad (3.2\text{-}2)$$

3.3 Air flow in intake manifolds.

Like other reciprocating internal combustion engines, air flow in the intake manifold of petrol engines occurs in a series of pulses, one going to each cylinder. The flow at the throttle will fluctuate as a consequence of the pulsed flow out of the manifold into the cylinders. At high intake vacuum, the flow will be continuously inward at the throttle and flow pulsations will be small. At wide-open throttle when the flow restriction at the throttle is a minimum, flow pulsations at the throttle location will be much more pronounced (Benson et al, 1974).

Under transient operating conditions, there is a slow response of air flow to the cylinders. For example, as the throttle is opened the air flow into the manifold increases with throttle opening. However, due to the finite volume of the manifold, the pressure level in the manifold increases more lowly than that would be the case if steady state conditions prevailed at each throttle position. Thus, the pressure difference across the throttle is larger than it would be under steady flow conditions. Because the air flow into each cylinder depends on the pressure in the manifold, this lags the throttle air flow. However, according to Aquino (1981), the lag of air flow is not very significant (some micro seconds).

The air flows to each cylinder of a multicylinder engine, even under steady operating conditions, are not identical because of differences of the lengths of the runners and branches of the intake manifolds and other geometric details of the flow path to each cylinder. Also, as each cylinder's intake flow commences, air is drawn from the branch and runner leading to the cylinder, the plenum, and the other runners and branches feeding the plenum, as well as past the throttle. Thus the air flow to each individual cylinder is affected by the detail of its own branch, the way that branch connects to the rest of the intake manifold, and the cylinder firing order (Chapman, M, 1979).

However, in conventional IC engines, these characteristics of air flow do not significantly affect air distribution between cylinders. According to Woods and Sag (1981), at high engine speed and load, variations in the average air mass flow rate to the individual cylinders are quite small, but at part load and under the changes of speed and load, the variations are higher, up to 2 to 3 percent.

3.4 Wall fuel film flow in intake manifolds.

The existence of a liquid fuel film on the wall of the intake manifold during engine operation has been confirmed by many investigators, such as Kay (1978), Nakajima et al (1978), Hosho et al (1985), Milton (1986), Hasson and Flint (1989), Nagaishi et al (1989), Abbass et al (1994) etc.

Wall fuel film flow is produced due to the impactions of fuel droplets on the walls of the induction system during transportation to the cylinders. The impactions depend on characteristics of fuel discharged from fuel nozzles and design characteristics of the induction system. Small droplets are more likely to pass through an inlet manifold without impaction, but larger fuel droplets are easier to impact onto manifold walls. It can be said that, the larger the droplets, the more the impactions occur. Trayser et al (1972) indicated that if the fuel droplets were produced at relatively small size (diameter of around 14 μm), then the proportion impacted on the flow passage walls in a 90 deg bend would vary between 56 and 100 per cent, depending on the mixture flow rate. If the droplet diameter was greater than 35 μm then total impaction would occur at all flow rate. Once the droplets impact, a film of fuel is formed and flows along the manifold walls. However, not all of the fuel droplets impacted on the wall of the induction system are kept in the film and flow into cylinders as liquid fuel, but most of fuel from the wall film evaporates and re-entrains to the main

stream (air stream) during flowing along the manifold (Brown and Ladommatos, 1991). If the vaporisation rate off the wall is sufficiently high, then a liquid film will not build up. Any liquid fuel film or pool on the manifold floor or walls is important because it introduces additional fuel transport processes (deposition, liquid transport, and vaporisation) which together have a much longer time constant than the air transport process. Thus changes of the air and fuel flow into each engine cylinder, during a change of engine load, will not occur in phase with each other unless compensation is made for the slower fuel transport.

The behaviour of wall fuel film flow in the intake manifold and its effect on mixture formation and fuel distribution in the engine cylinders depend on engine operating conditions, and design characteristics of the intake manifolds.

3.4.1 Wall fuel film flow during steady operations.

a) Characteristics of wall fuel film flow.

During steady operations, an equilibrium is established in the intake manifold of the engine; the quantity of the liquid fuel in the wall film is stable and the fuel film flows steadily along the manifold. Hayashi et al (1988) made measurements of film thicknesses in a carburetted engine running on methanol at full throttle using conductive probes and indicated that typical fuel film thicknesses range from 0.001 to 0.2 mm depending on engine speed, and vary around the circumference of the intake pipe: at low engine speed, the film thickness at the bottom of the pipe was up to five times greater than at the top, due to gravity. Using the same method, Kajitani et al (1990) also showed the film thickness being around 0.1 mm in a carburetted engine running at 2000 rpm and with an equivalence mixture ratio of 1.1. These results also agreed with the prediction made by Milton and Behnia (1989) who showed that the film builds up to about 1.2 mm by the end of a manifold of 80 mm length downstream of the throttle plate.

Hasson and Flint (1989) investigated effects of carburettor and manifold geometry on wall film quantities by determining the wall film flow rate, using a separator to remove the wall film from the core of the flow in the intake manifold of the engine operating at different mixture ratios and engine speeds. Four manifolds of different configurations were used in the investigations. The

results indicated that the wall film mass flow rate decreases with lean mixture. This is because the droplet deposition rate in the intake manifold is proportional to the concentration of droplets in the mixture; reducing fuel-air ratio (reducing the proportion of fuel in the mixture of fuel and air) means reducing the concentration of droplets in the mixture. This was also confirmed earlier by Hayashi et al (1984), and later by Abbass et al (1994) when investigating the effect of throttle configuration on wall fuel film flow rate. However, this characteristic is not very significant for studying engine performance because the range of fuel-air ratio of the mixture required at steady engine operating conditions is relatively small; the fuel-air ratio of the mixture supplied to the engines is then relatively stable at a certain value around stoichiometric (as mentioned in the previous chapter).

Increasing engine speed increases the wall film flow rate (Hasson and Flint, 1989) because a greater rate of fuel enters the induction system. However, the percentage of wall mass flow in relation to the total fuel mass flow entering the system decreases with the increase in engine speed. This is because at high engine speed, air velocity in the intake manifold is high, causing high turbulence of the flow, which leads to an increase in both the re-entrainment and evaporation rate of fuel from the wall film, while the rate of fuel entering the system does not vary linearly with engine speed. Hayashi,1984 and Abbass et al ,1994 also indicated similar results; Abbass further showed that the effect of air stream velocity on percentage of wall film flow rate in the manifold in relation to the total rate of fuel supplied is relatively small beyond the stream velocity of 100m/s. This can be seen in Figure 3.4-1 and Figure 3.4-2 based on experimental data.

A conclusion which can be drawn from the above experimental results is that the effect of fuel film flow on mixture formation at high engine speed is smaller than that at low engine speed. This also means that at higher engine speed or at higher air stream velocity in the manifold the conditions for mixture preparation is better. High stream velocity can be also reached at large throttle opening; however the opening position of the throttle plate also has another effect on fuel evaporation in general, and in particular on fuel film flow. The effect of the throttle opening on fuel film flow is found to be stronger in carburetted and single point injected engines than in port injected engines.

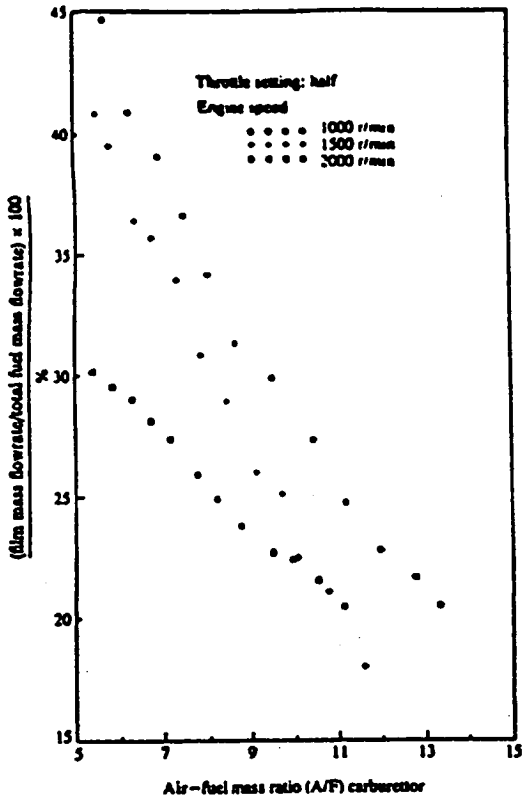

Figure 3.4-1. Effect of engine speed on per cent wall mass flow (Hasson and Flint, 1989).

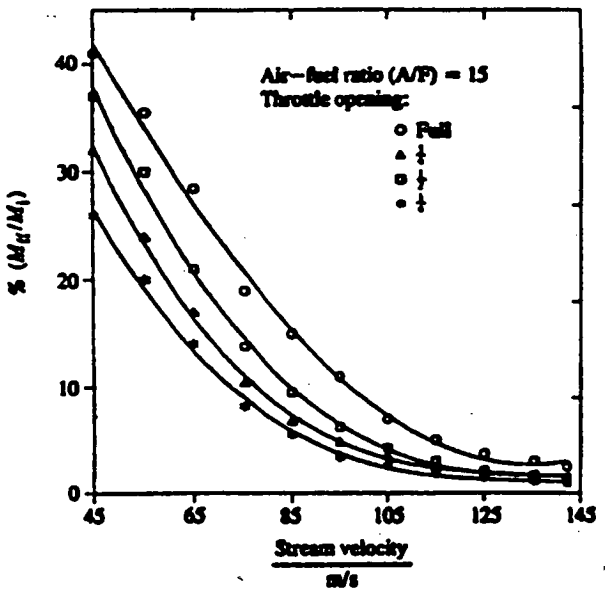

Figure 3.4-2. Effect of stream velocity on per cent wall mass flow (Abbass et al, 1994).

There have been some investigations on the effect of throttle plate on wall fuel film flow but the results vary slightly. Hasson and Flint (1989) showed that the percentage of wall fuel film flow has a maximum value at the half throttle position of the throttle plate, and then the fuel film quantity decreases successively with the engine operation at three-quarter throttle opening and full throttle opening because of increased stream velocity in the manifold. The lowest value of fuel film flow occurs during engine operation at a quarter throttle opening. The explanation for this may be that at small throttle opening, the stream of the fuel droplets from the carburettor impinges onto the throttle plate and then it is deflected as a liquid stream towards the manifold wall (the impingement and deflection of the fuel droplets are greatest at a quarter throttle opening). Near the tips of the throttle plate the liquid fuel is strongly sheared into small droplets due to the high velocity of the air and fuel vapour flowing through the throat of the restriction at small throttle openings. The small droplets are then re-entrained easily into the highly turbulent core, flowing down stream or evaporating. Moreover, at quarter-throttle opening operation, the manifold pressure significantly decreases, consequently the evaporation from the wall film is greater.

Abbass et al (1994) reached the same conclusion in the case of quarter-throttle operation. However, their experimental results contrast with Hasson as the throttle plate is further opened. Increasing the throttle opening increases the percentage of wall mass flow rate as indicated in Figure 3.4-3.

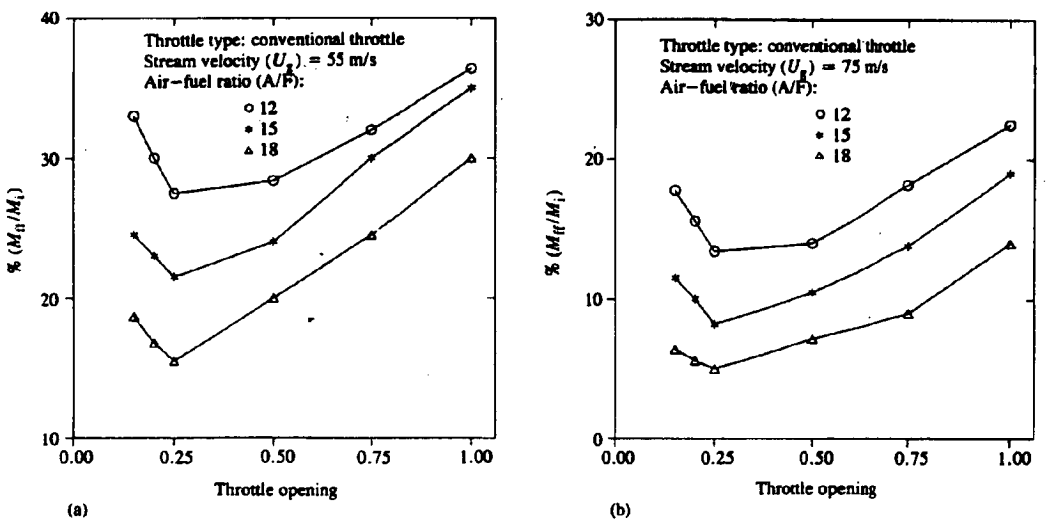

M_{ff} is fuel film mass flow rate

M_i is total mass flow rate of fuel supplied at the carburettor.

Figure 3.4-3. Wall mass flow versus throttle opening, (Abbass et al, 1994).

In fact, throttle openings can influence the fuel wall film in many ways. First, increasing the throttle opening leads to increasing the stream velocity in the manifold, which accelerates the evaporation and re-entrainment of the fuel from the wall film due to high turbulence of the stream, resulting in a decrease in film mass flow rate. However, the second effect of increasing throttle opening is that the shearing and re-entrainment of liquid fuel at the throttle decreases due to the decrease in the stream velocity at the large throttle opening. In addition, increasing throttle opening leads to a rise in the intake pressure, causing a relative decrease in fuel evaporation from the wall film and therefore an increase in fuel film flow rate. Depending on the design characteristics of the induction system and operating conditions of the engine, any of the factors above can have dominant effects on the wall film flow. That is why the results of experiments by the authors are found different.

Throttle plate itself also influences the rate of fuel film flow. At part throttle openings, a proportion of fuel sprayed into the stream usually impinges onto the throttle plate first, and then flows towards the tips of the throttle plate where some of the fuel can be atomised into smaller droplets owing to high stream velocity, but at larger throttle openings most of the fuel impinging on the throttle plate breaks up into large droplets and deposits on the wall of the manifold causing a large quantity of wall film. Abbass et al (1994) showed that in carburettors using a variable throttle for changing quantity of the mixture supplied to the engine, sprayed fuel is atomised better and the wall film flow rate is smaller than in the case of a conventional carburettor using throttle plate because the stream is not deflected to the manifold wall.

Configuration of the manifold also affects the wall film mass Flow rate because it influences the dynamic property of the stream. Hayashi et al (1984) and Hasson (1989) stated that increasing the length of the intake manifold leads to a decrease in the wall film mass flow rate. Wall mass flow rate in a straight manifold is smaller than in the manifold with a bend because in a straight manifold, fuel droplets sprayed from the fuel nozzle have less chance to impinge onto the wall of the intake manifold on the way to the intake port than they do in the case of a bend manifold.

Increasing inlet air temperature and manifold temperature decreases the quantity of wall fuel film significantly. Brown and Ladommatos (1991)

predicted that heating the inlet manifold to some temperature beyond the boiling point of the fuel can completely eliminate the fuel film.

In the case of port-injected engines, the wall film flow is strongly dependent on injection timing. Kajitani et al (1990) showed that the film thickness is around 0.1 mm at 100° crank angle before top dead centre (TDC) overlap, but decreases to 0.05 mm at 10° crank angle after TDC overlap. In general, wall film in the intake manifolds of port injected engines is significantly smaller than in carburetted engines and single point injected engines; according to Brown and Ladommatos, 1991, film thickness in this case is only about 0.002 to 0.04 mm.

b) Prediction of wall fuel film flow.

It is clear that the behaviour of liquid fuel film in the intake manifold is very complicated. It depends on so many factors, so establishing a mathematical model for calculating fuel film flow is not usually easy. Relying on different assumptions, some researchers established different models for prediction of fuel film flow.

With the assumptions that the intake manifold geometry is circular; and the liquid fuel film flows only on the lower half segment of the pipe and has a constant thickness, h, and that the liquid fuel film is a couette flow with no pressure gradient in the flow direction, and shear stresses at the gas stream and liquid film flow interface are equal, the mass flow rate and velocity of the fuel film can be calculated by equations (3.4-1) and (3.4-2) (Servati and Yuen, 1984).

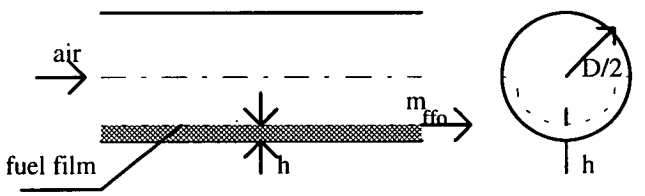

Figure 3.4-4 Model of wall film in the intake manifold.

The mass flow rate of the liquid fuel film flow:

$$m_{ffo} = \frac{\pi}{2} D \rho_f \frac{f_g \rho_g u_g^2}{4 m_f} h^2 \qquad (3.4\text{-}1)$$

The wall film mean flow velocity:

$$V_f = \left(\frac{m_{ffo} f_g \rho_g u_g^2}{2 p D m_f \rho_f}\right)^{1/2} \qquad (3.4\text{-}2)$$

Where m_{ffo} is mass flow rate of liquid fuel film flow.

D is intake manifold diameter.

ρ_f is liquid fuel density.

ρ_g is gas density in the intake manifold.

f_g is gas phase friction factor.

u_g is gas velocity.

μ_f is fuel viscosity

h is liquid fuel film thickness.

V_f is mean velocity of the film flow.

This model just simply expresses main factors influencing the fuel film, it is not convenient to be used to quantitatively determine fuel film flow because to do that , the thickness of the film must be measured first, needing an extensive experimentation.

A more precise prediction of fuel film flow can be made by solving the computer model established by Milton and Behnia (1989). The model consists of differential equations of conservation of energy, mass, and momentum of vapour, droplet, and liquid fuel film. In this model, fuel evaporation from the film is included. Therefore, it gives results that agree with experimental results.

c) Effect of wall fuel film on fuel distribution in the engine.

It is well-known that fuel maldistribution in petrol engines is inevitable. Compared with gaseous engines this problem is much more severe and it is believed to be mainly due to the wall fuel film flow in the intake manifold. In effect, wall fuel film flow can negatively affect fuel distribution in engines in several ways.

Firstly, it is accepted that total fuel delivered into a cylinder consists of fuel vapour, fuel droplets, and liquid fuel from the fuel film. Therefore, uneven flow rate of each form of fuel affects overall fuel maldistribution in the engines. Of these fuel forms, maldistribution of cylinder-to-cylinder wall fuel film flow is a major cause of mixture maldistribution between cylinders (Nightingale and Tsatsami, 1984). Nightingale and Tsatsami stated that uneven distribution of wall fuel film flow between cylinders is due to the inlet manifold design characteristics. That is the difference in shapes and lengths of the manifold leading to the cylinders; the cylinders that are closer to the carburettor (with shorter inlet pipe) receive more liquid fuel from fuel film than the others. In addition to this conclusion, Gardiner and Bardon (1986) indicated that different inclinations of the manifold runners also cause an uneven distribution of fuel film flow between cylinders due to gravitational effect of fuel. They also showed that reducing wall fuel film by improving fuel atomisation or heating inlet air and manifold significantly reduces fuel maldistribution between cylinders.

Secondly, the pulsations of the flow and non-identical conditions in different manifold runners can cause different rates of evaporation and re-entrainment of fuel from the fuel film to the air stream flowing to the different cylinders, causing fuel maldistribution between cylinders.

Moreover, wall fuel film entering cylinders will cause an inhomogeneity of mixture within individual cylinders because large liquid fuel droplets present in the cylinder do not have enough time to fully evaporate.

3.4.2 Wall film flow during transient operations.

a) Characteristics of wall fuel film flow during transient operations.

Wall fuel film quantity always varies during transient engine operations. According to Hires and Overington (1981), during engine acceleration there is a momentary increase in the volume of fuel deposition in the intake manifold as fuel film, causing a relative delay of fuel flow into the cylinders. The mechanism is that when fuel flow increases at the fuel nozzle of the carburettor with the increase in throttle opening, a portion of the fuel droplets first strikes the walls of the intake manifold, adhere there and remain in the form of liquid fuel film, and are thus held up for some time before evaporating, re-entraining

into the air stream or flowing into the cylinders. The delay of the liquid fuel film flow in the intake manifold causes a lean excursion of the mixture supplied to the engine. Mixture becomes momentarily leaner immediately after sudden throttle openings (Tanaka and Durbin, 1977, Hires and Overington, 1981, Aquino, 1981 and Taylor, 1985). Figure 3.4-4 indicates a transient air-fuel ratio excursion in the case of sudden opening of the throttle plate in throttle body injected engines. In the case of deceleration (sudden closing throttle plate), the situation is inverse, mixture becomes momentarily richer soon after sudden throttle closing.

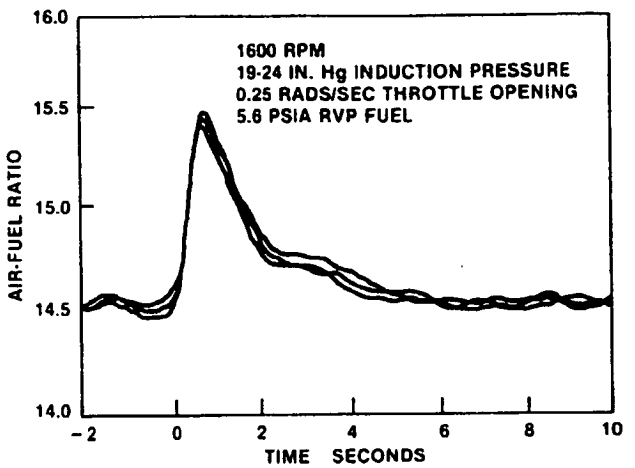

Fig. 3.4-4. Transient air fuel ratio for blended fuel in the case of sudden throttle opening. (Hires and Overington, 1981)

During engine start and warm-up, the temperature of the manifold wall and the air velocity are usually much lower than those during steady operations, so fuel evaporation and re-entrainment from the wall film are much lower. This leads to a larger rate of fuel accumulation in the wall film than the rate of fuel evaporation. The consequence is similar to the case of transient acceleration.

In injected engines, the delay in fuel entering the cylinders during transient operations is similarly found. Nagaishi et al (1989) showed that during acceleration a large proportion of the fuel injected from the injectors does not enter the cylinders, but remains on the walls of the intake system, increasing the fuel film quantity. The rate of fuel accumulation on the wall of the intake manifold as a film is strongly influenced by coolant temperature, intake pressure, and air velocity in the intake manifold. The experimental results show that increasing coolant temperature, air velocity or decreasing intake pressure leads to a significant decrease in the duration of fuel delay. The results for the

single point injection system seem to indicate that under conditions of low intake pressure, which corresponds to small throttle openings, fuel vaporisation and atomisation are promoted by high air flow velocity through the throttle valve. The nature of this is similar to that in carburetted engines.

In port-injected engines with direct fuel injection to the inlet valve, the amount of fuel delayed is very small compared with that in the case mentioned above.

In brief, during transient operating conditions (start, warm up, increase in load) most of the fuel discharged from the fuel nozzles is accumulated in the intake manifold, causing an increase in quantity of wall fuel film. This leads to the fact that fuel entering the cylinders decreases momentarily, and therefore air-fuel ratio becomes momentarily lean.

b) Mathematical models of wall fuel film flow during transient operations.

The fuel flow in the inlet manifold can be divided into two parts. One is the fuel vapour and fuel droplets suspended in the air stream, which flows together with the air stream in the middle of the inlet manifold. The other is the liquid film adhering to the inner surface of the inlet pipe, which flows slowly toward the cylinder dragged by the aspirated air (wall flow). The illustration of this is shown in Figure 3.4-5.

A simple model for determining the thickness of wall fuel film under a transient acceleration can be established based on the diagram in Figure 3.4-5 and the assumptions that the liquid fuel film has a constant thickness h in the circumferential direction of the circular inlet manifold, and the flow of fuel film has no pressure gradient in the flow direction and the flow is linearly proportional to the distance from the wall with the mean velocity V_f.

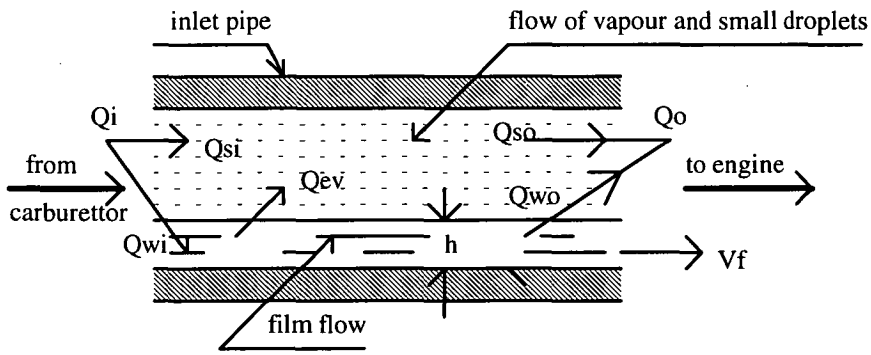

Figure 3.4-5 Fuel film flow model in inlet manifold.

We have

$$Q_i = Q_{si} + Q_{wi} \tag{3.4-3}$$

$$Q_o = Q_{so} + Q_{wo} \tag{3.4-4}$$

Where Q_i = total fuel flow rate at the inlet of the manifold.

Q_{si} = flow rate of vapour and droplet fuel at the inlet of the manifold.

Q_{wi} = liquid fuel film flow rate at the inlet of the manifold.

Q_o = total fuel flow rate at the outlet of the manifold.

Q_{so} = flow rate of vapour and droplet fuel at the outlet of the manifold.

Q_{wo} = liquid fuel film flow rate at the outlet of the manifold.

Obviously, under steady running conditions $Q_i=Q_o$, but under transient conditions, for example, during acceleration as mentioned previously, a part of fuel supplied, Q_i, is delayed in the manifold, increasing the thickness of the film. Hence, until the steady state is re-established, value Q_i is greater than Q_o.

While the fuel film flows along the inlet pipe, a part of the fuel will evaporate. Thus, we have

$$Q_{so} = Q_{si} + Q_{ev} \tag{3.4-5}$$

$$Q_{wo} = Q_{wi} + Q_{ev} \tag{3.4-6}$$

Where Q_{ev} is evaporation rate of fuel film.

Also, with the assumptions above, we can have

$$Q_{wo} = \pi D h V_f \tag{3.4-7}$$

Where D is the inner diameter of the inlet manifold.

h is the fuel film thickness.

V_f is the mean velocity of the fuel film flow.

Considering the mass balance of the liquid fuel film in the inlet manifold, we have

[liquid fuel flow into the manifold] = [liquid fuel stored in the film]

+ [liquid fuel flow out of the manifold]

+ [fuel evaporated from the film]

Assuming that the fuel film thickness after throttle movement termination at time t_o is h_o, and then the thickness of fuel film would increase to $h = h_o + dh$ during the time interval dt. Thus, we have

$$Q_{wio}\, dt = \pi DLdh + \pi DhV_{fo}\, dt + Q_{ev}\, dt \tag{3.4-8}$$

Where L is the length of the manifold.

subscript o denotes for the moment of the beginning of transient operation.

Combining equations (3.4-6), (3.4-7), and (3.4-8) gives:

$$\frac{dh}{dt} + \frac{1}{T}h = \frac{h_o}{T} \tag{3.4-9}$$

Where $T = \dfrac{L}{V_{fo}}$ is called a time constant.

Equation (3.4-9) describes characteristics of fuel film thickness and allows to determine the thickness of the fuel film as a function of time at a transient condition. To solve this equation, the thickness and mean velocity of the fuel film at the beginning or the end of the transient stage and the length of the pipe should be known.

With different assumptions, some authors presented different models for prediction of fuel film flow. According to Servati and Yuen (1984) with the assumptions that the liquid fuel film only flows on the lower half segment of the pipe and has a constant thickness, the thickness and velocity of the liquid fuel film in the intake manifold during transient operating conditions, with the throttle plate opened from position 1 to position 2, corresponding to the thickness of the fuel film increasing from h_1 to h_2 can be determined by the following equations.

The thickness of the fuel film at time t:

$$h(t) = h_2 \frac{1 - C_1 e^{\frac{-2V_{f2}}{L}t}}{1 + C_1 e^{\frac{-2V_{f2}}{L}t}} \tag{3.4-10}$$

The velocity of liquid fuel film:

$$V_f(t) = V_{f2}\, \frac{1 - C_1 e^{\frac{-2V_{f2}}{L}t}}{1 + C_1 e^{\frac{-2V_{f2}}{L}t}} \tag{3.4-11}$$

The film mass flow rate:

$$m_{ffo}(t) = m_{ffo_2}\left(\frac{1 - C_1 e^{\frac{-2V_{f2}}{L}t}}{1 + C_1 e^{\frac{-2V_{f2}}{L}t}}\right)^2 \qquad (3.4\text{-}12)$$

Where $C_1 = \frac{h_2 - h_1}{h_2 + h_1}$

h_1 is initial steady fuel film thickness.

h_2 is final steady fuel film thickness.

L is intake manifold length.

t is time (from the beginning of opening throttle plate).

V_{f2} is final steady fuel film thickness.

m_{ffo_2} is mass flow rate of liquid fuel film at a steady condition corresponding to position 2 of the throttle plate.

To predict velocity and mass flow rate of liquid fuel film by the above equations, the wall film thickness should be measured first. In practice, fuel film thickness varies along the intake manifold and around its circumference, depending on manifold design characteristics and operating variables. Therefore, the calculated value by the above equations may be different from the true value.

3.4.3 Summary.

The following conclusions can be drawn from the above analysis of wall fuel film flow in petrol engines.

1) There is always a large amount of liquid fuel present in the intake manifold of the engine as wall fuel film. Velocity of fuel film ranges from 40 to 150 mm/s and fuel film thickness from 0.001 to 1.2 mm, depending on the engine operating conditions and design characteristics of the induction system.

2) Wall film quantity in the intake manifold of carburetted engines is much more than in port-injected engines.

3) Under steady operating conditions, the wall film quantity increases with engine speed and load, but decreases with increasing engine temperature

(however, the effect of engine temperature on fuel film quantity has not been experimentally investigated). The wall film flow rate is also strongly dependent on the manifold configuration. It is greater in manifolds with bends than in straight manifolds.

4) Wall fuel film flow may be the main causes of fuel maldistributions in the engines.

5) During transient operating conditions, the wall film quantity changes, causing transient fuel air-ratio excursions (lean excursions during engine start, warm-up, and acceleration; and rich excursions during engine deceleration).

6) The effective methods to reduce fuel film quantity and its negative effect on engine operations are heating manifold walls and improving fuel atomisation.

3.5 Fuel droplets in intake manifolds.

Fuel droplets are always present in the intake manifold of the engines. They are formed from the atomisation of fuel jets sprayed into the air stream, the secondary atomisation of fuel at the throttle plate in the case of part load, or the re-entrainment of the fuel film during flow toward the cylinders. With carburettor and throttle body injection systems, fuel supplied to the induction system is atomised as it enters the air stream. In the carburettor venturi this occurs as the fuel-air emulsion from the fuel jets enters the high velocity air stream. With an injector, the velocity of the liquid jet as it exits the nozzle is high enough to shatter the flowing liquid, and its interaction with the coaxial air flow further atomises the fuel. Typical droplet size distributions are not well defined; size would vary over the load and speed range. Droplet diameters is found in the range of 5 to 250 μm (Fraidl, 1987). However, droplet diameters in the 25 to 100 μm range are usually assumed to be representative; of them, distributions of small and large droplet sizes are small.

Liquid fuel drops, due to their density being many times greater than that of the air, will not exactly follow the air flow. Droplet impaction on the walls may occur as the flow changes direction, and the greater inertia of the droplets causes them to move across the streamlines to the outer wall. Deposition on the manifold floor due to gravity may also occur.

3.6 Fuel evaporation in intake manifolds of petrol engines.

3.6.1 Introduction.

As mentioned earlier, the objective of mixture preparation process is to create a homogeneous air-fuel mixture and equally distribute it into the cylinders of the engine. Therefore, fuel evaporation in the intake manifold is a determinant factor for good mixture formation.

The evaporation of fuel in the intake manifolds of petrol engines occurs in complicated conditions. It takes place in a non-steady turbulent two-phase flow of air and fuel, and from both fuel film and fuel droplets during transportation to the cylinders. Fuel evaporation rate depends on design characteristics of the induction system and engine operating conditions.

In practice, not all of the fuel discharged from fuel nozzles can fully evaporate in the intake manifold during transportation to the cylinders, but some liquid fuel enters the cylinders and continues to evaporate until the end of the engine cycle. For example, by measuring air to fine-airborne-fuel ratio of the mixture supplied by the carburettor and air fuel ratio of the intake mixture entering each cylinder of a four-cylinder engine running at steady condition of 2500 rpm, Collins (1969) reported that an overall 69% of the petrol supplied is vaporised before entering the cylinders (at intake ports) at part load and 81% at full load.

Pao (1982) measuring the proportions of fuel forms by means of calorimetry and sampling probe techniques showed a similar result as the Collins's report. Under steady operating conditions, on passing the intake port of the cylinders, fuel vapour and fine fuel droplets represent 65 to 70%, small and large fuel droplets represent 30 to 35% of the total fuel supplied. However, these proportions vary with the running conditions.

Under transient conditions, the proportion of each fuel form entering the cylinders differs markedly from the data above, and varies continuously during operations before reaching a value at steady conditions. During warm up, the measurement results of Pao (1982) showed that the proportion of vaporised fuel increases with time. The proportion of large fuel droplets decreases, while the proportion of small fuel droplets fluctuates before decreasing to a steady state.

Theory and practice show that it takes some time for fuel to fully evaporate while the time available for fuel to evaporate in engines is very short (equal to the period of time for one engine cycle), so it is hard to get fully vaporised fuel in the cylinders by the time of ignition if large fuel droplets and net liquid fuel from the fuel film are introduced into the cylinders. This cause an inhomogeneous mixture in the cylinders, and has negative effects on the engine performance. In cylinders some fuel droplets cannot completely burn, and some continue to evaporate after the passage of the flame front, leading to an increase in CO and HC emissions and a decrease in engine efficiency and power output. As a result, fuel introduced into cylinders should be as much in the form of vapour and fine droplets as possible.

According to Winklhofer et al, 1992, in conventional petrol engines, by improving conditions of mixture preparation to get a good atomisation and evaporation of fuel in the intake manifold, most of the fuel supplied into the cylinders can fully evaporate by the time ignition occurs, and therefore good quality of combustible mixture in the engines can be obtained.

3.6.2 Mathematical models.

Both, the fuel droplets and the wall fuel film in the intake manifold of petrol engines evaporate during transportation to the cylinders.

Initial droplet sizes of the fuel sprayed from a nozzle vary in a certain range, depending on the method of spray and the size of fuel nozzle. The distribution of size is very difficult to experimentally determine. Assuming that initial droplet sizes produced by a nozzle of a carburettor are identical, it can be determined from equation (3.6-1) established by Ingebo and Foster (1957). The equation correlates the average droplet diameter with the size of the nozzle and air velocity at the fuel discharge area as follows.

$$D_O = 3.9\, d_O \left(\frac{We}{Re}\right)^{0.25} \qquad (3.6\text{-}1)$$

Where D_O is the initial volume-mean droplet diameter.

d_O is the diameter of the nozzle.

We is Weber number.

Re is Reynolds number based on d_O.

For the evaporation of a spherical liquid droplet in a moving gas stream, Sjenitzer (1962) presented an equation written as

$$\frac{d(y^2)}{d\theta} = -E[1 + A_o\ (zy)^{0.5}] \qquad (3.6\text{-}2)$$

Where $E = 8M_L\ D_G\ \Delta p / 9\eta_G\ RT_L$

$A_o = 0.30\ S_c^{0.33}\ \mathrm{Re}_o^{0.50}$

$z = (Va - V)/Va$ = Reduced relative velocity of droplets, depending on the time and can be determined from the Equation (3.3-3).

$$\frac{dz}{d\theta} = -2.25\mathrm{Re}_o^{0.16}\ z^{1.16}\ y^{-1.84} \qquad (3.6\text{-}3)$$

$y = D/D_o$ = Reduced diameter of droplets.

D_o = Initial diameter of droplet (m)

D =Diameter of droplet at any time (m)

$\theta = 9\eta t/\rho_L\ D_o^2$ = Reduced time

M_L = Molecular weight of liquid (kg/kmol)

D_G = Diffusivity in gas phase (m^2/sec)

Δp = Difference between vapour pressure of droplet and partial pressure of liquid in gas phase (N/m^2)

η_G = Dynamic viscosity of gas phase (kg/ms)

η = Dynamic viscosity of liquid phase (kg.ms)

R = Gas constant =8315 J/kmol K

T_L = Wet bulb temperature of liquid droplets (K)

S_C = Schmidt number in the gas phase

Re_o= Initial value of Reynolds number

t = Absolute time (sec)

ρ_L = Density of liquid phase (kg/m^3)

V = Absolute velocity of droplets (m/s)

V_a = Constant velocity of gas phase (m/s)

Rao and Lefebvre (1976) investigated evaporation characteristics of aviation kerosene sprays injected from a swirl-type, pressure atomisers into a flowing air stream in a constant area duct at atmospheric pressure and presented the following empirical expression for the rate of fuel evaporation.

$$\frac{N}{100-N} = 3.37\times10^{-6}\left[\frac{T_a}{1000}\right]^{4.32}\left[\frac{V_a}{100}\right]^{1.71}\left[\Delta P_f\right]^{0.56}\left[FN\right]^{-4.32}\left[L\right]^{1.57} \qquad (3.6\text{-}4)$$

Where N is percentage of spray evaporated

L : axial distance downstream of fuel injector, m

P : pressure, N/m^2

T_a : air temperature, K

V_a : air velocity, m/s

FN : atomiser flow number, $(litres/hr)/(N/m^2)^{0.5}$

ΔP_f : atomiser pressure drop, N/m2; higher atomiser pressure drop produces smaller mean droplet size.

ΔT : temperature difference between drop and air, K.

Equation (3.6-4) indicates that spray evaporation rates increase with increase in air velocity, air temperature, fuel injection pressure, axial distance from the injector and with reduction in atomiser flow number.

Equations (3.6-2) and (3.6-4) basically express evaporation rates of fuel spray in experimental conditions (mainly from fuel droplet) and allow us to understand characteristics of fuel evaporation and factors affecting the rate of fuel evaporation from droplet.

Fuel evaporation rates from fuel film on the walls of the intake manifold can be predicted by analogy with measured heat transfer rates. According to the theory of heat and mass transfer, if the heat transfer coefficient has been measured and written in the form:

$$Nu = C\,\mathrm{Re}^a\,\mathrm{Pr}^b \qquad (3.6\text{-}5)$$

Where Nu is Nusselt Number

Re is Reynolds Number

Pr is Prandtl Number

C, a, b are constants.

then the dimensionless mass transfer coefficient is by analogy:

$$\frac{h_D\, l}{\rho D} = C\,\mathrm{Re}^a\ Sc^b \qquad (3.6\text{-}6)$$

Where the values of a, b, and C in equations (3.6-5) and (3.6-6) are the same,

h_D is convective mass transfer coefficient (kg/m^{2}s)

l is diameter of the manifold (m)

ρ is density of air-vapour mixture (kg/m^3)

D is mass diffusion coefficient for fuel vapour in the mixture (m^2/s)

Sc is Schmidt number.

The mass flow rate of fuel evaporation from the fuel film on the surface of the manifold is given by:

$$\dot{m}_v = h_D \; AB \text{ (kg/s)} \tag{3.6-7}$$

Where $\dot{m}_v$ is mass flow rate of fuel evaporation from the fuel film

A is heat and mass transfer area (m^2)

$B = \dfrac{m_{fw} - m_{f\infty}}{1 - m_{fw}}$ is mass transfer driving force

m_{fw} and $m_{f\infty}$ are mass fraction of fuel vapour in air-vapour mixture at the wall and in the mainstream respectively.

However in this model, measurement of heat transfer rate between manifold wall and air stream and determination of constants *C, a, b* in equation (3.6-5) require extensive experimentations.

There are some mathematical models for calculating fuel evaporation rates from fuel droplet and fuel film in the intake manifold of petrol engines, which reflect more accurately the nature of fuel evaporation. Boam and Finlay (1979) and Milton and Behnia (1989) established numerical models of carburetted and single-point fuel systems, in an unbranched manifold with specific consideration of the requirements necessary for studying the liquid/vapour fuel proportion entering the cylinder, and the behaviour of fuel evaporation during transient operation. According to Milton and Behnia, droplet evaporation and wall film evaporation are expressed by the following equations.

$$\frac{d\dot{m}_{de}(j)}{dx} = -\pi \frac{N}{V_d} D_d^2 \beta_d(j)[p_{sd}(j) - p_v(j)] \tag{3.6-8}$$

$$\frac{d\dot{m}_{fe}(j)}{dx} = -S_{gf} \beta_f(j)[p_{sf}(j) - p_v(j)] \tag{3.6-9}$$

Where $\dot{m}_{de}(j)$ and $\dot{m}_{fe}(j)$ are rate of droplet evaporation and film evaporation of fuel component *j*, respectively (kg/s).

N is the number of droplets per time at a cross-section

V_d is droplet velocity (m/s)

D_d is droplet diameter (m)

$\beta_d(j)$ and $\beta_f(j)$ are the mass transfer coefficients of fuel component *j* (kg/m^2s)

$p_{sd}(j)$ and $p_{sf}(j)$ are the saturation vapour pressure of component *j* at droplet and film respectively (N/m^2).

$p_v(j)$ is the partial pressure of the vapour of component j (N/m^2)
x is the distance from the fuel nozzle along the manifold (m)
S_{gf} is the width of the film at a cross-section of the manifold (m).

Equations (3.6-8) and (3.6-9) are solved together with a system of differential equations expressing conservation of mass, conservation of energy, and conservation of momentum of air, fuel vapour, fuel droplets, and fuel film in the intake manifold.

In the case of port-injected engines, Brown and Ladommatos (1991) presented models for calculating droplet evaporation and wall-film evaporation in the intake manifold as flows.

Droplet mass evaporation rate:

$$\dot{m}_{L,s} = 4\pi r_s D_{m,s} \rho_{m,s} [1+0.3(Re)_d^{1/2}(Sc)^{1/3}] ln(B+1) \quad (3.6\text{-}10)$$

Where $\rho_{m,s} \approx \frac{p_{man}}{R_f T_{L,s}}$

$B = \frac{Y_{f,s} - Y_{f,b}}{1 - Y_{f,s}}$ is the Spalding mass transfer number.

Wall-film evaporation rate:

Wall-film evaporation rate when the inlet valve is open is calculated from equation (3.6-11):

$$\dot{m}_{F,s} = A_F \left(\frac{K_{F,s}}{R_f T_{F,s}} \right) (p_{sat,s} - p_{p,f}) \quad (3.6\text{-}11)$$

Where $K_{F,s} = 0.023 (Re)_{man}^{0.8} (Sc)^{0.4} \left(\frac{D_{m,s}}{d_{man}} \right)$ is mass transfer coefficient.

While the inlet valve is closed, wall-film evaporation rate is calculated from equation (3.6-12):

$$\dot{m}_{F,s} = A_F D_{m,s} \rho_{m,s} \left(1 - \frac{p_{p,f}}{p_{man}}\right)\left(1 - \frac{p_{sat,s}}{p_{man}}\right) \quad (3.6\text{-}12)$$

Nomenclature for equations (23-11) and (3.3-12) is below.

$\dot{m}_{L,s}$: mass evaporation rate at droplet surface (kg/s)
r_s : radius of droplet (m)

$D_{m,s}$: diffusivity at droplet surface (m^2/s)
$\rho_{m,s}$: density of air-fuel mixture at droplet surface (kg/m^3)
$(Re)_d$: Reynolds number based on droplet diameter
Sc : Schmidt number
p_{man} : manifold pressure (N/m^2)
R_f : specific gas constant of fuel vapour (J/kmol K)
$T_{L,s}$: temperature at droplet surface (K)
$Y_{f,s}$: mass fraction of fuel vapour at droplet surface
$Y_{f,b}$: mass fraction of fuel vapour at bulk mixture condition
$\dot{m}_{F,s}$: mass evaporation rate from fuel film surface (kg/s)
A_F : surface area of fuel film (m^2)
$T_{F,s}$: temperature at fuel film surface (K)
$p_{sat,s}$: saturation pressure at fuel film surface (N/m^2)
$p_{p,f}$: partial pressure of fuel vapour (N/m^2)
$(Re)_{man}$: Reynolds number based on manifold diameter
$D_{m,s}$: diffusivity of air-fuel vapour mixture at film surface (m^2/s)
d_{man} : manifold diameter (m).

3.6.3 Characteristics of fuel evaporation in petrol engines

a) Fuel evaporation in carburetted and single point injected engines.

A carburetted fuel system and a single point injected fuel system of petrol engines are similar in that fuel is introduced at one point before throttle plate. Therefore, the characteristics of fuel evaporation downstream in the intake manifold in these systems are similar. This section analyses characteristics of fuel evaporation in intake manifolds and factors influencing it.

Effect of droplet size on fuel evaporation in the intake systems.

Theory of droplet evaporation shows that the evaporation rate of a given amount of fuel increases with reducing initial droplet size. Initial droplet size of the fuel sprayed from the nozzle of a carburettor ranges from 5 μm to 250 μm (Fraidl, G. K. 1987), depending on the diameter of the nozzle and velocity of the air stream in the venturi of the carburettor. Distribution of droplet sizes are very difficult to determine practically. However, distribution functions show that proportions of small and large droplets are usually small.

After being formed, fuel droplets are dragged into the air stream and travel downstream through the throttle. The throttle plate can play the role of an

atomiser to atomise fuel droplets into smaller ones in such a way that the fuel droplet stream impinges onto the throttle plate and then is deflected to the restriction throttle where droplets are sheared by the high velocity of the stream. However, this is not usually the case. In theory, small droplets of 5-10 μm can be formed at the throttle, but some of these may migrate onto the wall and coalesce to form liquid fuel, from which they may subsequently be re-entrained as much larger droplets. Some large droplets may also be formed immediately after the throttle plate due to the combination of some smaller droplets at the throttle plate. The droplet size may thus increase with distance from the throttle. Therefore, droplet size of fuel downstream also varies in a large range and has effects on characteristics of fuel evaporation and transportation. However , the formation of larger droplets due to throttle plate is not significant, so the change of droplet size can be assumed to be due only to evaporation and their size to be identical without a significant penalty (Boam and Finlay,1979, and Milton and Behnia, 1989).

Clearly, the smaller the droplet size, the greater the rate of evaporation because the evaporation and heat transfer area of fuel droplets of smaller size is greater than that of greater size. The higher heat transfer to fuel droplets causes fuel droplets to reach higher temperature, which increases evaporation rate since the vapour pressure of the fuel droplets is extremely sensitive to the droplet temperature. This was confirmed by Yun et al (1976), Boam and Finlay (1979), and Brown and Ladommatos (1991).

Evaporation occurs from both fuel forms, droplets and film in the intake system from the venturi to the intake port. Yun et al (1976) stated that a small proportion of fuel supplied evaporates in the venturi (2-8 %) depending on the initial droplet size. Figure 3.6-1 shows the results of their prediction at certain running conditions.

The results showed that the effect of droplet size is exponential such that smaller droplets are more sensitive to the size change than larger droplets. With droplet size of 100μm, the proportion of fuel evaporation in the venturi is only about 2.5%, but it will increase to more than 8.0% if droplet size is reduced to 25μm. Although an improvement in fuel spray from fuel nozzle in the venturi for reducing initial droplet size does not increase the fuel evaporation in the venturi very much compared with the total fuel supplied, it will be an important factor increasing the fuel evaporation rate downstream of the throttle plate.

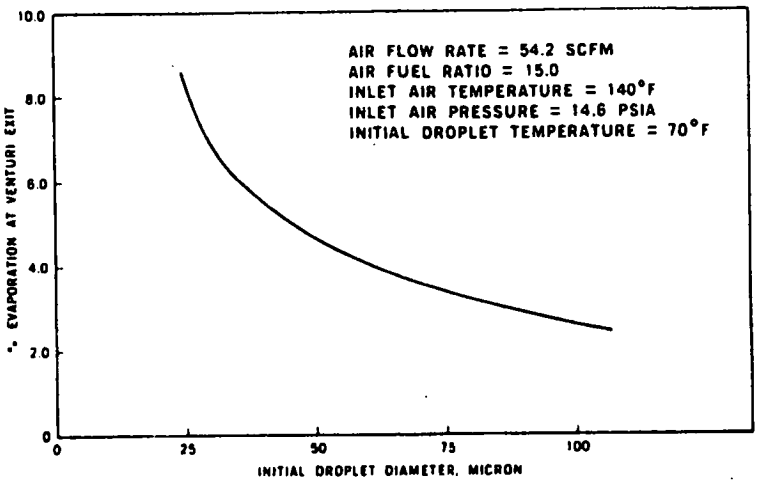

Figure 3.6-1. Effect of droplet size on fuel evaporation at venturi exit (Yun et al, 1976)

Evaporation of fuel downstream of the throttle plate in the intake system (between throttle plate and intake port) is very important for mixture formation. The percentage of fuel evaporation in this region increases with the distance from throttle plate because the amount of fuel evaporated increases with the time available for evaporation.

Theoretically, the effect of droplet size on fuel evaporation in this region is similar to that in the venturi. The evaporation is also affected by other variable parameters such as configuration and opening position of the throttle plate, and engine running conditions. The throttle plate can act as an atomiser to break up fuel droplets into smaller droplets, but secondary atomisation only occurs at part load. In the case of full load, the throttle plate is wide open and the high shearing stresses causing droplet break-up do not exist. Therefore, droplet size after the throttle plate can vary in a large range, depending on operating conditions. Fraidl (1987) investigated systematically the spray quality of different mixture preparation systems and showed that for carburetted fuel systems and single point injection systems, at part load the proportion of droplets of size from some μm to 50 μm is highest, but at full load most droplets are the size of 50 to 250μm.

Boam and Finlay (1979) showed that percentage of fuel evaporation increases with the distance from the throttle plate along the intake manifold. Without secondary atomisation, meaning large droplet size, (corresponding to full throttle opening), the percentage of fuel evaporation is smallest as indicated in Figure 3.6-2.

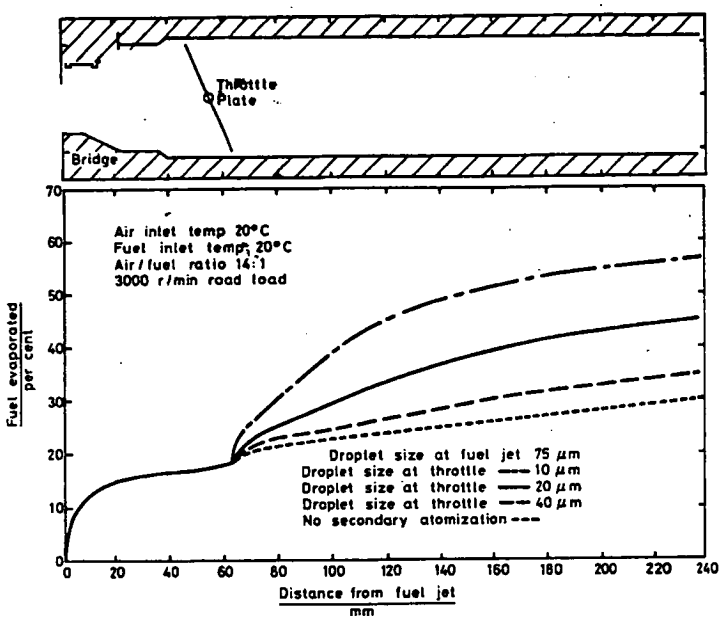

Figure 3.6-2. Effect of droplet size on fuel evaporation downstream, (Boam and Finlay, 1979)

Effect of mixture heating.

Obviously, heat is one of the active factors accelerating liquid evaporation. Therefore, adding heat to the mixture is an effective way to increase fuel evaporation rate. There are three ways to heat mixture. These are: heating the liquid fuel before its entry to the system (carburettor or injector), heating the air before its entry to the intake system, and heating the manifold wall downstream of the throttle.

- *Effect of inlet air heating.*

Heating the inlet air has a positive effect on droplet evaporation, especially when secondary atomisation is applied. This is because heat is transferred to the fuel droplets directly from the air stream, and fuel in smaller droplets has a larger total heat transfer surface area. The effect is seen both upstream and downstream of the throttle plate (Boam and Finlay, 1979).

Similarly, Rao and Lefebvre (1976) investigated experimentally the evaporation characteristics of aviation kerosene fuel injected into air streams at ambient pressure and indicated that an increase in air temperature raises fuel evaporation rates considerably at all velocities, however it is less effective in increasing vaporised fuel at high temperatures than at low ones. For example,

the change in air temperature at 300 K is twice as effective as that at 425 K for increasing fuel evaporation rate.

Heating the inlet air reduces air density effects on the metering characteristics of the carburettor but it also reduces air volumetric efficiency of the engine.

- *Effect of fuel heating.*

Although heating fuel before introducing it into the carburettor or injector is known to be a direct way to add heat to the fuel in the intake system for accelerating fuel evaporation, it is not widely applied in practice. Hohsho et al (1985) indicated that heating the liquid fuel before its supply into the manifold significantly reduces the delay in fuel entering cylinders at transient running conditions. This indicates an improved fuel evaporation by direct heating. However, heating the liquid fuel beyond the boiling point of the fuel can lead to a stoppage of fuel supply in the fuel metering system of the carburettor because evaporated fuel in the system then causes vapour lock.

- *Effect of manifold heating.*

Manifold heating is widely applied in petrol engines to improve fuel evaporation in the intake system. It can be done by using either exhaust gas or hot coolant from the engine. This is an effective way to add heat to the fuel film to accelerate the wall film evaporation.

The increase in fuel evaporation by wall heating is mainly due to fuel evaporation from fuel film. Milton and Behnia (1989) indicated that at the throttle opening of 15°, the heating of 100 kW/m^2 of manifold wall substantially reduces the film thickness at the end of the manifold to about 50% because of evaporation.

Boam and Finlay (1979) indicated that manifold heating is the best effective method of heating to improve fuel evaporation. This is illustrated in figure 3.6-3 that presents the effect of three methods of heating on percentage of fuel evaporation. The figure shows the prediction of fuel evaporation in each of the three methods with the addition of 100 W of heat at part load.

As can be seen from the Figure, the addition of 100W heat to the liquid fuel before its supply to the carburettor, which results in a fuel temperature at entry of 56°C, provides a very rapid flashing off of the lighter fractions of the fuel;

later, however, evaporation is slowed as the remainder become heavier. Adding heat to the inlet air takes much longer to have any effect as the heat then has to be transferred by convection to the liquid fuel before it can significantly affect evaporation. Wall heating provides a direct input of heat to the wall film and therefore helps fuel film evaporation significantly because most of the less volatile fuel fractions, which are difficult to vaporise without a heat addition, are usually present on the wall film.

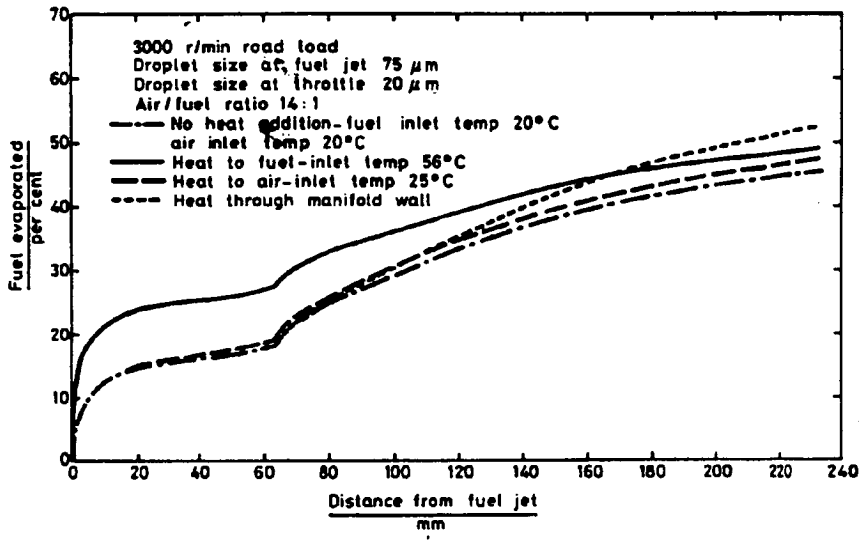

Figure 3.6-3. effect of method of heating on fuel evaporation, (Boam and Finlay, 1979)

Effect of engine speed and load.

Reducing load, which means reducing throttle opening, increases the degree of the secondary atomisation and therefore increases fuel evaporation. This effect only occurs beyond the throttle plate.

Investigating the effect of throttle opening on fuel evaporation, Milton and Behnia (1989) showed that the evaporated quantity of fuel after the throttle plate increases rapidly for the smallest throttle opening because of the large pressure drop at the throttle and the high degree of secondary atomisation. This can be seen in figure 3.6-4.

Rao and Lefebvre (1976) stated that at ambient temperature fuel evaporation in the intake manifold increases with the increase in air velocity. However, at part load percentage of fuel evaporation is greater at lower engine speed than at higher engine speed because at low engine speed convection around the fuel

droplets acts of a greater time that at high engine speed (Boam and Finlay, 1979).

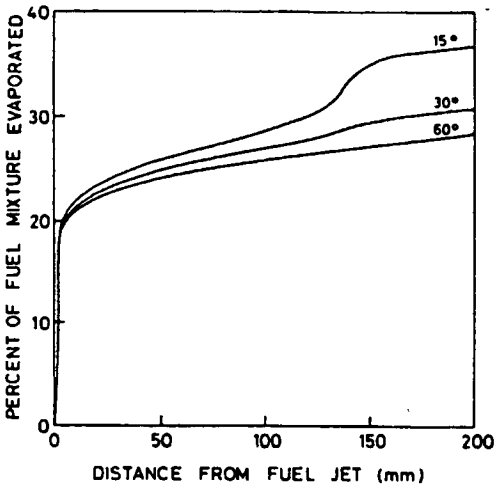

Figure 3.6-4. Effect of throttle plate opening angle on fuel evaporation (Milton and Behnia)

Effect of fuel characteristics.

The main property of fuel affecting evaporation is fuel volatility, whose effect on mixture formation has been discussed in Part 1. It is clear that under the same conditions, evaporation rate of fuel with higher volatility is higher than that of fuel with lower volatility.

b) Fuel evaporation in the intake manifold of a port injected engine.

In port injected engines the injectors are usually located close to the inlet valves, so the wetted length of the manifold is relatively short. The variation in the fuel temperature and fuel components along the manifold wall are therefore negligible. Consequently, the characteristics of fuel evaporation in the intake manifold of port-injected engines are very different from those of carburetted engines. This was theoretically investigated by Brown and Ladommatos (1991). They used heptane as the engine fuel in their study.

The droplet evaporation in the intake manifold was seen very small, representing less than 5 per cent of the injected fuel mass. Raising inlet air temperature has a very small effect on droplet evaporation. For example, raising the manifold air temperature from 20 to 100°C only increases the droplet and film evaporation by 2 to 3 per cent. This is because the time of

transportation of the fuel droplets in the intake manifold is relatively short due to the direct injection of fuel to the intake port.

Raising the wall temperature has a significant effect on fuel evaporation, particularly on film evaporation as shown in Figure 3.6-5.

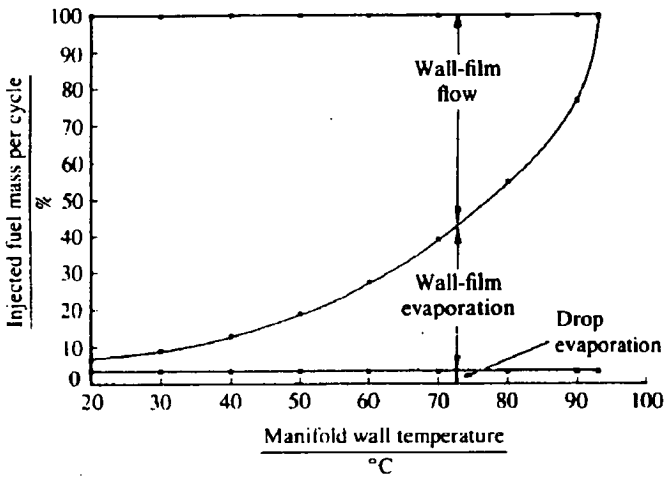

Fuel: haptane injected at 25 C
Injection timing end of compression
Droplet size: 0.0 80 mm
Engine speed: 1200 rpm
Engine load: 50 Nm

Figure 3.6-5 Effect of manifold wall temperature on fuel evaporation in port injected engines, (Brown and Ladomatos,1991)

As seen from the figure, at the wall temperature of 20°C (when engine starts) most injected fuel builds up on the manifold wall as wall fuel film (about 90%). Wall film evaporation rises to about 60% when the wall temperature reaches the boiling point of heptane at 81°C at manifold pressure. Beyond this point the film evaporation increases rapidly.

Droplet evaporation is very little affected by wall heating, the curve of drop evaporation is approximately a horizontal line. This is because heat transferred from the wall to the stream does not affect droplet evaporation very much due to limited time.

As in carburetted engines, fuel evaporation in port-injected engines is also strongly affected by droplet size. The result of Brown's investigation indicates that the effect of droplet size on fuel evaporation depends on engine temperature (or manifold wall temperature). In a hot engine, droplets of very small size (less than 40μm) can evaporate completely before the end of the engine cycle. Larger droplets usually impinge onto the manifold wall and

evaporate due to heat addition from the wall. According to Fraidl (1987), most droplets in multi-point injection systems are more than 50μm; therefore in this system with hot coolant, it can be concluded that fuel evaporation is almost entirely controlled by film evaporation. In contrast to the case of a hot engine, in a cold engine wall film flow represents a main part of fuel injected.

Injection timing and direction of fuel spray also have an effect on fuel evaporation. Nagaishi et al (1989) and Winklhofer et al (1992) stated that injecting fuel onto the surface of the intake valve improves fuel evaporation significantly, because the temperature of the intake valve is highest at intake port due to being heated directly by combustion and the heat then accelerates the evaporation of the wall film.

3.6.4 Summary.

The following conclusions can be drawn from the above analysis.

1) The evaporation rate of fuel increases with fuel temperature, inlet air temperature, and manifold wall temperature (or engine temperature).

- Raising the initial fuel temperature is an important factor to increase evaporation, particularly it is the most effective way of promoting evaporation early in the intake manifold.
- The inlet air temperature has a smaller influence on fuel evaporation from either fuel film or the fuel droplets than initial fuel temperature.
- Heating the manifold wall is the most effective method of achieving maximum fuel evaporation in the manifold for a given heat input in both carburetted engines and fuel injected engines. Therefore, it can be concluded that fuel evaporation in the intake manifold of petrol engines is mainly controlled by evaporation from wall film.

2) Fuel droplet size or secondary atomisation of fuel at throttle plate in carburetted engines and throttle body injected engines has a powerful influence on evaporation; that is, reducing fuel droplet size considerably increases the fuel evaporation rate.

3) The effects of other parameters such as pressure, velocity, and the properties of fuel and air on fuel evaporation in the intake manifold appear to be less significant than the effects of the parameters mentioned in (1) and (2).

4) Fuel evaporation is a determinant factor contributing to good mixture formation in petrol engines.

3.7 Mixing of fuel and air in intake manifolds of petrol engines.

3.7.1 Introduction.

Mixing of fuel vapour and air is an important factor in creation of a homogeneous mixture in petrol engines, which is always an objective of mixture preparation systems. In practice, creation of a completely homogeneous mixture of fuel and air is impossible in the conventional petrol engines. However, if attempts are made to increase the degree of mixing, an approximately uniform mixture can be obtained.

According to Yu (1963), mixture non uniformity results from one or more of the following phenomena. The first is time variations of fuel-air ratio (cycle-to-cycle mixture variation), which are caused partly by inherent instabilities in the flow of the liquid fuel film in the carburettor or manifold walls.

The second is geometric maldistribution of fuel and air between cylinders (the cylinder-to-cylinder mixture variations) resulting from the flow of fuel droplets and of a stratified fuel-air mixture through asymmetric or branched configurations of the carburettor and intake manifold. Because the fuel droplets have greater inertia than the gaseous mixture, they tend to continue in their original direction of movement whenever the direction of the flow is changed abruptly. As a result, there is a variation in air-fuel ratio between the cylinders, depending upon the cylinder location and the manifold design. This problem is more severe in carburetted engines and single point injected engines than port injected engines because fuel has to pass through a long route and different extractions of the induction system to reach the cylinders.

Another phenomenon of mixture non uniformity is the inhomogeneity in the mixture within individual mixture volumes. This results from a failure of the fuel vapour and fuel droplets to mix uniformly with the air and occurs even in the case of fully vaporised fuel because of limitations of time for mixing (Goulburn,1979).

The variations in the air-fuel ratios between different points in mixture volumes in the intake manifold lead to the variations of mixture between cylinders and within the individual cylinders. The inhomogeneity of the mixture within a cylinder is one of the causes of a cycle-to-cycle variation of the mixture.

A high degree of uniformity of mixture distribution can be obtained by minimising wall impaction and depositions of fuel droplets in the intake manifold by increasing the evaporation rate of fuel, and promoting mixing process of fuel and air in the intake manifold.

Thus, the first two possible approaches used to obtain a high degree of uniformity of the mixture is to produce a very finely atomised fog of droplets dispersed in the air and to vaporise the liquid component of the petrol in the air fuel mixture, giving a mixture of air and petrol vapour only. The third approach is mixing of fuel vapour and air.

3.7.2 Mixing of two gases.

The theory of mixing indicates that the mechanisms of mixing of two gases consist of *diffusion* and *convection*.

a) Diffusion.

If two gases are filled together in a container and kept in there for long enough, then the molecules will intermingle as a result of the concentration gradient and random molecular motions and form an uniform mixture on a submicroscopic scale. This is molecular diffusion. However, the molecular diffusion process alone is very slow for mixing requirements.

The diffusion process resulting from velocity gradients within the gases is another type of diffusion and more usually encountered in practice. In this case, low velocity gas or fluid becomes entrained in the faster moving streams when contacted with high velocity streams, which then causes the molecules from the two gases to intermingle quickly. If the flow is turbulent, then the random nature of the velocity fluctuations results in an even greater transfer of gas and the mixing process occurs much faster. This is **eddy diffusion**. In practice, eddy diffusion is generally the only mode of diffusion which can be viably used for mixing.

Mixing of air and fuel vapour or fine fuel droplet in the intake manifold of petrol engines can be considered to be a mixing of two gases. It occurs by molecular diffusivity and eddy diffusivity, and can be described by a total coefficient of diffusion.

$$D_t = D + E \tag{3.7-1}$$

Where D_t is a total coefficient of diffusion,

D is a coefficient of molecular diffusion,

E is a coefficient of eddy diffusion.

Smith (1934) indicated that the degree of mixing of two gases depends on the time of mixing, initial segregation distance of the two gases to be mixed, and their total coefficient of diffusion. This is expressed by equation (3.7-2).

$$\overline{F}_1-\overline{F}_2=\frac{8}{\pi^2}\sum_{n=1}^{n=\infty}\frac{1}{(2n-1)^2}e^{-\frac{(2n-1)^2\pi^2 tD_t}{\alpha^2}} \qquad (3.7\text{-}2)$$

Where $\overline{F}_1$ and $\overline{F}_2$ are mole fractions of gases involved in the mixture,

t is the time of mixing from the beginning of mixing to the moment considered (sec).

α is initial segregation distance of gases to be mixed (distance between the centerlines of two layers of gases) (m).

D_t is total coefficient of diffusion (m^2/s)

At a certain moment, the degree of mixing is defined as 1- ($\overline{F}_1-\overline{F}_2$), for example, 99% mixing occurs when $\overline{F}_1-\overline{F}_2=0.01$. Complete mixing will have occurred when $\overline{F}_1 - \overline{F}_2=0$, in other words, with complete mixing the mole fraction of the two gases is the same at every point in the volume of gases, but as can be seen from equation (3.7-2), this requires an infinite time. In engines the time available for mixing of fuel vapour and air is relatively short, so a complete mixing before the time of ignition is never obtained. This means that completely homogeneous mixture of air and fuel vapour is impossible.

However, it is possible to achieve a high degree of mixing to reach an approximately uniform mixture on a submicroscopic scale by improving mixing conditions. As can be seen from equation (3.7-2), for the same period of time t, increasing the total coefficient of diffusion D_t increases the degree of mixing. In other words, increasing the total coefficient of diffusion increases the degree of uniformity of the mixture.

According to Goulburn and Hughes (1979) molecular diffusion in engines was found to be much less significant than eddy diffusion. They showed, for example, that the value of coefficient of eddy diffusion was about 100 times greater than that of molecular diffusion. Thus, the total diffusivity is virtually independent of molecular diffusivity; that is, the rate of mixing is mainly

affected by turbulent mixing. Therefore, for a given intake system the effective method to increase the rate of mixing and to obtain a high degree of mixing is to create a turbulent motion of the air in the intake manifold and in the cylinder by using special devices.

Considering the mixing time t and assuming that t is the time of mixing in the intake manifold, it can be seen that the time t relates to the length and diameter of the mixing pipe. In an engine running under given conditions, the velocity of the mixture stream has a certain value depending on the air flow rate, and is determined by equation (3.7-3).

$$u = \frac{4w}{\pi d^2 \rho} \tag{3.7-3}$$

Where u is velocity of the mixture stream,

w is air mass flow rate which is determined by engine running conditions

d is diameter of the intake manifold,

ρ is air density.

It takes a time t to obtain the degree of mixing required, so the flow length l_t needed for mixing in the pipe of diameter d is determined by equation (3.7-4).

$$l_t = t * u = \frac{4wt}{\pi d^2 \rho} \tag{3.7-4}$$

Alternatively, the time of mixing in a given intake manifold is

$$t = \frac{l_t}{u} = \frac{l_t \pi d^2 \rho}{4w} \tag{3.7-5}$$

Thus, increasing the diameter and length of the inlet pipe increases the mixing time t, which in turn increases the degree of mixing. Also, increasing the diameter of the mixing pipe leads to a sharp increase in the mixing time t, so for a required degree of mixing, increasing the diameter of the pipe can avoid using a too long intake pipe. Therefore, it can be concluded that inlet pipe diameter should be as large as practicable for good mixing. However, increasing the diameter of the pipe reduces the velocity of the air stream in the induction system, leading to a decrease in evaporation of fuel spray and of wall film fuel flow (Nagaishi et al, 1989). Thus, there are constraints with mixing pipe diameter.

Equation (3.7-2) also shows that reducing the initial segregation distance α of the gases increases the degree of mixing. This can be obtained by finely atomising fuel and spraying it into a turbulent air stream.

b) Convection.

The second mechanism of mixing is convection. These are motions imparted to portions of material by virtue of the effects of inertial or gravitational forces. For example, the difference in temperature between mixture volumes in the intake manifold causes motion in the gas; or in the case of mixing chamber using a stirrer, a stirrer causes motion in the gas some distance from it. In the intake manifold of petrol engines, however, the effect of convection as described is relatively small compared with turbulent effect of the streams.

In brief, satisfactory mixing of fuel vapour and air could be achieved by increasing the length and diameter of the mixing pipe and air turbulence. However, the length of the pipe cannot be too long because of the problem of fitting the inlet system into the engine, so the method based on increasing the total coefficient of diffusion and reducing the initial segregation distance of fuel vapour and air is more convenient to be used. This can be achieved by breaking the stream down into a series of smaller streams and breaking down stratification patterns, then passing the streams across and through one another to redistribute major stratification patterns to speed up mixing.

3.7.3 Characteristics of mixing of fuel and air in petrol engines.

The quality of mixing of fuel and air in the intake manifold of petrol engines influences the uniform distribution of air-fuel mixture in the engine cylinders. A high degree of mixing (good mixing) will improve fuel distribution between cylinders and within the individual cylinders.

There are some methods of examining characteristics of mixing of fuel and air in the intake manifold of petrol engines, but perhaps, the good method to get a general picture of mixing is by observations. Some investigators studied fuel air mixing and fuel distribution in a transparent intake manifold and indicated that fuel does not equally distribute in the cross-section of the intake manifold. Two jets of fuel and air are formed in the throttle plate region, a larger quantity of fuel is concentrated on the jet in the direction of the plate opening in the

manifold, and in a whole intake manifold fuel (even fuel vapour) does not equally mix with air.

Liimatta et al (1971) studied this problem by hydraulic analogy method. They observed and photographed the flow field of water in the model of the two-dimensional carburettor and manifold runners, which was proved to be representative of the flow patterns that occur with a fuel-air mixture on an engine in a similar model under the same conditions, and reached similar results to that of the previous investigations. The results showed that a wake is formed in the region below the throttle plate and contains two vortices that rotate in opposite directions in two jets on the sides of the throttle plate. The particles usually remain within a given vortex. Therefore, it is possible that some fuel in an actual carburettor may become trapped within the wake and not have a chance to mix with the air around.

The jets do not interact, and there is little or no mixing of the jets issuing from either side of the throttle plate. As a result, if maldistribution of the fuel-air mixture occurs above the throttle plate in an actual carburettor, it definitely is not altered or corrected by the dynamic flow field located immediately below the throttle plate. For example, if the fuel in a carburettor is on the walls, it will remain on the walls; under an engine idle condition, the fuel usually enters the carburettor near the tip of the throttle plate, therefore, the possibility of equal distribution to either side is minimal. Thus, it can be concluded that characteristics of fuel sprays from the fuel nozzle and the arrangement of the nozzle relative to the air flow above the throttle plate are very important in improvement of fuel distribution in the engine.

At large throttle openings, observations of field flow show that the flow field is quite agitated in nature. Many of the vortices are stable only for an instant, and then are quickly swept downstream to the cylinders. In actual engine because fuel-air mixture in different vortices can be rich or lean, there will be cycle-to cycle variations.

Thus, it can be said that mixture distribution in an actual engine can be improved if good mixing of fuel and air occurs in the region immediately below the throttle plate and within manifold runners. Mixing conditions can be improved by increasing areas of shear in the flow field to remove the fuel attached to the walls and direct the jets issuing from either side of the throttle

plate against each other (for fuel droplet break up and mixing of fuel and air), and develop vortices or areas that are of differing relative velocity.

From the above analysis and as mentioned in section 3.7.2, methods for improving mixing conditions can be adjusting the length and the diameter of the manifold, or introducing some special devices into mixing region.

Goulburn and Hughes (1979) investigated mixing of propane and air in a pipe without chock (no throttle plate) and indicated the dependence of degree of mixing on the length of the pipe in figure (3.7-1).

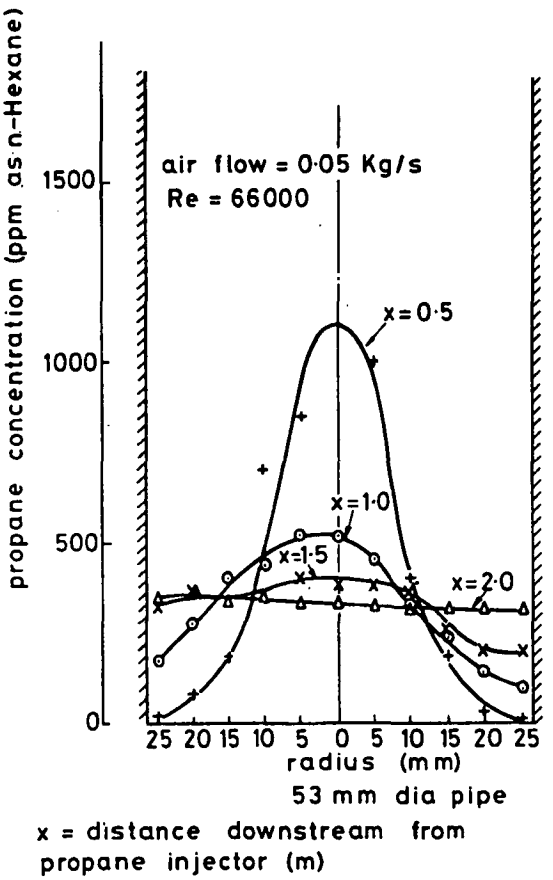

Figure 3.7-1. Typical concentration profiles across mixing pipe at different distance downstream from fuel nozzle (Goulburn and Hughes, 1979).

As can be seen from Figure (3.7-1), the difference in concentration of fuel at different points in a cross section of the pipe becomes smaller at longer distance from the fuel nozzle. This was also confirmed by Liimatta et al (1971). They indicated that short mixing lengths are not conducive to good mixing

conditions. As the length available for mixing is increased, there is more time for the air-fuel jets to spread and interact with one another, and the flow is more evenly divided into the manifold runners. However, the longer lengths do contain vortices that are not stable, and flow field can change with time.

3.7.4 summary.

1) Good mixing of fuel and air is only able to occur with vaporised fuel.

2) Mixing of fuel vapour and air in the intake manifold of petrol engines is mainly controlled by air turbulent flow.

3) The size of mixing pipe (length and diameter of the pipe) is also an important factor influencing mixing process.

4) In carburetted petrol engines, good mixing of fuel and air in the carburettor region and manifold runners significantly contributes to improving fuel distribution between cylinders. In other words, one of the causes of fuel maldistribution in carburetted engines is the failure of fuel and air to mix together in the region beneath the throttle plate.

5) Methods to increase degree of mixing to reach highly homogeneous mixture are increasing turbulent motion of air in the region beneath throttle plate, increasing the length (and the diameter) of the pipe in this region.

3.8 Conclusion.

So far it has been noted that quality of combustible mixture in the cylinders of petrol engines is mainly determined by the quality of mixture formation in the induction system, which is a combined result of such processes as fuel spray, fuel evaporation and transportation, and the mixing of fuel and air in the intake manifold.

The presence of large amount of liquid fuel in the intake manifold of the engines is inevitable and always supposed to be a major cause of fuel maldistribution between cylinders and inhomogeneity of the mixture within individual cylinders of an engine. Accelerating fuel evaporation to reduce liquid fuel deposition in the intake manifold is an effective way to reduce the

negative effect of this liquid fuel on fuel distribution. This can be done by the following methods.

- Using fuel with satisfactory volatility for a given engine.
- Atomising sprayed fuel into small droplets in the induction system.
- Heating the intake manifolds by exhaust gas or hot coolant from the engine.
- Avoiding a design of asymmetric and sharp bend manifold in multi-cylinder engines.
- Making intake manifold with satisfactory size and creating turbulent air motion in the intake manifold for good mixing of fuel and air.

However, the experimental data available are inadequate to evaluate in more detail the characteristics and the causes of mixture maldistribution in petrol engines, and its effect on engine performance.

The following section deals with the experimental investigation of fuel distribution and the causes of fuel maldistribution in petrol engines to contribute to clarifying the nature of mixture formation in petrol engines.

4. Mixture distribution in petrol engines.

4.1 Introduction.

Mixture distribution in multicylinder engines can be described as a measure of the uniformity of air-fuel charge between cylinders and within a given cylinder.

In a multi-cylinder engine, uniform distribution of air-fuel mixture is highly desirable as it prepares the way to equalising power generation between cylinders, a factor vital to achieving smooth operation of the engine. In addition, it allows to easily control the mixture supplied to the individual cylinders to achieve the optimum mixture in all the cylinders so that they can operate at optimum conditions. That is a factor to achieve clean, powerful, and efficient operation of the engine.

4.1.1 Mixture distribution between cylinders.

There are two direct factors leading to non-uniform distribution of mixture between cylinders. Those are the maldistribution of fuel mass flow rate and non-uniform distribution of air mass flow rate between cylinders, resulting in the difference of the quantities and fuel air ratios of the mixture supplied between the cylinders of an engine.

Therefore, there are two methods to evaluate the maldistribution of mixture between the cylinders of a multi-cylinder engine. The first is relying on the difference of the mass rates of air flow and fuel flow between cylinders. The second is relying on the difference of air fuel ratios of the mixtures and the mass rates of one of the followings: air, fuel, or mixture supplied to the cylinders.

In practice, the inlet induction system of an engine is usually designed optimally in terms of dynamic flow, to achieve maximum degree of uniformity of air distribution between cylinders. So in general, in conventional internal

combustion engines the difference of air flow rates to the cylinders is quite small. According to Collins (1969), Finlay et all (1985) and Sag (1988), the difference of air flow rates between the cylinders at wide throttle opening is very small and can be negligible; at low load and low engine speed it is up to only 2 percent. Therefore, it does not significantly affect engine performance. As a result, one is mainly interested in fuel distribution between the cylinders of the engine.

If the difference of air mass flow rates between cylinders is negligible, the mixture maldistribution between cylinders will be only due to the maldistribution of fuel supplied to them. The evaluation therefore can be based on measurement of fuel flow rates or air fuel ratios of the mixtures to the individual cylinders.

Measurement of fuel maldistribution by means of the difference of air/fuel ratios (or A/F equivalence ratios) between cylinders is practicable. In this method, fuel maldistribution can be characterised by the difference of A/F ratios between the cylinders that are supplied with leanest and richest mixtures. This is normally called **spread or delta air-fuel ratio**. Fuel maldistribution can be also characterised by a parameter called **maldistribution index** (MI), which is a ratio of the spread (in terms of A/F ratio or A/F equivalence ratio) and a normalising parameter of twice the average value of these parameters. For example, in terms of A/F ratio, maldistribution index is determined by equation:

$$MI = \frac{(A/F)_{\max} - (A/F)_{\min}}{2(A/F)_{mean}}.$$

There are a number of factors affecting fuel distribution between the cylinders of a petrol engine. Manifold wall fuel film, as analysed in section 3.2, is a dominant factor. The existence of considerable amount of liquid fuel in droplet form suspended in the main stream is another one. Therefore, any factor increasing wall fuel film quantity and fuel droplet deposition in the intake manifold can negatively affect fuel distribution in the engine. Factors causing a bad mixing of fuel vapour and fuel droplets with air in the intake manifold as mentioned in section 3.4 also significantly contribute to increasing fuel maldistribution between cylinders. All of these factors simultaneously affect fuel distribution in the engine.

Mahdi Ali (1989) investigated distribution patterns of air and fuel within a petrol engine manifold by using an experimental manifold with four extractions similar to four manifold branches for four engine cylinders as shown in figure 4.3-1 and showed that quantities of fuel entering the extractions are not even, but decrease from extraction 1 to extraction 4. Consequently, fuel-air ratio decreases from extraction 1 to extraction 4 as shown in figure 4.1-2. In the case of high air flow rate (high air velocity) the fuel distribution between extractions is better than that in the case of low air flow rate.

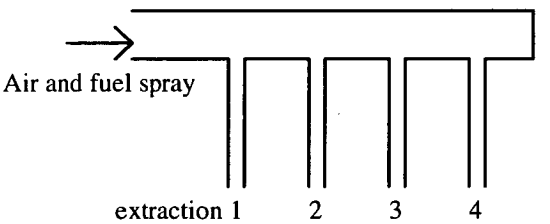

Figure 4.1-1 Diagram of experimental manifold of Mahdi Ali (1989)

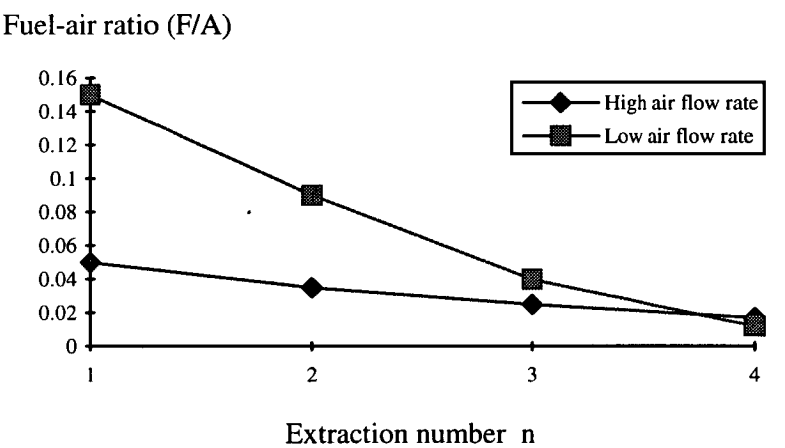

Figure 4.1-2 Fuel distribution between manifold branch (Mahdi Ali, 1989)

Thus, it can be deduced that in a petrol engine, the cylinders located closer to the carburettor (or to the throttle body in the case of a single-point injected engine) will receive a mixture richer than that the other cylinders receive. At high engine speed and full load, the fuel distribution between cylinders will be improved.

Spray and atomisation of fuel upstream of the throttle plate affect the shape of fuel jets passing through the throttle plate, and therefore affect the flow field beneath the throttle plate, and runner-to- runner variations in fuel-air ratio.

The problem of fuel distribution between cylinders in multi-cylinder port-injected engines may be not very significant because there is no problem of throttle plate effect and problem of fuel transportation in the intake manifold like in carburetted or single point injected engines. Fuel is metered separately to the intake port of each cylinder, so it can be metered accurately in the same amount to each cylinder.

4.1.2 Fuel distribution within a cylinder.

Distribution of the mixture within individual cylinders is called mixture quality distribution. In general, the quality distribution of mixture is not uniform. The composition of mixture varies from point to point within a cylinder as well as from time to time. Baritand and Heinze (1992) showed that the quality mixture distribution within a cylinder is strongly dependent on the engine running conditions and characteristics of the fuel supply system. At BDC the deviation of the mixture within a cylinder can be very high, during compression the mixture tends to homogenise, and at TDC approximately no droplets are found at normal running conditions of a conventional engine.

Characteristics of fuel supply has an important effect on the mixture distribution. According to Winkhofer et al (1992), who observed the fuel distribution in a research port-injected engine with a transparent cylinder liner by using the infra-red extinction technique, injection timing has a significant influence on the cycle-to-cycle variations of vapour concentration levels because it affects concentration of fuel vapour entering the engine.

The experiment showed that if fuel is injected into the intake port before the inlet valve is opened, a low degree of cycle-to-cycle variations of in-cylinder mixture is observed. This is because the valve and intake port surface, at higher temperature than the air stream, are wetted with liquid fuel which then evaporates rapidly and enters the cylinder during the initial period of the intake stroke. This high concentration of fuel vapour, first found near the intake valve before it is swept and diluted by the air entering the cylinder during intake, has

a long time to mix with air, so during compression, fuel vapour is well distributed and therefore compression ends with a highly homogeneous mixture.

Fuel injection during inlet valve opening into the high velocity air flow driven by the increasing piston velocity also results in highly repeatable fuel concentration levels at the end of compression; but during intake and at early compression, there are some cycle-to-cycle variations. In this case, with the start of injection, fuel is sprayed into the intake air stream and onto the port and valve surface. Some fuel is transported into the cylinder synchronously with injection by the intake air flow, so fuel air mixing is now affected by the spray propagation in the air flow and by the interaction of the air flow and the fuel wall film on the port and valve surface. The result is that mixture distribution at the end of compression is quite homogeneous, although during compression the mixture is less so.

With fuel injection in the period of maximum valve lift, there are significantly higher cyclic variations than earlier injection, which pertain until the end of compression. In this case there is a chance for parts of the spray to propagate directly into the cylinder, resulting in a highly inhomogeneous charge and in large fluctuations of local fuel concentration levels from cycle to cycle. This inhomogeneous fuel distribution pertains throughout the compression cycle.

In brief, composition of the mixture within individual cylinders varies from time to time due to the continuous evaporation and mixing of fuel and air, but the mixture tends to homogenise with time and get approximately homogeneous at the end of the compression stroke. Hence, it may be concluded that at the time of ignition in the cylinders of conventional petrol engines, the mixture is homogeneous enough to achieve good combustion.

Therefore, in multi-cylinder petrol engines in terms of fuel distribution, fuel distribution between cylinders is more important to consider than that within individual cylinders and is of interest to researchers. To contribute to this, the present study includes an experimental investigation of fuel distribution between the cylinders of multi-cylinder petrol engines in both types of engine, carburation engine and multi-point fuel injection engine.

4.2 Investigation of mixture distribution between cylinders.

4.2.1 Experimental objectives.

The objectives of the present experimental investigation are to determine the degree of uniformity of mixture distribution between the cylinders of multi-cylinder petrol engines and the factors influencing it.

The objectives are achieved by conducting experiments on the two engines, which are the same in size and arrangement except their fuel systems (one is equipped with a carburation system and the other with fuel injection system), using the method of analysis of exhaust gas from the individual cylinders.

4.2.2 Experimental facility and instrumentation.

Experiments were carried out based on the potential of the facility available in the Thermodynamic Laboratory of the Department of Civil and Mechanical Engineering. The facility and instruments used are as follows.

a) Engines.

Two petrol engines used for the investigation are the Peugeot 504 XN1 and Peugeot 504 XN2. These are four linear cylinder engines and mainly used in small motor vehicles. They are exactly the same in size and arrangement except in their fuel supply system. The 504 XN1 is equipped with the carburetion system using a twin-choke Solex carburettor 32-35 SEIEA while the 504 XN2 is equipped with the multi-point fuel injection system using KF5-92 014141 injection pump that is controlled by vacuum pressure in the intake manifold. According to the manufacturer's catalogue, the 504 XN2 engines with fuel injection system indicate more advantages in terms of power output and torque over the 504 XN1 carburetion engines. Beside the reason that volumetric efficiency of the injection engine is higher than that of the carburation engine, another reason for the power advantage of injection engine must be that quality of the mixture supplied in the injection engine is better than that of the carburation engine, ie. in terms of correct air-fuel ratio and homogeneity of mixture distribution. The main characteristics and performance of these two engines are shown in appendix C.

b) HPA, engine-stand dynamometers, No.201 and No.203, max power and speed range from 0.1 kW , 500 rpm to 300 kW, 6000 rpm.

c) Exhaust gas analysers:

The SERVOMEX model 1400B (1420B/1410B) O_2/CO_2 analysers: The device comprises two base units, the 1420B oxygen analyser using paramagnetic technology and the 1410B analyser using dual wavelength, single beam infrared technique.

The 1420B oxygen analyser measures the paramagnetic susceptibility of the sample gas using the world renowned Servomex paramagnetic transducer (a magneto-dynamic type measuring cell). Oxygen is virtually unique in being a paramagnetic gas, it is attracted into a magnetic field. In the Servomex measuring cell the oxygen concentration is detected by means of a dumb-bell mounted on a torque suspension in a strong, non-linear magnetic field. The higher the concentration of oxygen the greater this dumb-bell is deflected from its rest position. Based on this principle the concentration of oxygen is measured. The repeatability of this analyser is ±0.1% oxygen under constant conditions.

The 1410B CO_2 analyser measures carbon dioxide concentration using a single beam dual wavelength infrared technique. Accuracy of the device is ±2% FSD.

For both units, a dual range option is available for gas mixture concentration measurements required (for example, a low range is calibrated for 0-5% and a high range for 0-25%). The measured concentrations of gas are indicated in percentage by volume.

VANE, VP-760 emission analyser (CO and hydrocarbon (HC) analyser): The analyser operation is based on the ability to absorb infrared energy of the gas sample. CO absorbs energy of 4.65 micron wavelength and HC (C1 or $CH_{n/m}$) absorbs energy of 3.42 micron wavelength. The amount of energy absorbed by the gas sample is dependent on its concentration of carbon atoms. Meter readings are provided for percent of carbon monoxide (CO) and parts per million hydrocarbon (HC) in terms of $CH_{n/m}$. A dual scale is available for accuracy readings required. The accuracy of the device is ±3% of full scale for CO and HC.

d) Additional equipment:

- Closed circuit cooling system using HEA plate heat exchanger with GRUNDFOS UPS 32-80 180 pumps and expansion tanks. The system has

two coolant circuits. Engine coolant circulates in the engine closed circuit, gaining heat in the engine and transferring it to the water in the heat exchanger. The water in the secondary circuit takes heat from heat exchanger and transfers it to the air in the cooling tower. Therefore, the system permits to adjust engine temperature (engine coolant) as desired.

- Orifice plates and water gauge manometer.
- Tachometer, stroboscope, and electronic digital revolution counter.
- Heater for changing inlet air temperature with maximum power of 1700 W.
- Stop watch, pipette, thermocouples and temperature indicator.

e) Modification of the exhaust system of the engines:

In the current exhaust manifold, exhaust gases from each individual cylinder are passed through its own pipes and then mixed together in a common pipe to exit. The gases from cylinders 1 and 4 are mixed together in a common pipe, gases from cylinders 2 and 3 are mixed in another common pipe, and then these two pipes are joined together to conduct exhaust gas away. To take exhaust gas samples from the individual cylinders, the exhaust manifold was fitted with the stainless steel exhaust gas sampling tubes. To reduce the effect of mixing of exhaust gas from two cylinders on the gas samples, the tubes were located in such positions where they can take gas sample at about 1.5 cm from the back of the exhaust valves. The diagram of the arrangement of the gas sampling system is shown in appendix D.

4.2.3 Possible techniques in the investigation of mixture distribution.

In the present investigation, mixture distribution between the cylinders of a multi-cylinder engine can be evaluated by determination of difference of air/fuel ratios and of the quantities of the mixtures supplied to the individual cylinders. To evaluate factors affecting the mixture distribution, the experiments are carried out at different engine running conditions and on the two engines that are the same size, arrangement, but different in fuel supply system as presented earlier.

Parameters need to be determined in the experiments are overall measured and calculated air/fuel ratio of the mixture supplied to the engine, air/fuel ratio of the mixture and quantities of the mixture supplied to the individual cylinders at different operating conditions. Simple possible techniques are as follows.

a) Determination of overall air-fuel ratio.

The overall air-fuel ratio of the mixture supplied to an engine is determined from measurements of fuel consumption (fuel mass flow rate to the engine) and air consumption (air mass flow rate to the engine).

$$\text{Overall air-fuel ratio} = \frac{\text{Air mass flow rate to the engine}}{\text{Fuel mass flow rate to the engine}}$$

Fuel flow rate and air flow rate can be measured by flowmeters fitted in the fuel line and inlet air pipe. However, these instruments are expensive, so fuel flow rate and air flow rate can measured by using simple arrangements as follows.

Fuel flow measurement.

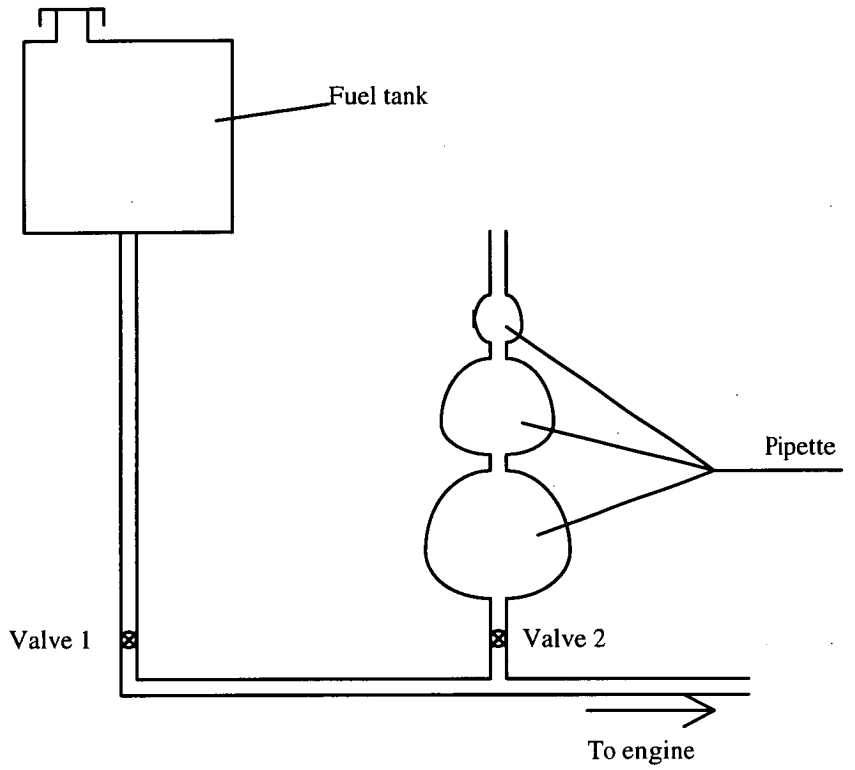

Figure 4.2-1 Fuel flow measurement

A normal measurement system to determine fuel flow rate is timing the consumption of a fixed volume fuel. This has to be converted to a gravimetric consumption by using the density as determined from a separate test. A typical arrangement for measuring fuel consumption is shown in figure 4.2-1.

In normal operation valve 1 is open, valve 2 is closed, fuel flows directly from the fuel tank to the engine. The pipette (calibrated volumes) are filled when

valve 2 is open. To measure fuel flow rate, valve 1 is closed, valve 2 is open and any fuel to the engine is drawn from the pipette. The different volumes are used to give the best compromise between accuracy and speed of taking readings.

Air flow measurement.

Air flow rate can be measured by using a volumetric air flow meter, hot wire method, or orifice plate. Using orifice plate is a simple and common method for determination of air flow rate in engine experimentation.

A simple system to measure the air flow rate is shown in figure 4.2-2. It is obtained by connecting the air intake pipe to a large rigid box with an orifice at its inlet. The box is to damp out the pulsations in air flow. The pressure drop across the orifice can be measured by a water or mercury tube manometer depending on the range of air flow rate to be measured.

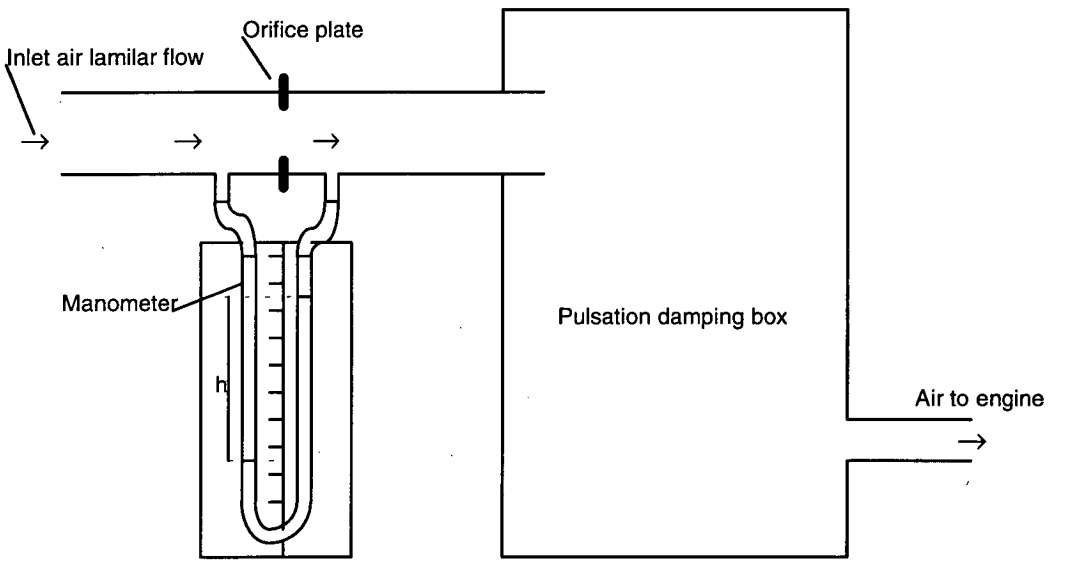

Figure 4.2-2 Diagram for air flow measurement

Because the flow velocity through the orifice plate is low (Mach No less than 0.3), the air can be considered to be incompressible. Therefore, , the air mass flow rate can be calculated from formula (4.2-1) (R. Stone, 1992).

$$\dot{m}_a = C_d \; A_o \sqrt{2gh\rho_f \; \rho_a} \qquad (4.2\text{-}1)$$

Where $\dot{m}_a$ = mass flow rate of air (kg/s)
C_d = discharge coefficient of the orifice
A_o = cross-sectional area of the orifice (m2)
g = acceleration due to gravity (m/s2)
h = height difference between liquid levels in the manometer (m)
ρ_f = density of manometer fluid (kg/m3)
ρ_a = density of air ($=p/RaT$) (kg/m3)

The accuracy of measurement of air mass flow rate by this method depends on knowing the discharge coefficient of the orifice. This should be checked against a known standard.

A more convenient and accurate method of calculation of air mass flow rate from pressure difference between upstream and downstream of the orifice plate applied for this method was presented by British Standard BS 1042 (Methods for the measurement of fluid flow in pipes, 1964) and is developed in detail for the present study in appendix E.

The overall air/fuel ratio is also determined by overall exhaust gas analysis as presented in the following section and compared to the direct measured values to determine the accuracy of method of determinations of air/fuel ratio of the mixture in the individual cylinders from exhaust analysis.

b) Determinations of air-fuel ratio of the mixture in individual cylinder.

A/F ratio of the mixture supplied to the individual cylinders of an engine can be determined by measuring air and fuel flow rates to that cylinder. However, unlike single cylinder engines, in multi-cylinder engines it is not easy to use simple methods for measuring air and fuel flow rates to each cylinder without modification of the induction system because in these engines the cylinders usually share a fuel supply system and an induction system. The determination of air-fuel ratio of the mixture supplied to each cylinder can also be done by using special devices such as flowmeters and air-fuel ratio meters fitted for the cylinder. However, these devices are usually expensive for a small laboratory. In practice, it is desirable to use indirect methods for this purpose.

Since air-fuel ratio of the mixture is one of the factors that have strongest effects on the output parameters of the engine (eg. exhaust emissions, imep, etc), it is possible to correlate air-fuel ratio of the mixture to these parameters, in particular, to the compositions of the exhaust gas and pressure rise in the

cylinders. Thus, air-fuel ratio can be evaluated and determined. There are some possible methods for this purpose.

Determination of air-fuel ratio from Cylinder Pressure-Time histories.

The fact that air-fuel ratio has an effect on the shape of the cylinder pressure trace has been well known. It is therefore possible to obtain the air-fuel ratio of mixture in an engine by examining the pressure trace if the engine speed, load, exhaust gas residual, and other engine running conditions are known.

Houpt and Andreadakis (1983) solved the problem by describing the pressure trace as a differential equation containing empirical combustion and heat transfer coefficients. It is possible to get the results. However, since the shape of cylinder pressure trace varies strongly with engine variables and many of the unknown parameters were assumed to be fixed values by the author to simplify the problem, the errors in estimating air-fuel ratio can be significant.

Gilkey and Powell (1985) directly used the cylinder pressure trace to correlate the changes of input parameters (engine variables) to cylinder pressure. Thus, the effects of all of the engine variables can be included in the problem. However, because cylinder pressure changes quickly with time and normal transducers usually have a response delay, pressure trace does not reflect the truth of the pressure in the cylinders. This leads to errors of the problem. In addition, in transient running conditions when the pressure trace is not stable, it is difficult to predict air-fuel ratio.

In brief, because of the complexity and inaccuracy, air-fuel ratio determination from Cylinder Pressure-Time histories as presented above is not very convenient to be used in evaluating the mixture quality.

Determination of air-fuel ratio by oxygen analysis: Air-fuel ratio analyser.

It is clear that products of **complete** combustion of hydrocarbon fuel include carbon dioxide, water vapour, and oxygen. The proportions of carbon dioxide and oxygen in the products express the air-fuel ratio of the mixture. Therefore, analysis of either oxygen concentration or carbon dioxide concentration in the products can indicate the air-fuel ratio of the mixture. Gerrish and Meem (1943) indicated a method to calculate air-fuel ratio from carbon dioxide concentration in a **fully oxidised** exhaust gas sample, but, according to subsequent authors, the method seems to be less accurate as the oxygen content

in the sample increases. Oxygen, on the other hand, is very Magnetochemically sensitive, so it can be used to indicate air fuel ratio in air-fuel ratio analysers.

For this purpose, a sample of the exhaust gas is taken and passed through a heated catalyst to fully oxidise any partial products of combustion (for rich mixture, an extra amount of air is added), and then, the oxygen level is evaluated. If the hydrogen/carbon/oxygen ratio of the fuel and the amount of added air are known, then the equivalence ratio (ϕ) or air/fuel ratio (A/F) can be deduced.

Consider first the combustion of a weak mixture with an equivalence air/fuel ratio ϕ (ϕ>1), the chemically balanced equation of complete combustion of fuel ($C_m\ H_n\ O_r$) in air is as follows.

$$\begin{aligned}(C_x\ H_y\ O_z)+\frac{(x+y/4-z/2)}{\phi}\left(O_2+\frac{79}{21}N_2\right) \rightarrow\ & xCO_2+\frac{y}{2}H_2O \\ &+\ (1/\phi-1)(x+y/4-z/2)\,O_2 \\ &+\ (1/\phi)(x+y/4-z/2)\frac{79}{21}N_2\end{aligned} \qquad (4.2\text{-}2)$$

Where x, y, z are the number of carbon atoms, hydrogen atoms, and oxygen atoms, respectively, in a molecule of hydrocarbon fuel.

It can be seen from the right hand side of equation (4.2-2) that the oxygen level in the exhaust gases enables the equivalence ratio to be found. Since the system is maintained at a temperature for which the water is vaporised, we have :

$$\%O_2=\frac{21(1-\phi)(x+y/4-z/2)}{21x\phi+21y\phi/2+(100-21\phi)(x+y/4-z/2)}\times 100 \qquad (4.2\text{-}3)$$

Equation (4.2-3) shows that if the oxygen level is evaluated, ϕ is the only unknown variable. In other words, equivalence ratio ϕ can be deduced from evaluating the oxygen level in the exhaust gas after being fully oxidised.

In the case of rich mixture burned, an extra amount of air, denoted by $d(O_2+79/21N_2)$, is added to fully oxidise partial products of combustion.

$$(C_xH_yO_z)+\frac{(x+y/4-z/2}{\phi}\left(O_2+\frac{79}{21}N_2\right)\Rightarrow \text{partial combustion product} \quad +$$

$$+d(O_2+\frac{79}{21}N_2) \Rightarrow$$

$$xCO_2+\frac{y}{2}H_2O+[(1/\phi-1)(x+y/4-z/2)+d]O_2+[(1/\phi)(x+y/4-z/2)+d]\frac{79}{21}N_2 \quad (4.2\text{-}4)$$

With equation (4.2-4), the equivalence ratio can be expressed in terms of the oxygen level in the exhaust, the fuel composition, and the extra air level (d):

$$\%O_2=\frac{(1/\phi-1)(x+y/4-z/2)+d}{x+y/2+(100/21\phi-1)(x+y/4-z/2)+100d/21}\times 100 \quad (4.2\text{-}5)$$

from which ϕ can be evaluated if d is known.

The oxygen level in a sample is evaluated by oxygen analysers. In practice, an air/fuel ratio analyser can be also an oxygen analyser which is calibrated to show air/fuel ratio or equivalence ratio of the mixture. However, this method is quite complicated because before analysing oxygen concentration, the sample gas must be fully oxidised; in addition, in the case of rich fuel mixture an accurate amount of added air must be determined. Therefore, although the oxygen analyser is available in the Thermodynamic Laboratory of the department, this method may not be convenient to be used in the present experiments.

Determination of air/fuel ratio from analysis of exhaust gas components.

It is known that combustion products relate to the composition of reactants. The generalised combustion of an oxygenate fuel is given by (4.2-6) (Taylor, 1985).

$$(C_x\,H_y\,O_z)+\frac{(x+y/4-z/2)}{\phi}\left(O_2+\frac{79}{21}N_2\right)\rightarrow a\,CO+b\,CO_2+c\,H_2O+d\,H_2$$

$$+e\,O_2+f\,C_m\,H_n+g\,NO_q+h\,N_2 \quad (4.2\text{-}6)$$

Coefficients a, b, c, d,e f, g, h are measured percentages of carbon monoxide, carbon dioxide, water, hydrogen, oxygen, unburnt hydrocarbon, oxides of nitrogen, and nitrogen by volume respectively in the exhaust gas. When the fuel composition is known (as the ratio of x:y and x:z), then there are four atomic balances and four unknowns, x and ϕ, and the concentration of the hydrogen

and water vapour in the products. If some assumptions are made on the relationships between the components of the products, it is possible to determine the air/fuel ratio of the mixture from the combustion products. However, in this case too many parameters should be measured and determined.

In the same principle but in a different way, Spindt (1965) studied this problem and showed that to calculate air-fuel ratio from exhaust gas components, only determinations of the percentage concentrations by mole of CO, CO_2, O_2, and percentage of hydrocarbons on the basis of carbon atom are needed. The equation for calculation of air-fuel ratio from exhaust gas analysis presented by him is as follows.

$$A/F = F_b \left[11.492 F_c \left(\frac{1+R/2+Q}{1+R}\right) + \left(\frac{120 F_h}{3.5+R}\right)\right] \qquad (4.2\text{-}7)$$

Where A/F is air to fuel ratio of the mixture supplied to the cylinder.

$$R = P_{CO}/P_{CO_2}$$

$$Q = P_{O_2}/P_{CO_2}$$

$$F_b = \frac{(P_{CO} + P_{CO_2})}{(P_{CO} + P_{CO_2} + P_{CH})}$$

P_{CO}, P_{CO_2}, P_{O_2}, and P_{CH} are percentage concentrations by mole of CO, CO_2, O_2, and concentration of unburnt hydrocarbon on the basis of carbon atom, respectively.

F_c and F_h are fractions of carbon and hydrogen by mass in the fuel.

This method has been checked by comparing the values of air fuel ratio received from direct measurements of air and fuel flow rates in a single cylinder engine and air fuel ratios calculated from the exhaust gas analysis method and showed that with good combustion, air fuel ratios determined from this method is about as accurate as those from direct measurement of air and fuel flow. The analysis shows that small errors in measurement do not significantly affect the air-fuel ratio determination, in particular, error in measurement of HC component. In fact, for a conventional petrol engine operating at normal conditions, concentrations of CO_2 usually ranges from 10 to 16%, CO from 8 to 0.1%, HC from 0 to 0.3% on the basis of carbon atom, so according to (4.2-7) error of measuring HC has a very little effect on the

calculated A/F ratio. In the case of poor combustion, Spindt stated that calculations based on equation (4.2-7) would give reasonably accurate results.

Thus, at normal running conditions of engines, this method of determination of air-fuel ratio from exhaust gas analysis can be used practically. The percentage concentration of oxygen by volume can be measured using paramagnetic technology, percentage concentrations by volume of CO and CO_2 can be measured using infrared technique, percentage concentration of HC on the basis of carbon atom can be measured by means of a flame ionisation detector.

In the Thermodynamics Laboratory, there are facilities available for measuring percentage concentrations by volume of O_2, CO, CO_2 as presented earlier, but there is not a flame ionisation detector for measuring percentage concentration of HC on the basis of carbon atom. Fortunately, the instrument available in the laboratory for measuring HC concentration provides meter readings in parts per million on the basis of hydrocarbon C1 ($CH_{n/m}$), so it can be translated to concentration of HC by volume and converted to the concentration of HC on the basis of carbon atom by multiplying the volume concentration of HC by the number of carbon atoms contained in a hydrocarbon molecule (in this case, only changing from part per million into percent is needed).

In other cases, it can also be determined by using any type of instrument for measurement of HC concentration in volume, and then translating into concentration on the basis of carbon atoms without significant error in the calculation result of A/F ratio from equation (4.2-7).

In effect, although petrol is a mixture of many hydrocarbons containing different number of carbon atoms, and it is difficult to determine exactly how many carbon atoms a hydrocarbon molecule has, it can be approximately determined. According to Gruse, W.A. and Stevens, D.R (1942), and Waddams, A.L. (1978), petrol is a mixture of light hydrocarbons that contain from 4 to 12 carbon atoms (C_4 *to* C_{12}) in their molecule. When reacting with oxygen in combustion, the large molecules of HC are broken into smaller ones, so the hydrocarbons in exhaust gas are very different from those in the fuel. Most of them are small molecule hydrocarbons. According to Kaiser, E.W. et al (1983), concentration of hydrocarbon species in exhaust gas from multicylinder petrol engines varies with the engine running conditions, but in every case, the concentration of heavy hydrocarbons is quite small, representing under 10% of

the total HC in exhaust gas. Hydrocarbon C_2 and C_3 (HC with 2 carbon atoms in their molecules) represents up to 40%. The rest is hydrocarbon C_1. Therefore, the average number of carbon atoms contained in a hydrocarbon molecule can be assumed to be 2. Now, percentage concentration of hydrocarbon on the basis of carbon atom P_{CH} can be determined.

$$P_{CH} = \frac{2 * (Volume\ concentration\ in\ ppm)}{10000}, \text{ percent}$$

For an engine in good conditions like the engine 504XN1 and 504 XN2 in the Thermodynamics Laboratory, the concentration of unburnt HC emission is very low, usually less than 500 ppm, the above assumption to calculate percentage concentration of HC on the basis of carbon atom would not significantly affect the error of the final results of determination of A/F ratio by this method. The accuracy of the calculations is presented in appendix F.

In brief, the method of determination of A/F ratio from exhaust gas components as presented by Spint is convenient to be used for the present experiment to investigate fuel distribution between the cylinders of a multi-cylinder petrol engine.

c) Determinations of mixture flow rates to the individual cylinders.

Quantity of charge (quantity of air-fuel mixture) supplied to a cylinder is determined by measurements of air flow rate and fuel flow rate. However, if air-fuel ratio is known, only either measurement of inlet air flow rate or inlet fuel flow rate is needed. This seems to be simple in single-cylinder engines, but in multi-cylinder engines direct measurements of inlet air flow rate or fuel flow rate to each cylinder is not a simple task. Therefore, possible alternative methods should be used.

Collins (1965) presented a method to determine the flow rates of air and fuel entering individual cylinder in multi-cylinder engines under steady running conditions as follows. By injecting additional liquid fuel at a given rate into the inlet port of a cylinder, the overall air-fuel ratio of the mixture entering the cylinder will change. The extent of the change depends on the rate of injection of fuel and the amount of air and fuel flowing from the carburettor to the cylinder. Because the rate of injection is known, a measurement of the change in air fuel ratio enables the amounts of air and fuel from the carburettor to be calculated. Assuming that the injection of small quantities of liquid fuel at a

rate of f g/s affects neither the air flow, A g/s, nor the fuel flow, F g/s, from the carburettor to the cylinder, the overall air-fuel ratio during injection is

$$AFR = A/(F+f),$$

$$\text{or} \qquad f = A(1/AFR) - F. \tag{4.2-8}$$

Equation (4.2-8) expresses a straight line with slope A and intercept F. Thus, by changing the amount of additional fuel injected into inlet port, f, and progressively determining AFR by exhaust gas analysis, and then plotting the results in the form of f against $1/AFR$, the slope and intercept of the line and therefore the air flow rate, A, and fuel flow rate, F, from the carburettor can be determined. Figure 4.3-3 illustrates the technique described above.

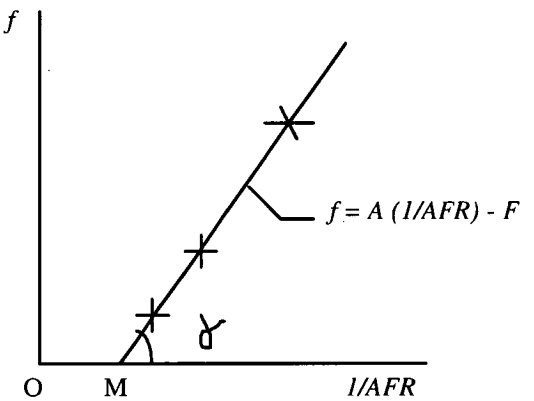

Figure 4.3-3. Diagram for determination of air and fuel flows into individual cylinders.

The values of air flow rate and fuel flow rate are calculated from the diagram as follows:

Air flow rate: $A = tan\,\gamma$

Fuel flow rate: $F = A \times$ OM.

The method described above is reasonable. It can be used to evaluate distributions of air and fuel between cylinders in multi-cylinder engines. However, the method indicates some disadvantages. First, errors can be significant if some of the additional liquid added at one inlet port finds its way into another cylinder. This is possible because of the pulsation of air flow in the intake manifold. Another is that overall air fuel ratio of the mixture entering the cylinders is changed because of additional fuel added. This leads to a limitation of the application of the method. For example, when studying the effects of fuel distribution between cylinders on engine performance, the method cannot be used.

Direct measurement of gas flow rate.

To overcome the disadvantages of the method described above, when studying the effects of mixture distribution in engines, it is possible to determine the distribution of charge (or air) between cylinders by direct measurements of air flows through individual cylinders at the exhaust pipe. To do this, the exhaust manifold will be replaced by separate pipes, approximately the same shape and size but connected to large steel tanks, which incorporated an orifice plate or a flowmeter at the outlet. The flow rate of the exhaust gas from each cylinder is then measured. A possible arrangement of instruments for such measurements is shown in Figure 4.2-4. This method is also only appropriate to measurements under steady running conditions.

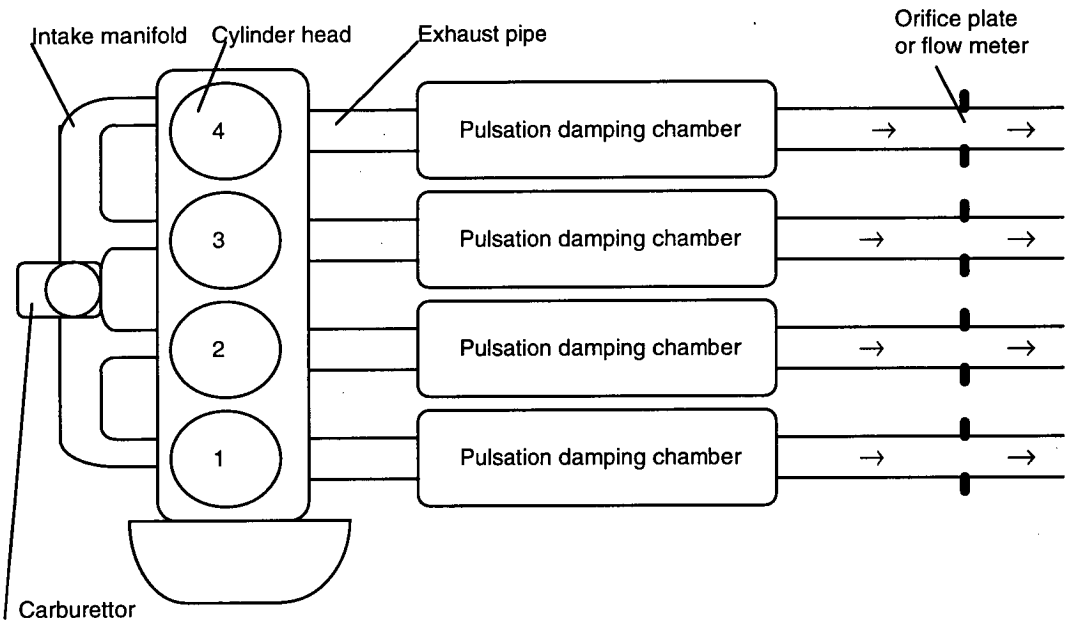

Figure 4.2-4. Block diagram for measurements of air distribution between cylinders.

After measuring the mass flow rate of exhaust gas coming out of each cylinder (also equal to mass flow rate of charge entering the same cylinder) and air-fuel ratio of the mixture, the air flow rate can be calculated from (4.3-9)

$$\text{Air mass flow rate} = \frac{(\text{exhaust mass flow rate}) \times (\text{air fuel ratio})}{(\text{air fuel ratio}) + 1}, \quad (4.2\text{-}9)$$

$$\text{and Fuel mass flow rate to a cylinder} = \frac{\text{exhaust mass flow rate}}{(\text{air fuel ratio}) + 1}, \quad (4.2\text{-}10)$$

This method is simple in its use and can give accurate measured results if measurement instruments are good.

Determination of mixture flow rate to the individual cylinders as presented is a bit sophisticated, requiring some facility and modifications of the system while the difference in air flow rate into the individual cylinders, as mentioned earlier, is very small and can be negligible. Therefore, in this experiments, measurement of air flow rate to the individual cylinders was omitted without significant effect on the error of the results of investigation. In this case, the air flow rate to the individual cylinders is assumed to be equal to the average air flow rate form all the cylinders. This means that air mass flow rate to each cylinder is equal to air mass flow rate to the engine, measured by orifice plates, divided by the number of cylinders, and

$$\text{Fuel mass flow rate to a cylinder} = \frac{\text{average air mass flow rate to each cylinder}}{\text{air fuel ratio}}$$

4.2-4 Techniques applied in the present study.

Based on the previous analysis and the facility available in the Thermodynamics Laboratory, the technique, which was chosen for investigation of mixture distribution between cylinders of a multi-cylinder petrol engine, is determination of A/F ratio in the individual cylinders from exhaust gas analysis presented by Spint (1965). The method of direct determination of overall A/F ratio presented in section 4.2-3 (a) is also applied to evaluate the accuracy of the indirect method by comparing the results. The distribution of air between the cylinders is assumed to be uniform.

4.2.5 Experimental procedure.

a) Measured parameters.

Parameters to be measured in the experiment include:

- Ambient air conditions: air temperature, air barometric pressure.
- Air mass flow rate; it is determined by measuring the pressure difference between upstream and downstream of the orifice plate, using a water pressure gauge, and then the data is translated in to air mass flow rate by referring to the charts in appendix E.

- Fuel mass flow rate; this is determined by measuring the time for running out of 0.1 litre of fuel, using a stopwatch, and then calculated with the specific gravity of the used fuel.
- Engine operating parameters; such parameters as brake load, engine speed, coolant temperature, inlet air temperature are measured with the instruments included in the dynamometer-engine system.
- The components of exhaust gas from the individual cylinders of the experimental engine; this is done by using gas analysers mentioned earlier.

b)Experimental procedure.

The following is the experimental procedure ued for both the 504 XN1 carburetion engine and the 504 XN2 fuel injection engine.

***Test 1**: Changing engine speed and brake load.*

The engines are run at different constant speeds: 1000, 1500, 2000, 2500, and 3000 rpm for a range of brake loads, 1.5, 3, 5.5, 8, 10, and 12 kgm. For the 504 XN2 injection engine, changing load to the above values is done by hanging objects of 1.5, 3, 5.5, 8, 10, and 12 kg at the end of the 1m lever attached at the housing rotor of the dynamometer. For the 504 XN1 engine, the objects of 2.46, 4.92, 9, 13.1, 16.4, or 19.7 kg are hanged at the end of the 0.61m lever attached at the housing rotor of the dynamometer. At each value of brake load and speed, the control valve of gas line to the analyser was switched one by one to the cylinders, at that position when steady conditions are established (based on the constancy with time of engine speed, brake load, exhaust gas temperature, and standard outlet cooling water temperature, 85±1°C) the desired data were then recorded, including engine speed, brake load, overall fuel flow rate (time for running out 100 ml of fuel), overall air flow rate (pressure difference in water gauge manometer), inlet air temperature, inlet and outlet cooling water temperature, and exhaust gas components were recorded. The data of exhaust components were recorded for each cylinder.

***Test 2**: Changing cooling water temperature.*

The engine was run at constant speed 2500 rpm with the range of brake load 1.5, 3, 5.5, 8, 10, and 12 kgm. Outlet water temperature was changed to 30, 50, 70, 85, and 100°C. At each steady state, the desired data were recorded. Changing cooling water temperature was done by adjusting the flow rate of water in the secondary circuit in the heat exchanger.

Test 3: Changing inlet air temperature.

The engine was run at 2500 rpm at standard cooling water temperature of 85± 1°C at different values of inlet air temperature corresponding to the amount of heat supplied to the inlet air of 0, 400, 800, 1200, and 1700 Watt. When reaching steady conditions the data were recorded. Changing inlet air temperature was done by adjusted power output of the heater for heating the inlet air.

4.2-6 Experimental data.

The data recorded in the experiments with the three tests described in the previous section for the two engines, Peugeot 504 XN1 carburation engine and Peugeot 504 XN2 multi-point injection engine, are printed in appendix F.

4.2.7 Data processing.

Calculation of overall fuel mass flow rate to the engine:

$$m_f = \frac{0.1}{\tau}[0.7333 - 0.00082(t - 15.5)] * 3600 \quad \text{kg/h}$$

Where m_f is overall fuel mass flow rate to the engine (kg/h),

τ is the time in second for the engine running out of 0.1 litre of fuel,

Specific gravity of the petrol fuel at 15.5°C is 0.7333 (the decrease in sp. gr/°C = 0.00082).

Calculation of overall air mass flow rate to the engine:

Air mass flow rate, was determined according to the reading values in the differential gauge by referring to figures (E-1) to (E-3) and then multiplying by the barometric pressure correction factor determined from figure E-4 in appendix E.

Overall direct measured air-fuel ratio $= m_f/m_a$.

Calculation of air fuel ratio in the individual cylinders:

Air fuel ratio of the mixture in individual cylinders was calculated by exhaust gas analysis based on the method presented by Spint, 1965, (was shown in equation 4.2-7).

$$A/F = F_b \left[11.492 F_c \left(\frac{1+R/2+Q}{1+R} \right) + \left(\frac{120 F_h}{3.5+R} \right) \right] \qquad (4.2\text{-}7)$$

$$R = P_{CO} / P_{CO_2}$$

$$Q = P_{O_2} / P_{CO_2}$$

$$F_b = \frac{(P_{CO} + P_{CO_2})}{(P_{CO} + P_{CO_2} + P_{CH})}$$

Compositions of the fuel used in experiment can be based on the compositions of super grade petrol:

F_h=H=14.4% by mass=0.144,
F_c=C=85.5% by mass=0.855,
S=0.1% by mass.

Exhaust gas components P_{CH}, P_{CO}, P_{CO_2}, P_{O_2} are denoted by HC, CO, CO_2, and O_2 respectively in the tables of test data printed in appendix F, in which the concentration of HC indicated in part per million (ppm) must be translated into percent before calculating in equation (4.2-7) above.

Delta air/fuel ratio and maldistribution index, MI:

As mentioned earlier, with air maldistribution being negligible, it is convenient to characterise mixture maldistribution between cylinders of a multi-cylinder engine by the terms *delta A/F ratio* or *maldistribution index, MI*, which were defined previously. Maldistribution index is a more appropriate characteristic of mixture maldistribution in the case of A/F ratio varying in a large range. In the present study with normal engine running conditions, because A/F ratio varies in a small range, it is more convenient to characterise mixture maldistribution by the term delta A/F ratio that is the difference between the A/F ratio in the cylinder supplied with leanest mixture and the A/F ratio in the cylinder supplied with richest mixture.

4.2-8 Results of calculations.

Results of calculations of overall measured A/F ratios, the A/F ratios in the individual cylinders, and the delta A/F ratio, in the cases of changing brake load, engine speed, coolant temperature, and changing inlet air temperature were tabulated and graphically presented in the following pages.

a) Results of experimental data processing on the Peugeot 504 XN1 engine.

Test1: A/F ratio and delta A/F ratio versus load at different engine speeds, 504 XN1 engine.
(coolant temperature $= 85 \pm 1^{o} C$*)*

Table 4.2-1: Calculated data

Engine speed, rpm	Brake load, kgm	Overall measured A/F ratio	Calculated A/F ratio					Delta A/F ratio	Maldistribution index
			Overall	Cylinder 1	Cylinder 2	Cylinder 3	Cylinder 4		
1000	1.5	16.25	16.63	17.12	16.37	15.83	17.21	1.38	0.0415
	3	16.11	16.29	16.88	16.05	15.73	16.48	1.14	0.035
	5.5	16.01	16.02	16.45	16.06	15.59	15.98	0.85	0.0266
	8	15.23	15.44	15.87	15.43	15.02	15.45	0.85	0.0276
	10	15.08	15.26	15.37	15.13	14.78	15.77	0.98	0.0323
	12	14.75	15.08	15.97	14.61	14.26	15.47	1.7	0.0564
1500	1.5	16.52	17	17.22	16.75	16.46	17.58	1.12	0.033
	3	16.31	16.69	16.9	17.16	16.55	16.15	1.01	0.0302
	5.5	16.18	16.32	16.47	16.73	16.15	15.93	0.8	0.0245
	8	16.01	16.18	16.62	16.06	15.77	16.27	0.85	0.0263
	10	15.82	15.94	16.53	15.56	15.48	16.18	1.04	0.0327
	12	15.39	15.57	16.29	14.84	15.32	15.83	1.46	0.0467
2000	1.5	16.48	16.69	17.17	16.56	16.23	16.8	0.95	0.0284
	3	16.17	16.29	16.73	16.44	16.13	15.87	0.86	0.0263
	5.5	15.6	15.64	15.75	16.05	15.26	15.52	0.8	0.0255
	8	15.01	15.12	15.1	15.12	14.69	15.59	0.9	0.0296
	10	14.69	14.82	14.98	14.61	14.25	15.43	1.18	0.0399
	12	14.51	14.59	14.65	13.92	14.48	15.31	1.39	0.0477
2500	1.5	16.01	16.17	15.99	15.75	16.35	16.6	0.86	0.0265
	3	15.23	15.53	15.92	15.15	15.71	15.32	0.77	0.0247
	5.5	14.95	15.16	15.25	15.04	14.76	15.6	0.84	0.0276
	8	14.4	14.53	15.08	14.64	14.02	14.4	1.06	0.0363
	10	14.13	14.29	14.96	14.08	13.68	14.47	1.28	0.0448
	12	13.85	14.11	14.83	13.95	13.47	14.18	1.36	0.048
3000	1.5	16.24	16.87	17.28	16.64	16.45	17.09	0.82	0.0244
	3	16.12	16.34	16.47	16.2	15.97	16.72	0.76	0.0232
	5.5	15.56	15.72	16.23	15.49	15.3	15.89	0.93	0.0297
	8	14.27	14.22	14.85	14.1	13.64	14.31	1.21	0.0426
	10	13.86	14	14.73	13.87	13.38	14.03	1.34	0.048
	12	13.59	13.81	14.58	13.77	13.2	13.71	1.38	0.0498

a)

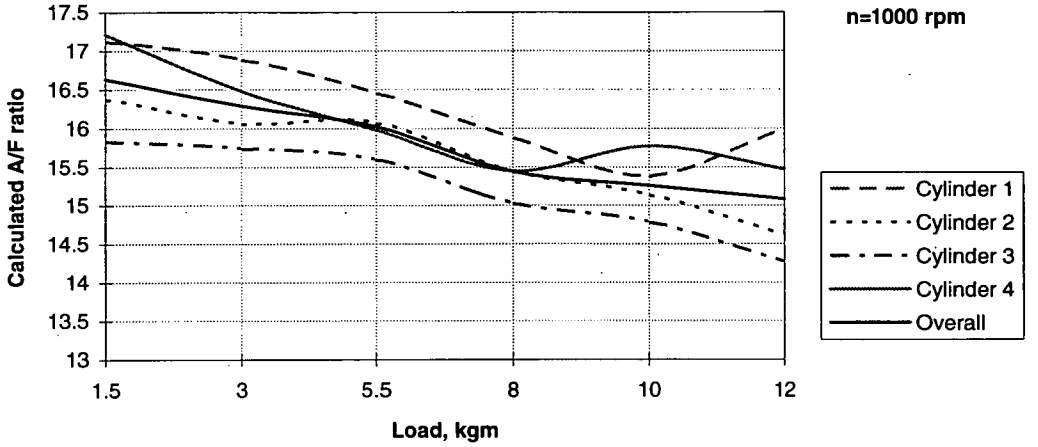

b)

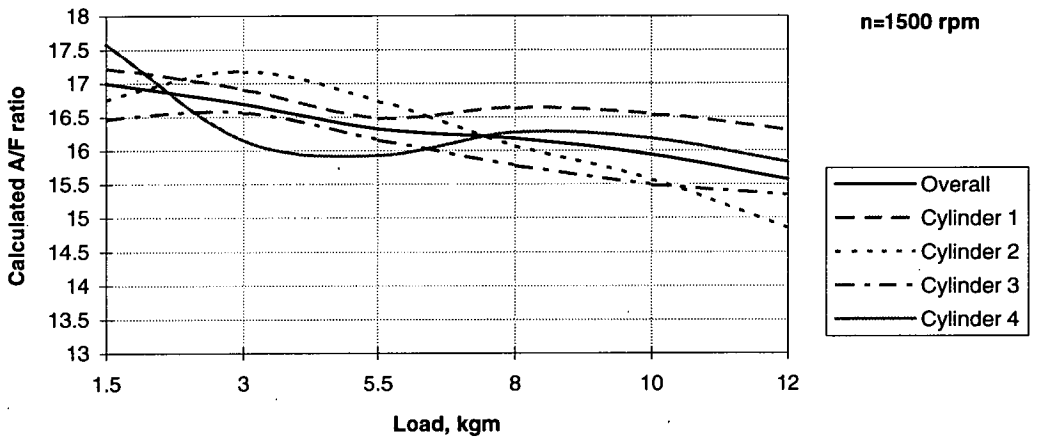

c)

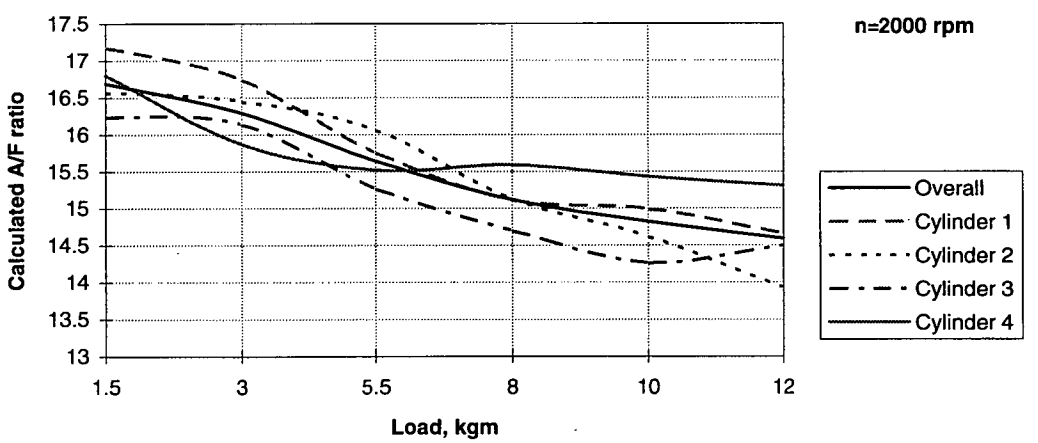

Figure 4.2-1(a,b,c): A/F ratio in the individual cylinders at different engine loads and speeds (504 XN1)
a) n=1000 rpm, b) n=1500 rpm, c) n=2000 rpm

d)

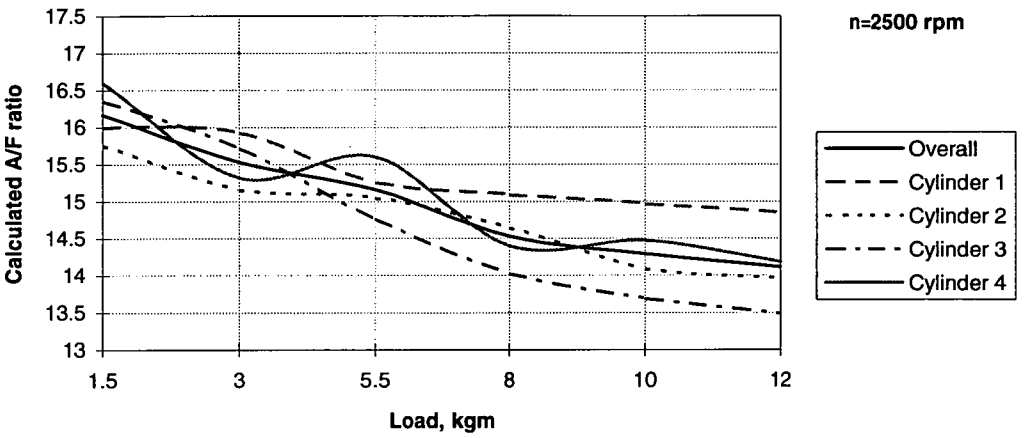

e)

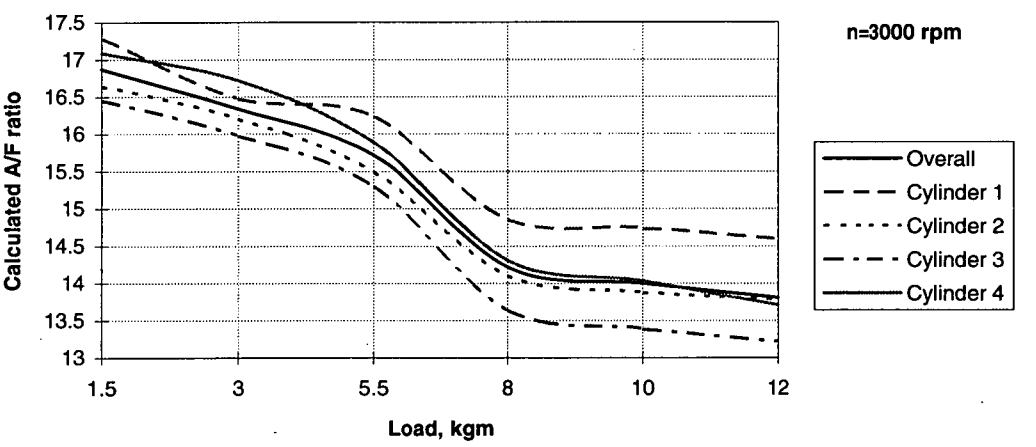

Figure 4.2-1(d,e): A/F ratio in the individual cylinders at different engine loads and speeds (504 XN1)
d) n=2500 rpm, e) n=3000 rpm

Test 2: A/F ratio and delta A/F ratio versus coolant temperature at different loads (504 XN1 engine, engine speed=2500 rpm)

Table 4.2-2: Calculated data

Brake load, kgm	Outlet coolant temperature	Calculated A/F ratio					Delta A/F ratio	Maldistribution index
		Overall	Cylinder 1	Cylinder 2	Cylinder 3	Cylinder 4		
1.5	30	16.42	16.88	15.66	16.18	16.95	1.28	0.0391
	50	16.39	16.71	15.77	16.07	17	1.22	0.0374
	70	16.39	16.56	15.87	16.15	16.97	1.1	0.0337
	85	16.17	15.99	15.75	16.35	16.6	0.86	0.0265
	100	15.97	16.38	15.53	15.79	16.17	0.85	0.0265
3	30	15.9	16.64	15.49	15.21	16.27	1.43	0.0448
	50	15.75	16.34	15.57	15.21	15.87	1.14	0.0361
	70	15.66	16.24	15.45	15.07	15.88	1.18	0.0375
	85	15.53	15.92	15.15	15.71	15.32	0.77	0.0248
	100	15.43	15.79	15.33	15.08	15.53	0.7	0.0228
5.5	30	15.86	16.6	15.16	15.47	16.22	1.45	0.0457
	50	15.73	16.38	15.43	15.14	15.96	1.24	0.0394
	70	15.33	15.89	15.41	15.18	14.83	1.05	0.0343
	85	15.16	15.25	15.04	14.76	15.6	0.84	0.0276
	100	15.16	15.28	15.03	14.79	15.54	0.75	0.0247
8	30	15.41	16.15	15.27	14.58	15.65	1.57	0.051
	50	14.79	15.49	14.65	14.14	14.9	1.35	0.0455
	70	14.61	15.23	14.58	14.04	14.58	1.19	0.0409
	86	14.53	15.08	14.64	14.02	14.4	1.06	0.0363
	100	14.49	14.98	14.51	14.02	14.44	0.96	0.033
10	30	15.12	16.06	14.74	14.36	15.31	1.7	0.0561
	50	14.72	15.53	14.52	14.03	14.81	1.51	0.0511
	70	14.68	15.41	14.94	14.37	14.02	1.39	0.0473
	85	14.29	14.96	14.08	13.68	14.47	1.28	0.0448
	100	14.33	14.89	14.19	13.77	14.49	1.12	0.0389
12	30	14.22	15.17	13.81	13.35	14.57	1.82	0.0638
	50	14.31	15.24	13.96	13.53	14.51	1.71	0.0596
	70	14.14	14.97	13.72	13.44	14.43	1.53	0.0539
	85	14.11	14.93	13.95	13.47	14.18	1.36	0.048
	100	14.23	14.85	13.83	13.9	14.37	1.02	0.0358

Tolerance of coolant temperature is about $\pm 1^0 C$

a)

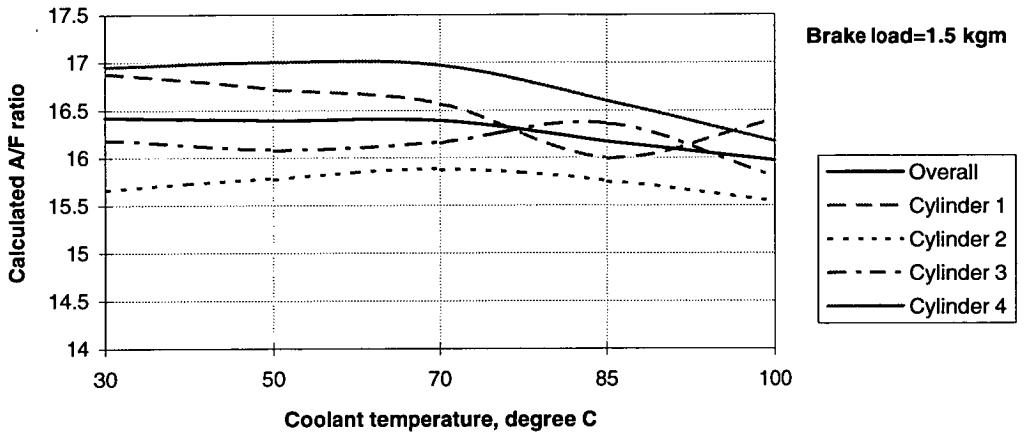

b)

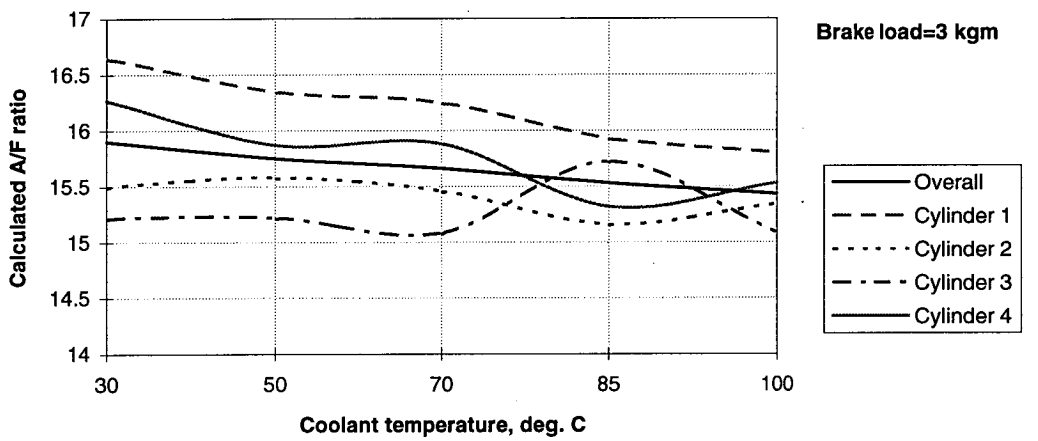

c)

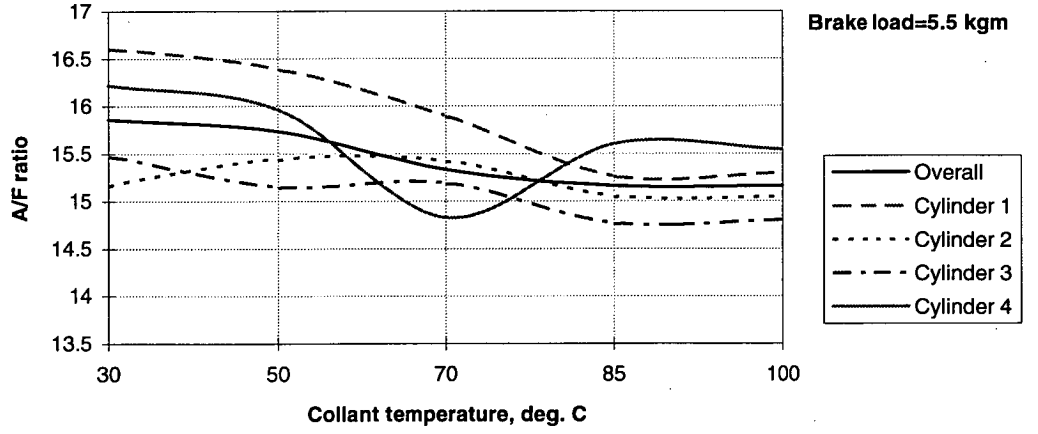

Figure 4.2-2(a,b,c) : A/F ratio&delta A/F ratio at different loads and coolant temperatures
504 XN1, a) Brake load=1.5 kgm, b) Brake load=3 kgm, c) Brake load=5.5 kgm

d)

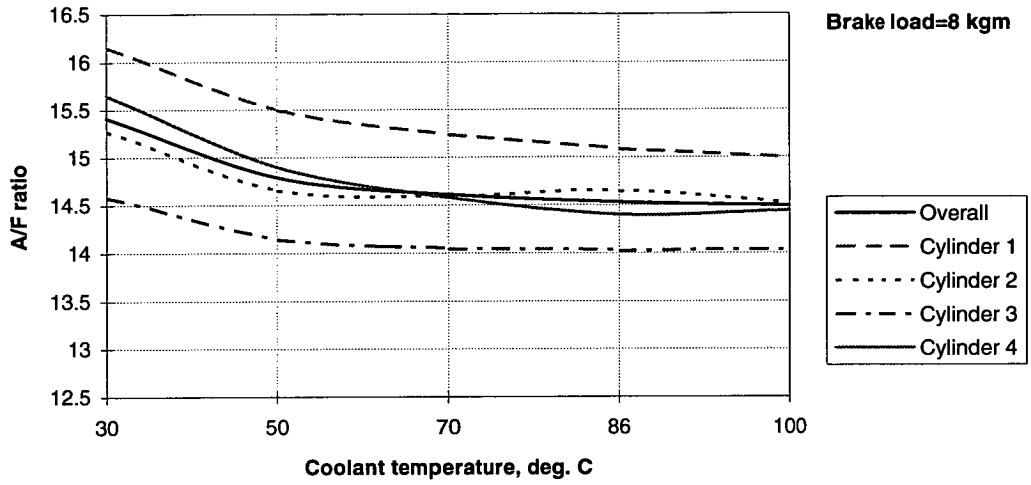

e)

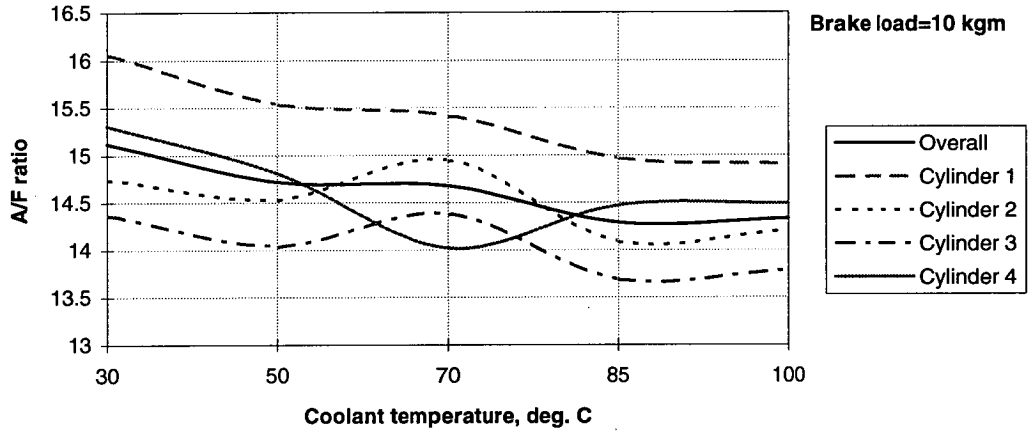

f)

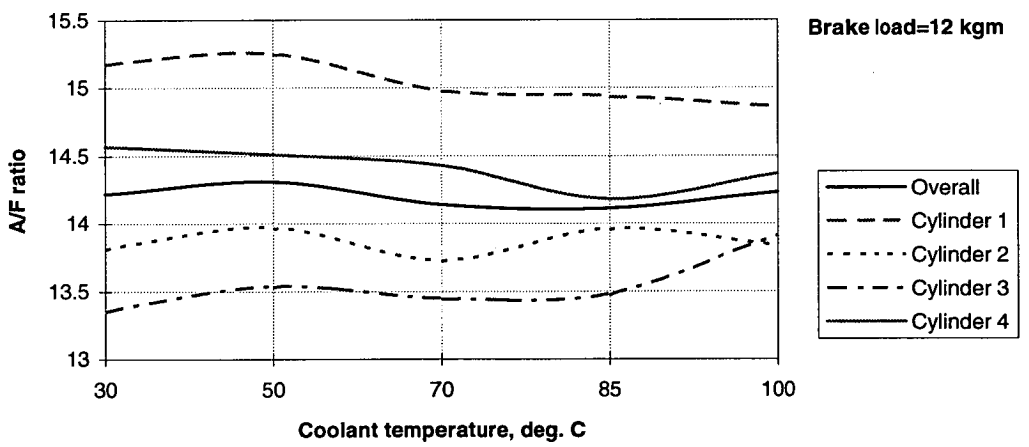

Figure 4.2-2(d,e,f) : A/F ratio in the individual cylinders at different loads and coolant temperatures 504 XN1, d) Brake load=8 kgm, e) Brake load=10 kgm, f) Brake load=12 kgm

Test 3: A/F ratio and delta A/F ratio versus inlet air temperatures at different loads, 504 XN1.
(coolant temperature $= 85 \pm 1^{o} C$, *engine speed* $= 2500 rpm$)

Table 4.2-3: Calculated data

Brake load, kgm	Heat supplied to inlet air,Watt	Inlet air temperature, degree C	Calculated A/F ratio					Delta A/F ratio	Maldistribution index
			Overall	Cylinder 1	Cylinder 2	Cylinder 3	Cylinder 4		
1.5	0	17	16.17	15.99	15.75	16.35	16.6	0.86	0.0265
	400	32	15.79	15.82	15.34	15.86	16.14	0.8	0.0254
	800	44	15.73	15.76	15.33	15.74	16.1	0.78	0.0247
	1200	55	15.58	15.6	15.2	15.58	15.93	0.73	0.0234
	1700	70	15.51	15.54	15.18	15.52	15.79	0.61	0.0197
3	0	17	15.53	15.92	15.15	15.71	15.32	0.77	0.0247
	400	31	15.83	16.02	15.32	15.92	16.05	0.72	0.0228
	800	42	15.77	15.89	15.3	15.88	16	0.7	0.0223
	1200	52	15.72	15.78	15.26	15.86	15.96	0.71	0.0225
	1700	68	15.69	15.89	15.24	15.73	15.89	0.64	0.0205
5.5	0	17	15.16	15.25	15.04	14.76	15.6	0.84	0.0276
	400	30	15.46	15.91	15.24	15.15	15.57	0.76	0.0245
	800	40	15.17	15.41	14.74	15.09	15.44	0.7	0.0229
	1200	50	15.06	15.33	14.67	14.95	15.29	0.66	0.0219
	1700	65	14.87	15.08	14.49	14.77	15.13	0.65	0.0217
8	0	17	14.53	15.08	14.64	14.02	14.4	1.06	0.0363
	400	28	14.99	15.59	14.63	14.6	15.15	1	0.0332
	800	39	14.98	15.54	14.66	14.63	15.1	0.91	0.0305
	1200	48	14.89	15.31	14.39	14.56	15.3	0.92	0.0308
	1700	61	14.81	15.19	14.32	14.54	15.2	0.88	0.0297
10	0	17	14.29	14.96	14.08	13.68	14.47	1.28	0.0448
	400	26	14.75	15.02	14.18	14.33	15.48	1.3	0.044
	800	35	14.58	15.19	14.36	13.97	14.82	1.22	0.0418
	1200	46	14.78	15.25	14.64	14.1	15.15	1.15	0.0388
	1700	60	14.57	15.2	14.33	14	14.73	1.2	0.0412
12	0	17	14.11	14.83	13.47	13.95	14.18	1.36	0.048
	400	25	14.39	15.23	14.1	13.94	14.3	1.3	0.045
	800	35	14.39	15.16	13.92	14.13	14.33	1.24	0.0431
	1200	47	14.2	14.98	13.72	13.89	14.22	1.26	0.0445
	1700	57	14.21	14.89	14.21	13.64	14.11	1.26	0.0442

a)

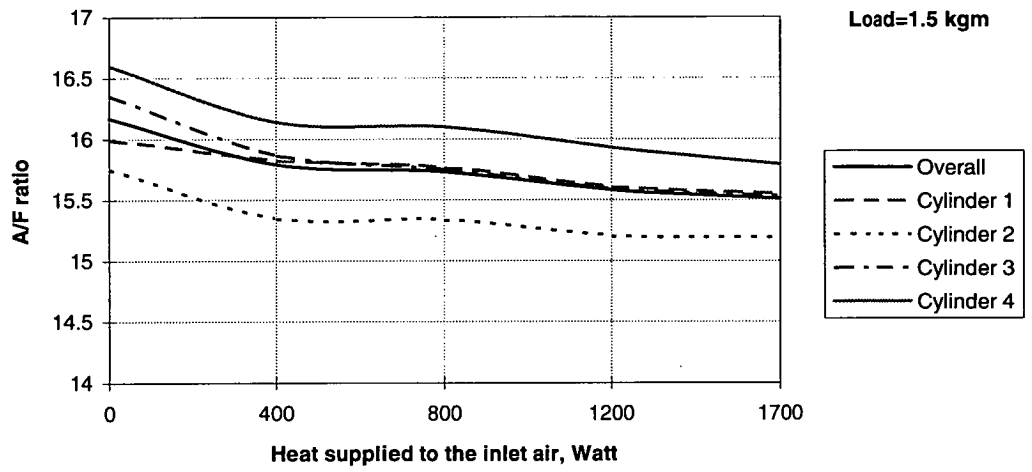

b)

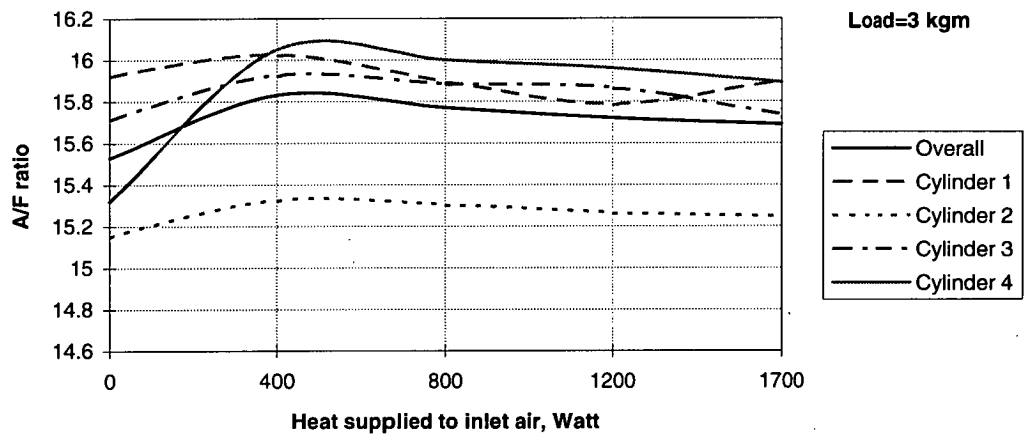

c)

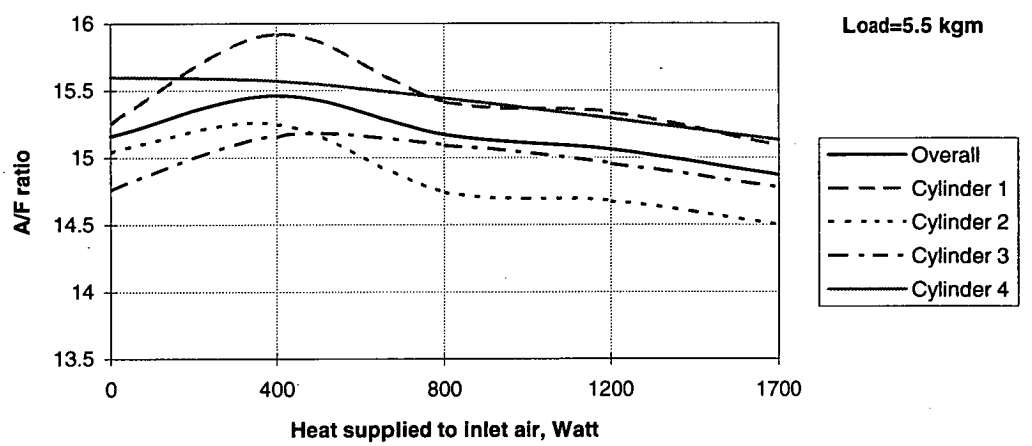

Figure 4.2-3(a,b,c) : A/F ratio in the individual cylinders with different degrees of inlet air heating 504 XN1, a) Load=1.5 kgm, b) Load=3 kgm, c) Load=5.5 kgm.

d)

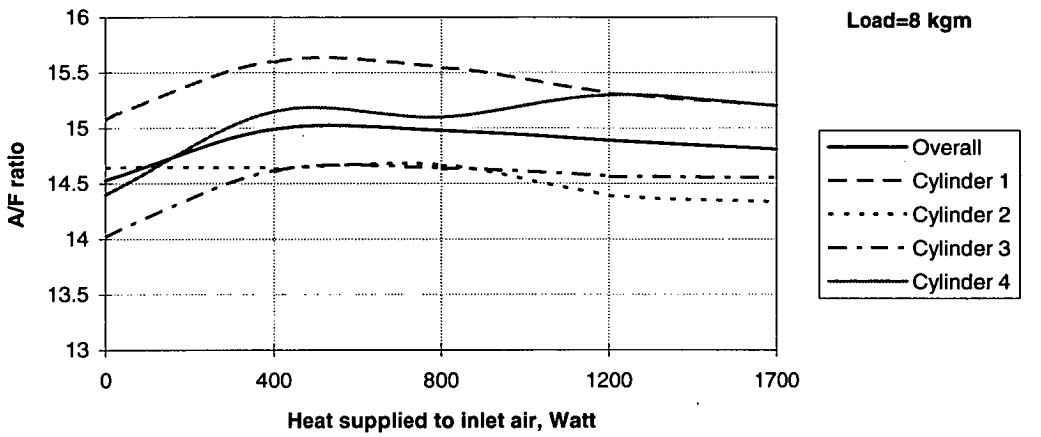

e)

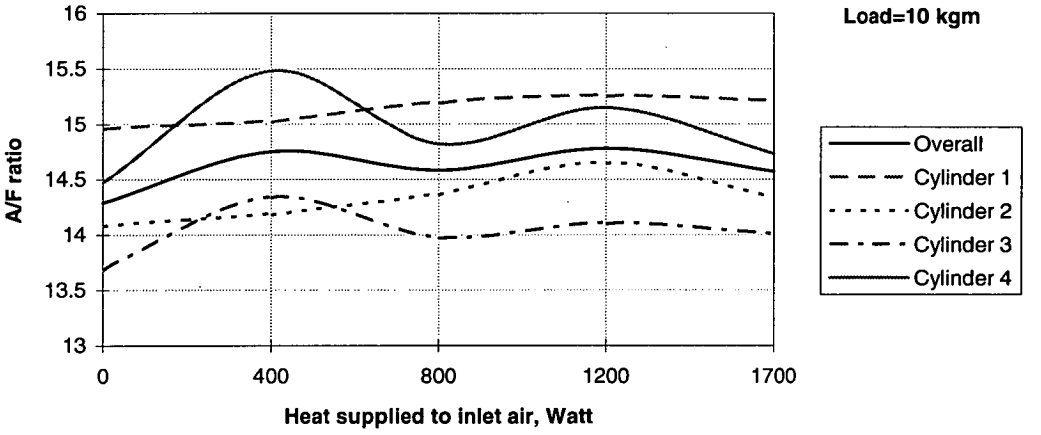

f)

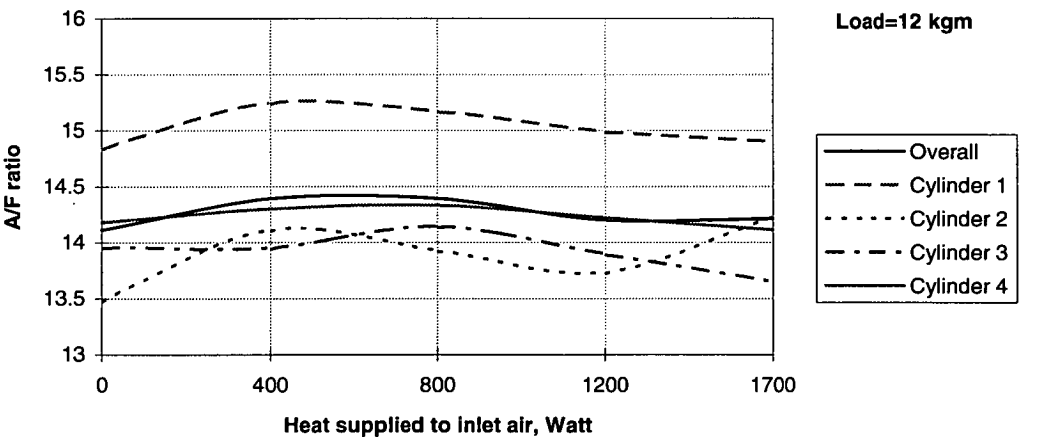

Figure 4.2-3(d,e,f): A/F ratio in the individual cylinders with different degrees of inlet air heating (504 XN1) n=2500 rpm, d) Load=8 kgm, e) Load=10 kgm, f) Load=12 kgm.

b) Results of experimental data processing on the Peugeot 504 XN2 engine

Test 1: A/F ratio and delta A/F ratio versus load at different engine speeds, 504 XN2 engine.
(coolant temperature $= 85 \pm 1^{o} C$*)*

Table 4.2-4: Calculated data

Engine speed, rpm	Brake load, kgm	Overall measured A/F ratio	Calculated A/F ratio					Delta A/F ratio	Maldistri-bution index
			Overall	Cylinder 1	Cylinder 2	Cylinder 3	Cylinder 4		
1000	1.5	15.82	15.91	15.53	16.01	15.87	16.23	0.7	0.022
	3	16	16.06	15.97	16.18	15.81	16.28	0.46	0.0144
	5.5	15.91	16.02	15.88	15.96	16.01	16.23	0.35	0.0109
	8	15.75	16.07	15.95	16.32	16.03	15.99	0.37	0.0115
	10	15.32	15.43	15.53	15.18	15.49	15.54	0.36	0.0119
	12	13.91	14.12	14.24	13.9	14.22	14.12	0.35	0.0123
1500	1.5	15.08	15.21	15.16	14.87	15.19	15.63	0.76	0.0249
	3	15.75	16.09	15.71	16.41	16.02	16.22	0.7	0.0217
	5.5	15.81	16	15.58	16.17	16.19	16.04	0.61	0.0192
	8	15.62	15.51	15.24	15.64	15.69	15.47	0.45	0.0146
	10	15.38	15.57	15.69	15.32	15.64	15.65	0.37	0.0118
	12	13.94	14.27	13.93	14.41	14.34	14.41	0.48	0.0168
2000	1.5	14.31	14.08	13.91	13.73	14.59	14.09	0.86	0.0305
	3	15.62	15.85	15.42	16.17	16.1	15.72	0.75	0.0237
	5.5	15.86	16.12	15.7	16.24	16.15	16.4	0.71	0.0219
	8	15.64	15.81	15.41	15.88	15.97	15.97	0.55	0.0176
	10	15.09	15.35	15.02	15.48	15.47	15.41	0.46	0.015
	12	14.23	14.49	14.26	14.7	14.78	14.21	0.57	0.0198
2500	1.5	13.18	12.95	12.51	13.42	12.87	12.99	0.9	0.0348
	3	15.04	15.21	15	15.39	14.76	15.69	0.93	0.0306
	5.5	15.78	15.86	15.35	16.15	15.76	16.17	0.82	0.0258
	8	15.43	15.57	15.18	15.78	15.63	15.69	0.6	0.0193
	10	14.87	14.91	14.73	15.23	14.97	14.71	0.52	0.0175
	12	13.7	13.84	13.55	13.83	14.15	13.85	0.6	0.0218
3000	1.5	13.56	13.73	13.48	14.27	13.82	13.37	0.9	0.0328
	3	15.47	15.55	15.1	16.01	15.45	15.65	0.91	0.0293
	5.5	15.5	15.43	14.97	15.9	15.47	15.39	0.93	0.0302
	8	15.32	15.67	15.22	16.07	15.72	15.68	0.85	0.0271
	10	15.19	15.41	15.26	15.79	15.5	15.1	0.69	0.0223
	12	14.62	15.01	14.75	15.2	15.37	14.72	0.65	0.0216

a)

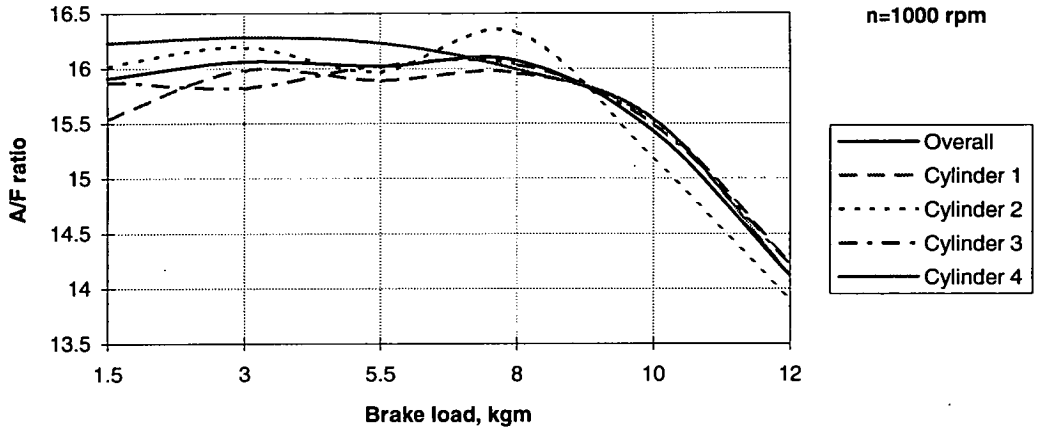

b)

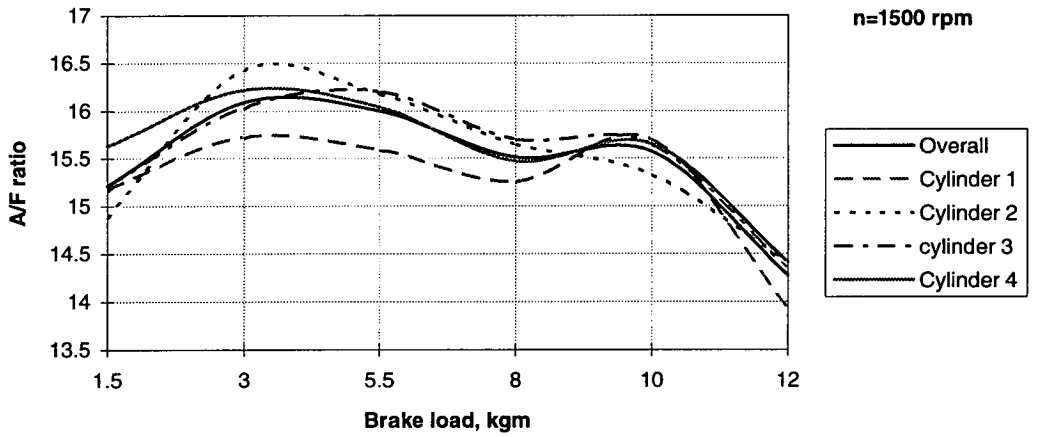

c)

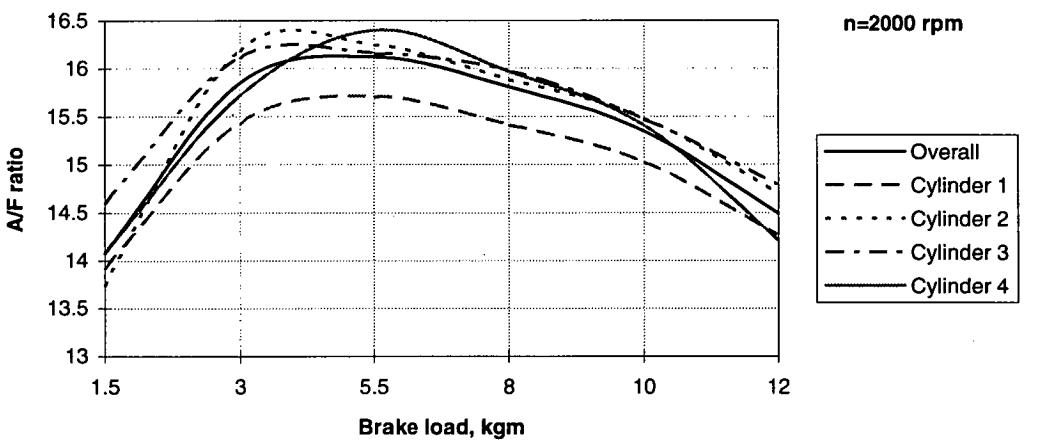

Figure 4.2-4(a,b,c): A/F ratio in the individual cylinders at different engine loads and speeds (504 XN2 engine)
a) n=1000 rpm, b) n=1500 rpm, c) n=2000 rpm

d)

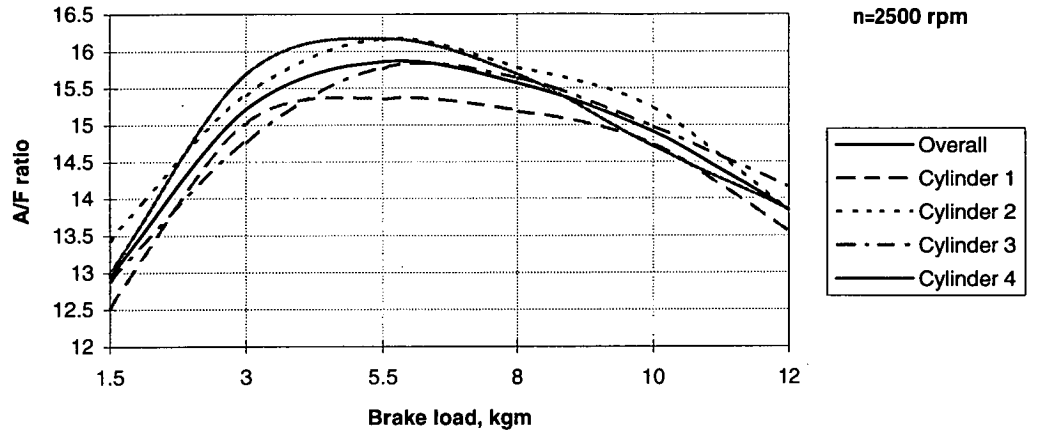

e)

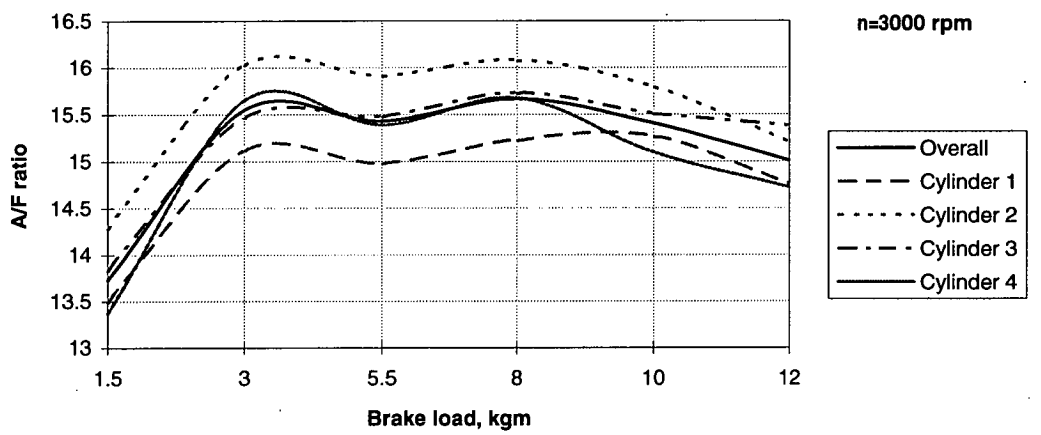

Figure 4.2-4(d,e): A/F ratio in the individual cylinders at different engine loads and speeds (504 XN2 engine)
d) n=2500 rpm, e) n=3000 rpm,

Test 2: A/F ratio and delta A/F ratio versus coolant temperature at different loads (504 XN2, engine speed n=2500 rpm)

Table 4.2-5: Calculated data

Brake load, kgm	Outlet coolant temperature, C	Calculated A/F ratio					Delta A/F ratio	Maldistribution index
		Overall	Cylinder 1	Cylinder 2	Cylinder 3	Cylinder 4		
1.5	30	12.15	11.65	12.59	11.96	12.4	0.94	0.0386
	50	12.98	12.68	12.86	12.83	13.54	0.85	0.0328
	70	13.05	12.7	13.62	12.96	12.93	0.91	0.035
	85	12.95	12.51	13.42	12.87	12.99	0.9	0.0348
	100	13.03	12.64	13.49	12.8	13.18	0.84	0.0323
3	30	12.52	12.13	12.53	12.41	13	0.87	0.0348
	50	14.91	14.61	14.88	14.73	15.41	0.8	0.0269
	70	15.22	14.85	15.66	15.07	15.32	0.81	0.0265
	85	15.21	15	15.39	14.76	15.69	0.93	0.0306
	100	15.27	14.9	15.57	15.11	15.51	0.68	0.0221
5.5	30	13.57	13.2	13.4	13.68	14.02	0.82	0.0304
	50	14.35	13.92	14.46	14.29	14.69	0.77	0.0269
	70	16.01	15.59	16.39	15.82	16.23	0.8	0.0251
	85	15.86	15.35	16.15	15.76	16.17	0.82	0.0258
	100	16.25	16.44	16.42	15.8	16.34	0.64	0.0197
8	30	15.43	14.8	15.62	15.58	15.7	0.9	0.0291
	50	15.31	15	15.1	15.32	15.82	0.82	0.0268
	70	15.81	15.4	15.9	15.83	16.12	0.72	0.0227
	85	15.57	15.18	15.78	15.63	15.69	0.6	0.0193
	100	15.41	14.96	15.58	15.53	15.58	0.62	0.0202
10	30	14	13.5	14.11	14.16	14.23	0.73	0.0259
	50	14.49	14.15	14.44	14.82	14.54	0.67	0.0231
	70	14.87	14.59	15.12	14.82	14.95	0.53	0.0179
	85	14.91	14.73	15.23	14.97	14.71	0.52	0.0175
	100	14.86	14.67	15.21	14.9	14.67	0.55	0.0183
12	30	13.66	13.4	13.66	13.66	13.91	0.51	0.0187
	50	13.99	13.7	13.96	13.98	13.32	0.62	0.0222
	70	13.92	13.6	13.94	13.92	14.21	0.6	0.0217
	85	13.84	13.55	13.83	14.12	13.85	0.57	0.0218
	100	14.14	13.89	14.21	14.05	14.42	0.52	0.0185

Tolerance of coolant temperature is about $\pm 1^0 C$

a)

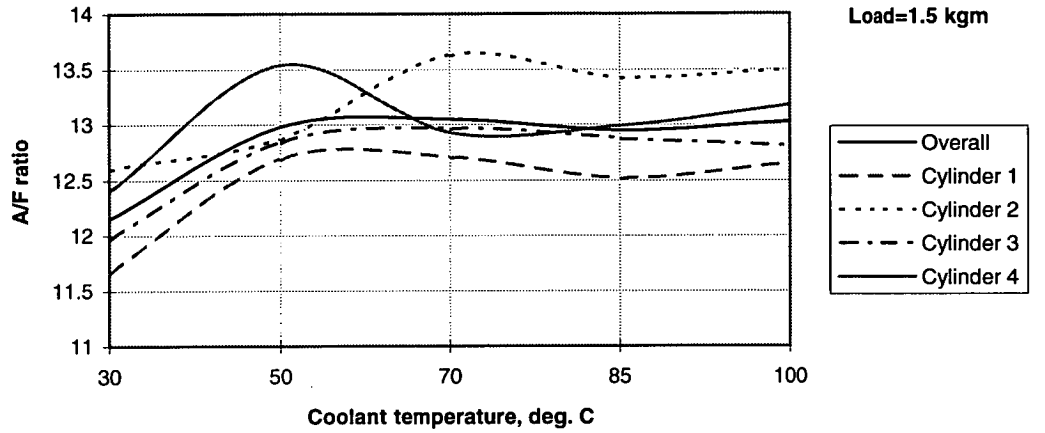

b)

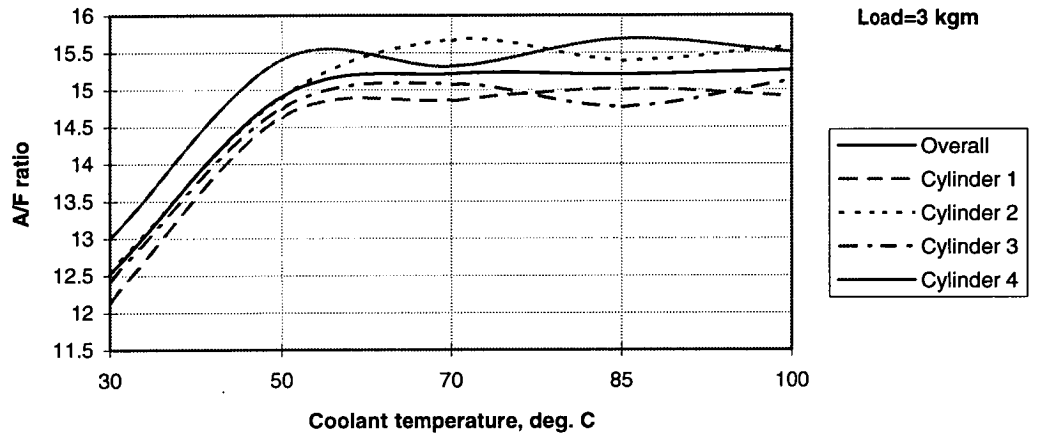

c)

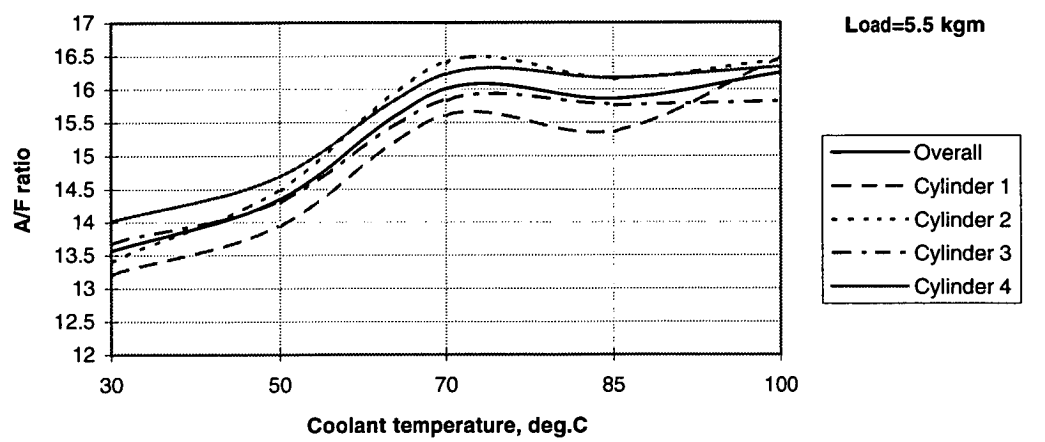

Figure 4.2-5(a,b,c): A/F ratio in the individual cylinders at different coolant temperatures and loads
504 XN2, a) Load=1.5 kgm, b) Load=3kgm, c) Load=5.5 kgm

d)

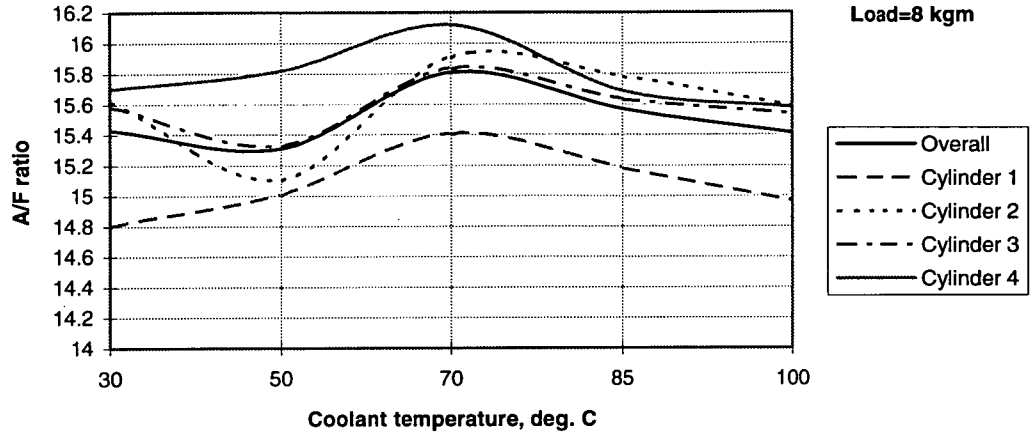

e)

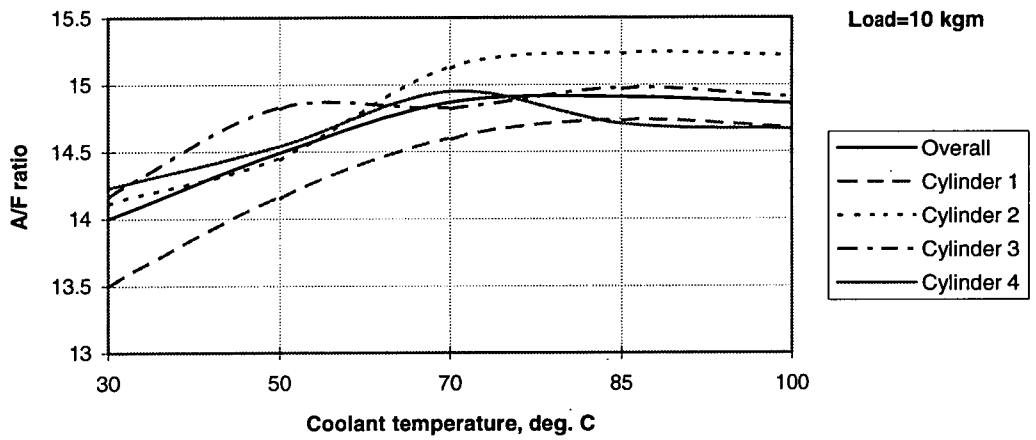

f)

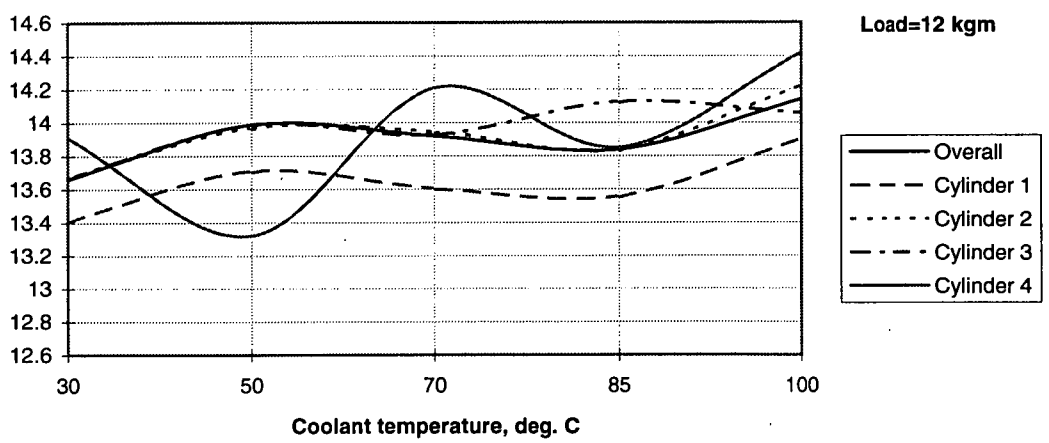

Figure 4.2-5(d,e,f): A/F ratio in the individual cylinders at different coolant temperatures and loads 504 XN2, d) Load=8 kgm, e) Load=10 kgm, f) Load=12 kgm

Test 3: A/F ratio and delta A/F ratio versus inlet air temperatures at different loads, 504 XN2
(coolant temperature $= 85 \pm 1^{o} C$, *engine speed* $= 2500 rpm$)

Table 4.2-6: Calculated data

Brake load, kgm	Heat supplied to inlet air, Watt	Inlet air temperature, degree C	Calculated A/F ratio					Delta A/F ratio	Maldistribution index
			Overall	Cylinder 1	Cylinder 2	Cylinder 3	Cylinder 4		
1.5	0	16.5	12.95	12.51	13.42	12.87	12.99	0.9	0.0348
	400	40	13.92	13.39	14.03	14.26	13.99	0.87	0.0312
	800	47	13.91	13.66	14.46	13.68	13.84	0.8	0.0289
	1200	60	13.88	13.5	14.34	13.89	13.79	0.84	0.0302
	1700	75	13.7	13.12	13.99	13.78	13.93	0.87	0.0318
3	0	16.5	15.21	15	15.39	14.76	15.69	0.93	0.0306
	400	39	15.99	15.57	16.42	15.82	16.15	0.85	0.0265
	800	46	15.86	15.4	16.26	15.77	16.01	0.86	0.0272
	1200	58	15.7	15.23	16.09	15.63	15.84	0.87	0.0276
	1700	73	15.6	15.14	15.68	15.61	15.95	0.82	0.0262
5.5	0	16.5	15.86	15.35	16.15	15.76	16.17	0.82	0.0258
	400	37	16.02	15.56	15.99	16.28	16.23	0.72	0.0225
	800	45	15.99	15.43	16.13	16.23	16.15	0.8	0.025
	1200	57	15.86	15.32	16.13	15.99	16.01	0.81	0.0255
	1700	70	15.79	15.29	16.07	15.88	15.93	0.78	0.0247
8	0	16.5	15.57	15.17	15.78	15.63	15.69	0.6	0.0193
	400	33	15.44	15.18	15.39	15.35	15.83	0.65	0.0209
	800	43	15.37	15.2	15.38	15.17	15.71	0.55	0.0178
	1200	55	15.32	15.07	15.31	15.21	15.67	0.6	0.0196
	1700	66	15.17	14.84	15.34	15.07	15.42	0.58	0.0191
10	0	16.5	14.91	14.73	15.23	14.97	14.71	0.52	0.0175
	400	31	15.08	14.76	15.28	15	15.28	0.51	0.0172
	800	42	14.97	15	14.75	14.81	15.3	0.55	0.0182
	1200	53	14.64	14.62	14.38	14.54	15.01	0.64	0.0217
	1700	64	14.4	14.49	14.12	14.38	14.6	0.48	0.0168
12	0	16.5	13.85	13.55	13.83	14.15	13.85	0.6	0.0216
	400	31	14.03	13.84	14.18	13.78	14.34	0.57	0.0201
	800	40	13.95	13.71	14.11	14.11	13.66	0.65	0.0233
	1200	52	13.38	13.16	13.51	13.15	13.73	0.58	0.0217
	1700	60	12.91	12.73	12.69	12.94	13.27	0.58	0.0224

a)

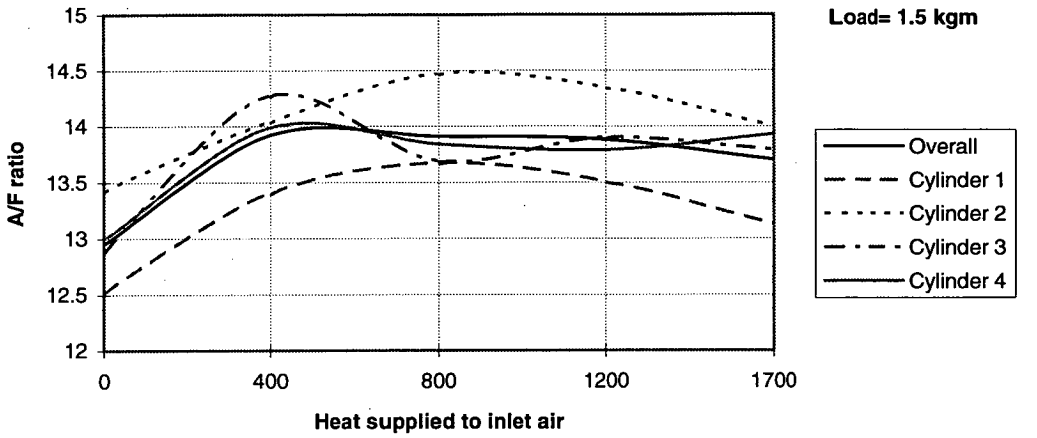

b)

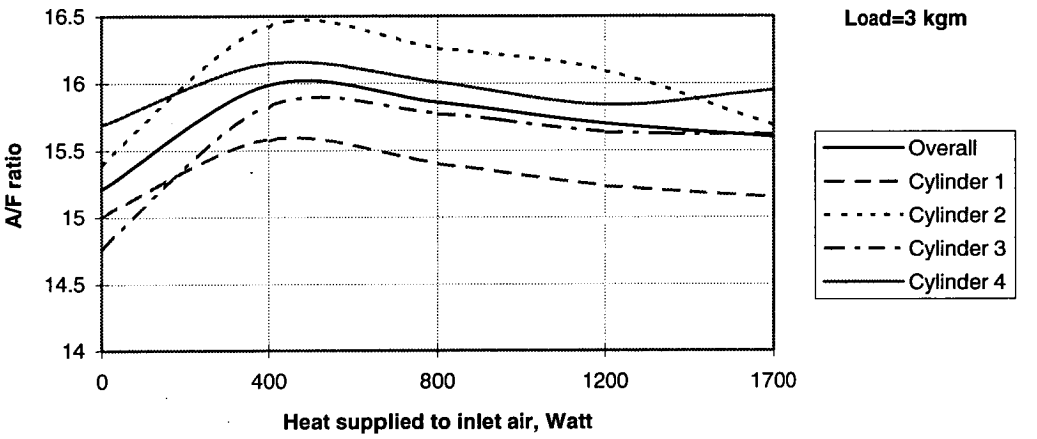

c)

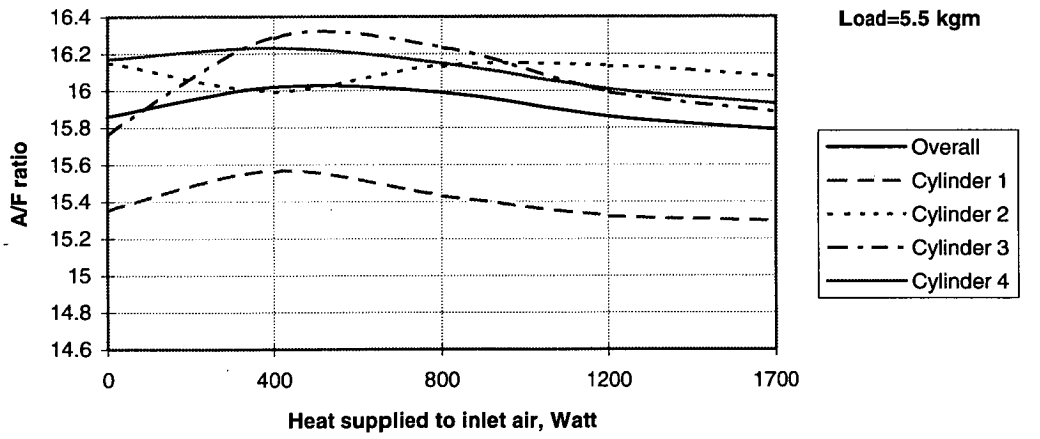

Figure 4.2-6 (a,b,c): A/F ratio in the individual cylinders with different degrees of inlet air heating (504 XN2)
a) Load=1.5 kgm, b) Load=3 kgm, c) Load=5.5 kgm.

d)

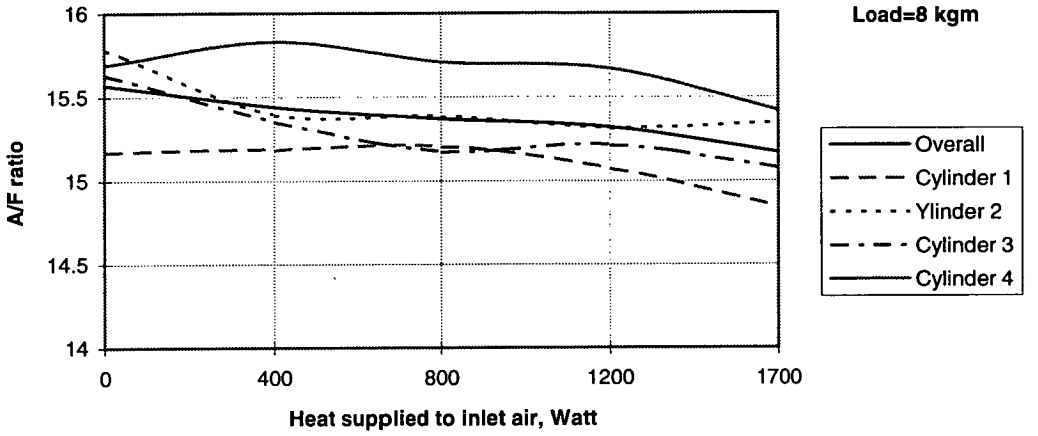

e)

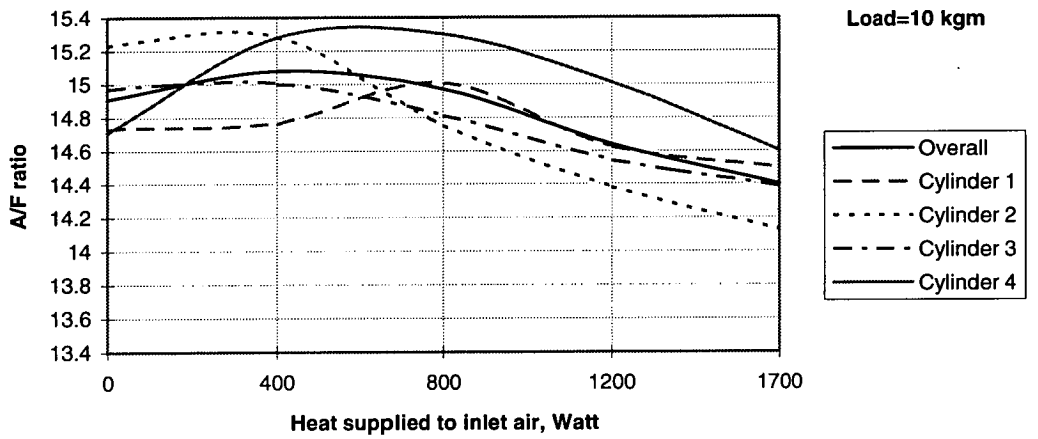

f)

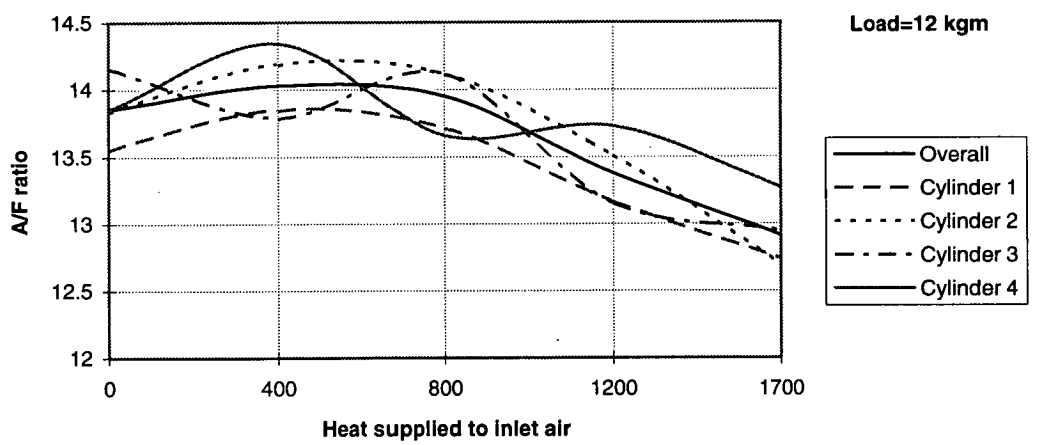

Figure 4.2-6 (d,e,f): A/F ratio in the individual cylinders with different degrees of inlet air heating (504 XN2)
d) Load=8 kgm, e) Load=10 kgm, f) Load=12 kgm.

c) Delta air/fuel ratio at different engine running conditions

Delta air/fuel ratio of the Peugeot 504 XN1 carburation engine.

Table 4.2-7: Delta A/F ratio versus load at different engine speeds
($Coolant\ temperature = 85 \pm 1^0\,C$)

Delta A/F ratio versus load and speed.					
Speed / Load	1000	1500	2000	2500	3000
1.5	1.38	1.12	0.95	0.86	0.82
3	1.14	1.01	0.86	0.77	0.76
5.5	0.85	0.8	0.8	0.84	0.93
8	0.85	0.85	0.9	1.06	1.21
10	0.98	1.04	1.18	1.28	1.34
12	1.7	1.46	1.39	1.36	1.38

Table 4.2-8: Delta air/fuel ratio versus degree of inlet air heating at different load
($Engine\ speed\ n = 2500\,rpm, coolant\ temperature = 85 \pm 1^0\,C$)

Delta A/F ratio versus degree of inlet air heating						
Load / Heat supply	1.5	3	5.5	8	10	12
0	0.86	0.77	0.84	1.06	1.28	1.36
400	0.8	0.72	0.76	1	1.3	1.3
800	0.78	0.7	0.7	0.91	1.22	1.24
1200	0.73	0.71	0.66	0.92	1.15	1.26
1700	0.61	0.64	0.65	0.88	1.2	1.26

Table 4.2-9:Delta air/fuel ratio versus coolant temperature at different loads, (n=2500 rpm)

Delta A/F ratio versus coolant temperature						
Load / Cooling temperature	1.5	3	5.5	8	10	12
30	1.28	1.43	1.45	1.57	1.7	1.82
50	1.22	1.14	1.24	1.35	1.51	1.71
70	1.1	1.18	1.05	1.19	1.39	1.53
85	0.86	0.77	0.84	1.06	1.28	1.36
100	0.85	0.7	0.75	0.96	1.12	1.02

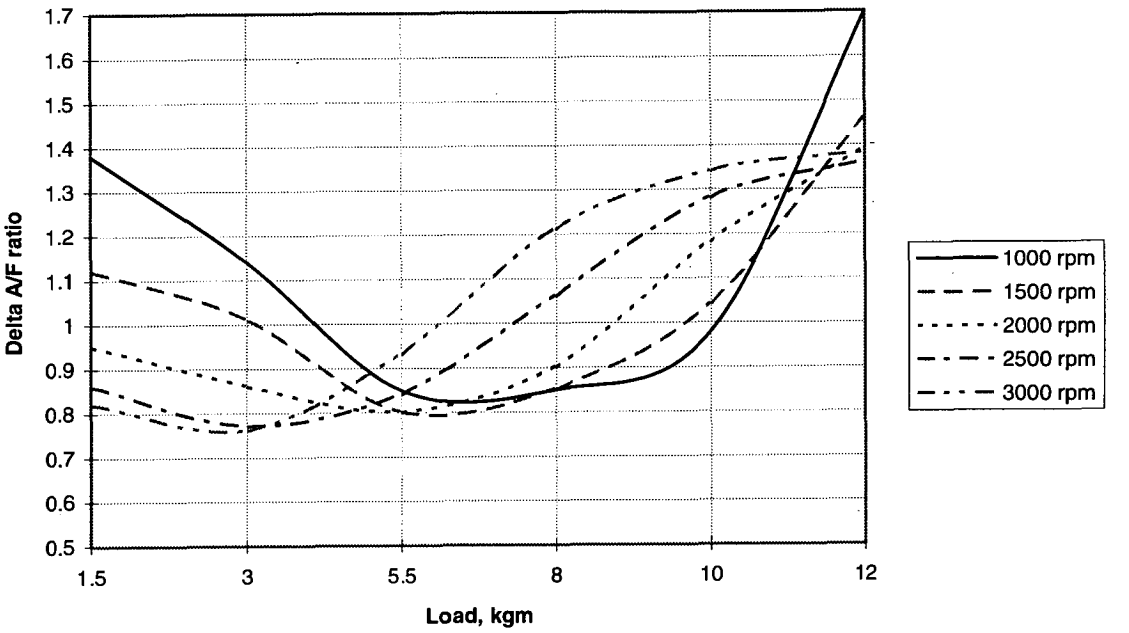

Figure 4.2-7: Delta A/Fratio versus load at different engine speeds (504 XN1 engine)

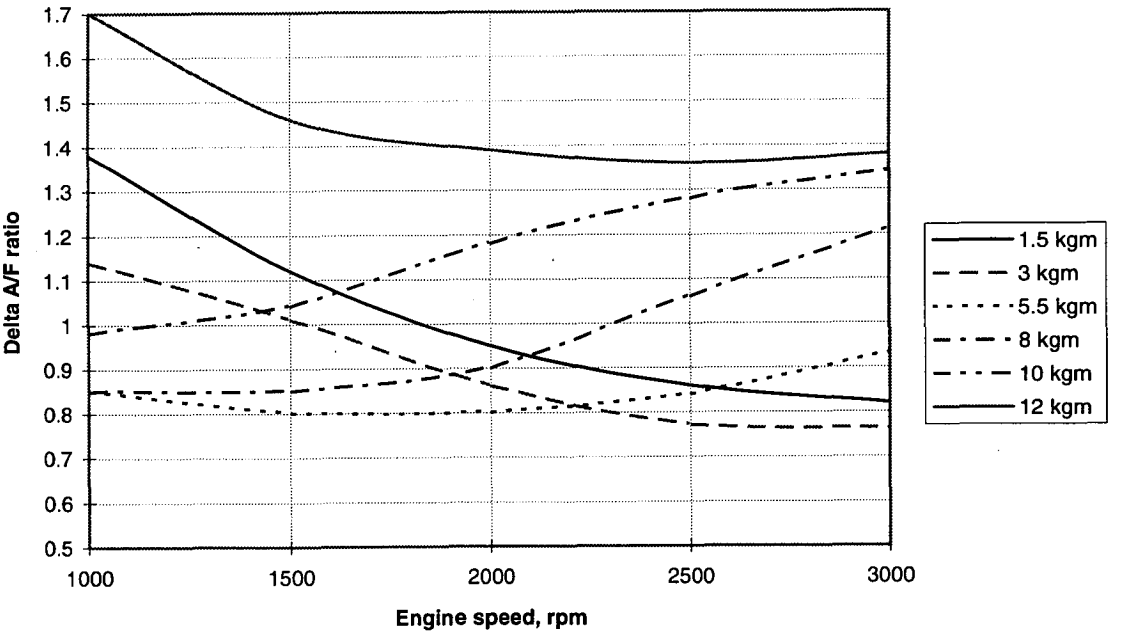

Figure 4.2-8: Delta A/F ratio versus engine speed at different loads (504 XN1 engine)

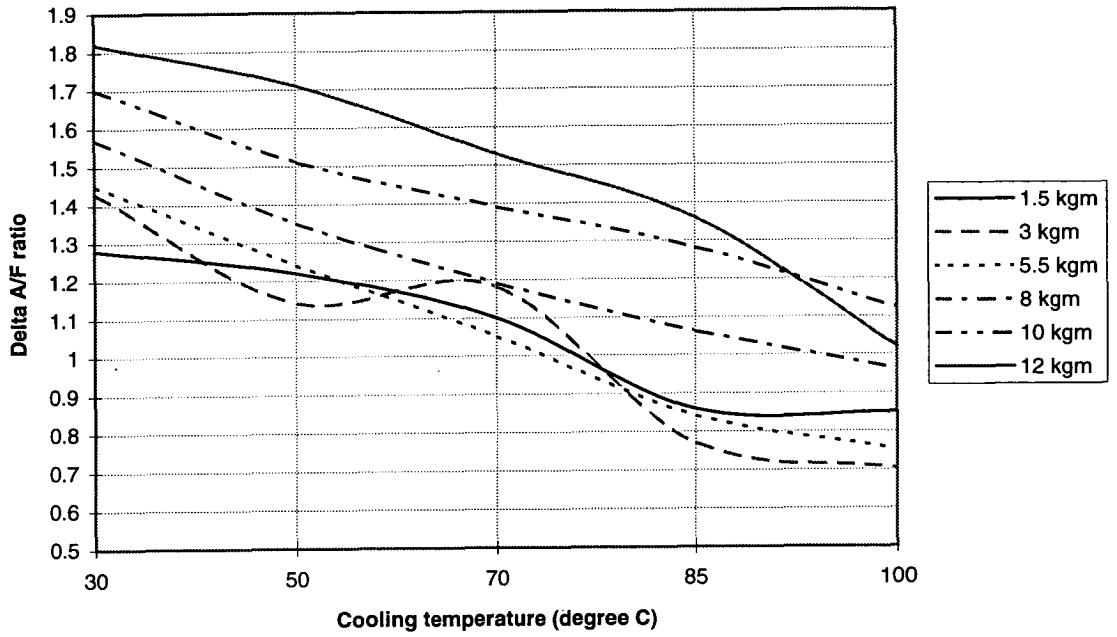

Figure 4.2-9: Delta A/F ratio versus coolant temperature at different loads (Peugeot 504 XN1 engine)

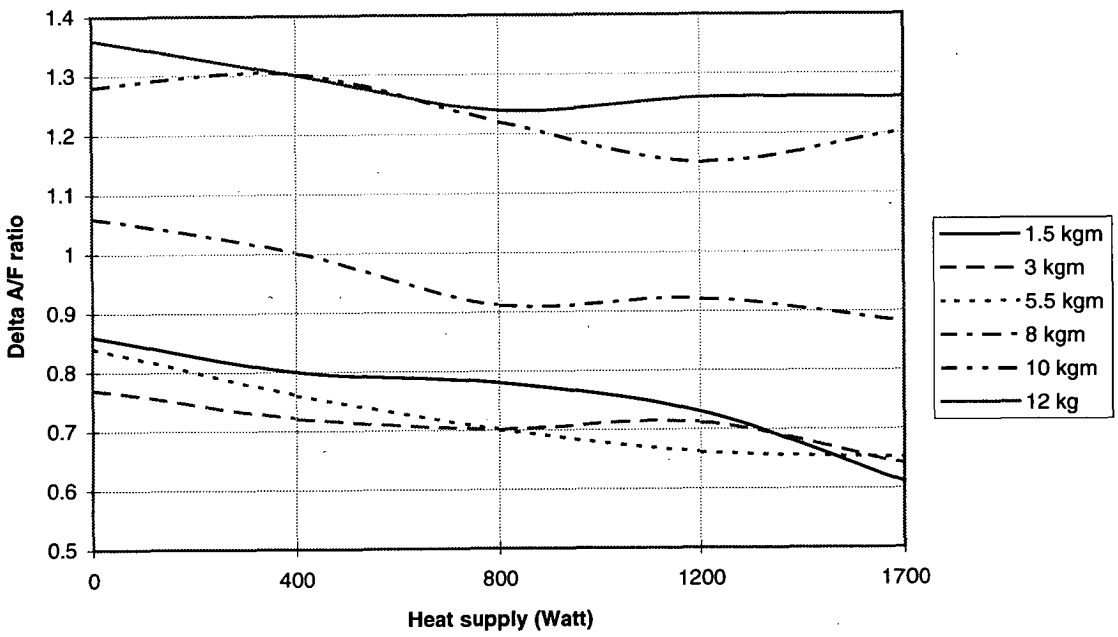

Figure 4.2-10: Delta A/F ratio versus degree of inlet air heating at different loads (504 XN1 engine)

Delta air/fuel ratio of the Peugeot 504 XN2 injection engine.

Table 4.2-10: Delta A/F ratio versus load at different engine speeds
($Coolant\ temperature = 85 \pm 1^0\,C$)

Delta A/F ratio versus load and spped.					
Speed / Load	1000	1500	2000	2500	3000
1.5	0.7	0.76	0.86	0.9	0.9
3	0.46	0.7	0.75	0.93	0.91
5.5	0.35	0.61	0.71	0.82	0.93
8	0.37	0.45	0.55	0.6	0.85
10	0.36	0.37	0.46	0.52	0.69
12	0.35	0.48	0.57	0.6	0.65

Table 4.2-11: Delta air/fuel ratio versus degree of inlet air heating at different loads
($Engine\ speed\ n = 2500\,rpm, coolant\ temperature = 85 \pm 1^0\,C$)

Delta A/F ratio versus idegree of inlet air heating						
Load / Heat supply	1.5	3	5.5	8	10	12
0	0.9	0.93	0.82	0.6	0.52	0.6
400	0.87	0.85	0.72	0.65	0.51	0.57
800	0.8	0.86	0.8	0.55	0.55	0.65
1200	0.84	0.87	0.81	0.6	0.64	0.58
1700	0.87	0.82	0.78	0.58	0.48	0.58

Table 4.2-12: Delta air/fuel ratio versus coolant temperature at different loads, (n=2500 rpm)

Delta versus cooling temperature						
Load / Cooling temperature	1.5	3	5.5	8	10	12
30	0.94	0.87	0.82	0.9	0.73	0.51
50	0.85	0.8	0.77	0.82	0.67	0.62
70	0.91	0.81	0.8	0.72	0.53	0.6
85	0.9	0.93	0.82	0.6	0.52	0.57
100	0.84	0.68	0.64	0.62	0.55	0.52

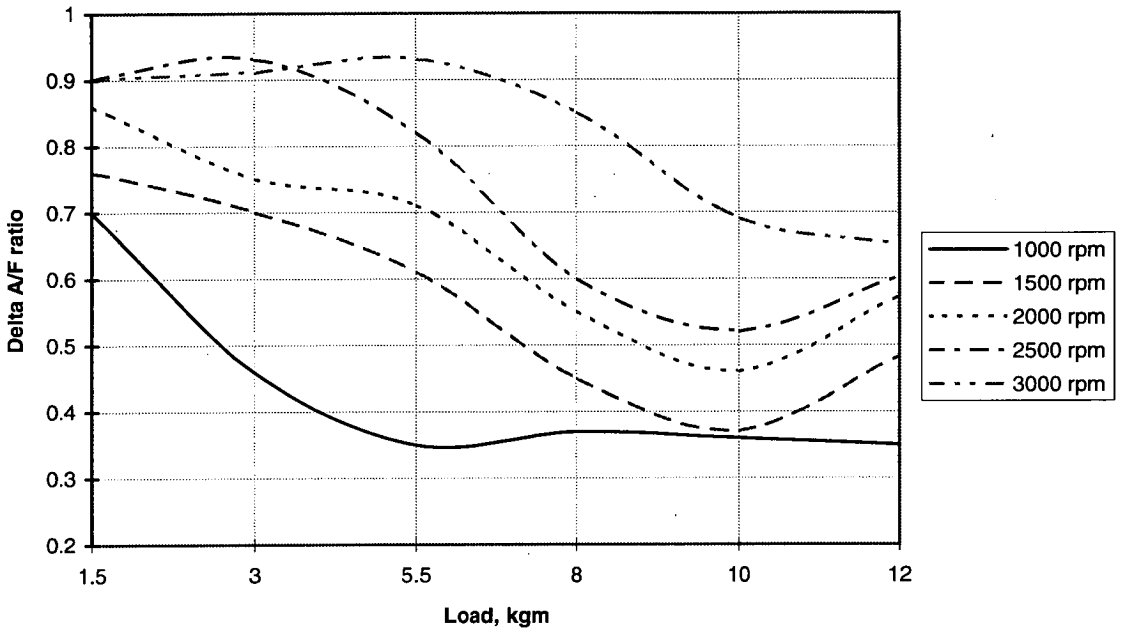

Figure 4.2-11: Delta A/F ratio versus load at different engine speeds (504 XN1 engine)

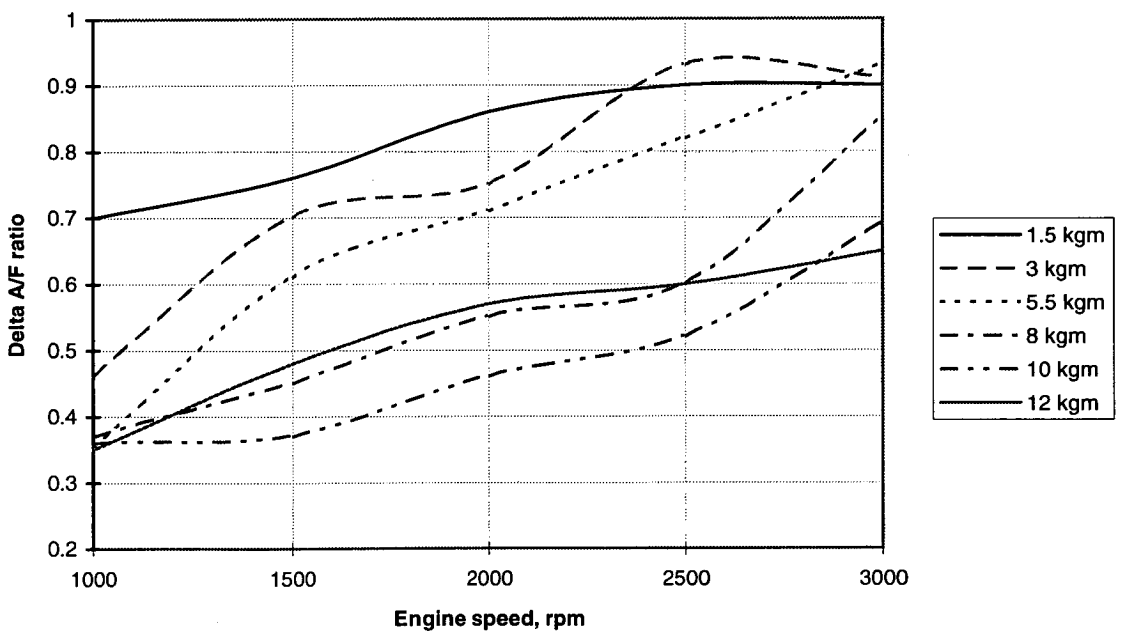

Figure 4.2-12: Delta A/F ratio versus engine speed at different loads (504 XN2 engine)

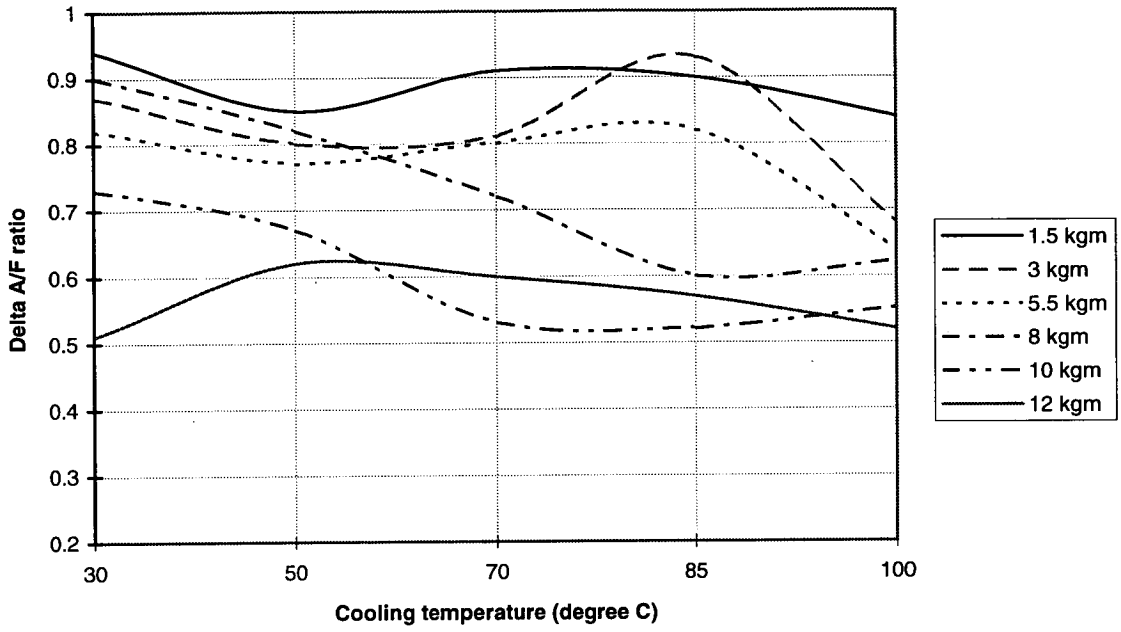

Figure 4.2-13: Delta A/F ratio versus coolant temperature at different loads (Peugeot 504 XN2 engine)

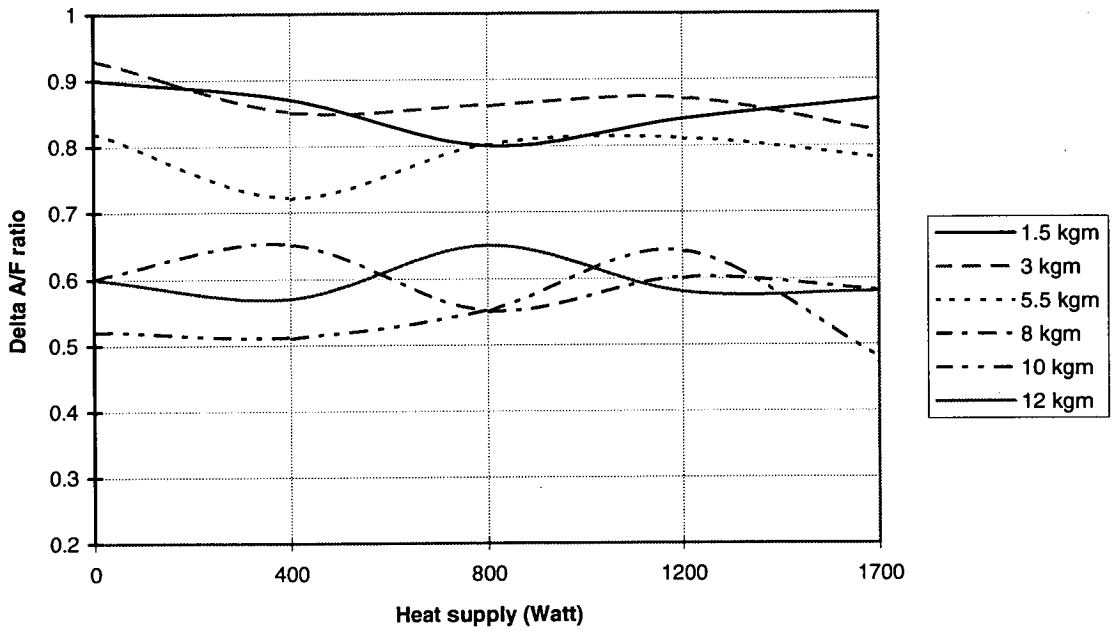

Figure 4.2-14: Delta A/F ratio versus degree of inlet air heating at different loads (504 XN2 engine)

4.3 Analysis and discussion of experimental results.

4.3.1 Accuracy of calculated results.

In test 1 for both the 504 XN1 and 504 XN2 engines, besides determinations of A/F ratio from exhaust gas analysis, overall A/F ratio was also determined by direct measurements of air flow rate and fuel flow rate to the engines. In practice, this method of determination of A/F ratio can give accurate values of A/F ratio, so comparing them with the values of A/F ratio determined by exhaust gas analysis can evaluate the accuracy of the determination of A/F ratio by the second method.

The values of A/F ratio determined by direct measurements of air flow rate and fuel flow rate and by exhaust gas analysis at different loads and engine speeds are printed in table 4.2-1 for the 504 XN1 engine and in table 4.2-4 for the 504 XN2 engine. Comparison of the values of A/F ratios determined by the two methods indicates that the discrepancies are relatively small. In effect, it can be seen from the tables that the differences between the values of A/F ratio determined by direct measurements of air and fuel flows and A/F ratio determined by exhaust gas analysis are up to 2.3% for the 504 XN1 engine and up to 2.7% for the 504 XN2 engine. The prediction of error in determination of air fuel ratio from exhaust gas analysis as presented in appendix G also indicated acceptable values of tolerance (between 1.7% and 2.1%). Therefore it can be concluded that the accuracy of the method of determination of A/F ratio from exhaust gas analysis is reasonable and the experimental data and the calculation results are accurate enough and acceptable for the present analysis.

However, the results printed in tables 4.2-1 and 4.2-4 show that in both engines the values of measured A/F ratios are usually smaller than the values of A/F ratio determined by exhaust gas analysis in all the range of load and speed. This may be due to the errors from the determinations of exhaust gas components, which can include one or more of the followings.

Firstly, in the experiment, some gas can be mixed with water trapped in the water trapper, leading to a decrease in concentrations of HC, CO, and CO_2 in the gas sample passing the analyser.

In addition, the gas line between the engine and the analyser may not be absolutely sealed, some air therefore can be drawn from outside, causing the

concentration of HC, CO, and CO_2 in the gas sample passing the analyser to be less than that in the typical exhaust gas sample from the cylinders while concentration of oxygen to be more.

The discrepancies can also come from the method of collections of experimental data. First, exhaust gas samples taken from the gas sampling tubes located at the fixed points close to the exhaust valves may not characterise the typical exhaust gas from the cylinder. In effect, as analysed earlier the mixture within a cylinder is not uniform, so exhaust gas is not uniform either. Its composition varies from time to time of the engine cycle and from point to point in the region close to exhaust ports. At a point close to the exhaust valves, exhaust gas from a cylinder has not been well mixed because of the shortage of time and room for mixing. This leads to the gas sample not typically reflecting the composition of the overall exhaust gas from a cylinder. This causes errors of determined A/F ratios by the exhaust gas analysis.

Second, experimental data successively recorded may not reflect the data at a given engine running condition. In fact, in this experiment the data at one set of engine running conditions were not recorded simultaneously, but successively during a certain time duration. During that time, the running condition can be changed a little due to the non-stability in operation of the engine. This means that the data of exhaust gas components from individual cylinders and data of measured A/F ratio are recorded at different conditions. To avoid this error, all the data needed at a certain engine running condition should be recorded simultaneously by an automatic device.

All the factors mentioned above cause not only discrepancies between the overall A/F ratio determined by direct measurement and overall A/F ratio determined from exhaust gas analysis, but also differences between A/F ratios from individual cylinders, causing errors in delta A/F ratio.

4.3.2 Air/fuel ratio in the individual cylinders.

a) A/F ratio at different engine running conditions.

A/F ratio versus load.

A/F ratios at different loads and engine speeds in the 504 XN1 engine and the 504 XN 2 engine at standard coolant temperature of the engines (85±1°C) and ambient inlet air temperature are determined in test 1.

Overall A/F ratio and A/F ratio in the individual cylinders versus load at different engine speeds are indicated in figure 4.2-1 for the 504 XN1 engine and in figure 4.2-4 for the 504 XN2 engine (in the same range of load for the two engines).

The figures show that A/F ratio decreases with load from medium load to high load. At high load (10 and 12 kgm), A/F ratio is smaller than stoichiometric A/F ratio that is equal to 14.78 in this case (as indicated in appendix B). In general, A/F ratio determined in the present experiment match the A/F ratio of the required mixture of the engines as analysed in section 1.5.

However, compared with the 504 XN1 engine, the 504 XN 2 engine has the A/F ratio versus load curves (as indicated in figure 4.2-4) closer to the required mixture of the petrol engines. That is at very low load and high load, the mixture is richer than stoichiometric mixture, and at other range of load between low load and high load the mixture is poorer (A/F ratio higher than the stoichiometric A/F ratio). This indicates that in the 504 XN2 injection engine, fuel is metered more accurately than in the 504 XN1 carburation engine to have correct mixture supplied to the engine.

A/F ratio versus coolant temperature.

A/F ratios versus coolant temperature at different engine loads are determined in test 2 and indicated in figure 4.2-2 for the 504 XN1 engine and in figure 4.2-5 for the 504 XN2 engine.

As shown in figure 4.2-2, A/F ratio in the 504 XN1 carburation engine mostly does not vary with coolant temperature whereas in the 504 XN2 injection engine, as shown in figure 4.2-5, A/F ratio increases rapidly with coolant temperature rising from 30 to 70 degree C and then increases steadily in the remained range of experiment temperature. This also indicates the more accurate metering of fuel in the injection engine than in the carburation engine to supply the rich mixture in the case of cold engine to compensate the amount of fuel not evaporating; when the engine gets hotter A/F ratio increases (mixture is then poorer). This is done in the Peugeot 504 XN2 injection engine by special devices including a temperature sensor and an enrichener. Coolant temperature is sensed by the sensor that then acts the enrichener of the mixture to adjust the quantity of the fuel supplied by the fuel injection pump. At low coolant more fuel is supplied to the engine than at high coolant temperature.

A/F ratio versus inlet air temperature.

Figure 4.2-3 and figure 4.2-6 show the dependence of A/F ratio on inlet air temperature in the 504 XN1 and 504 XN2 engines at different loads. As can be seen from these figures, in both engines inlet air temperature has small effect on A/F ratio. Increasing inlet air temperature reduces A/F ratio a little. For example, with a large amount of heat (1700 W) supplied to the inlet air, which increases inlet air temperature to 70 to 80 degree C, A/F ratios decrease by about 0.1 to 0.6 because volumetric efficiency of the engine decreases a little with increasing inlet air temperature.

b) Comparison of A/F ratios between individual cylinders.

In the Peugeot 504 XN1 carburation engine:

Calculated results of A/F ratio in the individual cylinders of the Peugeot 504 XN1 carburation engine in the three tests are presented in figures 4.2-1 to 4.2-3. Generally, the figures show that A/F ratios in the two mid cylinders (cylinder 2 and cylinder 3) are smaller than A/F ratios in the two end cylinders (cylinder 1 and cylinder 4); in other words, the two mid cylinders are supplied with richer mixture than the two end cylinders. There are some reasons for that. These may be the reasons of the shape and arrangement of the induction system of the engine. In this engine, the runner leading from the carburettor to cylinder 2 and cylinder 3 lies lower than the runners leading to cylinder 1 and cylinder 4, and faces directly to the mixture stream from the main venturi of the carburettor as illustrated in figure 4.2-15.

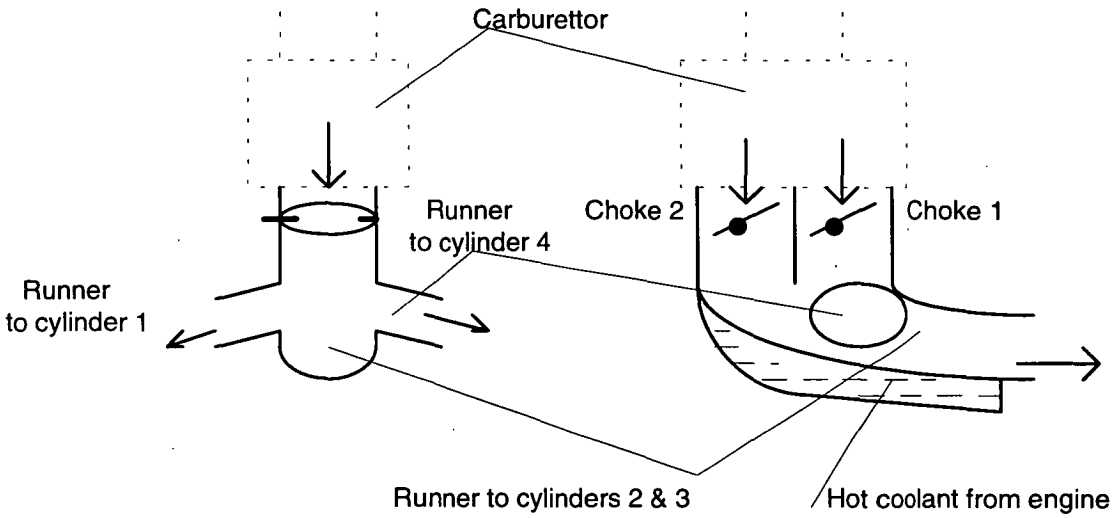

Figure 4.2-15: Diagram of a part of the induction system of the 504 XN1 engine.

In this case, mixture stream going to cylinder 2 and cylinder 3 travels along a shorter and straighter pipe than mixture stream going to cylinder 1 and cylinder 4, so due to inertia of fuel droplets, more fuel goes to cylinder 2 and cylinder 3 than to cylinder 1 and cylinder 4.

In effect, during the induction processes of cylinder 2 and cylinder 3 all the fuel supplied by the carburettor can be easily drawn to these cylinders, but for cylinder 1 and cylinder 4 it is not so. Because the mixture streams going from the carburettor to cylinder 1 and cylinder 4 have to travel through the sharp bends at the entries of the runners leading to these cylinders, some fuel droplets tend to go in straight direction due to inertia, so they are trapped at the entry of the runner leading to cylinder 2 and cylinder 3, reducing the quantity of fuel going to cylinder 1 and cylinder 4. During the induction processes of cylinder 2 and cylinder 3, the trapped fuel is drawn to these cylinders, adding to the normal fuel supplied to these cylinders. The result is that the two inside cylinders receives more fuel than the two end cylinders, and therefore its A/F ratio is smaller.

In addition, liquid fuel film has significant effects on the problem. In effect, fuel film in the induction system is mostly formed soon after the mixture stream travels through the throttle plate due to the impaction of fuel droplets on the walls of the pipe at the entries of the runners leading to different cylinders. At this region the runner leading to the two mid cylinders is lower and incliner than the runners to the two end cylinders, so the fuel film is easier to flow to the runner leading to the two mid cylinders due to its gravity. The result is that the two mid cylinders are supplied more fuel than the two end cylinders.

In the Peugeot 504 XN2 injection engine.

The calculated results as indicated in figure 4.2-4 to figure 4.2-6 show that cylinder 1 is supplied with richer mixture compared with other cylinders in most engine running conditions. For the three other cylinders, the mixture supplied to one cylinder is sometimes richer and sometimes poorer than the other two. The reason for that in this engine may be mainly the errors in manufacturing of the fuel injection pump, fuel injectors and other components of the fuel supply system, and may be uneven wear of the fuel injection pump and injectors.

4.3.3 Delta air/fuel ratio.

As analysed earlier, delta A/F ratio is used to quantitatively characterise fuel maldistribution between cylinders in an engine in the present study, maldistribution index is also calculated for additional reference.

a) Delta A/F ratio versus load.

Delta A/F ratios versus load at different engine speeds are indicated in table 4.2-7 and figure 4.2-7 for the 504 XN1 engine, and in table 4.2-10 and figure 4.2-11 for the 504 XN2 engine. Generally, the figures show that delta A/F ratio in the 504 XN2 engine is much smaller than delta A/F ratio in the 504 XN1 engine at the same level of engine load and speed. For example, at the engine speed of 3000 rpm and the range of load from 1.5 to 12 kgm, delta A/F ratio in the 504 XN2 engine varies between 0.65 and 0.93 while delta A/F ratio in the 504 XN1 engine varies between 0.76 and 1.38. The tendencies of changes of delta A/F ratio according to engine load and speed in these engine are very different. They are discussed below.

For the Peugeot 504 XN1 engine.

As can be seen from figure 4.2-7, delta A/F ratio in the 504 XN1 engine markedly changes with engine load. It decreases first with load, reaching a minimum at about 30 percent of total load, and then increases.

In the case of low load, the openings of the throttle plates are still small (for the loads lower than 30 percent, the throttle plate in choke 1 is open at about 40 percent and the opening of the throttle in choke 2 is still very small). Therefore, the throttle plates have significantly negative effects on the mixing of fuel and air in the region under them as investigated by Liimatta et al (1971) and discussed earlier in section 3.7.3. In effect, the length of the pipe between the carburettor and the entries of the runners leading to the cylinders is very short (only about 7 cm), so the fuel jets issued from the tips of the throttle plates have very little chance to mix together. At very low loads (small throttle openings), the fuel jets issued from the two tips of a throttle plate are very different; further opening the throttle plate, the fuel jets become less different and get closer to each other. That makes the mixture in the region before the entries of the runners more homogeneous. That is why the delta A/F ratio decreases when increasing load in the range of low load.

Further increasing load beyond about 50 percent (corresponding to large opening of the throttle plates), there are not clear fuel jets existing in the region between the carburettor and the entries of the runners leading to the cylinders (Liimatta et al, 1971). Therefore, in this case the throttle plate has very small effect on fuel distribution between cylinders. Fuel distribution between cylinders in this case for the 504 XN1 engine is affected mainly by the shape and arrangement of the induction system. Further opening the throttle plate makes the entry of the runner leading to cylinder 2 and cylinder 3 face more directly to the mixture stream from the carburettor, so the effect of flow dynamic of the fuel stream and inertia effect of fuel droplets and fuel film on fuel maldistribution between cylinders as discussed earlier become more significant. Therefore, increasing load beyond 50 percent leading to the increase in delta A/F ratio.

For the Peugeot 504 XN2 engine.

As indicated in figure 4.2-11, delta A/F ratio in the Peugeot 504 XN2 engine generally decreases with increasing load. The explanation for that may be as follows.

The 504 XN2 engine is equipped with the fuel injection system with pneumatic regulation (using KF5 injection pump), which employs the vacuum in the inlet manifold to ensure optimum air-fuel metering at all engine loads and speeds. Changing load is carried out by changing the air throttle openings but the air throttle is not linked mechanically to the injection pump. The control of the injection pump is obtained through the vacuum present in the inlet manifold, which in turn depends on the opening of the air throttle.

At low load (corresponding to a small air throttle opening), the vacuum present in the inlet manifold is high, so small variations of engine speed due to the unstable operation of the engine can cause significant pressure pulsations in the intake manifold. This may have a significant effect on the pneumatic controller of the fuel injection pump because the pressure regulator usually has a certain delay in its operation. This can lead to the pulsations of fuel pressure in the fuel injection pump and of the instantaneous pressure difference across the fuel injectors. The result is that the quantities of fuel supplied by the injectors may be pulsated and become different between cylinders.

In addition, at low load the relative effects of the error in manufacture and effect of uneven wear of the fuel injection pump and fuel injectors on the

inequality of fuel supplied from the injectors become more significant than in the case of high load. Therefore, the delta A/F ratio is high at low load and decreases with increasing load.

Summary:

As analysed above, the main factor causing fuel maldistribution in the 504 XN1 engine is the shape and arrangement of the induction system of this engine. This is an inevitable factor causing fuel maldistribution in carburation engines as mentioned in section 2. In the 504 XN2 engine, on the other hand, fuel maldistribution between cylinders may be mainly due to the error in manufacture and uneven wear of the fuel injection pump and injectors. Effects of these factors on fuel distribution can be minimised by improving the accuracy in manufacture and the operating conditions of the engine. That is why delta A/F ratio in the 504 XN1 engine is much bigger than in the 504 XN2 engine.

b) Delta A/F ratio versus engine speeds.

Delta A/F ratios at different engine speeds are indicted in table 4.2-7 and figure 4.2-8 for the 504 XN1 engine, and in table 4.2-10 and figure 4.2-12 for the 504 XN2 engine.

For the 504 XN1 engine.

Figure 4.2-8 shows that the tendency of change of delta A/F ratio against engine speed depends on the level of engine load. At low load, for example, 1.5 and 3 kgm (under about 30 percent of total load in general), delta A/F ratio decreases with increasing engine speed. In this range of load, the throttle plates have a significantly negative effect on fuel distribution as mentioned in section 3.7.3 and 4.3.2 due to the formation of different fuel jets and the bad mixing between them. With increasing engine speed, the velocities of the jets increase, creating more vortexes in the region below the throttle plates. This contributes to better mixing of fuel and air before the mixture is drawn to the different runners. Therefore the fuel distribution is improved and delta A/F ratio decreases.

At the medium range of load (8 to 10 kgm), delta A/F ratio increases with engine speed. This may be due to the increase in the dynamic effect of the stream of air and fuel droplets from the carburettor to the different runners leading to the cylinders with increasing engine speed. Effects of throttle plate become small in this range of load. Analysis for this is similar to that in the previous section. However, at high load (12 kgm), delta A/F ratio is again in

steady decrease with increasing engine speed. The reason may be that at total throttle opening, increasing engine speed increases the air velocity at the venturi of the carburettor very much, leading to a better atomisation of fuel sprayed from the fuel nozzles. Obviously, smaller fuel droplets relatively better contribute to reducing negative dynamic effect of the flow on fuel distribution.

For the 504 XN2 engine.

Figure 4.2-12 shows that delta A/F ratio in the 504 XN2 engine generally increases with engine speed in all range of load. In effect, as mentioned earlier, the 504 XN2 engine employs vacuum present in the intake manifold to control fuel metering of the fuel injection pump. At the same load, increasing engine speed increases vacuum in the intake manifold. High vacuum in the intake manifold causes high delta A/F ratio as mentioned in the previous section. Therefore, increasing engine speed leads to an increase in delta A/F ratio.

c) Delta A/F ratio versus coolant temperature.

In internal combustion engines at steady running conditions, coolant temperature reflects engine temperature (engine heating state). Effects of coolant temperature on delta A/F ratio is indicated in table 4.2-9 and figure 4.2-9 for the 504 XN1 engine, and in table 4.2-12 and figure 4.2-13 for the 504 XN2 engine.

For the 504 XN1 engine.

Figure 4.2-9 shows the dependence of delta A/F ratio on coolant temperature in the 504 XN1 engine at different loads and at the engine speed of 2500 rpm. It can be seen from this figure that delta A/F ratio decreases with increasing coolant temperature. For example, increasing coolant temperature from 30°C to 100°C will reduce delta A/F ratio by 0.43 at low load (1.5 kgm), and by 0.8 at high load (12 kgm). In effect, the induction system of this engine is heated by hot coolant from the engine as shown in figure 4.2-15. Therefore, increasing coolant temperature leads to an increase in the temperature of the inlet manifold, which in turn reduces liquid fuel deposit in the region before the entries of the runners leading to the cylinders due to fuel evaporation, so as discussed in sections 3.4, 3.6 and 4.3.2 the liquid fuel film effects decreases and delta A/F ratio decreases.

For the 504 XN2 engine.

As shown in figure 4.2-13, coolant temperature has little effect on delta A/F ratio in the 504 XN2 engine. Increasing coolant temperature leads to a slight

decrease in delta A/F ratio. For example, delta A/F ratio decreases by only about 0.1 to 0.2 when coolant temperature increases from 30°C to 100°C. The reason is not as in the 504 XN1 engine. In the 504 XN2 engine fuel is sprayed directly to the intake port of each cylinder so the temperature of the induction system does not affect the distribution of fuel between cylinders. The main reason may be that at higher coolant temperature the engine operates more stably, therefore as discussed in 4.3.2 vacuum pressure in the intake manifold is more stable, keeping the fuel injection pump more stable. Therefore fuel distribution is better and delta A/F ratio is lower.

d) Delta A/F ratio versus degree of inlet air heating.

For the 504 XN1 engine.

Table 4.2-8 and figure 4.2-10 show the dependence of delta A/F ratio on degree of inlet air heating in the 504 XN1 engine at different loads. Inlet air is heated by 400, 800, 1200, and 1700 W of heat supplied to reach different temperatures indicated in table 4.2-3. Figure 4.2-10 shows that delta A/F ratio steadily decreases with increasing the degree of inlet air heating. As analysed in section 2.6, heating inlet air is one of the methods of supplying heat to fuel droplets to accelerate their evaporation, so concentration of fuel droplets decreases with increasing inlet air heating. Therefore, as discussed in section 4.3.2, this reduces negative effects of fuel droplets on fuel distribution between cylinders. This means that delta A/F ratio decreases with increasing inlet air heating. In the present study, the maximum air heating is only 1700W that increases inlet air temperature by about 53°C at the load of 1.5 kgm (seen from table 4.2-3), which reduces delta A/F ratio by 0.25. At higher load (12 kgm) the air mass flow rate is higher, so with the same heat supplied the inlet air temperature increases by only 40°C, which reduces delta A/F ratio by 0.1.

For the 504 XN2 engine.

Table 4.2-11 and figure 4.2-14 present effect of inlet air heating on delta A/F ratio in the 504 XN2 engine. The figure shows that delta A/F ratio in this engine almost does not change with inlet air heating in the large scale.

4.3.4 Exhaust emissions.

The test data of the two engines at different conditions presented in appendix F showed that the 504 XN2 injection engine seems to give higher concentrations of CO and HC than the 504 XN1 carburation engine, particularly at low coolant

temperature. There are some reasons for that. First, the mixture supplied in the 504 XN2 was adjusted to be richer than mixture supplied in the 504 XN1 engine (A/F ratios in the 504 XN2 are about 0.2 to 1 unit smaller than A/F ratios in the 504 XN1 engine). Another reason is that relative quantity of liquid fuel introduced into the cylinders may be bigger in the 504 XN2 engine than in the 504 XN1 engine. In effect, in the 504 XN2 engine, fuel is sprayed into the intake port, so at the opening time of the intake valve most of the liquid fuel sprayed can be drawn directly from the injector to the cylinder. In the 504 XN1 engine, fuel has more time to evaporate in the intake manifold than in the 504 XN2 engine.

4.4 Summary.

The following main points are summarised from the results of the investigation of fuel distribution between cylinders of petrol engines.

The investigation was conducted on the two Peugeot engines, 504 XN1 carburation engine and 504 XN2 multi-point injection engine, at different conditions using the method of determination of A/F ratio by exhaust gas analysis.

The result showed that the use of the method of determination of A/F ratio in the individual cylinders from exhaust gas analysis for the purpose of evaluation of fuel distribution between cylinders of a multi-cylinder petrol engine is convenient.

Delta A/F ratio is significantly dependent on engine running conditions (engine speed and load)

Delta A/F ratio in the Peugeot 504 XN2 injection engine is much smaller than that in the Peugeot 504 XN1 carburation engine (delta A/F ratio range of 0.35 to 0.93 compared with delta A/F ratio range of 0.76 to 1.7) at normal running conditions.

In the 504 XN1 engine, the two mid cylinders are usually supplied with richer mixture than the two end cylinders. Heating the intake manifold is a good way to improve fuel distribution in this engine. Heating inlet air is less effective for this purpose.

In the 504 XN2 engine, the arrangement of the induction system seems not to affect delta A/F ratio. Fuel distribution may be most affected by the fuel injection pump and fuel injectors. Heating has significant effect on A/F ratio but it is found not very effective on improving fuel distribution in this engine.

The use of two engines that are the same in size and arrangement but equipped with different types of fuel supply systems (carburation and multi-point injection systems) in the present investigation indicated to be the most convenient method to investigate fuel distribution between the cylinders of petrol engines and the factors influencing it.

5. Conclusions and recommendations.

5.1 General conclusion.

The following conclusions can be drawn form the present study.

Deposition of liquid fuel in the intake manifold of engines.

In carburation and single point injection engines, a large amount of liquid fuel deposits in the intake manifolds as wall fuel film and fuel droplets. The amount of these liquid fuel forms varies with engine running conditions and with the air flow pulsation in the intake manifolds and depends on the shape of the intake manifolds. The liquid fuel is poorly distributed into different cylinders, causing maldistribution of mixture between cylinders and inhomogeneity of the mixture within a cylinder. During transient conditions, the deposition of fuel in the intake manifolds causes A/F excursion in the engines.

In multi-point injection engines, fuel is sprayed to the back of the exhaust valves so the deposition of liquid fuel in the intake manifolds and its negative effect on fuel distribution between cylinders is much less than that in carburation and single point injection engines.

Fuel evaporation in the intake manifolds.

In carburation and single point injection engines most of the fuel supplied at the throttle evaporates in the intake manifold. Evaporation rate depends much on heat transfer to fuel film and fuel droplets. Any methods to increase heat transfer to fuel in the intake manifolds, eg. heating intake manifold, inlet air heating, or atomising fuel, can increase fuel evaporation rate. Increasing fuel evaporation rate reduces fuel maldistribution between cylinders in multi-cylinder engines.

In multi-point injection engines, fuel evaporation is mostly from fuel film at the intake port and back of the exhaust valves. Evaporation rate is much dependent on the injection timing. Injecting fuel to the back of the intake valves before

their open is an effective way to increase fuel evaporation in this region. In these engines fuel evaporation rate has little effect on fuel distribution between cylinders.

Fuel distribution between cylinders.

Fuel distribution between cylinders in multi-point injection engines is much better than that in carburation and single point injection engines. Comparing the fuel distributions between the two investigated engines, the main causes of fuel maldistribution between the cylinders of petrol engines in general can be confirmed as follows.

In carburation and single point injection engines, fuel distribution depends much on the shape and arrangement of the induction system and fuel evaporation in the intake manifold. Asymmetric and sharp bend manifolds have significantly negative effects on fuel distribution between cylinders. The cylinders closer to the throttle body or the carburettor with straighter runners usually receive richer mixture than other cylinders.

Any method to increase fuel evaporation rate in the intake manifolds (eg. heating the intake manifold, inlet air and fuel, or atomising fuel etc.) and to increase good mixing of fuel and air immediately beneath the throttle plate can reduce the above effects and improve fuel distribution between cylinders. Heating the intake manifold is the best way of heating for this purpose.

In multi-point injection engines, the arrangement of the intake manifold and heating indicate little effect on fuel distribution between cylinders. The main reasons for fuel maldistribution between cylinders in the engines may be from the fuel injection pump and the way of its control, injectors, and other components of the injection system.

In general, it can be concluded that multi-point injection systems can meter fuel supplied to each cylinder more accurately and more equally than carburation and single point injection systems to get correct mixture ratio in a cylinder and uniform distribution of the mixture between cylinders. In other words, in multi-point injection engines, it is easier to control mixture supplied to the cylinders at different conditions for optimum engine operations than in carburation and single point injection engines.

5.2 Recommendations.

As discussed previously, the method applied in the present investigation of fuel distribution between cylinders of petrol engines is appropriate and convenient to achieve the objective. The results are found acceptable. However, they could have been better if all the possible sources of errors mentioned earlier had been eliminated. Possible changes to improve the experiments are as follows.

- To reduce transient time when switching the valve from one cylinder to the other to sample exhaust gas from each cylinder, the orifices of the switch valve should be larger than the diameter of the connecting tubes. The gas line should be as short as possible, and the valve should be located close to the gas analyser.
- To take good exhaust gas samples, it is best to replace the current exhaust manifold by a new one that has 4 longer branches, and the gas sampling tubes are located somewhere far from the exhaust ports and far from the common pipe as shown in the diagram below.

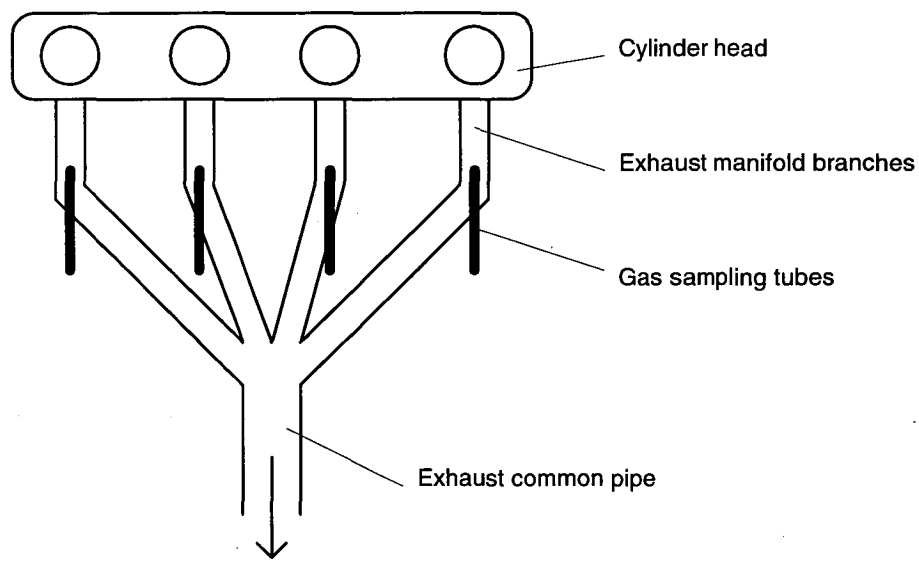

- It should be better to use one type of petrol for all the tests in the two engines.

Suggestions for further research.

This project can be extended for further research of the nature of mixture formation and distribution in petrol engines. The following works can be done

based on the potential of the facility available in the Thermodynamics Laboratory.

Experiments.

- Measurement of fuel film flow rate in the intake manifold of a carburation engine and study its effects on fuel distribution and engine performance by removing the fuel film from the stream to the cylinders, using a separator located at the intake port of the engine.
- Increasing fuel evaporation in the intake manifold of a carburation engine by local heating and study its effects on fuel distribution. For this purpose, an additional pipe is introduced into the induction system between the carburettor and the intake manifold. Fuel stream is directed by a special device to impinge onto the wall of this pipe which is heated by a heater.
- Increasing the degree of mixing of fuel and air in the intake manifold by introducing a special device to create vortex and turbulent air motion in the region immediately beneath the throttle plate and study the effects on fuel distribution.

Mathematical modes.

Establishing mathematical models of dynamic flow of fuel and air in the intake manifold.

Appendix A: Some definitions of engine operating parameters

1. Indicated mean effective pressure (imep, $\bar{p}_i$).

The net area enclosed on the pressure-volume trace or indicator diagram from an engine is the indicated work (Wi) done by the gas on the piston. The imep is a measure of the indicated work output per unit swept volume. It is independent of the size and number of cylinders in the engine and engine speed. The imep is defined as

$$\text{imep, } \bar{p}_i = \frac{\text{indicated work output (Nm) per cylinder per mechanical cycle}}{\text{Swept volume per cylinder (m}^3\text{)}}, \quad \text{N/m}^2$$

In a four-stroke cycle of naturally aspirated engines the negative work occurring during the induction and exhaust strokes is termed the pumping loss, and has to be subtracted from the positive indicated work of the other strokes. When an engine is throttled the pumping loss increases, thereby reducing the indicated work, imep and leading to reducing the engine efficiency.

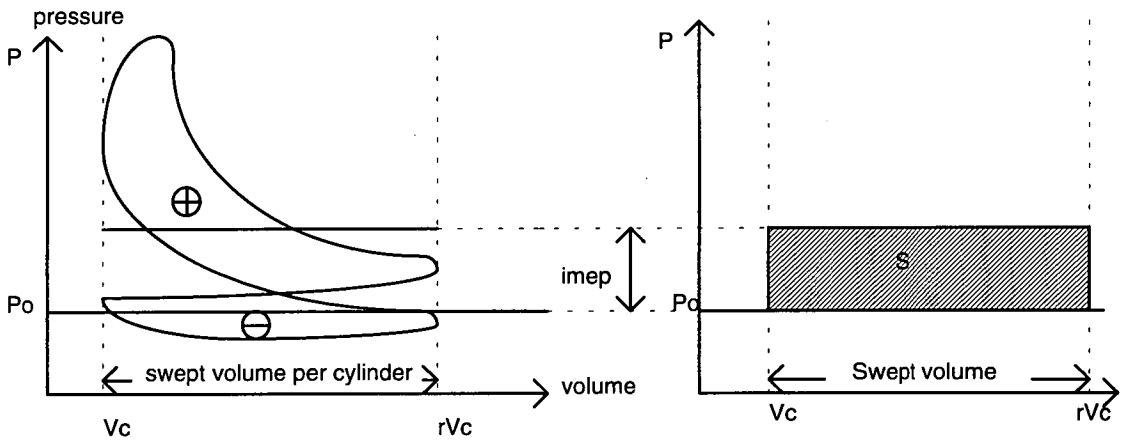

Area S = net cycle work output of a cycle in a cylinder

= The difference between the positive part and negative part of the area enclosed on the pressure-volume trace of a cycle.

$$\text{imep} = \frac{Area\ S}{Swept\ volume}$$

(*) Sometimes the imep does not always incorporate the pumping work.

2. Brake mean effective pressure (bmep), $\bar{p}_b$.

The brake mean effective pressure is defined as

$$\bar{p}_b = \frac{\text{brake work output (Nm) per cylinder per mechanical cycle}}{\text{swept volume per cylinder (m}^3\text{)}}, \text{ N /m}^2$$

Where brake work output per cylinder per mechanical cycle is calculated from the brake work output of an engine, which is the work output measured by a brake dynamometer. Bmep is a measure of work output from an engine, and not of pressure in an engine.

3. Indicated efficiency, η_i .

Indicated efficiency is used as a means of examining the thermodynamic processes in an engine. It is defined as the indicated power divided by calorific value of consumed fuel.

$$\eta_i = \frac{W_i}{\dot{m}_f \, .CV}$$

Where W_i is indicated power, kW

$\dot{m}_f$ is the mass flowrate of consumed fuel, kg/s,

CV is calorific value of fuel, kJ/kg.

4. Mechanical efficiency, η_m .

The difference between indicated work and brake work is accounted for by friction and work done in driving essential items such as the lubricating oil pump. This leads to the definition of mechanical efficiency, η_m

$$\eta_m = \frac{\text{break power}}{\text{indicated power}} = \frac{\text{bmep}}{\text{imep}},$$

5. Arbitrary overall efficiency (or brake thermal efficiency), η_o .

The arbitrary overall efficiency of an engine is defined as the brake power divided by calorific heat of consumed fuel.

$$\eta_o = \frac{\dot{W}}{\dot{m}_f \, CV} = \frac{W_i \, \eta_m}{\dot{m}_f \, CV} = \eta_i \, \eta_m \, .$$

6. Specific fuel consumption, sfc.

It is the rate of fuel consumption per unit power output,

$$\text{sfc}=\frac{\dot{m}_f}{\dot{W}}=\frac{1}{CV.\eta_o}\text{, kg/kWh,}$$

7. Volumetric efficiency, η_v.

Volumetric efficiency is a measure of the effectiveness of the induction and exhaust processes. It is defined as

$$\eta_v=\frac{\text{mass of air inhaled per cylinder per cycle}}{\text{mass of air to occupy swept volume per cylinder at ambient p and T}}$$

Assuming air obeys the perfect gas laws, this can be rewritten as

$$\eta_v=\frac{\text{volume of ambient density air inhaled per cylinder per cycle}}{\text{cylinder swept volume}}=\frac{V_a}{V_s N}$$

Where V_a is volumetric flow rate of air with ambient density,

V_s is engine swept volume,

N is number of cycle per revolution.

The output of an engine is related to its volumetric efficiency; this can be shown by considering the mass of fuel burnt ($\dot{m}_f$), its calorific value(CV), and the brake efficiency of the engine.

$$\dot{m}_f=\frac{\eta_v V_s \rho_a}{AFR}$$

Where AFR is the gravimetric air-fuel ratio,

ρ_a is the ambient air density.

The amount of brake work produced per cycle (Wb) is given by

$$W_b = \bar{p}_b V_s = \dot{m}_f \eta_b CV$$

Therefore

$$\bar{p}_b = \frac{\eta_v \eta_b \eta_a CV}{AFR}$$

Volumetric efficiency has a direct effect on power output as the mass of air in the cylinder determines the amount of fuel that can be burnt.

Appendix B: Air/fuel and fuel/air ratio.

1. Air/fuel and fuel/air ratio.

In engine testing, both the air mass flow rate m_a and fuel mass flow rate m_f are normally measured. The ratio of these flow rates is useful in defining engine operating conditions.

$$\text{Air/fuel ratio (A/F)} = \frac{m_a}{m_f}$$

$$\text{Fuel/air ratio (F/R)} = \frac{m_f}{m_a}$$

Both the concepts of air/fuel ratio and fuel/air ratio are used in studying engines. The normal operating range of the mixture for conventional petrol engine: $12 \le A/F \le 18$ or $(0.056 \le F/A \le 0.083)$.

2. Stoichiometric air/fuel ratio (fuel/air ratio).

Stoichiometric air/fuel ratio is the air/fuel ratio of the mixture that is chemically correct for complete combustion.

Assuming that mass fractions of carbon, hydrogen, oxygen, and other elements (non-fuel) in a fuel $C_xH_yO_z$ are *m, n, p, q,* respectively, (where *x, y,* and *z* are the numbers of carbon atoms, hydrogen atoms, and oxygen atoms respectively in a molecule of the fuel), it then can be deduced the stoichiometric air/fuel ratio from the following equation of the theoretically complete combustion.

$$(C_xH_yO_z) + (x + \frac{y}{4} - \frac{z}{2})(O_2 + \frac{79}{21}N_2) = xCO_2 + \frac{y}{2}H_2O + (x + \frac{y}{4} - \frac{z}{2})\frac{79}{21}N_2 \quad (1)$$

Amount of fuel involved in the combustion presented by the above equation is

$$F_C = (12x + y + 16z + Q) \text{ kg}$$

where Q is amount of other elements present in this amount of the fuel (kg).

Amount of air needed for complete combustion of F kg fuel is

$$A_c = (x + \frac{y}{4} - \frac{z}{2})(O_2 + \frac{79}{21}N_2) \text{ kg}$$

Stoichiometric air/fuel ratio of the mixture is

$$A_c/F_c = \frac{(x+\frac{y}{4}-\frac{z}{2})(O_2+\frac{79}{21}N_2)}{(12x+y+16z+Q)} \tag{B2}$$

Based on the mass fractions of the components of the fuel, *m, n, p, q,* we have:

$$m=\frac{12x}{(12x+y+16z+Q)}, \quad or \quad \frac{12x}{m}=(12x+y+16z+Q)$$

$$n=\frac{y}{(12x+y+16z+Q)}, \quad or \quad \frac{y}{n}=(12x+y+16z+Q)$$

$$p=\frac{16z}{(12x+y+16z+Q)}, \quad or \quad \frac{16z}{p}=(12x+y+16z+Q)$$

$$q=\frac{Q}{(12x+y+16z+Q)}, \quad or \quad \frac{q}{Q}=(12x+y+16z+Q)$$

And therefore

$$y=\frac{12n}{m}x, \quad z=\frac{12p}{16m}x, \quad \text{and} \quad Q=\frac{12q}{m}x \tag{B3}$$

Substituting (3) to (2) gives

$$A_c/F_c = \frac{\frac{412}{24m}(8m+24n-3p)}{\frac{12}{m}(m+n+p+q)} \tag{B4}$$

because $(m + n + p + q)=1$, (4) becomes

$$A_c/F_c = \frac{103}{72}(8m+24n-3p) \tag{B5}$$

Where m is mass fraction of carbon in the fuel,

n is mass fraction of hydrogen in the fuel,

p is mass fraction of oxygen in the fuel.

Thus, for any fuel, if fractions of the components are known, the stoichiometric air/fuel ratio can be determined by equation (5).

Petrol fuel usually does not contain oxygen (O_2=0). The main elements are C and H, fraction of other elements is very small (usually less than 0.1%). For

example, a super grade petrol contains 85.5% C, 14.4% H_2 0.1% S, its stoichiometric air/fuel ratio determined by (5) is A_C/F_C=14.78 kg/kg.

3. Fuel/air equivalence ratio, F_R and relative air/fuel ratio, λ:

$$F_R = \frac{(F/A)_{actual}}{(F/A)_{stoichiometric}}$$

$$\lambda = \frac{1}{F_R} = \frac{(A/F)_{actual}}{(A/F)_{stoichiometric}}$$

Both F_R and λ are used in the field of internal combustion engine. Under normal operating conditions of an engine, F_R and λ usually range from 0.8 to 1.2, but under transient conditions, the engine operates with much richer mixture.

Appendix C: Specifications of the test engines

The engines used for experiment are two petrol engines, Peugeot 504 XN1 and Peugeot 504 XN2, which are the same size and linear-cylinder arrangement but different in their fuel system. One engine is equipped with a carburation fuel system, the other is equipped with a fuel injection system. Main characteristics of these engines are as follows.

Description	504 XN1-Carburetted Engine	504 XN2 Injection Engine
Number of cylinders	4	4
Bore x stroke (in mm)	88x81	88x81
Cubic capacity (in cm^3)	1971	1971
Compression ratio	8.35/1	8.35/1
Solex carburettor	32-35 SEIEA (twin choke)	
KF injection pump		KF5-92 014141
Maximum power	98 hp - 72 kW	110 HP - 80.8 kW
at engine speed (r.p.m)	5600 rpm	5600 rpm
Maximum torque and corresponding engine speed (r.p.m)	17.2 mkg - 168.5 Nm 3000 rpm	18.1 mkg - 177 Nm 3000 rpm

Exhaust manifod:

The exhaust manifolds of the two engines are exactly the same. The runners from the individual cylinders join two separate branches of the manifold; the runners from cylinders 2 and 3 join one branch while the runners from cylinders 1 and 4 join another; and then these two branches join together to a common duct far from the exhaust ports of the cylinders.

Intake system:

The 504 XN1 carburetion engine uses a twin choke carburettor with two mixture chambers. From light load to about 20% of total load the mixture is

supplied from only one mixture chamber, and after that both butterfly valves open to supply more mixture to meet the engine's requirement. The base of the carburettor, which is faced to the mixture streams from the two venturis, is heated by the hot coolant from the engine. Three runners go from there to the cylinders. Two separate runners go to cylinder 1 and cylinder 4, the middle runner is responsible for supplying mixture to cylinder 2 and cylinder 3. The middle runner lies is 4 cm lower than the other two runners. The diagram of the intake system is shown below.

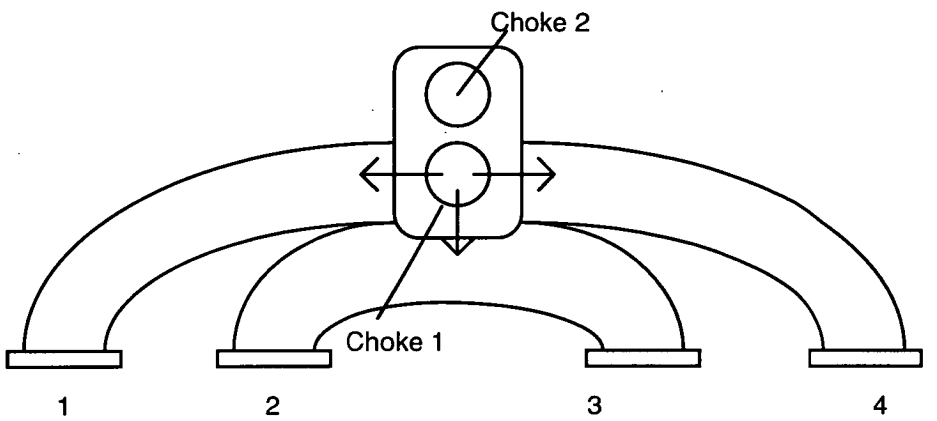

The inlet manifold of 504 XN2 fuel injection engine has a common pipe, from which 4 separate runners go to each cylinder as shown in the diagram below.

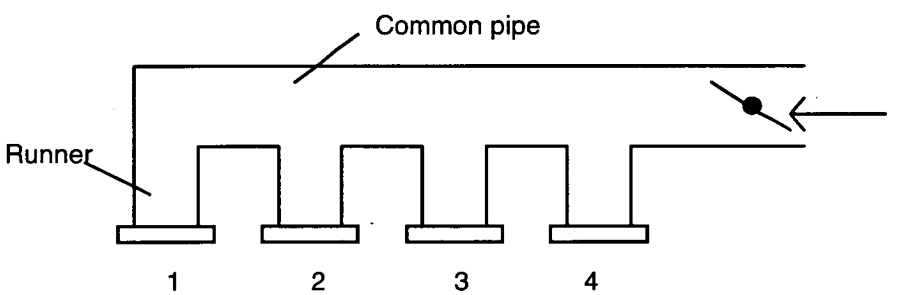

Appendix D: Exhaust gas sampling system

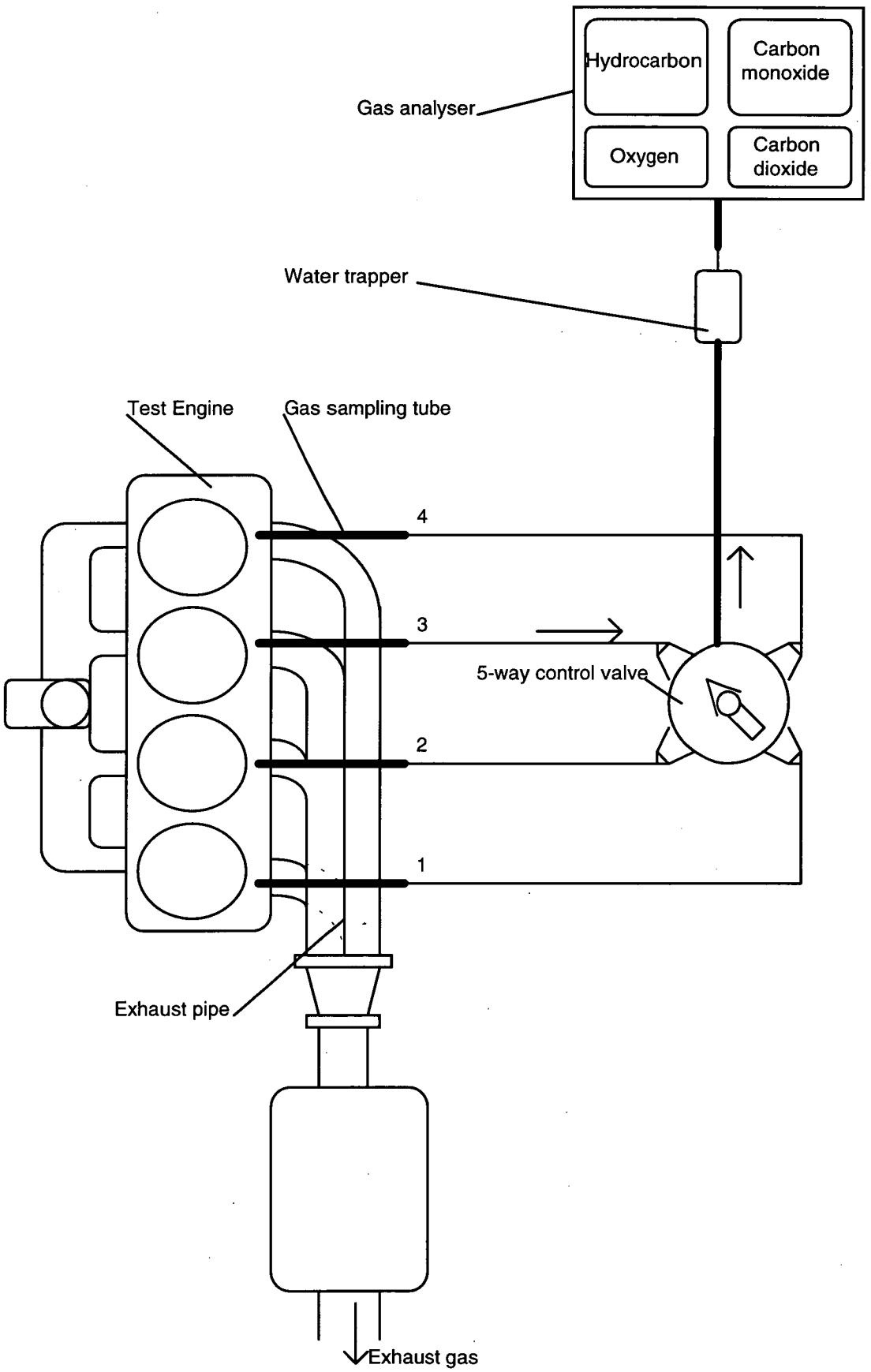

Location of gas sampling tube

1- Engine block
2- Piston
3- Combustion chamber
4- Exhaust valve
5- Cylinder head
6- Exhaust manifold
7- Tube fitting
8- Exhaust gas sampling tube
(Stainless steel tube)

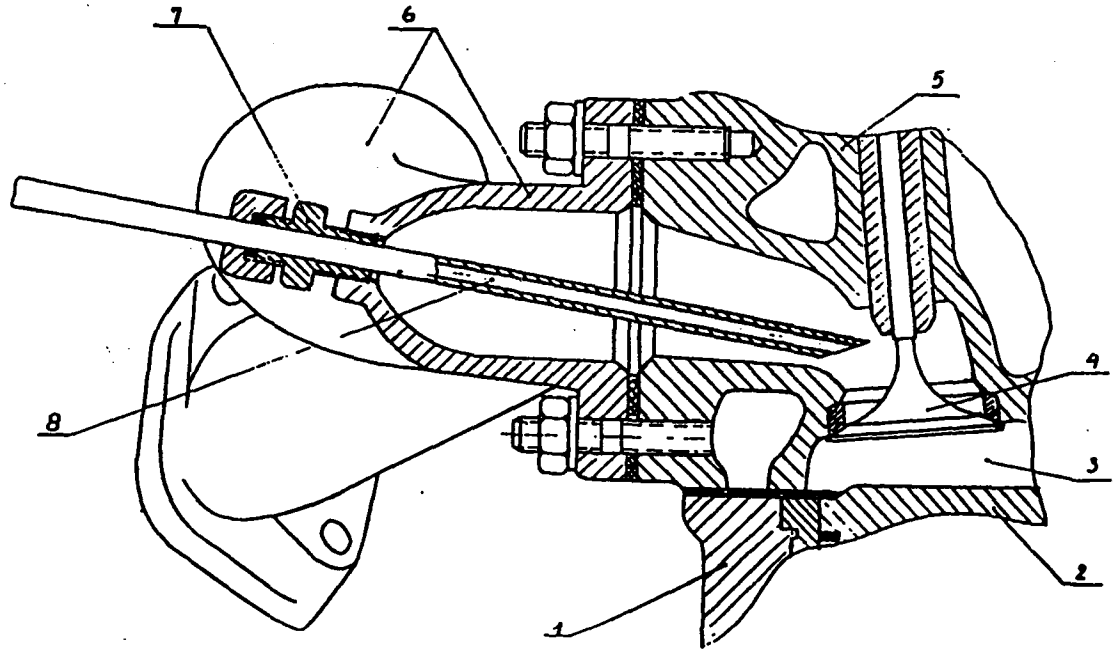

Appendix E: Measurement of air mass flow rate with using orifice plates.

The orifice plates used in the present experiments are orifice plates with D and D/2 tappings of 3 different sizes, 1", 1.5" and 2" to measure all range of inlet air mass flow rate corresponding to the range of load and speed of the test engines.

During experiment, the pressure difference between upstream and downstream of the orifice plate is measured. The data are interpreted into air mass flow rate based on the following calculations.

According to British Standard 1042 (Methods for the Measurement of fluid flow in pipes, part1, 1964) the mass rate of air flow in a pipe through an orifice plate is determined by the following equation.

$$W = 0.01252CZeEd^2\sqrt{h\rho} \tag{E-1}$$

$$E = \frac{1}{\sqrt{1-m^2}}, \quad m = (\frac{d}{D})^2 \tag{E-2}$$

Where W is the air mass flow rate (kg/h),

d is the diameter of the orifice (mm),

D is the internal diameter of the upstream pipeline (mm),

h is the pressure difference between upstream and downstream of the orifice plate (mmH_2O),

ρ is the density of the air (kg/m^3), and found from table of air properties.

C is the basic coefficient whose value is dependent on the area ratio m and can be found from the graph by BS 1042 (Fig.38a/page 120),

e is expansibility factor, which can be found from the graph by BS 1042 (from Fig. 39/page 122) according to h/P, m, and γ, where h is pressure difference (inH_2O), and P is absolute pressure upstream pipeline (lbf/in^2), γ is specific heat ratio of the air and can be found from tables of air properties.

Z is correction factor, and equal to $Z_R Z_D$,

Z_D is pipe size correction factor depending on m and D, and can be found from the graph by BS 1042, 1964 (Table 9/p.119 and Fig.38c/p. 121),

Z_R is Reynolds number correction factor depending on m and Reynolds number R_d. The method for the determination of Z_R is as follows. A provisional value of the rate of flow, W' (kg/h), is calculated from equation (E-1) with Z_R taken to be unity. This provisional rate is used in calculating the Reynolds number $Rd = \frac{3.54W'}{\mu d}$,

μ is dynamic viscosity of air (g/cms) and can be found from air tables.

d is diameter of the orifice (mm),

The Reynolds number correction factor is finally found from the graph by BS 1042, 1964 (Fig.38b/p.120).

In brief, after having measured the pressure difference, h, and determined all the other related parameters mentioned above, the mass rate of air flow is calculated by equation (E-1).

To interpret the pressure difference, h, into the air mass flow rate conveniently and quickly during experiment, the air mass flow rate is calculated in advance with different values of the pressure difference, and at different air temperature under the standard barometric pressure of 760 mmHg. The results are tabulated and presented in the graphs as seen in figure E-1 to figure E-4. The mass rate of air flow under the absolute pressure different from the standard barometric pressure is calculated by multiplying the air mass flow rate found in the graphs by a barometric pressure correction factor C_b.

Determination of the correction factor C_b:

In the range of barometric pressure 750 mmHg to 770 mmHg the properties of air (μ and γ) do not vary very much, so their values can be assumed to be equal to those at 760 mmHg, only the density changes. Therefore we have:

At 760 mmHg, $W_o = 0.01252CZeEd^2\sqrt{h\rho_o}$

At some pressure $W = 0.01252CZeEd^2\sqrt{h\rho}$

Defining $C_b = \frac{W}{W_o} = \sqrt{\frac{\rho}{\rho_o}} = \sqrt{\frac{P}{P_o}}$

Therefore $W = C_b W_o$

Accuracy.

The magnitude of the error of the quantity of air mass flow rate determined by this method can be estimated and expressed as a percentage of that quantity. It is denoted by the term *tolerance* and expressed by the following equation.

$$X_w = \sqrt{X_c^2 + X_{ZR}^2 + X_{ZD}^2 + X_e^2 + (\frac{2}{1-m^2})^2 X_d^2 + (\frac{2m^2}{1-m^2}) X_D^2 + \frac{1}{4}(X_\rho^2 + X_h^2)}$$

Where X_c, X_{ZR}, X_{ZD}, X_e, X_d, X_D, X_ρ and X_h are the tolerances (expressed as percentages) of the source of W, including C, Z_R, Z_D, e, d, D, ρ, and h as defined earlier. According to BS 1042, 1964

$X_{ZR} = 33(Z_R\text{-}1)$

$Z_e = 33(1\text{-}e)$

X_c and X_{ZD} can be found from graphs,

X_d and X_D are dimensional tolerances of the orifice and pipe,

X_h depends on the accuracy of the instrument,

X_ρ depends on the method of determination of air density.

Referring to the values of the above parameters for each of the 3 orifice plates to be used, calculated values of the tolerances of the mass flow rates measured by these orifice plates are as follows.

The 25.4 mm Orifice plate: $X_{W1} = \pm 1.1\%$

The 38.1 mm Orifice plate: $X_{W1.5} = \pm 1.3\%$

The 50.8 mm Orifice plate: $X_{W2} = \pm 1.6\%$

Interpretation of pressure difference into air mass flow rate is carried out by referring to tables (E-1) to (E-3) or graphs (E-1) to (E-3), and the multiplying the value found by the pressure correction factor found from graph (E-4).

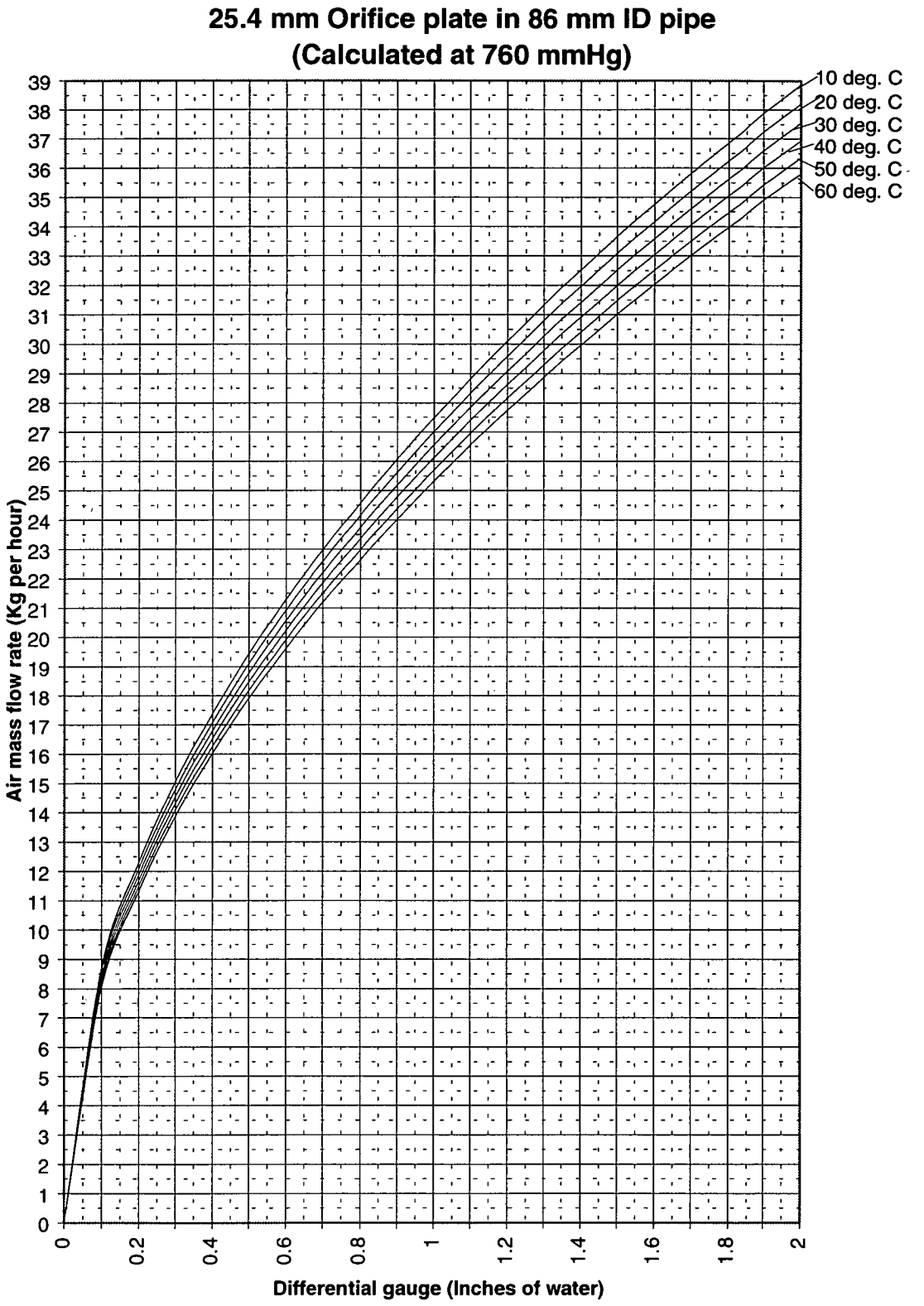

Figure E-1. Calibration curve for 25.4 mm orifice plate in 86 mm ID pipe at different temperatures.

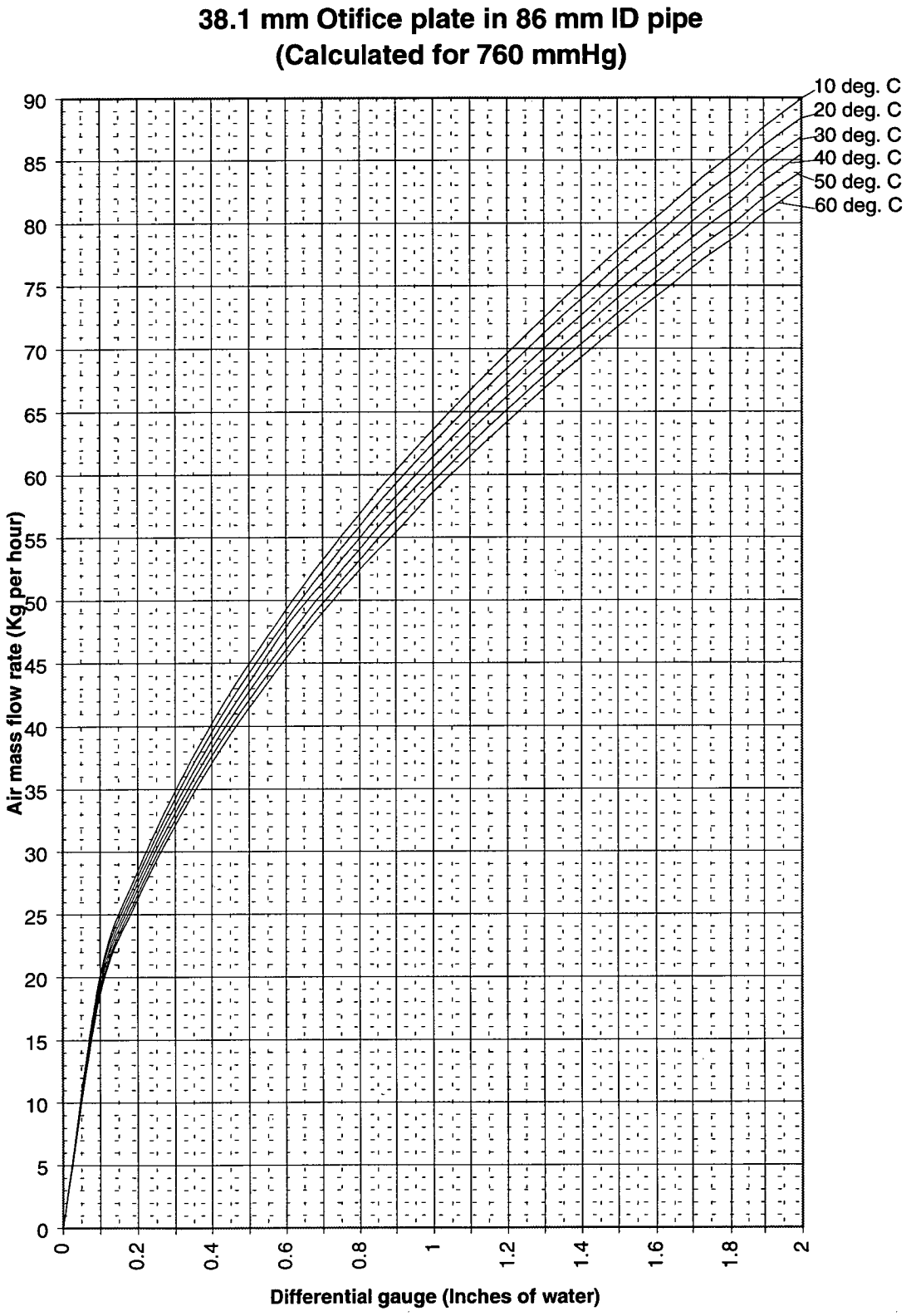

Figure E-2. Calibration curve for 38.1 mm orifice plate in 86 mm ID pipe at different temperatures.

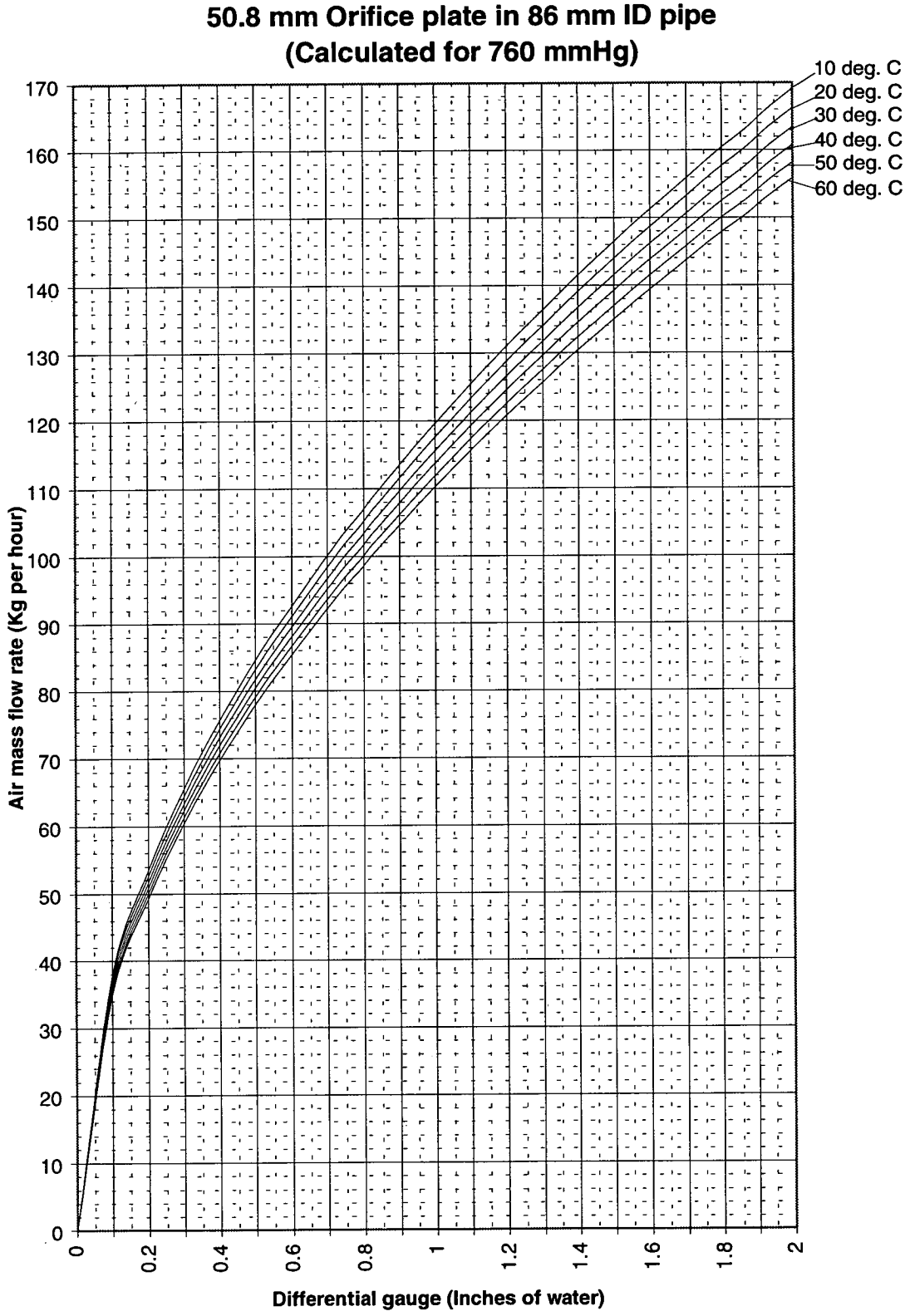

Figure E-3. Calibration curve for 50.8 mm orifice plate in 86 mm ID pipe at different temperatures.

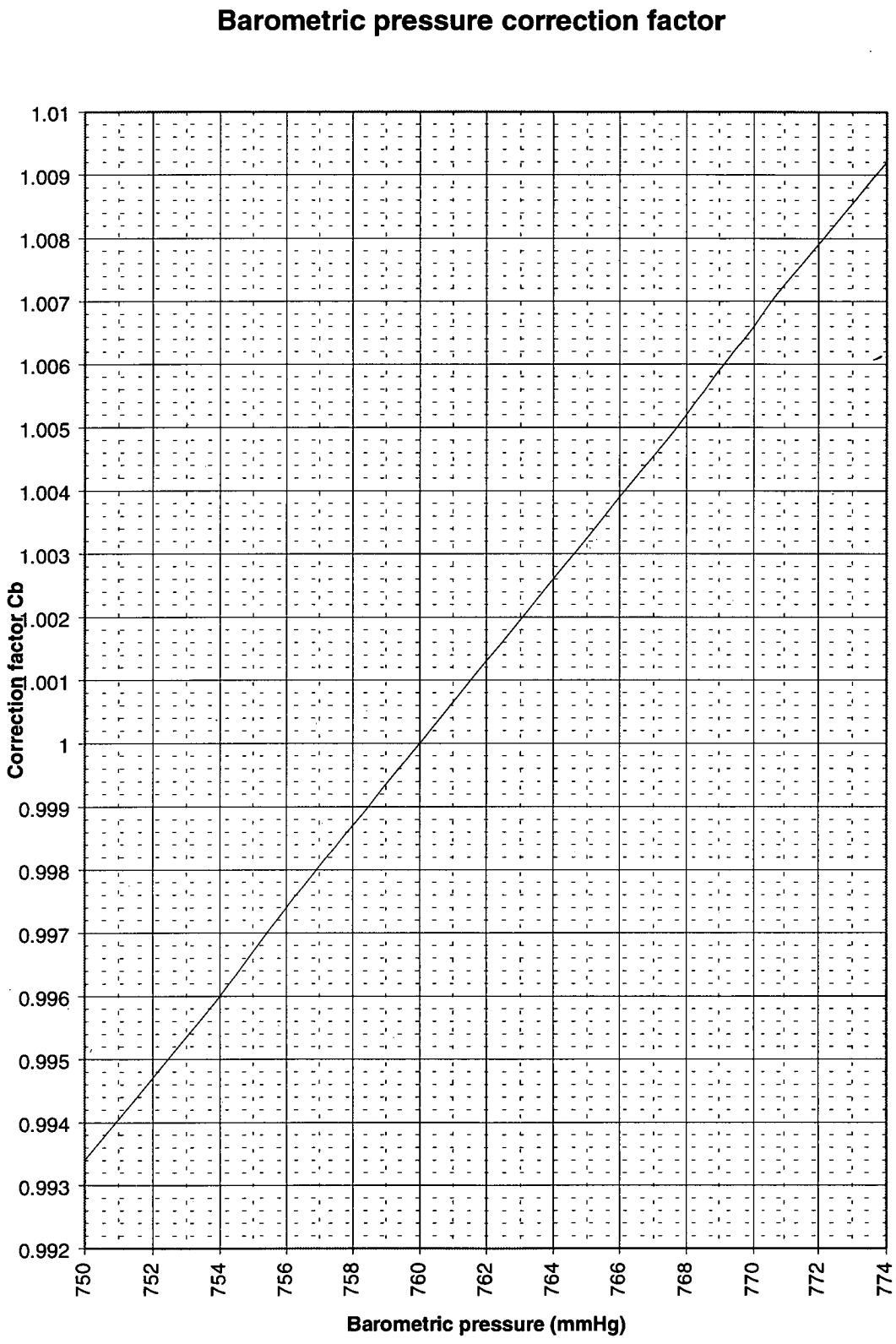

Figure E-4. Multiplying barometric pressure correction factor

Appendix F: Test data

Test 1 data of the Peugeot 504 XN1 carburation engine

Engine speed= 1000 rpm

Ambient temperature: 16.2 deg. C
Barometric pressure: 761 mmHg
Coolant temperature 85 ± 1 deg . C

Test No.	Brake load, (kgm)	Orifice plate, (inch)	Air rate (inch of water)	Fuel rate (s/100 mml)	Cylinder No.	Exhaust gas components			
						HC, (ppm)	CO, (%)	CO_2, (%)	O_2, (%)
1	1.5	1	0.42	252.41	1	220	1.71	12.2	4.5
					2	230	1.85	13.1	3.7
					3	240	2.1	13.4	3.1
					4	200	1.5	12.1	4.4
					Overall	222.5	1.79	12.7	3.93
2	3	1	0.56	210.16	1	230	1.81	12	4.2
					2	240	2.2	13.1	3.5
					3	200	2.4	13.6	3.2
					4	240	2	12.5	3.9
					Overall	227.5	2.1	12.8	3.7
3	5.5	1	0.82	172.48	1	290	1.9	12.7	3.8
					2	260	2.09	12.9	3.4
					3	250	2.7	13.5	3.2
					4	280	2.42	13.3	3.6
					Overall	270	2.28	13.1	3.5
4	8	1	1.44	125.25	1	290	2.99	11.7	3.7
					2	330	3.31	11.9	3.3
					3	300	3.91	12.3	3.1
					4	320	3.52	12.1	3.5
					Overall	310	3.43	12	3.4
5	10	1	1.77	111.23	1	350	3.61	11.4	3.4
					2	360	3.81	11.8	3.2
					3	320	4.17	12.2	2.9
					4	370	3.25	11	3.7
					Overall	325	3.71	11.6	3.3
6	12	1.5	0.42	96.37	1	470	3.3	10.6	4
					2	450	4.21	10.7	2.7
					3	400	4.7	12.1	2.4
					4	480	3.82	10.6	3.7
					Overall	450	4.01	11	3.2

Test 1 data of the Peugeot 504 XN1 carburation engine

Engine speed = 1500 rpm

Ambient temperature: 17.5 deg. C
Barometric pressure: 766 mmHg
Coolant temperature 85 ± 1 deg . C

Test No.	Brake load, (kgm)	Orifice plate, (inch)	Air rate (inch of water)	Fuel rate (s/100 mml)	Cylinder No.	Exhaust gas components			
						HC, (ppm)	CO, (%)	CO_2, (%)	O_2, (%)
1	1.5	1	0.74	191.39	1	230	0.9	13	4.1
					2	210	1.12	13.4	3.7
					3	180	1.2	13.8	3.4
					4	220	0.8	12.6	4.4
					Overall	210	1.01	13.2	3.9
2	3	1	1.19	149.19	1	230	1.21	13.4	4
					2	210	1	13.8	4.3
					3	220	1.42	13.1	3.6
					4	200	1.6	14.1	3.3
					Overall	215	1.31	13.6	3.8
3	5.5	1.5	0.37	113.88	1	280	1.66	13.7	3.8
					2	260	1.35	13.5	3.9
					3	250	1.75	13.9	3.4
					4	210	2.05	14.1	3.3
					Overall	250	1.7	13.8	3.6
4	8	1.5	0.52	92.99	1	320	1.4	13.6	3.8
					2	290	1.88	14.2	3.4
					3	220	2.2	14.6	3.2
					4	330	1.72	14	3.6
					Overall	290	1.8	14.1	3.5
5	10	1.5	0.65	83.1	1	330	1.36	14	3.7
					2	310	2.15	14.4	2.8
					3	250	2.44	14.6	2.9
					4	350	1.61	14.2	3.4
					Overall	310	1.89	14.3	3.2
6	12	1.5	0.9	69	1	380	1.81	13.9	3.7
					2	300	2.6	15.1	1.9
					3	350	2.25	14.7	2.5
					4	370	1.95	14.3	3.1
					Overall	350	2.15	14.5	2.8

Test 1 data of the Peugeot 504 XN1 carburation engine

Engine speed = 2000 rpm

Ambient temperature: 18.2 deg. C
Barometric pressure: 754 mmHg
Coolant temperature 85 ± 1 deg . C

Test No.	Brake load, (kgm)	Orifice plate, (inch)	Air rate (inch of water)	Fuel rate (s/100 mml)	Cylinder No.	Exhaust gas components			
						HC, (ppm)	CO, (%)	CO_2, (%)	O_2, (%)
1	1.5	1.5	0.22	150.49	1	240	0.75	13.4	4
					2	220	1.12	13.8	3.5
					3	200	1.35	14	3.2
					4	210	0.98	13.6	3.7
					Overall	217.5	1.05	13.7	3.6
2	3	1.5	0.37	111.8	1	280	1.26	13.4	3.8
					2	280	1.34	13.8	3.5
					3	250	1.66	14	3.3
					4	270	1.74	14.4	3
					Overall	270	1.05	13.9	3.4
3	5.5	1.5	0.52	90.95	1	340	2.4	13.1	3.2
					2	320	2.09	12.9	3.4
					3	270	2.91	13.5	2.8
					4	310	2.61	13.3	3
					Overall	310	2.5	13.2	3.1
4	8	1.5	0.75	73.11	1	320	2.41	14	2.2
					2	350	2.62	14.2	2.4
					3	300	2.99	14.5	1.9
					4	380	2.01	13.7	2.7
					Overall	337.5	2.51	2.3	15.1
5	10	1.5	1.07	60.21	1	380	2.52	14.4	2.1
					2	360	2.9	14.6	1.7
					3	310	3.32	14.9	1.3
					4	390	2.04	14.1	2.5
					Overall	360	2.7	14.5	1.9
6	12	1.5	1.17	56.47	1	410	2.92	14.9	1.8
					2	310	4.1	15.6	1.1
					3	370	3.13	15.3	1.6
					4	390	2	14.5	2.3
					Overall	370	3.04	15.07	1.7

Test 1 data of the Peugeot 504 XN1 carburation engine

Engine speed = 2500 rpm

Ambient temperature: 16.2 deg. C
Barometric pressure: 761 mmHg
Coolant temperature 85 ± 1 deg . C

Test No.	Brake load, (kgm)	Orifice plate, (inch)	Air rate (inch of water	Fuel rate (s/100 mml)	Cylinder No.	Exhaust gas components			
						HC, (ppm)	CO, (%)	CO_2, (%)	O_2, (%)
1	1.5	1.5	0.29	125.25	1	200	1.3	14.1	2.8
					2	270	1.48	14.8	2.6
					3	310	1.15	13.7	3.2
					4	300	1	13.4	3.4
					Overall	270	1.23	13.9	3
2	3	1.5	0.45	97.06	1	340	1.6	13.7	2.9
					2	230	2.41	14.7	2.3
					3	330	1.85	14	2.8
					4	300	2.14	14.4	2.4
					Overall	300	2	14.2	2.6
3	5.5	1.5	0.77	71.83	1	360	2.2	13.9	2.3
					2	340	2.4	14.1	2.1
					3	300	2.8	14.5	1.9
					4	320	1.76	13.4	2.5
					Overall	330	2.29	13.98	2.2
4	8	1.5	1.15	56.88	1	410	2	14.4	1.9
					2	430	2.5	15	1.5
					3	330	3.5	16	0.9
					4	390	2.9	15.4	1.3
					Overall	390	2.73	15.2	1.4
5	10	1.5	1.64	46.88	1	470	1.97	15.1	1.7
					2	400	3.25	15.7	0.9
					3	270	4.18	16	0.6
					4	460	2.69	15.3	1.3
					Overall	400	3.02	15.53	1.13
6	12	2	0.59	40.81	1	460	1.86	15.3	1.4
					2	430	3.55	16	0.8
					3	380	4.62	16.3	0.4
					4	450	3.07	15.6	1
					Overall	430	3.28	15.8	0.9

Test 1 data of the Peugeot 504 XN1 carburation engine

Engine speed = 3000 rpm

Ambient temperature: 17.7 deg. C
Barometric pressure: 768 mmHg
Coolant temperature 85 ± 1 deg . C

Test No.	Brake load, (kgm)	Orifice plate, (inch)	Air rate (inch of water	Fuel rate (s/100 mml)	Cylinder No.	Exhaust gas components			
						HC, (ppm)	CO, (%)	CO_2, (%)	O_2, (%)
1	1.5	1.5	0.41	110.87	1	300	0.6	13.3	4
					2	270	0.92	14	3.5
					3	200	1.1	14.3	3.4
					4	310	0.71	13.6	3.9
					Overall	270	0.83	13.8	3.7
2	3	1.5	0.47	98.76	1	320	1.1	14	3.4
					2	290	1.3	14.4	3.2
					3	210	1.5	14.7	3
					4	340	0.95	13.7	3.6
					Overall	290	1.21	14.2	3.3
3	5.5	1.5	1.06	64.06	1	390	1.2	13.9	3.1
					2	360	2.15	14.5	2.7
					3	290	2.31	14.9	2.5
					4	400	1.56	14.3	2.9
					Overall	360	1.81	14.4	2.8
4	8	1.5	1.61	46.95	1	510	1.64	15.3	1.3
					2	450	2.9	16.1	0.7
					3	310	3.85	16.3	0.3
					4	530	2.52	15.5	0.9
					Overall	450	2.73	15.8	0.8
5	10	1.5	1.91	42.51	1	550	1.8	15.2	1.2
					2	470	3.35	16.4	0.5
					3	390	4.6	17	10.1
					4	510	3.06	15.8	0.7
					Overall	480	3.2	16.1	0.63
6	12	2	0.84	33.65	1	570	1.43	15.5	0.7
					2	500	3.75	16.6	0.5
					3	320	5.39	17.1	0.1
					4	610	3.47	16	0.3
					Overall	500	3.51	16.3	0.4

Test 2 data of the Peugeot 504 XN1 carburation engine

Brake load = 1.5 kgm

Ambient temperature: 16.2 deg. C
Barometric pressure: 761 mmHg
Engine speed: 2500 rpm

Test No.	Outlet coolant temp. (C)	Cylinder No.	Exhaust gas components			
			HC, (ppm)	CO, (%)	CO_2, (%)	O_2, (%)
1	30	1	340	1.8	11	4
		2	320	2.32	12	2.9
		3	300	2.21	11.6	3.5
		4	330	1.6	11.4	4
		Overall	322.5	1.98	11.5	3.6
2	50	1	320	1.41	12.3	3.7
		2	300	1.98	12.7	3.3
		3	230	2.25	13.1	3.1
		4	350	1.26	12	3.9
		Overall	300	1.73	12.53	3.5
3	70	1	290	1.3	12.9	3.5
		2	270	1.87	13.5	3
		3	280	1.73	13.3	3.3
		4	295	1.02	12.7	3.8
		Overall	283.8	1.48	13.1	3.4
4	85	1	200	1.3	14.1	2.8
		2	270	1.48	14.4	2.6
		3	310	1.15	13.7	3.2
		4	300	1	13.4	3.4
		Overall	270	1.23	13.9	3
5	100	1	270	0.8	14	3
		2	200	1.49	15	2.3
		3	250	1.19	14.9	2.5
		4	280	1.05	14.1	2.9
		Overall	250	1.13	14.5	2.68

Test 2 data of the Peugeot 504 XN1 carburation engine

Brake load: 3 kgm

Ambient temperature: 18.8 deg. C
Barometric pressure: 752 mmHg
Engine speed: 2500 rpm

Test No.	Outlet coolant temp. (C)	Cylinder No.	Exhaust gas components			
			HC, (ppm)	CO, (%)	CO_2, (%)	O_2, (%)
1	30	1	410	2.2	11.3	4.1
		2	310	2.92	12.1	3.1
		3	370	3.05	12.5	2.8
		4	390	2.25	11.7	3.7
		Overall	370	2.6	11.9	3.42
2	50	1	380	1.78	12.3	3.5
		2	350	2.54	12.8	3
		3	300	2.9	13.1	2.7
		4	370	2.23	12.6	3.2
		Overall	350	2.36	12.7	3.1
3	70	1	310	1.43	12.6	3.1
		2	320	2.21	13.4	2.6
		3	300	2.5	13.7	2.2
		4	315	1.63	13.1	2.8
		Overall	311.2	1.94	13.2	2.67
4	85	1	300	1.6	13.7	2.9
		2	230	2.41	14.7	2.3
		3	330	1.85	14	2.8
		4	340	2.14	14.4	2.4
		Overall	300	2	14.2	2.6
5	100	1	290	1.42	14.2	2.6
		2	2.5	1.82	14.9	2.2
		3	200	2.15	15	2
		4	260	1.7	14.3	2.4
		Overall	250	1.77	14.6	2.3

Test 2 data of the Peugeot 504 XN1 carburation engine

Brake load = 5.5 kgm

Ambient temperature:17.2 deg. C
Barometric pressure: 749 mmHg
Engine speed: 2500 rpm

Test No.	Outlet coolant temp. (C)	Cylinder No.	Exhaust gas components			
			HC, (ppm)	CO, (%)	CO_2, (%)	O_2, (%)
1	30	1	480	2.13	11.8	4.1
		2	280	3.32	12.6	2.9
		3	400	3.04	12.3	3.2
		4	440	2.39	12.1	3.8
		Overall	400	2.72	12.2	3.5
2	50	1	410	1.8	12.5	3.6
		2	360	2.65	13.3	2.9
		3	300	2.9	13.6	2.6
		4	370	2.17	12.7	3.3
		Overall	360	2.38	13.03	3.1
3	70	1	420	2	13	3.1
		2	370	2.29	13.3	2.6
		3	300	2.52	13.7	2.4
		4	310	2.91	14.1	2.1
		Overall	350	2.43	13.53	2.55
4	85	1	360	2.2	13.9	2.3
		2	340	2.4	14.1	2.1
		3	300	2.8	14.5	1.9
		4	320	1.76	13.4	2.5
		Overall	330	2.29	13.98	2.2
5	100	1	340	1.97	14.3	2.2
		2	320	2.25	14.7	2
		3	240	2.45	14.9	1.7
		4	400	1.8	14.1	2.5
		Overall	325	2.12	14.5	2.1

Test 2 data of the Peugeot 504 XN1 carburation engine

Brake load =8 kgm

Ambient temperature: 18.8 deg. C
Barometric pressure: 752 mmHg
Engine speed: 2500 rpm

Test No.	Outlet coolant temp. (C)	Cylinder No.	Exhaust gas components			
			HC, (ppm)	CO, (%)	CO_2, (%)	O_2, (%)
1	30	1	520	2.5	12.1	3.8
		2	420	3.31	12.5	3.1
		3	270	3.7	13.1	2.2
		4	470	2.93	12.3	3.4
		Overall	420	3.11	12.5	3.13
2	50	1	480	2.31	12.6	2.7
		2	410	3.05	13.4	1.9
		3	300	3.53	13.8	1.3
		4	450	2.72	13	2.1
		Overall	410	2.9	13.2	2
3	70	1	470	2.1	13.4	2.2
		2	390	2.5	14.2	1.4
		3	280	3.42	14.5	1
		4	420	3.1	13.9	1.8
		Overall	390	2.78	14	1.6
4	85	1	410	2	14.4	1.9
		2	430	2.5	15	1.5
		3	330	3.5	16	0.9
		4	390	2.9	15.4	1.3
		Overall	390	2.73	15.2	1.4
5	100	1	420	1.92	15.4	1.7
		2	360	2.3	16.1	1.1
		3	2.8	3.25	16.5	0.7
		4	390	2.8	15.8	1.3
		Overall	362	2.57	15.95	1.2

Test 2 data of the Peugeot 504 XN1 carburation engine

Brake load = 10 kgm

Ambient temperature: 19.6 deg. C
Barometric pressure: 751 mmHg
Engine speed: 2500 rpm

Test No.	Outlet coolant temp. (C)	Cylinder No.	Exhaust gas components			
			HC, (ppm)	CO, (%)	CO_2, (%)	O_2, (%)
1	30	1	520	2.82	11.9	3.9
		2	450	3.98	12.8	2.7
		3	320	4.25	13.1	2.2
		4	500	3.35	12.3	3.2
		Overall	447.5	3.6	12.53	3
2	50	1	500	2.3	13	2.8
		2	430	3.52	13.4	2
		3	320	4.2	14.1	1.5
		4	460	3.07	13.5	2.2
		Overall	427.5	3.27	13.5	2.13
3	70	1	470	2.22	14	2.6
		2	430	2.9	14.3	2.3
		3	380	3.25	14.7	1.5
		4	400	3.86	15.1	1.2
		Overall	420	3.06	14.53	1.9
4	85	1	470	1.97	15.1	1.7
		2	400	3.25	15.7	0.9
		3	270	4.18	16	0.6
		4	460	2.69	15.3	1.3
		Overall	400	3.02	15.53	1.13
5	100	1	440	2	15.7	1.6
		2	370	3.12	16.1	1
		3	250	3.74	16.3	0.5
		4	400	2.5	15.8	1.2
		Overall	365	2.84	15.97	1.08

Test 2 data of the Peugeot 504 XN1 carburation engine

Brake load = 12 kgm

Ambient temperature:18.6deg. C
Barometric pressure: 754 mmHg
Engine speed: 2500 rpm

Test No.	Outlet coolant temp. (C)	Cylinder No.	Exhaust gas components			
			HC, (ppm)	CO, (%)	CO_2, (%)	O_2, (%)
1	30	1	600	3.3	11.1	2.9
		2	490	4.81	12.1	1.7
		3	300	5.65	12.5	1.3
		4	570	4.17	11.6	2.6
		Overall	490	4.48	11.83	2.13
2	50	1	570	2.5	13	2.5
		2	470	3.97	13.6	1.3
		3	300	4.89	13.9	1
		4	530	3.21	13.2	1.8
		Overall	467.5	3.64	13.43	1.65
3	70	1	560	1.8	14.1	1.6
		2	400	4.31	15	0.9
		3	290	5	15.2	0.7
		4	530	2.72	14.4	1.3
		Overall	445	3.46	14.68	1.13
4	85	1	460	1.86	15.3	1.4
		2	430	3.55	16	0.8
		3	380	4.62	16.3	0.4
		4	450	3.07	15.6	1
		Overall	430	3.28	15.8	0.9
5	100	1	510	1.2	15.5	1
		2	400	3.37	16.5	0.4
		3	230	3.4	16.9	0.5
		4	460	2.22	15.8	0.8
		Overall	400	2.55	16.18	0.68

Test 3 data of the Peugeot 504 XN1 carburation engine

Brake load: 1.5 kgm

Ambient temperature: 17 deg. C
Barometric pressure: 51 mmHg
Engine speed: 2500 rpm
Coolant temperature 85 ± 1 deg . C

Test No.	Heat supplied, Watt	inlet air temp. deg. C	Cylinder No.	Exhaust gas components			
				HC, (ppm)	CO, (%)	CO_2, (%)	O_2, (%)
1	0	17	1	200	1.3	14.1	2.8
			2	270	1.48	14.8	2.6
			3	310	1.15	13.7	3.2
			4	300	1	13.4	3.4
			Overall	270	1.23	13.9	3
2	400	32	1	270	2.5	13.3	3.4
			2	240	2.85	13.6	2.9
			3	260	2.6	13	3.5
			4	290	2.4	13	3.8
			Overall	2.65	2.59	13.23	3.4
3	800	44	1	250	2.8	13	3.5
			2	240	2.9	13.4	2.9
			3	280	2.9	12.5	3.5
			4	290	2.63	12.8	3.9
			Overall	265	2.81	12.92	3.45
4	1200	55	1	250	3	12.9	3.4
			2	280	3.2	13.1	2.9
			3	280	3.2	12.6	3.5
			4	310	3	12.6	3.9
			Overall	280	3.1	12.8	3.43
5	1700	70	1	300	3.3	12.4	3.5
			2	290	3.4	12.7	3
			3	300	3.5	12.2	3.6
			4	320	3.45	12.2	4
			Overall	302.5	3.41	12.37	3.53

Test 3 data of the Peugeot 504 XN1 carburation engine

Brake load: 3 kgm

Ambient temperature: 17 deg. C
Barometric pressure: 761 mmHg
Engine speed: 1000 rpm
Coolant temperature 85 ± 1 deg . C

Test No.	Heat supplied, Watt	inlet air temp. deg. C	Cylinder No.	Exhaust gas components			
				HC, (ppm)	CO, (%)	CO_2, (%)	O_2, (%)
1	0	17	1	340	1.6	13.7	2.9
			2	230	2.41	14.7	2.3
			3	330	1.85	14	2.8
			4	300	2.14	14.4	2.4
			Overall	300	2	14.2	2.6
2	400	31	1	300	2.2	14.2	3.6
			2	270	2.7	14.3	2.8
			3	280	2.6	13.8	3.7
			4	340	2.5	13.5	3.8
			Overall	297.5	2.5	13.95	3.48
3	800	42	1	300	2.4	13.8	3.5
			2	280	2.65	14	2.7
			3	320	2.7	13.6	3.7
			4	340	2.6	13.5	3.8
			Overall	310	2.59	13.73	3.43
4	1200	52	1	290	2.8	13.5	3.6
			2	290	3.18	13.5	3
			3	320	3.1	12.8	3.9
			4	370	3	12.9	4
			Overall	317.5	3.02	13.18	3.63
5	1700	68	1	290	3	13.2	3.9
			2	285	3.2	13.6	3
			3	335	3.2	13.2	3.8
			4	380	3	13.1	3.9
			Overall	322.5	3.1	13.28	3.65

Test 3 data of the Peugeot 504 XN1 carburation engine

Brake load: 5.5 kgm

Ambient temperature: 16.2 deg. C
Barometric pressure: 761 mmHg
Engine speed: 1000 rpm
Coolant temperature 85 ± 1 deg . C

Test No.	Heat supplied, Watt	inlet air temp. deg. C	Cylinder No.	Exhaust gas components			
				HC, (ppm)	CO, (%)	CO_2, (%)	O_2, (%)
1	0	16.2	1	360	2.2	13.9	2.3
			2	340	2.4	14.1	2.1
			3	300	2.8	14.5	1.9
			4	320	1.76	13.4	2.5
			Overall	330	2.29	13.98	2.2
2	400	30	1	330	2.2	14.1	3.4
			2	300	2.3	15.1	2.4
			3	380	3.4	13.7	3
			4	390	3	13.4	3.4
			Overall	350	2.73	14.08	3.05
3	800	40	1	340	2.6	14.5	2.9
			2	300	3	15.2	2
			3	410	3.4	13.7	2.9
			4	380	3	13.6	3.2
			Overall	357.5	3	14.25	2.75
4	1200	50	1	350	2.8	14.3	2.9
			2	325	2.9	15.2	1.8
			3	430	3.6	13.5	2.8
			4	420	3.2	13.5	3.1
			Overall	381.3	3.13	14.13	2.65
5	1700	65	1	370	3.3	13.7	2.8
			2	255	3.42	14.8	1.8
			3	450	3.9	13.2	2.7
			4	420	3.6	13.1	3.1
			Overall	373.7	3.56	13.7	2.6

Test 3 data of the Peugeot 504 XN1 carburation engine

Brake load: 8 kgm

Ambient temperature: 16.2 deg. C
Barometric pressure: 761 mmHg
Engine speed: 1000 rpm
Coolant temperature 85 ± 1 deg . C

Test No.	Heat supplied, Watt	inlet air temp. deg. C	Cylinder No.	Exhaust gas components			
				HC, (ppm)	CO, (%)	CO_2, (%)	O_2, (%)
1	0	16.2	1	410	2	14.4	1.9
			2	430	2.5	15	1.5
			3	330	3.5	16	0.9
			4	390	2.9	15.4	1.3
			Overall	390	2.73	15.2	1.4
2	400	28	1	375	2.22	15.3	3
			2	260	2.6	16.2	1.5
			3	400	3.8	14.1	2.3
			4	380	3.4	13.7	3
			Overall	353.7	3.01	14.83	2.45
3	800	39	1	340	2.6	14.2	3.1
			2	280	2.8	15.9	1.7
			3	420	4	13.7	2.5
			4	410	3.8	13.1	3.2
			Overall	362.5	3.3	14.1	2.63
4	1200	48	1	390	2.8	14.9	2.9
			2	280	3.58	15.6	1.7
			3	430	4.19	14	2.5
			4	380	3.9	13	3.6
			Overall	370	3.62	14.38	2.68
5	1700	61	1	400	3	14.2	2.8
			2	300	3.46	15.2	1.5
			3	440	4.2	13.4	2.5
			4	450	4	12.7	3.5
			Overall	397.5	3.67	13.88	2.58

Test 3 data of the Peugeot 504 XN1 carburation engine

Brake load: 10 kgm

Ambient temperature: 16.2 deg. C
Barometric pressure: 761 mmHg
Engine speed: 1000 rpm
Coolant temperature 85 ± 1 deg . C

Test No.	Heat supplied, Watt	inlet air temp. deg. C	Cylinder No.	Exhaust gas components			
				HC, (ppm)	CO, (%)	CO_2, (%)	O_2, (%)
1	0	16.2	1	470	1.97	15.1	1.7
			2	400	3.25	15.7	0.9
			3	270	4.18	16	0.6
			4	460	2.69	15.3	1.3
			Overall	400	3.02	15.53	1.13
2	400	36	1	390	2.4	15	2.1
			2	240	3.8	15.8	1.4
			3	400	3.6	13.6	1.7
			4	400	2.3	13.1	2.7
			Overall	357.5	3.03	14.38	1.98
3	800	35	1	390	2.75	13.8	2.6
			2	250	3.05	15.3	1.3
			3	410	4.45	13.6	1.6
			4	400	3.51	13	2.5
			Overall	362.5	3.44	13.92	2
4	1200	46	1	390	2.5	13.5	2.5
			2	390	3.2	12.7	2
			3	280	4.05	14.5	1.5
			4	400	3.6	12.3	3.1
			Overall	365	3.34	13.25	2.28
5	1700	60	1	380	2.62	13.2	2.5
			2	290	3.3	13.7	1.5
			3	390	4.4	12.7	1.7
			4	410	3.7	12.1	2.5
			Overall	367.5	3.51	12.92	2.05

Test 3 data of the Peugeot 504 XN1 carburation engine

Brake load: 12 kgm

Ambient temperature: 16.2 deg. C
Barometric pressure: 761 mmHg
Engine speed: 1000 rpm
Coolant temperature 85 ± 1 deg . C

Test No.	Heat supplied, Watt	inlet air temp. deg. C	Cylinder No.	Exhaust gas components			
				HC, (ppm)	CO, (%)	CO_2, (%)	O_2, (%)
1	0	16.2	1	460	1.86	15.3	1.4
			2	430	3.55	16	0.8
			3	380	4.62	16.3	0.4
			4	450	3.07	15.6	1
			Overall	430	3.28	15.8	0.9
2	400	25	1	410	1.8	16.2	2.1
			2	250	3.4	15.9	1
			3	430	4.72	13.7	1.7
			4	390	3.2	15.4	1.3
			Overall	370	3.28	15.3	1.53
3	800	35	1	410	2	15.8	2.1
			2	250	4.13	15.7	1.1
			3	450	4.4	13.2	1.9
			4	380	3.4	15.1	1.5
			Overall	372.5	3.48	14.95	1.65
4	1200	47	1	400	2.2	15.6	1.9
			2	280	4.64	15.6	1
			3	450	4.8	13.3	1.7
			4	380	3.4	15	1.3
			Overall	377.5	3.76	14.87	1.48
5	1700	57	1	420	2.43	15.4	1.9
			2	270	3	15.3	1
			3	440	4.8	12.8	1.3
			4	400	3.7	14.8	1.3
			Overall	382.5	3.48	14.58	1.38

Test 1 data of the Peugeot 504 XN2 injection engine

Engine speed: 1000 rpm

Ambient temperature: 18.16 deg. C
Barometric pressure: 762 mmHg
Coolant temperature 85 ± 1 deg . C

Test No.	Brake load, (kgm)	Orifice plate, (inch)	Air rate (inch of water)	Fuel rate (s/100 mml)	Cylinder No.	Exhaust gas components			
						HC, (ppm)	CO, (%)	CO_2, (%)	O_2, (%)
1	1.5	1	0.33	275.71	1	170	2.4	14.1	2.9
					2	150	2.28	14	3.6
					3	190	2.3	14.1	3.4
					4	130	1.83	14.1	3.6
					Overall	160	2.2	14.08	3.38
2	3	1	0.48	221.38	1	240	1.95	14.1	3.3
					2	200	1.83	13.9	3.5
					3	240	2.2	13.8	3.2
					4	190	1.3	14.4	3.3
					Overall	217.5	1.82	14.05	3.33
3	5.5	1	0.77	175.63	1	420	1.85	13.3	3
					2	370	1.56	13.4	2.9
					3	390	1.71	13.4	3.1
					4	350	1.41	13.5	3.2
					Overall	382.5	1.63	13.4	3.05
4	8	1	1.31	137.23	1	450	1.25	14.6	2.8
					2	380	1.2	14.3	3.3
					3	440	1.4	14.2	3
					4	400	1.17	14.6	2.8
					Overall	417.5	1.26	14.43	2.98
5	10	1.5	0.33	112.62	1	380	2.33	13	2.8
					2	380	2.35	14.1	2.3
					3	460	2.45	13	2.8
					4	430	2.41	13.3	2.9
					Overall	412.5	2.37	13.35	2.7
6	12	1.5	0.65	73.63	1	610	5.5	9.7	3.1
					2	570	4.86	10.1	2.1
					3	550	5.3	9.9	2.9
					4	590	5.1	10.1	2.6
					Overall	580	5.19	9.95	2.68

Test 1 data of the Peugeot 504 XN2 injection engine

Engine speed: 1500 rpm

Ambient temperature: 20.5 deg. C
Barometric pressure: 751 mmHg
Coolant temperature 85 ± 1 deg . C

Test No.	Brake load, (kgm)	Orifice plate, (inch)	Air rate (inch of water)	Fuel rate (s/100 mml)	Cylinder No.	Exhaust gas components			
						HC, (ppm)	CO, (%)	CO_2, (%)	O_2, (%)
1	1.5	1	0.67	174.01	1	220	3.1	14.6	2.8
					2	310	3.25	14.7	2.4
					3	300	2.85	14.8	2.7
					4	200	2.41	14.4	3.1
					Overall	257.5	2.9	14.3	2.75
2	3	1	0.92	164.36	1	290	1.48	13.9	2.5
					2	230	0.63	14	2.9
					3	280	1.25	13.9	2.8
					4	250	1	13.9	2.9
					Overall	262.5	1.09	13.92	2.78
3	5.5	1	1.64	122.49	1	280	0.96	15.1	2
					2	230	0.82	14.7	2.8
					3	290	0.74	14.2	2.7
					4	320	0.86	14.4	2.6
					Overall	280	0.84	14.6	2.53
4	8	1.5	0.46	96.34	1	370	1.4	15.7	1.8
					2	380	0.95	14.9	2.1
					3	360	1.25	14.9	2.4
					4	420	1.45	15	2.2
					Overall	382.5	1.26	15.13	2.13
5	10	1.5	0.7	78.69	1	370	1.9	14	2.8
					2	330	1.75	14.2	2.1
					3	380	1.9	13.7	2.7
					4	370	2.15	13.7	2.9
					Overall	362.5	1.93	13.9	2.63
6	12	1.5	1.35	51.42	1	450	5	10.4	2.2
					2	500	5.3	9.7	3.2
					3	580	5.2	10.3	3
					4	550	4.9	10.4	2.9
					Overall	520	5.1	10.2	2.83

Test 1 data of the Peugeot 504 XN2 injection engine

Engine speed: 2000 rpm

Ambient temperature: 18.6 deg. C
Barometric pressure: 762 mmHg
Coolant temperature 85 ± 1 deg . C

Test No.	Brake load, (kgm)	Orifice plate, (inch)	Air rate (inch of water)	Fuel rate (s/100 mml)	Cylinder No.	Exhaust gas components			
						HC, (ppm)	CO, (%)	CO_2, (%)	O_2, (%)
1	1.5	1	1.19	127.14	1	420	5	10	2.2
					2	330	5.57	9.8	2.3
					3	300	4	10.8	2.5
					4	350	4.6	10.1	2.2
					Overall	350	4.79	10.18	2.3
2	3	1.5	0.25	115.04	1	300	1.62	14.8	2.2
					2	240	0.9	15	2.9
					3	270	1.3	14.2	3
					4	275	1.7	14.2	2.7
					Overall	271.3	1.38	14.55	2.7
3	5.5	1.5	0.52	95.6	1	310	1.22	16.2	2.5
					2	300	1.17	14.7	3.2
					3	360	1.24	15.3	3.2
					4	270	0.88	15.2	3.3
					Overall	310	1.13	15.35	3.05
4	8	1.5	0.82	73.5	1	310	1.06	16.5	1.9
					2	380	1.6	15.1	3
					3	400	1.33	15.5	3
					4	360	1.5	15.3	3.1
					Overall	362.5	1.37	15.6	2.75
5	10	1.5	1.25	57.13	1	380	1.15	17.6	1.3
					2	440	0.89	16.2	1.9
					3	480	1.09	15.7	2
					4	480	0.95	15.9	1.8
					Overall	445	1.02	16.35	1.75
6	12	1.5	1.55	48.31	1	330	2.6	16.3	0.8
					2	470	2.2	15.1	1.4
					3	440	2.73	14.7	1.9
					4	470	2	15.3	0.4
					Overall	427.5	2.38	15.35	1.13

Test 1 data of the Peugeot 504 XN2 injection engine

Engine speed: 2500 rpm

Ambient temperature:18.6 deg. C
Barometric pressure: 762 mmHg
Coolant temperature 85 ± 1 deg . C

Test No.	Brake load, (kgm)	Orifice plate, (inch)	Air rate (inch of water)	Fuel rate (s/100 mml)	Cylinder No.	Exhaust gas components			
						HC, (ppm)	CO, (%)	CO_2, (%)	O_2, (%)
1	1.5	1.5	0.26	106.15	1	450	7.85	8.7	1.9
					2	380	6	9.6	2.1
					3	400	7.3	8.2	2.3
					4	370	7	9.1	2.1
					Overall	400	7.04	8.9	2.1
2	3	1.5	0.37	104.31	1	320	2.5	13.7	2.1
					2	350	2.3	13.7	2.6
					3	370	3.52	13.1	2.4
					4	380	2	13.1	2.8
					Overall	367.5	2.58	13.4	2.48
3	5.5	1.5	0.77	77.23	1	350	1.48	16.5	2.1
					2	375	0.8	15.6	2.9
					3	400	1.3	15.4	2.6
					4	360	0.96	15.2	3
					Overall	371.3	1.14	15.68	2.65
4	8	1.5	1.38	55.88	1	320	1	18	1.5
					2	360	1.05	16	2.5
					3	450	0.7	16.1	2
					4	375	0.66	15.3	2
					Overall	376.3	0.85	16.35	2
5	10	2	0.53	46	1	330	2	16.6	1.3
					2	480	1.6	16.8	2
					3	480	1.9	16.1	1.7
					4	470	1.87	16.6	1.2
					Overall	440	1.84	16.53	1.55
6	12	2	0.72	36.97	1	360	4.22	15.8	0.4
					2	600	4.4	14.9	1.2
					3	620	4.5	15	1.9
					4	610	4.2	15.2	1.1
					Overall	532.5	4.33	15.23	1.15

Test 1 data of the Peugeot 504 XN2 injection engine

Engine speed: 3000 rpm

Ambient temperature:18.6 deg. C
Barometric pressure: 762 mmHg
Coolant temperature 85 ± 1 deg . C

Test No.	Brake load, (kgm)	Orifice plate, (inch)	Air rate (inch of water)	Fuel rate (s/100 mml)	Cylinder No.	Exhaust gas components			
						HC, (ppm)	CO, (%)	CO_2, (%)	O_2, (%)
1	1.5	1.5	0.39	91.25	1	330	6	10.9	2
					2	250	4.67	11.5	2.4
					3	280	5.3	11.2	2.1
					4	320	5.7	11	1.6
					Overall	295	5.42	11.5	2.03
2	3	1.5	0.55	87.5	1	270	1.75	16.2	1.8
					2	240	0.75	15.6	2.6
					3	300	1.4	14.8	2.1
					4	230	1.1	15	2.2
					Overall	260	1.25	15.4	12.17
3	5.5	1.5	1.03	63.75	1	330	0.55	18.1	0.8
					2	320	0.32	16.4	2.2
					3	300	0.2	16.9	1.4
					4	350	0.23	16.9	1.3
					Overall	325	0.33	17.08	1.43
4	8	2	0.45	52.5	1	320	0.9	17.9	1.5
					2	370	0.56	15.1	2.5
					3	410	0.5	16	2
					4	370	0.65	15.6	2
					Overall	367.5	0.65	16.15	2
5	10	2	0.64	43.75	1	320	92	18	1.6
					2	370	1.02	16	2.5
					3	410	0.65	16.9	1.8
					4	400	0.52	17	1
					Overall	375	0.78	16.98	1.73
6	12	2	0.86	36.25	1	350	1.8	18.2	1.2
					2	470	1.5	17.5	1.9
					3	470	1.4	18.2	2.2
					4	460	1.7	18.1	1.1
					Overall	437.5	1.6	18	1.6

Test 2 data of the Peugeot 504 XN2 injection engine

Brake load: 1.5 kgm

Ambient temperature: 20.5 deg. C
Barometric pressure: 751 mmHg
Engine speed: 2500 rpm

Test No.	Outlet coolant temp. (C)	Cylinder No.	Exhaust gas components			
			HC, (ppm)	CO, (%)	CO_2, (%)	O_2, (%)
1	30	1	700	9.3	7.3	1.7
		2	1500	8.05	6.2	3
		3	720	8.9	7.1	2.1
		4	700	8.4	7.2	2.5
		Overall	905	8.66	6.95	2.33
2	50	1	500	7.6	8.9	2
		2	510	7.6	8.5	2.4
		3	480	7.4	8.6	2.2
		4	450	6.72	9.3	2.8
		Overall	485	7.33	8.82	2.35
3	70	1	450	7.1	8.7	1.8
		2	440	6.75	9	3
		3	420	7	8.9	2.1
		4	380	7.1	8.5	2.2
		Overall	422.5	6.99	8.78	2.28
4	85	1	450	7.85	8.7	1.9
		2	380	6	9.6	2.1
		3	400	7.3	8.2	2.3
		4	370	7	9.1	2.1
		Overall	400	7.04	8.9	2.1
5	100	1	450	7.4	8.2	2
		2	380	6.6	8.9	2.7
		3	390	7.5	8.6	2.2
		4	400	6.8	8.6	2.4
		Overall	405	7.08	8.58	2.33

Test 2 data of the Peugeot 504 XN2 injection engine

Brake load: 3 kgm

Ambient temperature: 19.5 deg. C
Barometric pressure: 753 mmHg
Engine speed: 2500 rpm

Test No.	Outlet coolant temp. (C)	Cylinder No.	Exhaust gas components			
			HC, (ppm)	CO, (%)	CO_2, (%)	O_2, (%)
1	30	1	690	8	9.2	1.2
		2	670	8	8.5	2.1
		3	750	8	8.5	1.9
		4	700	7.4	9.1	2.4
		Overall	702.5	7.85	8.83	1.9
2	50	1	400	3	13.7	1.8
		2	450	3.2	13.1	2.4
		3	490	3.4	12.6	2.3
		4	420	2.85	12.8	3
		Overall	440	3.11	13.05	2.38
3	70	1	410	2.7	14	2
		2	340	2.23	14	3
		3	420	2.9	13.4	2.5
		4	400	2.6	13.7	2.7
		Overall	392.5	2.61	13.87	2.55
4	85	1	320	2.5	13.7	2.1
		2	350	2.3	13.7	2.6
		3	370	3.52	13.1	2.4
		4	380	2	13.1	2.8
		Overall	367.5	2.58	13.4	2.48
5	100	1	340	2.9	13.3	2.2
		2	320	1.92	13.7	2.6
		3	370	3	12.6	2.6
		4	340	2.5	13.1	2.9
		Overall	342.5	2.58	13.18	2.58

Test 2 data of the Peugeot 504 XN2 injection engine

Brake load: 5.5 kgm

Ambient temperature: 17 deg. C
Barometric pressure: 761 mmHg
Engine speed: 2500 rpm

Test No.	Outlet coolant temp. (C)	Cylinder No.	Exhaust gas components			
			HC, (ppm)	CO, (%)	CO_2, (%)	O_2, (%)
1	30	1	560	6	12.8	1.2
		2	530	6.2	11.5	1.9
		3	560	5.3	11.9	1.8
		4	580	5.85	11.6	2.8
		Overall	557.5	5.84	11.95	1.93
2	50	1	460	4.2	14.3	1.3
		2	470	3.6	13.4	2
		3	530	3.8	13.2	1.8
		4	520	4.08	13.2	2.7
		Overall	495	3.92	13.53	1.95
3	70	1	360	1	16.8	2.2
		2	390	0.8	15.6	3.3
		3	420	1	15.6	2.5
		4	350	1.05	15.4	3.2
		Overall	380	0.96	15.85	2.8
4	85	1	350	1.48	16.5	2.1
		2	375	0.8	15.6	2.9
		3	400	1.3	15.4	2.6
		4	360	0.96	15.2	3
		Overall	371.3	1.14	15.68	2.65
5	100	1	300	1.2	16.2	38
		2	325	0.7	15.3	3.2
		3	380	1.34	15.4	2.7
		4	280	0.9	15.1	3.2
		Overall	321.3	1.03	15.5	3.22

Test 2 data of the Peugeot 504 XN2 injection engine

Brake load: 8 kgm

Ambient temperature: 17 deg. C
Barometric pressure: 761 mmHg
Engine speed: 2500 rpm

Test No.	Outlet coolant temp. (C)	Cylinder No.	Exhaust gas components			
			HC, (ppm)	CO, (%)	CO_2, (%)	O_2, (%)
1	30	1	640	3.2	13.8	2.3
		2	510	2.8	12.7	3.3
		3	510	2.5	12.6	3
		4	480	2.4	12.6	3.1
		Overall	535	2.73	12.93	2.93
2	50	1	380	2.9	14.7	2.4
		2	500	2.5	14.3	2.3
		3	500	2.6	13.3	2.7
		4	480	2.4	12.8	3.3
		Overall	465	2.6	13.77	2.68
3	70	1	340	1.46	16.9	2.2
		2	400	1.2	14.8	2.7
		3	460	1	15.3	2.5
		4	400	0.95	15.1	2.9
		Overall	400	1.15	15.53	2.58
4	85	1	320	1	18	1.5
		2	360	1.05	16	2.5
		3	450	0.7	16.1	2
		4	375	0.66	15.3	2
		Overall	376.3	0.85	16.35	2
5	100	1	330	1.8	17.2	1.6
		2	360	1.15	15.7	2.2
		3	440	0.95	15.9	2
		4	410	1.3	15.4	2.3
		Overall	385	1.3	16.05	2.03

Test 2 data of the Peugeot 504 XN2 injection engine

Brake load: 10 kgm

Ambient temperature: 18.6 deg. C
Barometric pressure: 762 mmHg
Engine speed: 2500 rpm

Test No.	Outlet coolant temp. (C)	Cylinder No.	Exhaust gas components			
			HC, (ppm)	CO, (%)	CO_2, (%)	O_2, (%)
1	30	1	400	4.7	15.7	0.6
		2	510	4.3	14.7	1.7
		3	590	4	15	1.6
		4	570	4.1	14.9	1.8
		Overall	517.5	4.28	15.08	1.43
2	50	1	380	3	16.9	0.8
		2	490	2.5	16.3	1.1
		3	490	2.6	16.4	1.9
		4	490	2.5	16	1.3
		Overall	462.5	2.65	16.4	1.28
3	70	1	350	2	18	1
		2	500	1.32	17	1.6
		3	500	1.55	17	1.2
		4	450	1.8	16.5	1.6
		Overall	450	1.67	17.12	1.35
4	85	1	330	2	16.6	1.3
		2	480	1.6	16.8	2
		3	480	1.9	16.1	1.7
		4	470	1.87	16.6	1.2
		Overall	440	1.84	16.53	1.55
5	100	1	380	2.15	17.7	1.2
		2	400	1.56	16.4	1.9
		3	450	1.8	16.6	1.5
		4	410	1.85	15.9	1.1
		Overall	402.5	1.82	16.65	1.43

Test 2 data of the Peugeot 504 XN2 injection engine

Brake load: 12 kgm

Ambient temperature: 16.2 deg. C
Barometric pressure: 761 mmHg
Engine speed: 2500 rpm

Test No.	Outlet coolant temp. (C)	Cylinder No.	Exhaust gas components			
			HC, (ppm)	CO, (%)	CO_2, (%)	O_2, (%)
1	30	1	400	4.9	15	0.6
		2	700	4.9	14.7	1.2
		3	710	4.6	14.9	1
		4	690	4.45	15	1.4
		Overall	625	4.71	14.9	1.05
2	50	1	380	4.1	16.2	0.6
		2	650	3.9	15.6	1.1
		3	650	3.7	15.9	1
		4	620	3.73	15.8	1.7
		Overall	575	3.86	15.7	1.1
3	70	1	390	4.3	15.5	0.6
		2	570	4.1	15.2	1.2
		3	670	4	15.5	1.1
		4	640	3.9	15.5	1.6
		Overall	567.5	4.08	15.42	1.13
4	85	1	360	4.22	15.8	0.4
		2	600	4.4	14.9	1.2
		3	620	4.5	15	1.9
		4	610	4.2	15.2	1.1
		Overall	532.5	4.33	15.23	1.15
5	100	1	300	3.5	16.5	0.6
		2	480	3.2	16.1	1.1
		3	500	3.5	15.7	1
		4	500	3.3	15.6	1.6
		Overall	445	3.38	15.98	1.08

Test 3 data of the Peugeot 504 XN2 injection engine

Brake load: 1.5 kgm

Ambient temperature: 16.4 deg. C
Barometric pressure: 746 mmHg
Engine speed: 2500 rpm
Coolant temperature 85 ± 1 deg . C

Test No.	Heat supplied, Watt	inlet air temp. deg. C	Cylinder No.	Exhaust gas components			
				HC, (ppm)	CO, (%)	CO_2, (%)	O_2, (%)
1	0		1	450	7.85	8.7	1.9
			2	380	6	9.6	2.1
			3	400	7.3	8.2	2.3
			4	370	7	9.1	2.1
			Overall	400	7.04	8.9	2.1
2	400		1	450	7.7	8.6	3.3
			2	400	7	9.2	3.8
			3	400	6.8	9.6	4
			4	400	7.3	8.7	4
			Overall	412.5	7.2	9.03	3.78
3	800		1	430	7.3	9.1	3.4
			2	410	6.2	9.8	3.9
			3	410	7.6	8.7	3.7
			4	420	7.6	8.4	4
			Overall	417.5	7.18	9	3.75
4	1200		1	400	8.1	8.3	3.8
			2	420	6.55	9.2	4
			3	420	7.3	9	3.8
			4	440	7.1	9.8	3.4
			Overall	420	7.26	9.07	3.75
5	1700		1	440	7.7	8.8	2.8
			2	410	7.3	8.7	4
			3	480	7.5	8.7	3.8
			4	420	7.5	8.3	4.1
			Overall	437.5	7.5	8.63	3.68

Test 3 data of the Peugeot 504 XN2 injection engine

Brake load: 3 kgm

Ambient temperature: 16.4 deg. C
Barometric pressure: 746 mmHg
Engine speed: 1000 rpm
Coolant temperature 85 ± 1 deg . C

Test No.	Heat supplied, Watt	inlet air temp. deg. C	Cylinder No.	Exhaust gas components			
				HC, (ppm)	CO, (%)	CO_2, (%)	O_2, (%)
1	0		1	320	2.5	13.7	2.1
			2	350	2.3	13.7	2.6
			3	370	3.52	13.1	2.4
			4	380	2	13.1	2.8
			Overall	367.5	2.58	13.4	2.48
2	400		1	330	2.3	13.9	2.9
			2	300	1.75	13.1	3.7
			3	370	2.5	13.2	3.4
			4	390	2.4	12.8	3.8
			Overall	347.5	2.24	13.25	3.45
3	800		1	340	2.54	14	2.8
			2	380	2.2	12.8	3.8
			3	380	2.6	13.2	3.4
			4	360	2.2	13.5	3.5
			Overall	365	2.39	13.37	3.38
4	1200		1	350	2.8	13.9	2.7
			2	340	2.07	13.3	3.5
			3	370	2.8	12.9	3.3
			4	375	2.9	12.7	3.7
			Overall	358.8	2.64	13.2	3.3
5	1700		1	360	2.6	13.8	2.4
			2	350	2.5	13.4	3.2
			3	370	2.7	13	3.2
			4	370	2.8	12.7	3.8
			Overall	362.5	2.65	13.23	3.15

Test 3 data of the Peugeot 504 XN2 injection engine

Brake load: 5.5 kgm

Ambient temperature: 16.4 deg. C
Barometric pressure: 746 mmHg
Engine speed: 1000 rpm
Coolant temperature 85 ± 1 deg . C

Test No.	Heat supplied, Watt	inlet air temp. deg. C	Cylinder No.	Exhaust gas components			
				HC, (ppm)	CO, (%)	CO_2, (%)	O_2, (%)
1	0		1	350	1.48	16.5	2.1
			2	375	0.8	15.6	2.9
			3	400	1.3	15.4	2.6
			4	360	0.96	15.2	3
			Overall	371.3	1.14	15.68	2.65
2	400		1	270	1.5	15.4	2.4
			2	350	1.5	14.2	3
			3	340	1.35	13.9	3.3
			4	320	1.3	13.4	3.1
			Overall	320	1.41	15.23	2.95
3	800		1	280	1.6	14.7	2.2
			2	350	1.6	13.4	3.2
			3	360	1.38	13.6	3.2
			4	300	1.43	13.5	3.1
			Overall	322.5	1.5	13.8	2.93
4	1200		1	300	1.75	14.3	2.1
			2	330	1.6	13.5	3.2
			3	350	1.62	13.5	3
			4	340	1.66	13	3
			Overall	330	1.66	13.58	2.83
5	1700		1	295	1.97	14.1	2.2
			2	370	1.79	13	3.2
			3	360	1.7	13.5	2.9
			4	330	1.8	13	3
			Overall	338.8	1.82	13.4	2.83

Test 3 data of the Peugeot 504 XN2 injection engine

Brake load: 8 kgm

Ambient temperature: 17 deg. C
Barometric pressure: 746 mmHg
Engine speed: 1000 rpm
Coolant temperature 85 ± 1 deg . C

Test No.	Heat supplied, Watt	inlet air temp. deg. C	Cylinder No.	Exhaust gas components			
				HC, (ppm)	CO, (%)	CO_2, (%)	O_2, (%)
1	0		1	320	1	18	1.5
			2	360	1.05	16	2.5
			3	450	0.7	16.1	2
			4	375	0.66	15.3	2
			Overall	376.3	0.85	16.35	2
2	400		1	230	2.08	16.6	2.2
			2	380	2.5	14.7	2.8
			3	380	1.95	15.7	2.4
			4	350	2.15	14.7	3.3
			Overall	335	2.17	15.42	2.67
3	800		1	270	2.6	16.5	2.6
			2	360	2.4	14.4	2.7
			3	380	2.16	15.4	2.2
			4	360	2.3	14.5	3.2
			Overall	342.5	2.37	15.2	2.68
4	1200		1	270	2.53	16.2	2.3
			2	375	2.4	14.7	2.6
			3	375	2.2	15.3	2.3
			4	370	2.6	13.8	3.3
			Overall	347.5	2.43	15	2.63
5	1700		1	280	2.9	16	2.1
			2	380	2.5	14.2	2.7
			3	420	2.4	15.1	2.2
			4	375	2.65	13.7	2.9
			Overall	363.8	2.61	14.75	2.48

Test 3 data of the Peugeot 504 XN2 injection engine

Brake load: 10 kgm

Ambient temperature: 17 deg. C
Barometric pressure: 746 mmHg
Engine speed: 1000 rpm
Coolant temperature 85 ± 1 deg . C

Test No.	Heat supplied, Watt	inlet air temp. deg. C	Cylinder No.	Exhaust gas components			
				HC, (ppm)	CO, (%)	CO_2, (%)	O_2, (%)
1	0		1	330	2	16.6	1.3
			2	480	1.6	16.8	2
			3	480	1.9	16.1	1.7
			4	470	1.87	16.6	1.2
			Overall	440	1.84	16.53	1.55
2	400		1	220	2.53	15.9	1.7
			2	370	2	13.8	2.2
			3	410	1.9	14.1	1.7
			4	400	2	13.6	2.2
			Overall	350	2.11	14.35	1.95
3	800		1	300	2.3	16	2
			2	440	2.5	15.5	1.7
			3	440	2.5	15.5	1.8
			4	420	2.24	13.4	2.4
			Overall	400	2.39	15.1	1.98
4	1200		1	475	3	15.1	1.8
			2	240	2.9	16.3	1.2
			3	490	2.8	15.7	1.5
			4	400	2.7	15.1	2.3
			Overall	401.2	2.85	15.55	1.7
5	1700		1	410	3.1	15.3	1.6
			2	250	3.5	15.7	1.1
			3	475	3.1	15.5	1.4
			4	480	3.2	14.7	1.9
			Overall	403.7	3.22	15.3	1.5

Test 3 data of the Peugeot 504 XN2 injection engine

Brake load: 12 kgm

Ambient temperature: 17 deg. C
Barometric pressure: 746 mmHg
Engine speed: 1000 rpm
Coolant temperature 85 ± 1 deg . C

Test No.	Heat supplied, Watt	inlet air temp. deg. C	Cylinder No.	Exhaust gas components			
				HC, (ppm)	CO, (%)	CO_2, (%)	O_2, (%)
1	0		1	360	4.22	15.8	0.4
			2	600	4.4	14.9	1.2
			3	620	4.5	15	1.9
			4	610	4.2	15.2	1.1
			Overall	532.5	4.33	15.23	1.15
2	400		1	230	5	14.3	1.6
			2	480	5	12.9	2.4
			3	510	5.1	13.2	1.7
			4	520	3.94	13	2
			Overall	435	4.76	13.35	1.93
3	800		1	250	5.5	13.9	1.7
			2	500	5.3	12.5	2.5
			3	520	5.4	12.9	1.7
			4	540	5.15	12.1	2.8
			Overall	452.5	5.34	12.85	2.17
4	1200		1	270	7	12.5	1.7
			2	530	6.5	11.4	2.3
			3	560	6.78	11.4	1.8
			4	620	6.5	10.7	2.8
			Overall	495	6.69	11.5	2.15
5	1700		1	325	8	11.6	1.6
			2	640	7.82	10.7	1.7
			3	610	7.8	10	2.3
			4	680	7.2	10.3	2.5
			Overall	563.8	7.71	10.65	2.03

Appendix G: Estimation of error of experimental results

A calculated result from experimental data is a function of many independent variables, each of which is determined from the measurements in the experiment. Therefore, error is unavoidable. To evaluate the experimental results, the error must be estimated.

The error in a measurement can be determined from the accuracy of the measuring instrument and from other factors such as errors from human factors in recording data, so the resulting error in the calculation of the desired variable can be determined based on the theory of error.

Consider a function U=f(x,y,z), where x, y, z are independent variables and have errors (expressed by tolerances of δx, δy, δz) attached to them, then the resulting error of U (expressed by tolerance δU) can be determined from the following equation (derived from the Taylor expansion for function U).

$$\delta U = \frac{\partial U}{\partial x}\delta x + \frac{\partial U}{\partial y}\delta y + \frac{\partial U}{\partial z}\delta z \qquad \text{(G-1)}$$

or approximately and more conveniently, it can be applied the equation below.

$$\delta U = \sqrt{\left(\frac{\partial U}{\partial x}\delta x\right)^2 + \left(\frac{\partial U}{\partial y}\delta y\right)^2 + \left(\frac{\partial U}{\partial z}\delta z\right)^2} \qquad \text{(G-2)}$$

If expressing the tolerance of each variable as the percentage of that variable, X_U, X_x, X_y, X_z, (where $X_U = \frac{\delta U}{U}$, etc), the resulting tolerance of U (expressed as percentage of the value U) is determined from the following equation.

$$X_U = \frac{1}{U}\sqrt{\left(x\frac{\partial U}{\partial x}X_x\right)^2 + \left(y\frac{\partial U}{\partial y}X_y\right)^2 + \left(z\frac{\partial U}{\partial z}X_z\right)^2} \qquad \text{(G-3)}$$

1. Error of the measured air/fuel ratios.

Measured air/fuel ratio is determined from

$$(A/F)_m = \frac{m_a}{m_f}$$

Where: $(A/F)_m$ is measured air/fuel ratio
m_a is air mass flow rate (kg/h),
m_f is fuel mass flow rate (kg/h).

Therefore, according to the method presented above (G-3), tolerance of measured air/fuel ratio, expressed as percentage of measured air/fuel ratio, is given by

$$X_{(A/F)m} = \sqrt{X_{ma}^2 + X_{mf}^2}$$

Where: X_{ma} is tolerance of the air mass flow rate, expressed as percentage of air mass flow rate, and is determined from appendix E.

X_{mf} is tolerance of the fuel flow rate, expressed as percentage of fuel flow rate, and is determined in terms of tolerance of time, X_τ , and tolerance of measured fuel volume, X_{vf}, corresponding to measurement time.

$$X_{mf} = \sqrt{X_\tau^2 + X_{vf}^2}$$

X_τ and X_{vf} include errors of the instruments and errors of readings, X_τ =0.1%, X_{vf} = 0.05%.

Therefore X_{mf}=0.11% and $X_{(A/F)m}$=1.11%, 1.31%, and 1.6% corresponding to the 25.4 mm, 38.1 mm, and 50.8 mm orifice plates, respectively.

2. Error of calculated air/fuel ratio from exhaust gas analysis.

Air/fuel ratio from exhaust gas analysis, U, is determined from equation (4.2-7) as presented section 4.2and is rewritten below.

$$U = A/F = F_b \left[11.492 F_c \left(\frac{1 + R/2 + Q}{1 + R}\right) + \left(\frac{120 F_h}{3.5 + R}\right)\right]$$

$$R = P_{CO} / P_{CO_2}$$

$$Q = P_{O_2} / P_{CO_2}$$

$$F_b = \frac{(P_{CO} + P_{CO_2})}{(P_{CO} + P_{CO_2} + P_{CH})}$$

P_{CO}, P_{CO_2}, P_{O_2}, and P_{CH} are percentage concentrations by mole of CO, CO_2, O_2, and concentration of unburnt hydrocarbon on the basis of carbon atom, respectively.

F_c and F_h are fractions of carbon and hydrogen by mass in the fuel.

Applying equation (G-3) and denoting X_i for the tolerance of the source i, for example $X_{P_{co}}$ is tolerance of P_{CO} (expressed as percentage of Pco), tolerance of calculated air/fuel ratio is determined as follows.

$$X_U = \sqrt{A_{Fb}^2 + A_{Fc}^2 + A_R^2 + A_Q^2 + A_{Fh}^2}$$

Where:

$$A_{Fb}^2 = X_{Fb}^2$$

$$A_{Fc}^2 = \left[\frac{11.492 F_b \left(\frac{1 + R/2 + Q}{1 + R} \right)}{U} \right]^2 X_{Fc}^2$$

$$A_R^2 = \left[\frac{F_b \left(11.492 F_c \left(\frac{1/2 + Q}{(1+R)^2} \right) + \frac{120 Fh}{(3.5+R)^2} \right) R}{U} \right] X_R^2$$

$$A_Q^2 = \left[\frac{11.492 F_b F_c \frac{Q}{1+R}}{U} \right]^2 X_Q^2$$

$$A_{Fh}^2 = \left[\frac{\frac{120}{3.5+R} F_h}{U} \right]^2 X_{Fh}^2$$

$$X_{Fb}^2 = \left(\frac{P_{CH}}{P_{CO} + P_{CO_2}}\right)^2 \left[X_{P_{CH}}^2 + \left(\frac{P_{CO}}{P_{CO} + P_{CO_2}}\right)^2 X_{P_{CO}}^2 + \left(\frac{P_{CO_2}}{P_{CO} + P_{CO_2}}\right)^2 X_{CO_2}^2 \right]$$

$$X_Q^2 = X_{P_{O2}}^2 + X_{P_{CO2}}^2$$

$$X_R^2 = X_{P_{CO}}^2 + X_{P_{CO2}}^2$$

$X_{P_{O2}}$, $X_{P_{CO}}$, $X_{P_{CO2}}$, $X_{P_{CH}}$ are tolerances of measured concentrations of exhaust components P_{O_2}, P_{CO}, P_{CO_2}, P_{CH}, respectively, and expressed as percentages of these concentrations. Their values include the errors of the instruments and errors of readings. According to accuracy of the instruments presented earlier and the ability of reading from the measurement scales of the instruments and the stability of the instruments during experiments, the values of these tolerances are as follows.

$X_{P_{O2}} = 2\%,$
$X_{P_{CO}} = 3\%,$
$X_{P_{CO2}} = 2\%,$
$X_{P_{CH}} = 50\%$

High error in concentration of HC on the basis of carbon atom is assumed due to the uncertainty of the method of interpretation from concentration by volume as presented in section (4.2-3).

Calculations are carried out by programming in Pascal language with measured data of exhaust gas components at all experimental conditions. The results show the calculated values of tolerances of calculated air/fuel ratio range from 1.7 to 2.1%. Even the tolerance $X_{P_{CH}}$ is large (say 1000%), the error of the calculated air fuel ratio is still in the range of 1.7 to 2.1% because HC concentration in the exhaust gas for the experiment engines are relatively small (less than 500 ppm).

References.

1. **Abbass, H. A., N. Raman, and M. V. Narasimhan**, "Effect of Throttle Configuration on Wall Flow Behaviour of Fuel in a Carburetted Induction System", *Proceedings of Institution of Mechanical Engineers*, Part D, Vol. 208, 1994.
2. **Ahtisham, A., Nizami, Surendra Singh and Nicholas P. Cernasky** (1982), "Formation of Oxides of nitrogen in monodisperse spray combustion of hydrocarbon fuels", *Combustion Science and Technology*, Vol. 28, pp. 97-106.
3. **Ali, E. Mahdi**, "Flow and Distribution Patterns Within the Gasoline Engine Manifold", In *Heat and Mass Transfer in Gasoline and Diesel Engines* (Eds **D. B. Spalding and N. H. Afgan**), 1989 (Hemisphere, New York).
4. **Aquino, C. F.**, "Transient air/fuel (A/F) control characteristics of the five litre central fuel injection engine," *SAE paper 810494*, 1981.5) **Aricl, O., Tabaczynski, R. J., and Arpaci, V. S.** (1983), "A model for the lean misfire limit in spark-ignition engines". *Combustion Science and Technology*, Vol. 30, pp. 31-45.
5. **Ball, Kenneth**, "*Workshop manual for Peugeot 504*", England 1972.
5. **Benson, Rowland S. and Whitehouse, N. D.**, *Internal Combustion Engines*, Vol. I, Pergamon, Oxford, 1979.
6. **Benson, Rowland S. and Whitehouse, N.D.**, *Internal Combustion Engines*, Vol. II, Pergamon, Oxford, 1979.
7. **Boam, D. J., I. C. Finlay, and G. S. Fairhead**, "The Optimisation of Fuel Enrichment Patterns with Throttle Body Injection", P*roceedings of Institution of Mechanical Engineers,* Vol.202, No.D1, 1989.
8. **Boam, D. J., Finlay, I. C., Biddulph, T. W., Lee, R., Richardson, S. H., Bloomfield, J., Green, J. A. and Woods, W. A.** (1994), "The sources of unburnt hydrocarbon emissions from spark ignition engines during cold starts and warm-up", *Proceedings of Institution of Mechanical Engineers*, Vol. 208, Part D, pp.1-11.
9. **Brown, C. N. and N. Ladommatos**, "The Effects of Mixture Preparation and Trapped Residuals on the Performance of a Spark-Ignition Engine with Air-Shrouded Port Injectors, at Low Load and Low Speed", *Proceedings of Institution of Mechanical Engineers*, Vol.205, Part D, 1991.
10. **Boam, D. J. and I. C. Finlay**, "A Computer Model of Fuel Evaporation in The Intake System of a Carburetted Petrol Engine", I Mech E Conference on *FuelEconomy and Emissions of Lean Burn Engines*, paper C89/79, 1979, pp.25-37.

11 **British Standard 1042**, *Methods for the Measurement of Fluid Flow in Pipe, part1: Orifice plates, Nozzles and Venturi tubes*, British Standard Institution, 1964.

12 **Brown, C. N. and Ladommatos, N.**, "A Numerical Study of Fuel Evaporation and Transportation in the Intake Manifold of a Port-Injected Spark-Ignition Engine", *Proceedings of Institution of Mechanical Engineers*, Vol.205, 1991.

13 **Charles Aquino and William D. Plensdort**, "An Evaluation of Local Heating as a Means of Fuel Evaporation for Gasoline Engines", *SAE paper 860246*, 1986.

14 **Collins, M. H.**, "A technique to characterise quantitatively the air fuel mixture in the inlet manifold of a gasoline engine". *SAE paper 690515*, 1969, pp. 1842-1848.

15 **Fendell, F., Fink, S. and Feldman, P.** (1983), "A note on unburned hydrocarbon emissions from automotive engines", *Combustion Science and Technology*, Vol.30, pp. 47-57.

16 **Finlay, I. C. and Welsh,N.**, "Photographic study of fuel atomisation and distribution in air-valve carburettors," *Automotive engineer, vol. 3, No. 1*, 1978.

17 **Fraidl, G. K.**, "Spray Quality of Mixture Preparation Systems", *EAEC Int. Conf.on New Developments in Powertrain and Chassis Engineering* Strasbourg, Vol.1, pp.232-46.

18 **Gardiner, D.P. and Bardon, M. F.** "Mixture maldistribution due to manifold films in a methanol fuelled engine", *SAE paper 860234*, 1986.

19 **Gat, N. and Kauffman, C. W.**, "The effect of exhaust gas recirculation and turbulence on the burning velocity, dead space thickness, and minimum ignition energy in premixed methane-air combustion", *Combustion Science and Technology*, Vol. 23, 1980, pp1-15.

20 **Gilkey, J. C. and Powell, J. D.**, "Fuel- Air Ratio Determination From Cylinder Pressure Time Histories", *Transactions of the ASME, Journal of Dynamic Systems,Measurement, and Control*, Vol.107, December 1985.

21 **Goulburn, J. R. and D. W. Hughes**, "Mixing of Vaporized Petrol and Air in Automobile Engine Inlet Systems", I Mech E Conference on *Fuel Economy and Emissions of Lean Burn Engines*, paper C96/79, 1979, pp.97-105.

22 **Gruden, D. and Hahn, R.** (1979), "Performance, exhaust emissions and fuel consumption of an I C engine operating with lean mixtures", I Mech E Conference on *Fuel Economy and Emissions of Lean Burn Engines*, paper C111/79, pp. 177-184.

23 **Gruse, William A.** and **Stevens, Donald R.**, *The chemical Technology of Petroleum, McGraw-Hill*, New York, 1942.

24 **Harrow, G. A., Mills, W. D., Thomas, A. and Finlay, I. C.**, "The vapipe - a practical system for producing homogeneous gasoline-air mixture". *SAE paper 760564*, 1976.

25 **Hasson, D. A. and W. L. Flint**, "An Investigation of the Liquid Petrol Wall Film in the Manifold of a Carburetted Spark Ignition Engine: Effect of Carburettor and Manifold Geometry on Wall Film Quantities, Engine Performance and

Emissions", *Proceedings of Institution of Mechanical Engineers*, Vol.203, Part D, 1989.

26 **Hayashi, S. and Norihiro Sawa**, "A Study on the Transient Characteristics of Small SI Engines", *Bulletin of JSME*, Vol. 27, No. 224, February 1984.

27 **Hires, S. D. and Overington, M. T.**, " Transient mixture strength excursions -An investigation of their causes and the development of a constant mixture strength fuelling strategy," *SAE paper 810495*, 1981.

28 **Hohsho, Y., Kokichi Kanno, Hiroyuki Nakai, and Toshikazu Kadota** "Characteristics of Response of Carburetted SI Engine under Transient Conditions", *Bulletin of JSME*, Vol. 28, No. 242, August 1985.

29 **Houpt, Paul K. and Stamatios K. Andreadakis**, "Estimation of Fuel-Air Ratio from Cylinder Pressure in Spark Ignited Engines", *SAE paper 830418*, International Congress & Exposition Detroit, Michigan February 28 - March 4, 1883.

30 **Humberg, D. R. and Hyland, J. E.**, "A vaporized gasoline metering system for internal combustion engine", *SAE paper 760288*, 1976.

31 **Jones, B. E. and Mackwoth, J. D.**, "Induction Swirl in Spark Ignition Engines", Conference on *Combustion in Engines* sponsored by the Automobile Division of the Institution of Mechanical Engineers in association with the school of Automotive Studies, Cranfield Institute of Technology 7-9 July 1975. pp.41-48.

32 **Kaiser, E. W., Rothschild, W. G. and Lavoie, G. A.** (1983), "The effect of fuel and operating variables on hydrocarbon species distributions in the exhaust from a multicylinder engine", *Combustion Science and Technology*, Vol. 32, pp. 245-265.

33 **Kashiwaya, M., Kosuge, T., Nakagawa, K. and Okamoto, Y.**, " The effect of atomisation of fuel injectors on engine performance". *SAE paper 900261*, 1990.

34 **Lancaster, D.R., Krieger, R.B. and J.H. Lienesch**, "Measurement and analysis of engine pressure data", *SAE paper 750026*, 1975.

35 **Lavoie, G.A.**, "Spectroscopic measurement of nitric oxide in spark-ignition engines", *Combustion and Flame*, 15, 97, 1970.

36 **Liimatta, D. R., R. F. Hurt, R. W. Deller, and W. L. Hull**, "Effects of Mixture Distribution on Exhaust Emissions as Indicated by Engine Data and the Hydraulic Analogy", *SAE paper 710618*, Mid-Year Meeting Montreal, Que.,Can. June 7-11, 1971.

37 **Lorusso, J. A., Kaiser, E. W. and Lavoie, G. A.** (1981), "Quench layer contribution to exhaust hydrocarbons from a spark-ignited engine", *Combustion Science and Technology*, Vol. 25, pp. 121-125.

38 **Lorusso, J. A., Kaiser, E. W. and Lavoie, G. A.** (1983), "In-cylinder measurements of wall layer hydrocarbons in a spark ignited engine", *Combustion Science and Technology*, Vol. 33, pp. 75-112.

39 **Ma, T. H.**, "Effect of Cylinder Charge Motion on Combustion", Conference on *Combustion in Engines* sponsored by the Automobile Division of the Institution

of Mechanical Engineers in association with the school of Automotive Studies, Cranfield Institute of Technology 7-9 July 1975. pp.1-12.

40 **Marsee, F. J., Olree, R.M. and Adams, W. E.**, "Compression ratio effects with lean mixtures", *SAE paper 770640*, Detroit, Michigan, February 28 - March 4, 1977.

41 **Masaaki Takizawa, Tatsuo Uno, Toshiaki Oue, and Tadayoshi Yura**, "A Study of Gas Exchange Process Simulation of an Automotive Multi-Cylinder Internal Combustion Engine", *SAE paper 820410*, 1982.

42 **Milton, B. E. and M. Behnia**, "A Numerical Study of the Interchanging Vapor, Droplet, and Film Flows in a Gasoline Engine Manifold", In *Heat and Mass Transfer in Gasoline and Diesel Engines* (Eds D. B. Spalding and N. H. Afgan), 1989 (Hemisphere, New York).

43 **Nagaishi, H., Hiromichi Miwa, Yoshihisa Kawamura, and Masaaki Saitoh**, "An Analysis of Wall Flow and Behavior of Fuel in Induction Systems of Gasoline Engines", *SAE paper 890837*, 1989.

44 **Nakajima, Y., Sugihara, K. and Takagi, Y.** (1979), "Lean mixture or EGR - Which is better for fuel economy and NO_x reduction", I Mech E Conference on *Fuel Economy and Emissions of Lean Burn Engines*, paper C94/79, pp.81-86.

45 **Nakajima, Y., Saito, T., Takagi, Y., Katoh, K. and Iijima, T.** " The influence of fuel characteristics on vaporisation in the SI engine cylinder during cranking at low temperature". *SAE paper 780612*, 1978, pp.2234-2250.

46 **Newhall, H.K. and Starkman, E.S.**, "Direct spectroscopic determination of nitric oxide in reciprocating engine cylinders", *SAE paper 670122*, 1967.

47 **Newhall, H.K. and Shahed, S. M.**, "Kinetics of nitric oxide formation in high pressure flames", *13th International Symposium on combustion*, Salt Lake City, 365, 1971.

48 **Nightingale, C. J. E. and Tsatsami, V.** "Improved mixture preparation for cold starting of SI engines". *Automotive engineer*, vol. 9(5), 1984.

49 **Ohata, A. and Ishida, Y.**, "Dynamic Inlet Pressure and Volumetric Efficiency of Four Cycle Four Cylinder Engine", *SAE paper 820407*, International Congress & Exposition Detroit, Michigan February 22-26,1982.

50 **Pao, H. C.**, "The Measurement of Fuel Evaporation in the Induction System During Warm-up", *SAE paper 820409*, 1982.

51 **Quader, A.A.** "Lean combustion and misfire limit in spark ignition engines". *SAE paper 741055*, 1974.

52 **Rao, K. V. L. and A. H. Lefebvre**, " Evaporation characteristics of kerosenesprays injected into a flowing air stream," *Combustion and flame, vol. 26, 1976*, pp. 303-309.

53 **Sano, Taeko**, (1982), "NO_2 formation in laminar flames", *Combustion Science and Technology*, Vol. 29, pp261-275.

54 **Sjenitzer, F.**, "The evaporation of a liquid spray injected into a stream of gas,"*Chemical Engineering Science*, vol.17, 1962.

55 **Spindt, R. S.**, "Air-Fuel Ratios from Exhaust Gas Analysis", *SAE paper 650507*, Mid-Year Meeting Chicago,III. May 17-21,1965.

56 **Servati, Hamid B and Walter W. Yuen**, "Deposition of Fuel Droplets in Horizontal Intake Manifolds and the Behavior of Fuel Film Flow on Its Walls", *SAE paper 840239*, 1984.

57 **Shayler, P. J., R. M. Isaacs, and T. H. Ma**, "The Variation of In-Cylinder Mixture Ratios During Engine Cranking at Low Ambient Temperatures", *Proceedings of Institution of Mechanical Engineers,* Vol. 206, Part D, 1992.

58 **Shyy, W. and Adamson, T. C.** (1983), "Analysis of hydrocarbon emissions from conventional spark-ignition engines", *Combustion Science and Technology*, Vol. 33, pp. 245-260.

59 **Stone, R.**, *Introduction to Internal Combustion Engines*, 1992. Macmillan Press, London.

60 **Takemura, J., Sanbuyashi, D. and Ando, H.** "Effect of turbulence in the intake port of MPI engine, fuel transport phenomena and nonuniformity of fuel/air mixing in cylinder". *SAE paper 900162*, 1990.

61 **Tanaka, M. and Durbin, E.J.**, "Transient response of a carburettor engine," *SAE paper 770046*, 1977.

60. **Taylor,C. F.** (1985a). *The Internal Combustion Engine in Theory and Practice*, Vol.I, MIT Press, Cambridge, Massachusetts.

61. **Taylor,C. F.** (1985b). *The Internal Combustion Engine in Theory and Practice*, Vol.II, MIT Press, Cambridge, Massachusetts.

62. **Trayser, D. A.** *et al*, "A study of the influence of fuel atomization, vaporization, and mixing processes on pollutant emissions from motor-vehicle powerplants", *Battelle Memorial Institute Report*, Ohio,USA, 1972.

63. **Watfa, M. and Daneshyar, H.**, "Formation of Nitric Oxide (NO), Carbon Monoxide (CO) and Unburnt Hydrocarbons (HC) in Spark Ignition Engines", Conference on *Combustion in Engines* sponsored by the Automobile Division of the Institution of Mechanical Engineers in association with the school of Automotive Studies, Cranfield Institute of Technology 7-9 July 1975. pp.165-183.

64. **Waddams, A. Lawrence**, *Chemical from Petroleum, an Introductory Survey*, London, 1978.

65. **Woods, W. A. and Sag, O. K.**, "A Study of Cylinder-to-Cylinder Distribution of Charge in a six Cylinder Spark Ignition Engine", *Transactions of the ASME,Vol.110, July 1988, Journal of Engineering for Gas Turbines and Power.*

66. **Winklhofer, E., G. K. Fraidl and A. Plimon**, "Monitoring of Gasoline Fuel Distribution in a Research Engine", *Proceedings of Institution of Mechanical Engineers,* Vol.206, Part D,1992.

67. **Yu, Henry T.C.** "Fuel distribution - A new look at an old problem," *SAE transactions*, Vol. 71, 1963, pp.596- 613.

68. Yun, H. J., R. S. Lo, and T. Y. Na, "Theoretical Studies of Fuel Droplet Evaporation and Transportation in a Carburettor Venturi", *SAE paper 760289,* Detroit, Michigan 1976.

69. Servomex, 1410 B Infrared Analyser Instruction Manual and 1420 B Oxygen Analyser Instruction Manual, 1987.

70. VANE VP-760 Emissions Analyser Manual, 1982.